SIMULATION OF SOLUTE TRANSPORT IN UNSTEADY STREAMFLOWS

A THESIS

Submitted in fulfilment of the
requirements for the award of the degree
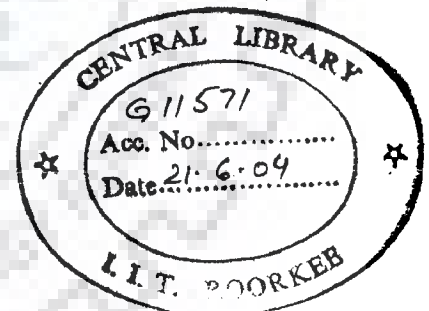*of*

DOCTOR OF PHILOSOPHY

in

WATER RESOURCES DEVELOPMENT

By

SEEPANA BALA PRASAD

WATER RESOURCES DEVELOPMENT TRAINING CENTRE
INDIAN INSTITUTE OF TECHNOLOGY ROORKEE
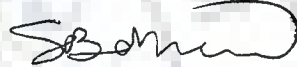ROORKEE–247 667 (INDIA)

SEPTEMBER, 2002

INDIAN INSTITUTE OF TECHNOLOGY ROORKEE
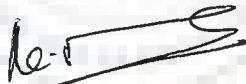## ROORKEE

CANDIDATE'S DECLARATION

I hereby certify that the work which is being presented in the thesis entitled **"SIMULATION OF SOLUTE TRANSPORT IN UNSTEADY STREAMFLOWS"** in fulfilment of the requirement for the award of the Degree of Doctor of Philosophy and submitted in the Water Resources Development Training Centre, Indian Institute of Technology, Roorkee, is an authentic record of my own work carried out during a period from July 1999 to September 2002 under the supervision of **Dr. U.C. Chaube**, Professor, WRDTC, Indian Institute of Technology, Roorkee, **Dr. M. Perumal**, Associate Professor, Centre for Continuing Education, Indian Institute of Technology, Roorkee, and **Dr. C.S.P. Ojha**, Associate Professor, Department of Civil Engineering, Indian Institute of Technology, Roorkee.

The matter presented in this thesis has not been submitted by me for the award of any other degree of this or any other institute/university.

(SEEPANA BALA PRASAD)

This is to certify that the above statement made by the candidate is correct to the best of our knowledge.

(Dr. C.S.P. Ojha)	(Dr. M. Perumal)	(Dr. U. C. Chaube)
Assoc. Professor	Assoc. Professor	Professor
Dept. of Civil Engineering	Centre for Continuing Education	Water Resources Dev. Training Centre

Indian Institute of Technology Roorkee, Roorkee

Dated : September 20 , 2002

The Ph. D. Viva-Voce examination of **Seepana Bala Prasad**, Research Scholar, has been held on 14 . 11. 2002

Signature of Supervisor(s)   Signature of H. O. D.   Signature of External Examiner

i

ABSTRACT

The subject of pollutant mixing and its transport in streams has been at the forefront of research for the determination of pollutant concentration along the river course and for regulating disposal of pollutants in rivers. While abundant literature is available for solute transport modelling under steady flow conditions, only a few researchers have studied the problem of solute transport in rivers under unsteady streamflow conditions. Majority of the studies available in literature employ complex numerical algorithms for solution of the governing equations of flow and solute transport phenomena, which require river cross-section details at close spatial intervals, in addition to flow and solute concentration measurements at those locations. The existing models do not allow the integration of flow and solute transport model parameters and simultaneous flow and solute routing. Further, existing transient storage models for simulating solute transport in the presence of transient storage zones along river reach require complex numerical solution algorithms. The present study attempts to overcome the above limitations in modelling the longitudinal dispersion of solutes under unsteady flow conditions using the following approach:

1. Simplification of the Advection-Dispersion (AD) equation for solute transport modelling and coupling it with a flow routing model based on the Approximate Convection- Diffusion (ACD) equation for simultaneous routing of flow and solute.

2. Simplification of the governing equations of the Transient Storage (TS) model for solute transport modelling along the river reach and coupling it with the flow routing model based on the ACD equation.

Important assumptions used in the development of this approach, are: i) the flow in small reach length Δx is steady and uniform over a routing time interval Δt, but varies from one time interval to the next interval, and ii) the concentration varies linearly within a small reach length Δx.

Similarity between the simplified form of the (AD) equation governing the solute transport, and the Approximate Convection-Diffusion (ACD) equation (Perumal and Ranga Raju, 1999) governing the flow transport is established. The similarity of the simplified forms of the flow transport and solute transport equations has enabled the development of the AD-VPM model for studying solute transport in rivers under steady flow conditions. The appropriateness of the AD-VPM model is first tested under steady flow conditions by reproducing the analytical solution of the AD equation for a given uniform pulse input and for different combinations of flow velocity (U) and dispersion coefficient (D_L). It is found from the analysis of a number of numerical experiments that analytical solution of the AD model is closely reproduced by the proposed AD-VPM model as indicated by the Nash-Sutcliffe criterion, $\eta \geq 99\%$, when $D_L \leq 415.64$ $U^{1.71}$ defining the applicability domain of the AD-VPM model. The proposed AD-VPM model has also been verified under steady flow conditions using i) two laboratory test data, and ii) three field experiments data, (the Colorado River, the Rhine river, and the Missouri river). The dispersion coefficient, which is a parameter in the AD-VPM model is estimated using the relationship suggested by McQuivey and Keefer (1974) because of its simplicity and accuracy. Satisfactory reproduction of the C-t curves demonstrates the suitability of the AD-VPM model for its application under steady flow conditions, within its applicability domain.

The acceptable performance of the AD-VPM model for steady flow conditions, has enabled to extend it for studying solute transport under unsteady flow conditions. This is achieved by integrating the parameters of the AD-VPM model with the parameters of the VPM flow routing model for simultaneous routing of the solute under unsteady flow conditions. Numerical experiments on two hypothetical channels having a width of 50m and 100m, characterised by different Manning's roughness coefficient and bed slope values, demonstrate the ability of the AD-VPM model for solute transport by reproducing the results obtained from the numerical solution of the coupled Saint-Venant equations for flow routing and the AD equations (SVE-AD

for an uniform pulse input, and ii) using two field experiments data (Mimram river and Uvas Creek). Since the form of the ATS model is same as that of the AD model, the applicability criterion of the ATS-VPM model under steady flow conditions is considered as the same as that obtained for the AD-VPM model with U replaced by the solute transport velocity (U_s) and D_L replaced by the ATS dispersion coefficient (D_{Ls}).

The ATS-VPM model has been extended to study solute transport in rivers under unsteady flow conditions, following the same approach as adopted in the case of AD-VPM model. Numerical experiments on three hypothetical channels of different characteristics demonstrate the adequacy of the ATS-VPM model, by satisfactorily simulating the C-t curves as obtained by the numerical algorithm solutions of the Saint-Venant's Equations and the TS equations (SVE-TS model). The ATS-VPM model has also been verified for its applicability using the field experiments data of Huey creek recorded under unsteady flow conditions (Runkel et al., 1998).

Based on the study it is concluded that the proposed AD-VPM and ATS-VPM models simulate the solute transport in rivers and streams under steady as well as unsteady flow conditions satisfactorily within their applicability ranges.

ACKNOWLEDGEMENT

CONTENTS

LIST OF TABLES

LIST OF FIGURES

NOTATIONS

A	cross-sectional area of flow, $[L^2]$;
A_s	storage zone cross-sectional area normal to the flow, $[L^2]$;
$A(z^{-1})$	polynomial in z^{-1};
A'	area at four nodes, $[L^2]$;
B	width of the channel, $[L]$;
$B(z^{-1})$	polynomial in z^{-1};
C	cross-sectional averaged concentration, $[ML^{-3}]$;
$\overline{C}$	mean concentration of solute in the cell, $[ML^{-3}]$;
C_a	mean concentration of solute in the main stream, $[ML^{-3}]$;
C_b	initial concentration, $[ML^{-3}]$;
$C_{c,i}$	i^{th} computed concentration ordinate, $[ML^{-3}]$;
C_d	mean concentration of solute in the dead zone, $[ML^{-3}]$;
C_I	inflow concentration of solute, $[ML^{-3}]$;
C_{IO}	concentration of solute in injected solution, , $[ML^{-3}]$;
C_O	output concentration of solute, $[ML^{-3}]$;
$C_{Ob,i}$	i^{th} observed concentration ordinate, $[ML^{-3}]$;
$\overline{C_{Ob,i}}$	mean of the observed concentration ordinates, $[ML^{-3}]$;
C_p	peak concentration, $[ML^{-3}]$;
C_s	cross-sectional averaged concentration in the storage zone, $[ML^{-3}]$;
$C(0,t)$	concentration of solute at x=0 and time,t, $[ML^{-3}]$;
$C(x_1,t)$ and $C(x_2,t)$	concentration of solute at distances x_1 and x_2 at time t, $[ML^{-3}]$;
$C(x, 0)$	concentration of solute at distance x and time t = 0, $[ML^{-3}]$;
$C(x, t)$	concentration of solute at distance x and time t, $[ML^{-3}]$;
c_{sp}	concentration in side pockets, $[ML^{-3}]$;
c_k	wave celerity, $[LT^{-2}]$;
D_f	flow diffusion coefficient, $[L^2T]$;

D_L	longitudinal dispersion coefficient, $[L^2T^{-1}]$;
D_{La}	longitudinal dispersion coefficient in DZ model, $[L^2T^{-1}]$;
D_{Lts}	ATS dispersion coefficient, $[L^2T^{-1}]$;
D_{ts}	longitudinal dispersion coefficient in the main channel in TS model, $[L^2T^{-1}]$;
DF	dispersive fraction;
d/s	downstream
F_M	Froude number at the middle of the reach Δx;
G_1, G_2 and G_3	Muskingum coefficients for flux routing;
g	acceleration due to gravity, $[LT^{-2}]$;
g_a	adsorbed solute mass per unit volume in storage zone, $[ML^{-3}]$;
g_a	dissolved solute mass per unit volume in storage zone, $[ML^{-3}]$;
I_b	initial steady flow, $[L^3T^{-1}]$;
I_p	peak flow, $[L^3T^{-1}]$;
i	space discretisation index;
j	time discretisation index;
K_C	reach travel time of solute of the AD-VPM model, $[T]$;
K_{cts}	reach travel time of solute of the ATS-VPM model, $[T]$;
K_f	reach travel time in the Muskingum flow routing method, $[T]$;
K_m	reach travel time in the Muskingum flux routing method, $[T]$;
L	characteristic length of the reach, Δx, $[L]$;
L_B	overall bend length measured along the centerline of the channel, $[L]$;
M	mass of conservative solute, $[M]$;
M_r	mass flow rate of conservative solute past a section, $[MT^{-1}]$;
m	constant (=2/3 for Manning's friction law and =1/2 for Chezy friction law);
N_c	Courant number;
N_{CI}	number of sub-reaches;
Nr	number of sub-reaches;
n	total number of ordinates;
P	wetted perimeter, $[L]$;
P_e	Peclet number;
Q	rate of flow, $[L^3T^{-1}]$;
Q_I	rate of inflow, $[L^3T^{-1}]$;

Q_O	rate of outflow, [L^3T^{-1}];
q	lateral flow rate per unit length, [$L^3T^{-1}L^{-1}$];
q_w	discharge per unit width of channel, [$L^3T^{-1}L^{-1}$];
R	hydraulic radius, [L];
r	radius of the pipe, [L];
r_c	radius of curvature of bend, [L];
S	storage of flow in the reach, [L^3];
S_c	mass storage per unit volume in the reach;
S_0	bed slope;
S_f	friction slope;
T_r	residence time parameter, [T];
$\bar{t}$	travel time, [T];
t	temporal co-ordinate, [T];
$\bar{t}_1$ and $\bar{t}_2$	mean times of passage of tracer cloud at measuring stations located at longitudinal distance x_1 and x_2 from the section of solute injection, [T];
t_p	time to peak flow, [T];
t_{cp}	time to peak concentration, [T];
U	ensemble mean cross-sectional velocity, [LT^{-1}];
U'	mean of velocities at four nodes, [LT^{-1}];
U_*	shear velocity, [LT^{-1}];
U_a	actual velocity measured in the river, [LT^{-1}];
U_r	velocity in the representative trapezoidal cross-section, [LT^{-1}];
u'	deviation of velocity from the cross-sectional mean velocity, [LT^{-1}];
V	volume of each cell, [L^3];
V_{IO}	volume of injected solution, [L^3];
x	notation denoting longitudinal distance co-ordinate, [L];
y	depth of flow, [L];
y_m	maximum depth, [L];
y_d	dead zone depth in the channel, [L];
y_n	normal depth of flow in the main channel, [T]; and
z	back shift operator;

Symbols

erfc(z)	complimentary error function;
β	ratio of the storage area to the main channel area;
κ	Von Karman's coefficient;
ω_{K1}, ω_{K2}, and ω_{K3}	Muskingum coefficients for the exponential scheme;
ε_1 ε_2 and ε_3	Muskingum coefficients for flow routing;
ω_1, ω_2, and ω_3	coefficients of the AD-VPM model routing equation;
$\omega_{ts1}, \omega_{ts2}$, and ω_{ts3}	coefficients of the ATS-VPM routing equation;
ϕ	relational constant;
η	Nash-Sutcliffe's criterion;
ψ	velocity conversion coefficient;
γ_c	skewness factor for concentration distribution;
γ	skewness factor for flow distribution;
θ_f	weighting parameter of the Muskingum flow routing method;
θ_c	weighting parameter of the AD-VPM model;
θ_{cts}	weighting parameter of ATS-VPM model;
θ_m	weighting parameter of flux routing;
λ	applicability criterion parameter;
ε_t	transverse mixing coefficient, $[LT^{-2}]$;
α	stream storage exchange coefficient, $[T^{-1}]$;
α_d	mass exchange coefficient between the main flow and the dead zone, $[T^{-1}]$;
τ	time variable, $[T]$;
τ_d	time delay, $[T]$;
Γ_a	ratio of the interfacial area between the mainstream and dead zone to the mainstream volume; and
Γ_d	ratio of the interfacial area to the dead zone volume;
ξ	dummy variable;
Δt	routing time interval, $[T]$; and
Δx	reach length, $[L]$

The other notations have been described in the section as they first appear.

INTRODUCTION

1.1 GENERAL

In recent years, with the increasing industrialisation and urbanisation, generation of waste has increased manifold. Rivers have been traditionally used as sinks for waste disposal with or without treatment. This has resulted in the deterioration of water quality in many rivers in recent times because of the limited capacity of these rivers to assimilate the pollutants without endangering the associated ecosystem. Moreover, the inadvertent usage of fertilizers, pesticides and herbicides in agriculture and their consequent deterioration in quality of return flows is becoming an added problem while dealing with the water quality management of rivers. Therefore, to keep the waste disposal within the self-purification capacity of a river, it is necessary to know the transport characteristics of the pollutants disposed off into a river. Hence, acquisition of knowledge of the pollutant transport in rivers has been at the forefront of research for determination of pollutant concentration along the river courses and for regulating disposal of pollutants in rivers. During the solute transport in a river, the flow of water may be (i) steady and uniform, or (ii) steady and non-uniform or (iii) unsteady. Wastes in water are generally characterised by various forms of pollutants. Solute is defined as any dissolved substance or entity (pollutant such as pesticides, hydrocarbons, trace elements etc.) in a fluid solvent (herein water). The solute transport along a river course may be classified into three–dimensional, two-dimensional and one-dimensional processes based on the mixing mechanism. The solute transport process is (i) three–dimensional in the near–field where the advection and dispersion occur in vertical, transverse and longitudinal directions, (ii) two-dimensional in the mid-

field where the advection and dispersion are predominant in transverse and longitudinal directions, and (iii) one-dimensional in the far-field where the advection and dispersion are primarily important in longitudinal direction only. Near-field and mid-field together are commonly referred to as advective zone or initial mixing zone or convective zone and the far-field is commonly referred to as dispersive zone or equilibrium zone. Present study deals with the study of one-dimensional (longitudinal) transport of conservative solutes in rivers.

Over the past two decades, a number of approaches have been developed to study the one-dimensional transport of pollutant in solute form in rivers (Taylor, 1954; Elder, 1959; Fischer, 1968; Banks, 1974; Beltaos, 1982; Jirka, 1982; Bencala and Walters, 1983; and Beer and Young, 1983). Further, most of the studies on solute transport to date pertain to the periods of low flow in which flow in rivers may be assumed steady (Runkel et al., 1998).

This chapter presents (i) a brief description of solute transport studies in rivers under steady flow conditions, (ii) the relevance of solute transport in rivers under unsteady flow conditions, (iii) a brief description of solute transport studies under unsteady flow conditions, and the scope of the present study, (iv) the objectives of the present study, and (v) the details of the organization of the thesis.

1.2 BACKGROUND

Brief background pertinent to the solute transport study is presented in the following sections.

1.2.1 Studies on Solute Transport Under Steady Flow Conditions

Several researchers have studied solute transport in open channels under steady flow conditions using Advection-Dispersion (AD) model and its modifications (Elder, 1959; Fischer, 1968; Liu and Cheng, 1980; Beltaos, 1982,

2

Koussis, 1983, and Komatsu et al., 1997). Experimental studies by Godfrey and Frederick (1970), Nordin and Sabol (1974), and Day (1975) show that the AD equation fails to simulate the observed concentration time profiles (C-t curves), particularly with long tails, of rivers with dead zones or transient storage zones. In an attempt to explain the observed long tails in C-t curves, some researchers have postulated Dead Zone (DZ) model (Thackston and Krenkel, 1967; and Valentine and Wood, 1977), Transient Storage (TS) or One-dimensional Transport with Inflow and Storage (OTIS) model (Bencala and Walters, 1983; and Runkel, 1998), and Aggregated Dead Zone (ADZ) model (Beer and Young, 1983). Among these alternative approaches, Transient Storage model is the one which suitably incorporates the dead zone concept, considered as responsible for the development of elongated tails in observed C-t curves (Bencala and Walters, 1983). The analytical solution of the governing equations of the TS model is not possible (Nordin and Troutman, 1980; and Czernuszenko and Rowinski, 1997). Complex numerical solution schemes are necessary to solve the governing equations of the TS model simultaneously. Therefore, it may be desirable in practice to have a simplified model, which serves the same purpose as the TS model. In an attempt to simplify the DZ model formulation, the ADZ model, which is a conceptual approximation to the DZ model, was developed (Beer and Young, 1983).

The flow in rivers is usually non-uniform due to variations in channel cross-sections, bed slope and channel roughness, which play an important role in the flow transport and solute transport phenomena (Wallis, 1994). Recognising the importance of streamflow variability on solute transport, Li and Zhou (1997), Zoppou and Knight (1997), Guymer (1998), and Ranga Raju et al. (1997) studied the longitudinal dispersion under steady and non-uniform flow conditions. Thus, majority of the models developed so far is suitable for longitudinal dispersion of solute under steady flow conditions only.

1.2.2 Need to Study Solute Transport in Rivers Under Unsteady Flow Conditions

Often the major mechanisms of water quality and ecological change in rivers are closely linked to seasonal flow conditions in river (steady or unsteady flow) and in-stream mixing mechanisms (Orlob, 1983). Several situations arise in practice in which solute transport under unsteady flow conditions is important, such as

(i)   Water quality disruptions in rivers during storms resulting from a combination of point discharges of accumulated urban waste and persistent lateral inflow from non-point sources. The input rates are often quite high and of relatively short duration. Further, the interaction of basin topography and storm pattern may result in several flood waves during a storm. In order to determine the permissible waste loads, it is necessary to predict the water quality disruptions caused by storms (Bedford et al., 1983).

(ii)   Streams affected by mine drainage and acid rain as well as large geo-chemical changes occurring in response to rainfall and snowmelt events (Runkel et al., 1998).

(iii) Operation of water and wastewater treatment facilities wherein the operation cost can be significantly reduced by planning the waste disposal in accordance with the flow variation in a river. This is particularly important during monsoon season and could be effectively utilised in situations where it may be quite expensive to treat the wastewater from different sources.

1.2.3 Studies on Solute Transport Under Unsteady Flow Conditions

Modelling unsteady flow transport and associated river water quality is essential in water resources and environmental studies for pursuing an effective application of river water quality management and control (Orlob, 1983; and Thomann and Mueller, 1987). Many researchers (Whitehead et al., 1979,1981; Runkel, 1998; and Camacho, 2000) have foreseen the need, advantages, and

increased capabilities of developing a time-varying water quality perspective to address intrinsically dynamic water quality problems. Flow and solute transport models provide the time scales of system residence times that govern physical, biological and chemical interactions. Therefore, rigor in the descriptions of solute transport process under time varying flow condition should not be neglected or underestimated. However, if the time varying flow is considered along with transient storage mechanism in a river, then the governing equations become still more complex. Therefore, it would be desirable to develop simplified models considering the effects of transient storage in solute transport process.

Studies on longitudinal dispersion of pollutant under unsteady flow conditions in rivers are much less compared to the studies of pollutant dispersion during steady flow because of the complexities involved in modelling the phenomena. During unsteady flow, pollutant transport is dominated by advection process and solute concentrations are more of a consequence of advection, rather than dispersion (Bedford et al., 1983). The problem of less understood pollutant transport in time-varying flow regime was studied using coupled flow and transport models (Keefer and Jobson, 1978; Price, 1982; Runkel et al., 1998; Gabriele and Perkins, 1998; and Camacho, 2000). Graf (1995), and Krein and Symader (2000) studied the dispersion phenomena by performing field experiments during unsteady flow. Pollutant transport phenomena under unsteady flow conditions requires better description of the flow transport as well. Accuracy of the mass transport model depends on the accuracy of the flow routing model. In flow routing studies the use of simplified methods to model flow transport is sufficient for many field conditions (NERC, 1975) besides the reason that these methods are simple to formulate, and more suitable for operational purposes. Further, problems associated with numerical solution techniques of the governing equations of the flow routing transport problems, such as numerical instability, oscillations and mass conservation are absent in simplified methods.

1.3 SCOPE OF THE PRESENT STUDY

A physically based flood routing method, popularly known as the Muskingum method, has been widely used to model flood wave movement in streams and rivers. Several investigators have studied the Muşkingum method and suggested its modifications (Cunge, 1969; Koussis, 1978; Ponce and Yevjevich, 1978; and Perumal, 1994a). Koussis et al., (1983) presented an approach to model unsteady solute transport process in streams under steady flow conditions, using a Muskingum type method derived on the basis of the concept of matching the numerical dispersion with the physical diffusion of flood wave. Solute transport modelling in unsteady streamflows necessitates the selection of an appropriate flow routing model for proper understanding of the solute transport process. Variable Parameter Muskingum method (Perumal, 1994a), derived directly from the Saint-Venant Equations (SVE), is one such method which has been selected to route the flow, in the present study. The solute transport process under unsteady streamflow conditions can be studied appropriately, if the model structure adopted is same for both flow and transport phenomena.

The model structures for solute routing and flow routing advocated by Koussis (1983) are the same. However, there are logical errors in the development of the solute routing method, which is derived using the concept of matched diffusivity approach employed in the Muskingum flow routing method. The logical errors arise due to the fact that while the concept of employing one-to-one relationship between stage and discharge is responsible for the development of flow routing equation (Koussis, 1983), the same concept cannot be employed for solute transport phenomenon, as there is no other variable available to relate with the concentration, as in the case of flow with the stage. Further, the AD equation governing the solute transport process has been developed using the analogy of the Fick's law, which states that the mass flux is proportional to the concentration

6

gradient, implying that the concentration gradient induces diffusion. Hence, adoption of a governing equation based on advection only (i.e. physical dispersion is absent) to describe the solute transport process in a manner similar to that of the governing equation describing the flow transport process as envisaged by Cunge (1969) and Koussis (1978), is not logically correct. Further, there are process description inadequacies and application problems commonly associated with most one-dimensional models that include the inability to simultaneously model solute transport and unsteady flow processes. In particular, previous attempts often do not clearly distinguish between different flow and solute transport residence times and propagation velocities. One of the reasons that the existing methods do not allow one to route both the flow and solute simultaneously, is that the flow and solute transport phenomena are solved using different numerical schemes, and, thereby, increasing the complexities.

1.4   OBJECTIVES OF THE STUDY

In the light of the scope for improvement of the existing methods of solute transport modelling under unsteady streamflow conditions, the major objective of the present study is to investigate the solute transport process in streams and rivers under unsteady flow conditions by developing physically based simplified methods. Only conservative solutes are considered in this study.

The following are the objectives of the present study:

1.   To develop a simplified Advection-Dispersion equation governing the solute transport process in rivers under steady flow conditions, having a form same as that of the Approximate Convection-Diffusion equation governing the unsteady flow in rivers, and also to develop a solution algorithm for this simplified equation.

2.   To extend the above simplified model for simulating solute transport process in rivers under unsteady flow conditions.

7

3. To derive a simplified transient Storage model having a form similar to that of the Advection-Dispersion model, which is amenable to solution using simplified algorithms, and

4. To develop a solution algorithm for this simplified transient storage model for simulating solute transport in rivers under steady as well as unsteady streamflow conditions.

1.5 ORGANISATION OF THE THESIS

The research work consists of development of simplified longitudinal dispersion solute transport models with and without considering transient storage mechanism in the transport process, under steady as well as unsteady flow conditions. The ability of these models to simulate solute transport process under unsteady flow conditions depends on the ability of the sub-components of these models in simulating 1) the solute transport process under steady flow conditions, and 2) the unsteady flow process in which the solute transport takes place. The suitability of these models to serve the respective intended purposes is tested using various data sets such as (i) hypothetical test data from analytical and numerical solutions, (ii) laboratory experimental data, and (iii) field data collected from experiments conducted in rivers and streams. In order to make it easy to comprehend the research work, models development and their extensions are discussed in separate chapters alongwith the applicability analysis. Figure 1.1 shows the modelling approach and its presentation in thesis.

The research work on solute transport in rivers under unsteady streamflow conditions is presented in seven chapters as follows:

Chapter 1: In this chapter a general introduction of the investigations carried out and background for the present research work is presented.

Chapter 2: Solute transport process is explained in brief. It is followed by literature review focussing on the conservative solute transport under steady and unsteady streamflow conditions. Study of the solute transport under unsteady flow

conditions, requires the use of the flow routing model. Therefore, literature on flow routing, which is specifically relevant to the present study has been reviewed. Based on the literature review, conclusions with regard to the need for this research study are arrived at.

Chapter 3: In this chapter, an approximate Advection-Dispersion equation, which governs conservative solute transport phenomenon under steady flow conditions has been developed from the AD equation. Using this approximate Advection-Dispersion equation, the solute routing equation having a form similar to that of the VPM routing equation has been developed. The AD based VPM (henceforth, abbreviated as AD-VPM) model has been studied for solute dispersion under steady flow conditions and tested using hypothetical, laboratory and field data.

Chapter 4: The AD-VPM model has been studied for solute transport under unsteady streamflow conditions and tested using numerical solution of coupled Saint-Venant Equations and AD (SVE-AD) model due to hypothetical input (SVE for flow routing and AD for solute transport), and also using the data of Colorado River.

Chapter 5: An Approximate Transient Storage (ATS) model, which is a simplified form of the TS model for solute transport modelling has been developed. The analytical solution of the ATS equation is presented. Based on the developed ATS equation, solute routing equation similar to VPM (henceforth, abbreviated as ATS-VPM) method has been developed.

Chapter 6: The applicability criterion of the ATS model is developed by simulating the complete solution of the TS model using the ATS-VPM model. The developed ATS-VPM model has been tested against the analytical solution of the ATS model and the field data under steady flow conditions, and against the numerical solution of SVE coupled with TS model for hypothetical input and the field data of Huey creek under unsteady flow conditions.

Chapter 7: The conclusions based on the study are presented. Recommendations for further research work are made.

```
                          ┌─────────────────────┐
                          │     AD Equation     │
                          └─────────────────────┘
                                     │
                                     ▽
                    ┌──────────────────────────────────┐
                    │     Approximate AD Equation      │
                    └──────────────────────────────────┘
                                     │
                                     ▽
┌──────────────────────┐  ┌──────────────────────────────────────────┐
│ Solute transport under│  │ Development of AD-VPM model for solute    │
│ steady flow conditions│─▷│ routing using the concept of Variable     │
│      Chapter 3        │  │ Parameter Muskingum (VPM) model for flow  │
│                       │  │ routing                                   │
└──────────────────────┘  └──────────────────────────────────────────┘
                                     │
                                     ▽
┌──────────────────────┐  ┌──────────────────────────────────────────┐
│ Solute transport under│  │ Integrating parameters of AD-VPM model for│
│unsteady flow conditions│─▷│ solute routing with parameters of VPM model│
│      Chapter 4        │  │ for flow routing                          │
└──────────────────────┘  └──────────────────────────────────────────┘
                                     │
                                     ▽
┌──────────────────────┐  ┌──────────────────────────────────────────┐
│ Solute transport with │  │ ⊙ Development of Approximate Transient     │
│transient storage in channel│ │   Storage (ATS) model to account for transient│
│   under steady flow   │─▷│   storage mechanism in channel in solute  │
│     conditions        │  │   dispersion                              │
│      Chapter 5        │  │ ⊙ Development of ATS-VPM model using the   │
│                       │  │   concept of VPM model under steady flow  │
│                       │  │   conditions                              │
└──────────────────────┘  └──────────────────────────────────────────┘

┌──────────────────────┐  ┌──────────────────────────────────────────┐
│ Solute transport with │  │ Integration of parameters of ATS-VPM model for│
│ transient storage in  │─▷│ solute routing with parameters of VPM model for│
│ channel under unsteady│  │ flow routing                              │
│   flow conditions     │  │                                           │
│      Chapter 5        │  │                                           │
└──────────────────────┘  └──────────────────────────────────────────┘
```

Figure 1.1 Modelling Approach

10

LITERATURE REVIEW

2.1   GENERAL

In several branches of aquatic science, the need arises to predict the concentration of solutes being transported in rivers. Solute transport in rivers becomes one-dimensional when vertical and transverse concentration gradients are relatively insignificant. One-dimensional solute transport (often referred as longitudinal dispersion) involves two kinds of mechanisms, viz. advection and dispersion. Over the past two decades, different one-dimensional approaches have been developed that can represent the effects of solute transport phenomena in rivers in distributed and lumped manner. But, still there is no unified and widely adopted modelling approach to study the solute transport process. In this chapter, the state-of-the-art of modelling of one-dimensional solute transport under steady and unsteady flow conditions in streams is reviewed. As longitudinal dispersion of solute under unsteady streamflow conditions is the main topic of research in the present study, this subject matter is discussed in more details. The review has been classified into three main categories as follows:

i)   Solute transport under steady streamflow condition,

ii)   Studies on dispersion coefficient, and

iii)   Solute transport under unsteady streamflow condition

2.1.1   Solute Transport Process

In a stream, when pollutant or solute is disposed, it is carried away from point of disposal by the current through a process termed advection, and it spreads out because of the process of dispersion. Advection is the bodily movement of a parcel of fluid resulting from an imposed current. Advection transports any solute

that may be dissolved or suspended. The spreading of solute or tracer resulting from the mixing of dissolved substances due to Brownian motion is termed as molecular diffusion. Turbulence or eddy diffusion refers to mixing of dissolved and fine particulate substances caused by microscale turbulence. The interaction of turbulent diffusion with velocity gradients caused by shear forces in water body causes a greater degree of mixing, known as dispersion. In flow region close to the point of solute disposal, termed as near-field, advection and dispersion are important in all three co-ordinate directions. In mid-field, once the solute has mixed uniformly over the complete channel depth, vertical concentration gradients are not important. In this mid-field zone the dispersion becomes two-dimensional, i.e., varying in longitudinal and transverse directions. In far-field, solute mixes uniformly over the entire channel cross-section. Beyond that point, vertical and transverse concentration gradients become relatively negligible, and so the solute transport process has been termed as one-dimensional or longitudinal dispersion. The laws of conservation of water mass, momentum, energy and mass of water quality constituents form the basis of most flow and water quality models. Reynolds analogy states that transport of mass, momentum, and heat is analogous (Taylor, 1954). Taylor (1953,1954) studied the diffusion process in pipes based on Fick's law of diffusion and Reynolds analogy. Taylor's analysis led to the suggestion that in stationary and homogeneous turbulence, turbulent diffusion could also be modelled using Fick's law analogy provided sufficient time has elapsed since solute injection. Since turbulence in irregular natural channels is seldom homogeneous or stationary, the theoretical models are only an approximation of reality. Based on Fick's gradient law analogy, the solute transport in near-field is governed by three-dimensional advection-diffusion equation. In the mid-field, solute transport process is governed by two- dimensional advection-dispersion equation, obtained by averaging three-dimensional advection-diffusion equation over the depth. In the far-

12

field, attention can be focused on the rate at which the cross-sectional averaged concentration is advected downstream and dispersed longitudinally making it predominantly a one-dimensional process (Rutherford, 1994). The time period required for attaining uniform concentration distribution over the entire cross-section is known as 'initial mixing time' or 'convective time', and the distance traveled is known as 'initial mixing zone or advective zone'. The period beyond convective zone is known as dispersive period, and the zone is called as dispersive zone or equilibrium zone.

One-dimensional solute transport (often termed as longitudinal dispersion) has been modelled by averaging the three-dimensional advection-diffusion equation over the entire channel cross-sectional area to yield the one-dimensional Advection-Dispersion equation in open channel (Orlob, 1983; and Rutherford, 1994),

$$\frac{\partial C}{\partial t} + U\frac{\partial C}{\partial x} = \frac{1}{A}\frac{\partial}{\partial x}\left(AD_L\frac{\partial C}{\partial x}\right) \tag{2.1}$$

where, C is the ensemble cross-sectional averaged concentration, $[ML^{-3}]$; U is the ensemble mean cross-sectional velocity, $[LT^{-1}]$; A is the cross-sectional area, $[L^2]$; and D_L is the longitudinal dispersion coefficient, (hence forth referred as dispersion coefficient) $[L^2T^{-1}]$, x and t are the longitudinal distance and temporal coordinates, respectively. Using Eqn. (2.1) the advection-dispersion equation for one-dimensional solute transport in rivers under steady flow condition, i.e., when A, U, and D_L are all constant with respect to time and distance, is expressed as

$$\frac{\partial C}{\partial t} + U\frac{\partial C}{\partial x} = D_L\frac{\partial^2 C}{\partial x^2} \tag{2.2}$$

Equation (2.2) is generally referred as Advection-Dispersion (AD) equation. AD equation represents two kinds of transport mechanism, viz., advection represented by

$$\frac{\partial C}{\partial t} + U\frac{\partial C}{\partial x} = 0 \tag{2.3}$$

and dispersion represented by

$$\frac{\partial C}{\partial t} = D_L \frac{\partial^2 C}{\partial x^2} \tag{2.4}$$

Longitudinal dispersion arises because vertical and transverse shear carries the solute downstream more slowly near bed and banks than in mid-channel. Transverse shear velocity in a river channel makes a greater contribution to longitudinal dispersion of solute compared to vertical shear (Fischer et al., 1979).

Following the study by Elder (1959), one-dimensional solute transport in rivers has been mainly studied using AD model. But other models such as Cells-in-Series (CIS) model, Dead Zone (DZ) model, Transient Storage (TS) model, and Aggregate Dead Zone (ADZ) model have also been used.

2.2   SOLUTE TRANSPORT UNDER STEADY FLOW CONDITIONS

2.2.1   Advection-Dispersion Approach

In 1921 Taylor published a classic paper in which he made a theoretical analysis of the spreading of a cloud of tracer particles released into stationary, homogeneous turbulence. This analysis remains even today the key to quantify turbulent diffusion. Taylor's analysis demonstrates that in stationary homogeneous turbulence, the variance of the tracer cloud increases linearly with time at asymptotically large times (Fischer et al., 1979). The assumptions of the Fickian model (Eqn. 2.2) are (Chatwin, 1980; and Chatwin and Allen, 1985):

i)   The solute cloud has been evolving for a sufficiently long time,

ii)   The turbulence is statistically stationary and homogeneous,

iii)   The flow cross-section is independent of x and t, and

iv)   The solute is passive or it has no effect on the flow.

14

Taylor's concept was extended by Elder (1959) to describe the dispersion of the pollutant or solute in the turbulent flow in open channels. Eqn. (2.2) has been used to simulate the variation of concentration with time (C-t curve) by solving it analytically and numerically.

2.2.1.1 Analytical solution

Analytical solution of the AD equation (Eqn. 2.2), for steady and uniform flow conditions in a river, and for uniform step input boundary condition ($C(x,0)=0$, and $C(0,t)=C_I$), popularly known as Ogata and Banks (1961) solution is expressed as

$$C(x,t) = \frac{C_I}{2}\left[erfc\left(\frac{x-Ut}{2\sqrt{D_L t}}\right) + \exp\left(\frac{Ux}{D_L}\right)erfc\left(\frac{x+Ut}{2\sqrt{D_L t}}\right)\right] \qquad (2.5)$$

where $erfc(z)$ is complimentary error function given by

$$erfc(z) = 1 - \frac{2}{\sqrt{\pi}}\int_0^z \exp(-\xi^2)d\xi \qquad (2.6)$$

Analytical solution of the AD equation for an impulse injection of conservative solute mass M has been given as (Sayre, 1968)

$$C(x,t) = \frac{M}{A\sqrt{4\pi D_L t}}\exp\left[\frac{-(x-Ut)^2}{4D_L t}\right] \qquad (2.7)$$

Analytical solution of the AD equation for uniform pulse input of duration, τ, is given by Eqn. (2.5) for $t \leq \tau$ and for $t > \tau$, it is expressed as (Runkel, 1996)

$$C(x,t) = \frac{C_I}{2}\left\{\begin{bmatrix}erfc\left(\frac{x-Ut}{2\sqrt{D_L t}}\right) - erfc\left(\frac{x-U(t-\tau)}{2\sqrt{D_L(t-\tau)}}\right)\end{bmatrix} + \\ \exp\left[\frac{Ux}{D_L}\right]\begin{bmatrix}erfc\left(\frac{x+Ut}{2\sqrt{D_L t}}\right) - erfc\left(\frac{x+U(t-\tau)}{2\sqrt{D_L(t-\tau)}}\right)\end{bmatrix}\right\} \qquad (2.8)$$

Dispersion in open channel has been well studied by Fischer (1967,1968) presenting the dispersion mechanism, the pollutant concentration response

distribution (C-t curve), and the solution procedure to compute the dispersion coefficient. Fischer (1967) first recognized the importance of transverse velocity profiles. It was shown that longitudinal dispersion caused by the interaction of transverse velocity gradients and concentration completely dominates those caused by vertical velocity gradients. It has been shown (Fischer, 1968) that the one-dimensional analysis is applicable only in the dispersive zone. Fischer (1968) obtained analytical solution of the AD equation (Eqn. 2.2). The observed C-t curve at a section located at a longitudinal distance x_1 from the solute injection section is used as the initial tracer distribution. The C-t curve at a downstream section located at a distance x_2 ($x_2 > x_1$) from the solute injection section is predicted using the solution given by Fischer (1968) and is expressed as

$$C(x_2,t) = \int_{-\infty}^{+\infty} C(x_1,t) \exp\left[\frac{-\{U(\bar{t}_2 - \bar{t}_1 - t + \tau)\}^2}{4D_L(\bar{t}_2 - \bar{t}_1)}\right] \frac{U}{\sqrt{4\pi D_L(\bar{t}_2 - \bar{t}_1)}} d\tau \qquad (2.9)$$

where, $C(x_2,t)$ is concentration of solute at a distance x_2 and at time t, $C(x_1,t)$ is concentration of solute at a distance x_1 and at time t, U is the cross-sectional mean flow velocity, $\bar{t}_1$ and $\bar{t}_2$ are mean times of passage of tracer cloud at measuring stations located at longitudinal distance at x_1 and x_2 from the section of solute injection, respectively.

Analytical solution of the AD equation can be obtained only by making simplified assumptions. A generalised closed-form solution to this equation is not available. Due to mathematical complexities and availability of analytical solutions for specific solute input conditions only, as discussed above, numerical methods have been proposed by various researchers to solve the AD equation for practical cases employing various discretisation schemes.

2.2.1.2 Numerical solution

The AD equation, given by Eqn. (2.2), is a linear parabolic partial differential equation. Therefore, generally, the AD equation has been solved using

finite difference numerical methods. However, numerical solution of this equation is cumbersome and not accurate because of the generated numerical dispersion, which may be several times greater than the physical dispersion, and thus the solution may differ from the actual one. Numerical solutions have been given by several investigators, based on combined operator approach (Bella and Dobbins, 1968; Stone and Brian, 1963; Keefer and Jobson, 1978; Jaque and Ball, 1994; and Ranga Raju et.al., 1997), and split operator approach (Holly and Preissmann, 1977; Koussis, 1983; Li, 1990; Schohl and Holly,1991; and Komatsu et al., 1997). In split operator approach, numerical solution of the AD equation is obtained through independent solution of advection (Eqn. 2.3) and dispersion (Eqn.2.4) equations. In combined operator approach, advection and dispersion processes of the AD equation (Eqn. 2.2) are solved together using a numerical method. Most of the numerical methods which solve the advective part of Eqn. (2.2) are generating artificial numerical dispersion in addition to the physical dispersion, and also causing oscillatory results (Jobson, 1980; and Islam and Chaudhry, 1997). Method proposed by Koussis et al. (1983) is devoid of artificial dispersion problem and it is able to simulate the advection dominated solute transport phenomena closely. As the solution approach adopted in the present study employs a routing equation of the Muskingum type, similar to the one used by Koussis et al. (1983), it is pertinent to dwell on the method proposed by Koussis et al. (1983) to solve AD equation.

Koussis et al. (1983) proposed a procedure to solve the AD equation known as the Matched Advection Diffusion (MAD) scheme. It is based on the concept of matching the numerical dispersion (obtained by solving Eqn. (2.2), assuming dispersion coefficient equal to zero) with the physical dispersion given by the quotient of $\partial^2 C/\partial x^2$. Koussis et al. (1983) obtained the following solute routing equation in a form similar to that of the well known Muskingum flood routing

equation given in the hydrology literature (Chow et al., 1988).

$$C_{i+1}^{j+1} = \omega_{K1}.C_i^j + \omega_{K2}.C_i^{j+1} + \omega_{K3}.C_{i+1}^j \tag{2.10}$$

in which i and j are the space and time discretisation indices respectively. Expressions for $\omega_{K1}, \omega_{K2},$ and ω_{K3} were given, based on the exponential scheme in which the input variation was assumed linear over the routing time interval Δt, as

$$\omega_{K1} = \frac{1-\beta_c}{N_c} - \beta_c \tag{2.11a}$$

$$\omega_{K2} = 1 - \frac{1-\beta_c}{N_c} \tag{2.11b}$$

$$\omega_{K3} = \beta_c = \exp\left(-\frac{N_c}{1-\theta_c}\right) \tag{2.11c}$$

where, N_c is the Courant number, $(= \Delta t/K_C)$ and θ_c is the weighting parameter. The travel time K_C and θ_c are expressed as

$$K_C = \frac{\Delta x}{U} \tag{2.12}$$

and

$$\theta_c = 1 - N_c \left\{ \ln\left[\frac{2D_L + (1+N_c)U\,\Delta x}{2D_L + (1-N_c)U\,\Delta x}\right] \right\}^{-1} \tag{2.13}$$

Though the solution equation given by Eqn. (2.10) is able to closely reproduce the specific analytical solution and some field observations (C-t curves) as demonstrated by Koussis et al. (1983), there are logical errors involved in the development of Eqn. (2.10). In mass transport process, the dispersive flux is proportional to the concentration gradient. The AD equation governing the solute transport process has been developed using the analogy of the Fick's law, which states that the presence of concentration gradient induces dispersion. Hence, the presence of concentration gradient $\partial C/\partial x$ implies the presence of dispersion. Considering the presence of concentration gradient $\partial C/\partial x$ and absence of

18

dispersion is not consistent with the logic of Fick's law. Further, the Matched Advection Diffusion (MAD) scheme proposed by Koussis et al. (1983) follows a concept similar to that employed in the Muskingum-Cunge method (Cunge, 1969) for flood routing, in which it is assumed that there is a one-to-one relationship between stage and discharge during the passage of floods. But the same concept is not applicable for solute transport in rivers, as there is no second variable, like stage, to relate with the solute concentration, C. Hence, there are logical in consistencies in the development of the solute routing method by Koussis (1983) while adopting the concept employed in the flow routing advocated by Cunge (1969). Koussis et al. (1983) claimed that his exponential numerical scheme of Eqn. (2.2) is better than the fractional numerical scheme advocated by Cunge (1969). Koussis et al. (1983) approach does not allow the usage of unequal temporal step sizes, as the weighting parameter is a function of spatial and temporal step sizes (Eqn. 2.13).

Koussis et al. (1983) suggested that his routing procedure could be used to (i) approximately describe the AD processes in rivers with spatially variable characteristics by adjusting scheme parameters through spatial averaging to reflect changes in U, A, and D_L over individual segments, and (ii) to accommodate variations of U with respect to time. But Koussis et al. (1983) did not consider these two extensions any further.

The theoretical assumptions underlying the derivation of the AD equation ensures that, at asymptotically long times, the concentration distribution is Gaussian. The analytical or numerical solutions of the AD equation also result in Gaussian distribution. However, many observed data at long distances from the sources do not indicate a Gaussian shape as predicted by the AD model. The deficiencies of the AD model stimulated the investigators to develop alternative approaches including modification of the AD equation.

2.2.2 Cells-In-Series Model

As an alternative to the AD model, Cells-in-Series (CIS) model has been developed to study the longitudinal dispersion (Banks, 1974; Stefan and Demetracopoulos, 1981; and Beltaos, 1982). The Cells-in-Series model conceptualises the river reach under consideration to be consisting of cells arranged in series having the same filling time T_r. The governing equation of the CIS model is a first-order ordinary differential mass transport equation expressed as (Banks, 1974; and Stefan and Demetracopoulos, 1981)

$$V\frac{d\overline{C_o}}{dt} = QC_I - Q\overline{C_o} \qquad (2.14)$$

where V is the volume of each cell, $[L^3]$; Q is the rate of flow, $[LT^{-3}]$; C_I is inflow concentration, $\overline{C_o}$ is average concentration in the cell. The basic assumption in CIS model is that the solute in a cell is thoroughly mixed over the entire volume of the cell. In other words, the outflow solute concentration of a cell is equal to the mean solute concentration within the cell.

It was identified that the CIS model has a fixed relationship between number of cells, travel time of solute and dispersive properties (Beltaos, 1982; and Rutherford, 1994). The CIS model describes the dispersion properties, but does not reproduce the persistence skewness, which is usually observed in the C-t curves in rivers. Unknown number of cells are required to represent observed advection and dispersion characteristics in a single river reach. Stefan and Demetracopoulos (1981) studied the comparison of the CIS model and AD model. Stefan and Demetracopoulos (1981) also stated that further study on the relationships between number of cells and river hydro-geometric characteristics is needed.

It is pertinent to point out herein that there exists a similarity between the form of the governing equation of the well known Muskingum flood routing method

20

and that of the characteristic reach of the CIS model. If the weighting factor is equal to zero, the Muskingum method for flow routing gives an equation that is similar to the governing equation of the CIS model (Eqn. 2.14). Therefore, it can be inferred that the CIS model resembles as a special case of the Muskingum method, if rate of inflow and outflow are replaced by the input and output concentrations and the weighting factor is equal to zero.

Godfrey and Frederick (1970), Nordin and Sabol (1974), and Day (1975) have investigated solute transport in rivers from an extensive series of experiments in rivers. Based on the experimental results, it is concluded that the observed C-t curves in most of the rivers are almost invariably skewed with steeper rising limbs and elongated tails. Moreover, in many solute transport experiments, it is observed that the variance of the C-t curves grows more rapidly, and the peak concentration attenuates more rapidly than predicted by the one-dimensional AD model (Nordin and Sabol, 1974; and Day, 1975). It is widely recognized that the AD model and the CIS model fail to simulate the long tails that are, in general, common features of the C-t curves observed in rivers. Hence, modified Fickian models have been developed to simulate the observed C-t curves.

2.2.3 Modified Fickian Approach

The failure of the AD and CIS models to simulate the observed concentration time distributions (C-t curves) in natural channels stimulated researchers to modify the AD model. Much of the past research work has been concerned with the development of appropriate modification in the AD equation to account for the observed non-Gaussian behaviour of dispersants and solutes by introducing one or more parameters in addition to the existing ones (Beltaos, 1980; and Liu and Cheng, 1980). Chatwin (1980) incorporated higher-order moments into the AD equation in order to quantify the skewness and kurtosis. But these models

21

fail to simulate the long tails satisfactorily even with the additional parameters (Liu and Cheng, 1980). A common method for simulating these long tails has been to allow for 'storage zones' or 'dead zones' along the stream channel which has been widely used in present day research.

2.2.4 Dead Zone Model

In an attempt to explain the skewness in observed C-t curves in rivers, some researchers postulated Dead Zone Models (Thackston and Krenkel, 1967; Thackston and Schnelle, 1970; and Valentine and Wood, 1977). In these formulations, the mechanism responsible for skewness has been incorporated in a dead zone equation in addition to the modified AD equation. The dead zone models are by nature the modified Fickian models. The governing equations of the Dead Zone models are (Nordin and Troutman, 1980; and Beer and Young, 1983)

$$\frac{\partial C_a}{\partial t} + U \frac{\partial C_a}{\partial x} = D_{La} \frac{\partial^2 C_a}{\partial x^2} + \alpha_d \Gamma_a (C_d - C_a) \tag{2.15a}$$

$$\frac{\partial C_d}{\partial t} = \alpha_d \Gamma_d (C_a - C_d) \tag{2.15b}$$

in which C_a is the concentration in the main stream, C_d is the concentration in the dead zone, D_{La} is the longitudinal dispersion coefficient, α_d is the mass exchange coefficient between the main flow and the dead zone, Γ_a is the ratio of the interfacial area between the main stream and dead zone to the main stream volume, and Γ_d is the ratio of the interfacial area to the dead zone volume. The existence of dead zones, the channel irregularities and channel non-uniformity is responsible for prolongation of the travel time of the solute cloud, if there is an exchange of the solute between the main channel flow and the dead zones (Valentine and Wood, 1977; and Liu and Cheng, 1980). In a river reach with dead zone mechanism, the solute transport velocity and the mean flow velocity are different, and the relationship between these is given as (Valentine and Wood, 1977)

22

$$U_s = \frac{U}{1+\beta} \qquad (2.16)$$

where $\beta = Ay_d/y_n$ (2.17)

y_d is the dead zone depth in the channel, and y_n is the normal depth of flow in the main channel.

2.2.5 Aggregated Dead Zone Model

Beer and Young (1983) conceptualised Aggregated Dead Zone (ADZ) modelling approach to represent the advective and dispersive behaviour of a solute in streams with transient storage mechanism. The underlying concept in the development of the ADZ model is that the dead zones are primarily responsible for observed dispersion and, thus, the dispersion coefficient of the AD equation characterising the longitudinal dispersion in the main channel no longer needs to appear in the model. In the ADZ model, fundamental importance lies with the residence time of the solute. The ADZ model incorporates an advective time delay parameter that is mainly responsible for solute advection.

In the ADZ model, each reach of the river has been treated as being composed of an advective cell in which the solute undergoes pure plug flow with a concentration C_I and then enters the mixing tank representing the aggregated dead zones emerging with a concentration C_O. (Fig.2.1). Governing equation of the ADZ model is an ordinary differential delay equation expressed as (Beer and Young, 1983; and Rutherford, 1994):

$$V\frac{dC_O}{dt} = Q[C_I(t-\tau_d)-C_O] \qquad (2.18)$$

where, τ_d is the cell time delay. T_r is the ADZ residence time parameter, which is equal to V/Q. The travel time ($\bar{t}$) defines the total time a solute spends in the

reach being advected and dispersed, given by $\bar{t} = T_r + \tau_d$. Eqn. (2.18) can be written in discrete form as (Beer and Young, 1983)

$$C_O(k) = -a_1 C_O(k-1) + b_o. C_I(k-\tau_d) \qquad (2.19)$$

where $C_O(k)$ and $C_O(k-1)$ are the output concentrations of the reach at times $k\Delta t$ and $(k-1) \Delta t$. C_I is the input concentration at the input section of the aggregate dead zone. τ_d is the time delay in an integral number of sampling instants $a_1 = -\exp(-\Delta t/T_r)$ and $b_o = 1+a_1$.
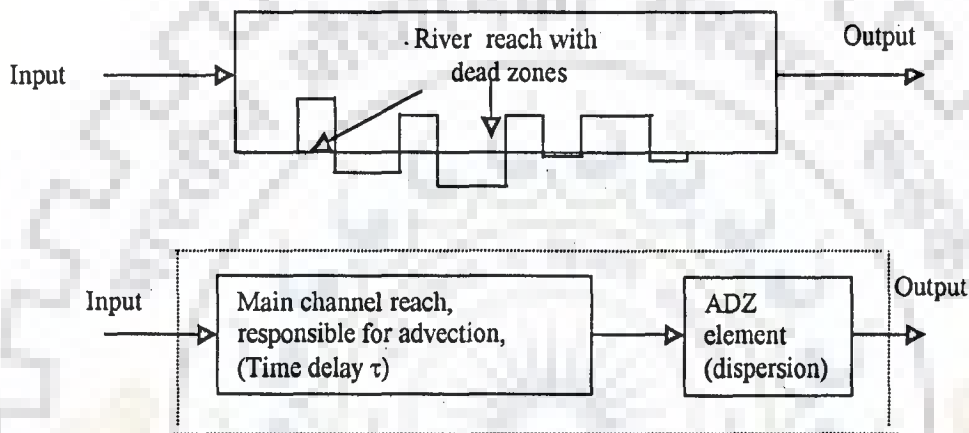
Figure 2.1 Conceptualisation of the river reach (top) by the ADZ model (bottom)

An important assumption made in the ADZ model is that the output concentration $C_o(t)$ is linearly related to the mean concentration of the solute in the reach, $\bar{C}(t)$ (Lees et al., 2000).

$$\bar{C}(t) = DF. C(t) \qquad (2.20)$$

where DF is the dispersive fraction that defines the mixing characteristics of the solute in the reach. It is important to note that in a continuously stirred tank reactor (CSTR) or completely mixed cell, the concentration in the reactor is identical to the output concentration, i.e., DF = 1. Interestingly if DF=1 and lag, τ_d =0, the ADZ formulations will reduce to the CIS model implying that the CIS model is a special

case of the ADZ model. The ADZ river reach is considered as an imperfectly mixed system in which the volume that can be considered as fully mixed volume is only a fraction of the total reach volume V_a. Serial or parallel connections of the first order ADZ models may be required to describe the observed higher order transport mechanisms (Young and Wallis, 1993). A generalised multi-order ADZ model, consists of several first-order ADZ elements with different time constants ($1/T_r$) and time delay (τ) are combined in series and/or parallel, in discrete form is given by (Beer and Young, 1983)

$$C_O(k) = \frac{B(z^{-1})}{A(z^{-1})} \cdot C_I(k - \tau) \qquad (2.21)$$

where $A(z^{-1})$ and $B(z^{-1})$ are polynomials in z^{-1} defined as

$$A(z^{-1}) = 1 + a_1 z^{-1} + \text{----} + a_n z^{-n} \qquad (2.22a)$$

$$B(z^{-1}) = b_0 + b_1 z^{-1} + \text{---} + b_m z^{-m} \qquad (2.22b)$$

z^{-1} is the backward shift operator, i.e., $z^{-1} C(k) = C(k-1)$. n and m are respectively the order of polynomials $A(z^{-1})$ and $B(z^{-1})$ which define the number of values of $C_o(k)$ and $C_I(k-\tau_d)$ needed to explain the observed C-t curves. $C_o(k)$ and $C_I(k-\tau_d)$ represent the concentrations at the appropriate upstream and downstream locations of the channel. Aggregated Dead Zone model can explain solute transport in rivers more satisfactorily compared to the AD equation with constant dispersion coefficient, and the CIS model. The assumption of incomplete mixing implicit in the residence time parameter T_r is contributing to the ADZ model's ability to describe skewed distributions

Rutherford (1994) interpreted the ADZ model as a variant of the CIS model. The main difference between the CIS and ADZ models is that in the ADZ model a pure time delay is introduced into the input concentration. The time delay introduced in the ADZ model allows advection and dispersion to be decoupled. The ADZ formulation is not derived from a detailed physical understanding of the

mechanisms which cause dispersion, but rather is an intuitive description of the combined effects of dead zones and advective transport (Rutherford, 1994). The practical difficulty of the ADZ model is in the identification and estimation of the number of model coefficients (Eqn. 2.22). It is not easy to interpret the physical significance of the model coefficients, viz. cell residence time, cell time delay and the number and arrangement of cells (Rutherford, 1994). Further work is needed before model coefficient can be predicted from hydro-geometric channel characteristics.

2.2.6 Transient Storage Model

Bencala and Walters (1983) presented the Transient Storage (TS) model based on the inference that " *there is in fact a mechanism that presents itself as a transient storage of solute mass along the length of the stream. Hence we do not believe that a strict dead zone model is a physical description of the processes occurring in mountain streams, but rather that the observed 'transient storage' can be empirically simulated using the identical equations*". Transient storage zones, on the riverbed and on the riverbanks, may trap some part of the solute temporarily and release it at a later stage (Fig. 2.2). Delayed release of these trapped portions of solute back into the main flow may result in the observed long tails and, thus, larger skewness of the concentration-time curves at fixed locations. The TS model is an extension of the dead zone model with the identical governing equations and different interpretation of the temporary trapping and release mechanism of solute in rivers. Bencala (1983) further stated that "*with the dead zone model, the hydrologic system is separated into two interacting compartments: first, the flowing stream channel and second, the storage zones which mix with the stream channel water, but have no longitudinal velocity. The storage zones will include both, water visible in the channel and water concealed from view in the coarse gravel and cobble bed*".
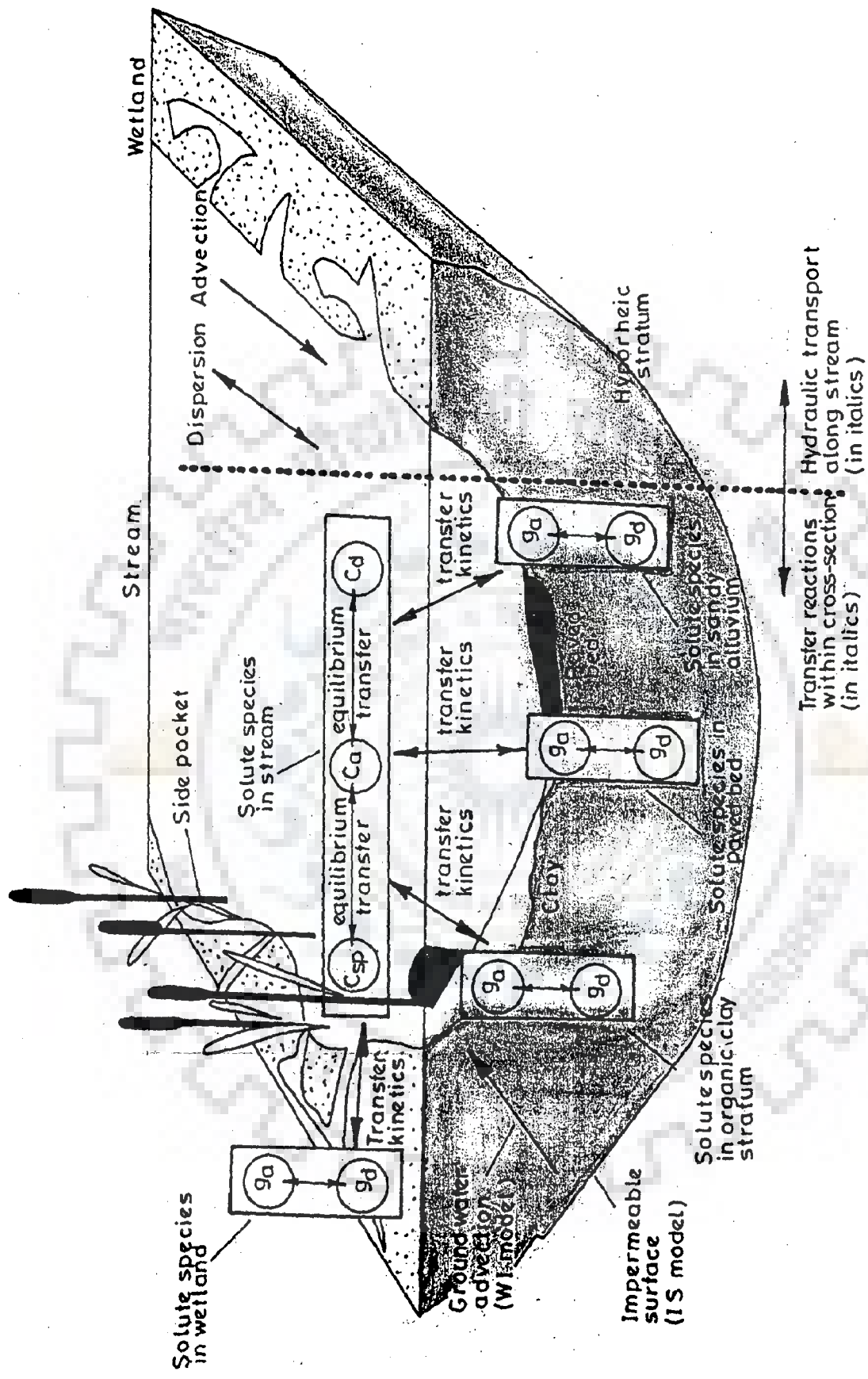
Figure 2.2 Solute transport in streams and river affected by transient storage mechanism (Source: Worman, (2000)).

Transient Storage approach includes the effects of the transient storage in longitudinal solute transport model using a first-order mass transfer equation in which all underlying mechanisms have been averaged in a non-dimensional form. The governing equations of the TS model, under steady and uniform flow conditions, are (Bencala and Walters, 1983; Runkel and Chapra, 1993; and Seo and Cheong, 2001).

$$\frac{\partial C}{\partial t} + U\frac{\partial C}{\partial x} = D_{ts}\frac{\partial^2 C}{\partial x^2} + \alpha(C_s - C) \qquad (2.23a)$$

$$\frac{\partial C_s}{\partial t} = \alpha\frac{A}{A_s}(C_s - C) \qquad (2.23b)$$

where C_s is the concentration in the storage zone [ML^{-3}], C is the concentration in the main or active channel [ML^{-3}], A_s is the storage zone cross-sectional area normal to the flow [L^2], α is the exchange coefficient [T^{-1}], D_{ts} is the longitudinal dispersion coefficient in the main channel [L^2T^{-1}], and x is longitudinal distance [L]. It is to be noted that the values of D_L and D_{ts} are not the same. The following are the assumptions involved in the development of the TS model (Bencala and Walter, 1983; and Runkel, 1998)

i)   There exist storage zones and these are assumed to be stagnant relative to the longitudinal flow of the stream.

ii)   Within the storage zone, solute is uniformly and instantaneously distributed.

iii) The transport of solute between the storage zone and the main channel obeys a first–order mass transfer type of exchange relationship. That is, the exchange of solute between the main stream channel and a storage zone is proportional to the difference in concentration between the stream and the storage zone.

Bencala and Walters (1983) solved Eqn. (2.23) using both the finite difference and the finite element numerical methods. Runkel and Chapra (1993) solved Eqn. (2.23) using Crank-Nicolson implicit numerical scheme by decoupling Eqns. (2.23a) and (2.23b). However, as stated by Manson et al. (2001), solution of the numerical scheme suggested by Runkel and Chapra (1993) give oscillatory results when it is used to solve the advection dominated solute transport.

Lees et al. (2000) obtained an expression, which is same as Eqn. (2.16), relating flow and solute transport velocities using a parameter β ($\beta = A_s / A$). The dead zone model and transient storage model differ only in the interpretation of the storage zone and the parameters describing the storage zone. Even though, TS model can simulate the observed C-t curves, it is not possible to get an analytical solution of the Eqn. (2.23) to compute the concentration $C(x,t)$ (Nordin and Troutman, 1980; and Czernuszenko and Rowinski, 1997). The model equations need to be solved numerically using efficient numerical schemes to obtain solutions. Moreover, considerable uncertainty remains in determining the physically realistic values of the parameters. It is not easy to obtain unique calibration values of D_{ts}, α, and β in a particular channel reach (Rutherford, 1994). In addition, it is not feasible to theoretically estimate α from hydro-geometric characteristics of a river. As more number of parameters are involved, this may pose problem related to parametric uncertainty. Therefore, its practical utility has been limited because of the complexities involved in the estimation of parameters (Rutherford, 1994). Hence, it is desirable to model solute transport in rivers affected by transient storage mechanism using simplified equations.

29

2.3 STUDIES ON DISPERSION COEFFICIENT

Dispersion coefficient, D_L of the AD equation is a parameter that represents the dispersive characteristics of a stream. It can be estimated using either theoretical methods or empirical expressions, some of which are discussed below.

2.3.1 Theoretical Method

Elder (1959) derived an equation to compute the longitudinal dispersion coefficient for an uniform flow in an infinitely wide open channel. Elder assumed Von Karman's logarithmic velocity profile, and similarity between the momentum transfer coefficient and mass transfer coefficient in the vertical direction as

$$D_L = \left[\frac{0.404}{\kappa^3} + \frac{\kappa}{6}\right] y U_*$$

(2.24)

where κ is the Von Karman's coefficient, and U_* is the shear velocity. However, further studies suggested that Eqn. (2.24) was not able to estimate the dispersion coefficient in natural streams (McQuivey and Keefer, 1974; Fischer et al., 1979; and Seo and Cheong, 1998). An alternative expression to compute the D_L has been given by (Fischer et al., 1979)

$$D_L = -\frac{1}{A}\int_0^B u'y \int_0^y \frac{1}{\varepsilon_t y}\int_0^B u'y \, dy dy dy$$

(2.25)

where u' is the deviation of velocity from the cross-sectional mean velocity, y is the depth of flow, and ε_t is the transverse mixing coefficient. It is difficult to estimate D_L using Eqn. (2.25) because of the data requirements and accuracy needed in the estimation of transverse mixing coefficient. Therefore, alternative methods as discussed below have been suggested to estimate the dispersion coefficient based on the observed C-t curves and hydro-geometric characteristics of a river.

2.3.2 Determination of Dispersion Coefficient Using Concentration Curves

Dispersion coefficient, D_L can be estimated from observed C-t curves using either the change of moment method (Fischer et al, 1979) or the routing procedure (Fischer, 1968) or the diffusive transport method (Fischer, 1968). The change of moment method is simple to use. However, it may not provide the physically meaningful dispersion coefficient, because the variance of the C-t curve that is used in the change of moment method gets significantly affected by the skewed concentration distributions. Mathematically, the routing method is a convolution of the input distribution with a linearised one-dimensional response function given by Eqn. (2.9). The routing procedure gives better estimates of D_L compared to the change of moment method, but its application is limited to the simplified form of Eqn. (2.1). When U, A and D_L are varying, this method also cannot be used. Diffusive transport method gives good results when: (i) the channel is uniform and its geometry must be accurately defined (ii) measurement of concentrations is made at sufficient number of points in the cross-section to adequately define the concentration variation, and (iii) measurement of C_I is accurate.

2.3.3 Empirical Relations for Dispersion Coefficient

Several investigators have proposed different empirical equations to estimate D_L in terms of the known hydro-geometric characteristics of a stream based on experimental studies. Empirical equations for the estimation of D_L, as recommended by various investigators, are presented in Table 2.1. It is important to note that even after four decades of research, till date, there is no generally acceptable expression to estimate D_L.

Among the various empirical expressions developed, McQuivey and Keefer (1974)'s expression (Sl. No. 9, Table 2.1) is simple for predicting longitudinal dispersion coefficient. The similarity between the mathematical formulations of

31

flow and solute transport was exploited for the development of the expression for

D_L. McQuivey and Keefer's expression for D_L predicts the measured or observed

values relatively well (Seo and Cheong, 1998) and is consistent with the observation

that the value of the dispersion coefficient increases with increase in discharge

(Rutherford, 1994). The standard error of estimation of D_L was referred as

approximately 30% (McQuivey and Keefer, 1974).

Table 2.1 The empirical equations for estimation of dispersion coefficient

Sl. No	Investigator	Equation	Remarks
1.	Taylor (1954)	$D_L = 10.1 U_* r$; where, r is the radius of the pipe	Pipe flow, dispersion mainly due to diffusive transport.
2.	Elder (1959)	$D_L = 6.3 U_* y$; where, y is the depth of flow	Wide channel; considering Von Karman's vertical log velocity profile.
3.	Yotsukura and Fiering (1964)	$D_L = 9.0$ to $13.0\ U_* y$	For hydraulically rough and smooth boundary.
4.	Fischer (1966)	$D_L = 0.011 \dfrac{U^2 B^2}{y U_*}$	Using data for smooth and rough laboratory flume and field data.
5.	Thackston and Krenkel (1967)	$D_L = 7.25 U_* y \left(\dfrac{U}{U_*} \right)^{\frac{1}{4}}$	Using both the laboratory and the field data.
6.	Sooky (1969)	$D_L = K_1' + K' + K''$ $K_1' = 0.2222 \dfrac{U_*}{\kappa^2} \dfrac{y_m}{a}$ $K^* = \dfrac{1}{9} a \kappa\, U_* y_m$; $K' = aK''$	Considering shape of the stream and velocity distribution. y_m is max depth in x-section. a is proportionality constant. κ is Von Karman constant.
7.	Sumer (1969)	$D_L = 6.23\ U_* y$	Considering velocity profile and vertical turbulent diffusion.
8.	Fukuoka and Sayre (1973)	$\dfrac{D_L}{R U_*} = 0.8 \left[\dfrac{r_c^2}{L_B y} \right]^{1.4}$ where, R is the Hydraulic radius	Considering the meandering effect, r_c is the radius of curvature of bend and L_B is the overall bend length measured along the centerline of the channel.

Table 2.1 (Contd...)

Sl. No	Investigator	Equation	Remarks
9.	McQuivey and Keefer (1974)	$D_L = 0.058 \dfrac{Q}{S_o B}$	Based on data from 18 rivers using analogy between flow and solute dispersion. S_o = bed slope and Q is discharge.
10.	Jain (1976)	$D_L = \dfrac{U^2 B^2}{kAU_*}$	Considering shape of the stream, $k = 0.1$ to 0.2 and increases with B/y.
11.	Beltaos (1978)	$\dfrac{D_L}{RU_*} = \alpha_1 \left(\dfrac{B}{R}\right)^2$	Used Sooky's finding. α_1 is the proportionality constant.
12.	Liu (1978)	$D_L = \dfrac{Q^2}{2U_* R^3}\left(\dfrac{U_*}{U}\right)^2$	Considering transverse diffusion coefficient, $\varepsilon_t = 0.23 \, yU_*$.
13.	Marivoet and Craenenbroeck (1986)	$D_L = 0.0021 \dfrac{U^2 B^2}{yU_*}$	Based on data from canals.
14.	Asai et al. (1991)	$\dfrac{D_L}{yU_*} = 2.0 \left(\dfrac{B}{R}\right)^{1.5}$	By analysing field and lab data.
15.	Ranga Raju et.al, (1997)	$\dfrac{D_L}{q_w S_o} = 0.4 P_t$ $P_t = \left(\dfrac{B}{R}\right)^{2.16}\left(\dfrac{U}{U_*}\right)^{-0.82}(S_o)^{-0.70}$	Using gradient search technique. q_w is the discharge per unit width of channel.
16.	Koussis and Mirasol (1998)	$D_L = \phi \dfrac{\sqrt{gRS_o}}{y} B^2$	Used Von Karman's law of velocity profiles. Mean $\phi = 0.6$.
17.	Seo and Cheong (1998)	$\dfrac{D_L}{yU_*} = 5.915 \left(\dfrac{B}{y}\right)^{0.620}\left(\dfrac{U}{U_*}\right)^{1.4}$	Used 56 river data sets.
18	Kezhong and Yu. (2000)	$\dfrac{D_L}{yU_*} = 3.5 \left(\dfrac{B}{y}\right)^{1.125}\left(\dfrac{U}{U_*}\right)^{0.25}$	Using genetic algorithm.

2.4 SOLUTE TRANSPORT UNDER UNSTEADY FLOW CONDITIONS

Majority of the studies to date relate to solute transport under steady flow conditions only. Attempts have also been made by few researchers to study the transport process under non-uniform streamflow conditions (Li and Zhou, 1997; Zoppou and Knight, 1997; and Guymer, 1998). Guymer (1998) studied the effects of varying cross-section under different discharges. Variations of longitudinal dispersion with discharge have been attributed to longitudinal changes of cross-sectional area. Even in situations (chapter 1, section 1.2) where the assumption of steady streamflow conditions does not hold good, steady streamflow condition has been assumed in majority of models. Such models are unable to accurately simulate the transport process under unsteady streamflow conditions.

Solute transport under unsteady streamflow conditions deals with both flow routing and solute transport processes. Therefore, study of solute transport phenomenon in streams under unsteady flow conditions require the knowledge of flow variation with time. The accuracy of mass transport model under unsteady flow condition would depend on the accuracy of the flow model. Hence, coupled flow and solute routing models need to be developed. A brief review of the studies available on the coupled flow and solute routing models is presented herein.

2.4.1 Flow Routing

Flow transport in a natural stream is a distributed process because geometric characteristics of the channel, i.e., cross-sectional area, roughness coefficient and bed slope, and flow conditions, i.e., discharge, depth, and velocity vary with distance. It is well recognised that one-dimensional (1-D) models can provide acceptable approximations of flow transport in a river (Price, 1982). Present work concentrates on the study of one-dimensional flow modelling approaches that can be potentially used with their correspondent one-dimensional solute transport

modelling approaches for studying the solute transport phenomenon in streams under unsteady flow conditions.

The governing partial differential equations for distributed one-dimensional unsteady open channel flow are popularly known as the Saint-Venant Equations (SVE).

The continuity equation without lateral flow is given as

$$\frac{\partial Q}{\partial x} + \frac{\partial A}{\partial t} = 0 \tag{2.26}$$

and the momentum equation is

$$S_f = S_0 - \frac{\partial y}{\partial x} - \frac{Q}{gA}\frac{\partial U}{\partial x} - \frac{1}{g}\frac{\partial U}{\partial t} \tag{2.27}$$

where, Q is the rate of flow, S_f is the friction slope, S_0 is the bed slope, and g is the acceleration due to gravity. Because of the complexities and numerical problems involved in solving the complete Saint-Venant equations, simplified methods have been developed for flood routing studies. Hayami (1951) proposed a simplified diffusive wave flow routing technique using convection–diffusive equation expressed as

$$\frac{\partial Q}{\partial t} + c_k\frac{\partial Q}{\partial x} = D_f\frac{\partial^2 Q}{\partial x^2} \tag{2.28}$$

where, c_k is the wave celerity, and D_f is the flow diffusion coefficient expressed as

$$D_f = \frac{Q}{2S_o B} \tag{2.29}$$

Simplified methods have been considered to be important tools of flood routing because of their simplicity in application, lesser data requirements for their solution and practical applicability. Among the simplified methods, the Muskingum method and its modifications have been widely used in flood routing studies (Price, 1982). The governing equations of the Muskingum method are

$$\frac{dS}{dt} = Q_I - Q_O \qquad (2.30)$$

Q_I and Q_O are rate of inflow and outflow respectively and S represents the storage in the reach and is expressed as

$$S = K_f \left[\theta_f Q_I + (1 - \theta_f) Q_O \right] \qquad (2.31)$$

where the parameter K_f denotes the travel time, and θ_f is the weighting parameter. The routing equation is expressed as

$$(Q_O)_j = \varepsilon_1 (Q_I)_j + \varepsilon_2 (Q_I)_{j-1} + \varepsilon_3 (Q_O)_{j-1} \qquad (2.32)$$

where $(Q_I)_j$ and $(Q_O)_j$ are the rate of inflow and outflow at time $j\Delta t$ respectively.

$(Q_I)_{j-1}$ and $(Q_O)_{j-1}$ are the rate of inflow and outflow at time $(j-1)\Delta t$ respectively, where Δt is the routing time interval. The Muskingum coefficients ε_1 ε_2 and ε_3 are expressed as

$$\varepsilon_1 = \frac{-K_f \theta_f + \Delta t/2}{K_f (1 - \theta_f) + \Delta t/2} \qquad (2.33a)$$

$$\varepsilon_2 = \frac{K_f \theta_f + \Delta t/2}{K_f (1 - \theta_f) + \Delta t/2} \qquad (2.33b)$$

$$\varepsilon_3 = \frac{K_f (1 - \theta_f) - \Delta t/2}{K_f (1 - \theta_f) + \Delta t/2} \qquad (2.33c)$$

The parameters K_f and θ_f are expressed in terms of physical characteristics of flow and channel geometry (Cunge, 1969; and Koussis, 1978). The Muskingum method has the defect of producing unrealistic initial outflow commonly referred to as negative or reduced flow. Ponce and Yevjevich (1978) proposed a variable parameter Muskingum method based on the matched diffusivity approach. The technique of varying the parameters was not physically based in this method (Perumal, 1994a).

Perumal (1994a) developed a Variable Parameter Muskingum (VPM) flood routing method based on the concept that during flood flow there exists a unique relationship between the stage at a given section and the corresponding steady discharge, occurring not at the same section, but somewhere downstream from that section. In developing the VPM method, it has been assumed that the water surface and discharge are varying linearly along the small reach length Δx. Perumal (1994a) used the Saint-Venant equations to arrive at the expressions for the parameters K_f and θ_f. The VPM method is a physically based method which has the advantage of routing both stage and discharge simultaneously with systematic variation of parameters from one time interval to another time interval.

Using the Saint-Venant equations, Perumal and Ranga Raju (1999) derived the Approximate Convection-Diffusion (ACD) equation as:

$$\frac{\partial Q}{\partial t} + c_k \frac{\partial Q}{\partial x} = 0 \tag{2.34}$$

They stated that "*ACD equation in discharge formulation enables one to develop a Variable Parameter Muskingum (VPM) method as proposed by Perumal (1994a) which has the inherent ability to model the physical diffusion of a flood wave, without attributing the diffusion exhibited by it to any numerical scheme as theorized by Cunge (1969)*".

2.4.2 Solute Routing

Under unsteady flow conditions in a river, the advection and dispersion of flow and solute occur simultaneously. The solute transport under unsteady flow conditions in a river is an advection dominated process (Bedford et al., 1983). Analysis of unsteady flow induced solute transport is a difficult problem requiring the solution of coupled nonlinear equations. However, the analysis may be made less complicated by adopting two step solution process: First, using the flow model

37

to arrive at the unsteady flow information, which then is subsequently used for solving the solute transport problem. This approach may be considered appropriate as the flow transport process affects the solute transport process and not vice-versa. Studies on solute transport under unsteady streamflow conditions are not many, because of the complexities involved in modelling the phenomena. Some of the available studies are reviewed in the following paragraphs.

2.4.2.1 Based on the advection-dispersion model

Keefer and Jobson (1978) studied the solute transport under unsteady flow conditions coupling both flow and solute transport equations and solving them using implicit finite difference numerical schemes. Flow model uses one-dimensional continuity equation and momentum equation for gradually varied flow. Forward linear implicit scheme identical to Amein and Fang scheme (1970) was used for flow modelling. Variant of Stone and Brian (1963) numerical scheme was used to solve the transport equation is expressed as

$$\frac{\partial(AC)}{\partial t} + \frac{\partial(AUC)}{\partial x} = \frac{\partial}{\partial x}\left(AD_L\frac{\partial C}{\partial x}\right) \tag{2.35}$$

In solving Eqn. (2. 37), $D_L = 0$ was assumed as the numerical scheme adopted to solve Eqn. (2.37) itself generated numerical dispersion which was more than the physical dispersion introduced by D_L. The velocities required in solute transport simulations are computed from the flow model. The flow and solute transport equations are solved using different numerical schemes.

Price (1982) presented numerical solution of the AD equation with lateral flow

$$\frac{\partial C}{\partial t} + U\frac{\partial C}{\partial x} = D_L\frac{\partial^2 C}{\partial x^2} + \frac{q}{A}C \tag{2.36}$$

where, q is the lateral inflow or out flow per unit length normal to the direction of flow. Considering C as the ratio of rate of mass flow past a section, M_r to the rate of flow at the section, $C = M_r/Q$, and using

38

$$\frac{\partial A}{\partial t} + \frac{\partial Q}{\partial x} = q \qquad (2.37)$$

in Eqn. (2.36) gives

$$\frac{\partial(M_r/U)}{\partial t} + \frac{\partial M_r}{\partial x} = AD_L \frac{\partial^2}{\partial x^2}(M_r/Q) \qquad (2.38)$$

Equation (2.38) has been solved using a finite difference scheme similar to the one used in the Variable Parameter Muskingum-Cunge (VPMC) method. The relation between the weighting parameter of the Muskingum method and the dispersion properties of solute is not clearly established. Price (1982) did not take into account the variation of flow on the dispersion coefficient.

Graf (1995), and Krein and Syamder (2000) studied the solute transport phenomenon under unsteady flow condition by conducting experiments in rivers. Graf (1995) studied the dispersion process under steady and unsteady stream flow conditions, by conducting experiments on Colorado River. To date, this is an unique experiment conducted to study the effect of flow variations on solute transport process.

Gabriele and Perkins (1997) studied the metal transport for Aberjona river watershed. Metal transport has been strongly influenced by different flow components of Aberjona river watershed. Metal flux transport was modelled by assigning metal concentration to each stream flow. It has been observed that three stream flow components viz., quick flow, slow flow and base flow play a significant role in determining the total transport of contaminants in the Aberjona River. The Muskingum method was used to route the stream flow, the suspended sediments, and the metals through channels. Gabriele and Perkins (1997) interpreted the storage of the Muskingum method as a sum of two compartments: one compartment, S_I, a function of inflow Q_I only and the second compartment S_Q function of outflow Q_O only. Considering a pollutant mass, M, is being carried with

inflow discharge Q_I and outflow discharge Q_O. C_I denotes the concentration of the input mass, C_O denotes the concentration of the output mass, M_{SI} the mass of solute in S_I compartment and M_{SO} is the mass of solute in S_O compartment, and the total mass M_S is given by

$$M_S = M_{SI} + M_{SO} \tag{2.39}$$

By analogy with the flow system

$$\frac{dM_S}{dt} = Q_I C_I - Q_O C_O \tag{2.40}$$

$$M_S = K_m \theta_m (Q_I C_I) + K_m (1 - \theta_m)(Q_O C_O) \tag{2.41}$$

where, K_m is time between the centroids of the input and output mass flux distributions and θ_m is the weighting parameter used to weigh the relative effects of input and output on the mass stored in the reach. The finite difference solution of Eqn. (2.40) combining with Eqn. (2.41) gives

$$(Q_O C_O)_{j+1} = G_1 (Q_I C_I)_{j+1} + G_2 (Q_I C_I)_j + G_3 (Q_O C_O)_j \tag{2.42}$$

and $G_1, G_2,$ and G_3 are the coefficients of Muskingum method for mass flux routing expressed as

$$G_1 = \left[\frac{1}{U_i^{j+1}} - N_{CI} - \frac{2A'D_L}{Q_i^{j+1}U'\Delta x} \right] \Big/ \left[\frac{1}{U_{i+1}^{j+1}} + N_{CI} + \frac{2A'D_L}{Q_{i+1}^{j+1}U'\Delta x} \right] \tag{2.43a}$$

$$G_2 = \left[\frac{-1}{U_i^j} - N_{CI} + \frac{2A'D_L}{Q_i^j U'\Delta x} \right] \Big/ \left[\frac{1}{U_{i+1}^{j+1}} + N_{CI} + \frac{2A'D_L}{Q_{i+1}^{j+1}U'\Delta x} \right] \tag{2.43b}$$

$$G_3 = \left[\frac{-1}{U_{i+1}^j} + N_{CI} - \frac{2A'D_L}{Q_{i-1}^j U'\Delta x} \right] \Big/ \left[\frac{1}{U_{i+1}^{j+1}} + N_{CI} + \frac{2A'D_L}{Q_{i+1}^{j+1}U'\Delta x} \right] \tag{2.43c}$$

$$A' = \frac{1}{4}\left(A_{i+1}^{j+1} + A_i^{j+1} + A_i^j + A_{i+1}^j \right) \tag{2.44}$$

$$U' = \frac{1}{4}\left(U_{i+1}^{j+1} + U_i^{j+1} + U_i^j + U_{i+1}^j \right) \tag{2.45}$$

where j denotes the time step, i denotes the space step, N_{cI} is inverse of Courant speed,$(\Delta t/\Delta x)$, A′ is mean of areas at four nodes i, i+1, j, and j+1. U′ is mean of velocities at four nodes i, i+1, j, and j+1.

Equation (2.42) is similar to the Muskingum routing equation for stream flow. They recognized that the contaminant mass flux distribution and the associated hydrograph do not travel at the same speed through a channel reach, and relative effects of input and outputs on the solute and flow transport processes may not be the same. Even after recognising the differences between velocity of propagation of solute cloud and flow hydrograph, Gabriele and Perkins (1997) have chosen to set K_m and θ_m equal to the K_f and θ_f values of Muskingum stream flow routing method. In reality $K_m \neq K_f$ and $\theta_m \neq \theta_f$. This is because of the differences (i) between velocity of flow propagation and that of solute transport, and (ii) between the flow diffusion coefficient and the solute dispersion coefficient.

2.4.2.2 Based on the transient storage model

Runkel et al. (1998) presented an application of the TS solute transport model under unsteady flow conditions for the Huey Creek, an Antarctic stream. The modelling framework couples the kinematic wave flow routing approximation with a TS model of solute transport. Flow equations are based on channel routing algorithm of Alley and Smith (1982), as referred in Runkel et al. (1998). Time varying discharges and cross-sectional areas computed by means of the flow routing model are used as input data to the one-dimensional solute transport model, which Runkel (1998) termed as One-dimensional Transport with Inflow and Storage (OTIS) model. The governing equations of transport model have been solved using the Crank-Nicolson numerical scheme proposed by Runkel and Chapra (1993). A tracer experiment under unsteady flow varying between 50 lt/s and 120 lt/s was performed in the Huey Creek by injecting a solution containing Lithium Chloride

(LiCl) and Lithium Bromide (LiBr) at a constant rate for about 3.75 hours. Runkel et al. (1998), obtained good calibration results of Lithium (Li) C-t curves at four sampling stations along a 1-km long stretch. The modelling framework proposed by Runkel et al. (1998) does not allow simultaneous flow and solute routing. In this approach, flow details need to be computed prior to the solute transport modelling. As already stated, the numerical method used to solve the TS model equations (Runkel and Chapra, 1993) fails to give satisfactory results in advection dominated dispersion process, which is prominent under unsteady flow condition.

2.4.2.3 Based on the aggregated dead zone model

An extension of the ADZ solute transport model integrated with a Multilinear Discrete Lag Cascade (MDLC) flow routing model, which has a similarity with the ADZ model, was developed by Camacho (2000) for the study of longitudinal dispersion under unsteady flow conditions. The proposed MDLC-ADZ modelling framework of Camacho, (2000), is a model involving two-parameter, viz., DF, the ratio of the residence time of solute to the total travel time of the solute in the reach, and β, the solute lag coefficient. It works well during steady flow, but fails to model dispersion during unsteady flow. Similarly, single-parameter (β) model that works satisfactorily for dispersion studies during unsteady flow fails to model dispersion during steady flow. As steady flow is a special case of unsteady flow, the model applicable for dispersion during unsteady flow should also be capable of modelling dispersion under steady flow conditions. The Camacho (2000) model lacks this capability. Moreover, the model used for dispersion studies during unsteady flow results in amplified outflow peak concentrations which, is contradictory to the characteristics of dispersion process of conservative solutes. This implies that there is some deficiency in the Camacho's (2000) model. Camacho (2000) even fails to suggest either a single or two-parameter model for the study reach considered.

2.5   CONCLUSIONS

Based on the review of literature presented in the preceding sections of this study, certain conclusions which are relevant in the context of objectives (Chapter 1, section 1.5) of this study have been drawn. These are stated below:

1. In majority of the studies available in literature, one–dimensional solute transport was modelled using the Advection–Dispersion equation under steady streamflow conditions. Based on the AD equation, a finite difference method similar to that of the Muskingum flow routing method was proposed by Koussis et al. (1983) to study the solute transport in a river under steady flow conditions. Though the model structures for flow routing using the Muskingum method and for solute routing using the Matched Advection Diffusion method advocated by Koussis et al. (1983) are the same, there exist logical inconsistencies in the development of the solute routing method, which is based on the concept of matched advective diffusivity approach used in the flow routing method (Cunge, 1969). Koussis et al. (1983) assumed dispersion coefficient to be zero implying absence of dispersion. However, at the same time considered the presence of concentration gradient ($\partial C / \partial x$), which is inconsistent with the logic of Fick's law. Further, the concept of one-to-one relationship between stage and discharge used in the development of the Muskingum-Cunge flow routing method is not applicable for the solute routing method advocated by Koussis et al. (1983), as there is no second variable, like stage to relate with the solute concentration.

2. Cells-In-Series (CIS) model was developed as an alternative to the AD model. In the CIS model, there exists a fixed relationship between the number of cells, the reach travel time, and the dispersive characteristics, for a series of equal cells. This model is sensitive to the number of cells, in which a river reach is divided.

3. It has been widely recognized that the AD model and the CIS model fail to simulate the long tail of the observed C-t curves in rivers. Hence, the Dead Zone, the Transient Storage and the Aggregated Dead Zone models were developed to simulate the long-tails of C-t curves observed in rivers affected by transient storage mechanism.

4. Transient storage model is capable of simulating the observed C-t curves even with long–tails satisfactorily. However, it is difficult, if at all possible, to obtain an analytical solution of the TS model for general boundary conditions. Efficient numerical methods are required to solve the governing equations of the TS model. It is not easy to obtain an unique set of calibration values of D_{ts}, α, and β in a particular channel reach. It is also not possible to theoretically estimate α from hydro-geometric characteristics of a river. Hence, the practical utility of the TS model has been limited. Therefore, it is desirable to model solute transport in rivers affected by transient storage mechanism using simplified equation.

5. Aggregated Dead Zone model is an approximation of the Dead Zone model. It has also been interpreted as a variant of the CIS model. It simulates the C-t curves observed in rivers satisfactorily. However, it is difficult to identify and estimate the model coefficients. Moreover, it is not easy to interpret the physical significance of the model coefficients.

In view of the problems stated above with the TS model and the ADZ model, it is necessary to explore an alternative method for solute transport in rivers affected by transient storage mechanism. The alternative method should be reliable and also simple in comparison to the TS and ADZ models.

6. The modelling framework coupling flow and solute transport models was used to study the one-dimensional solute transport under unsteady flow conditions. The flow routing models were coupled either with the AD equation (Keefer and Jobson, 1978, Price, 1982) or with the TS equations (Runkel et al. 1998). However, the modelling framework does not allow the integration of model parameters and simultaneous flow and solute routing. Flow routing equations and solute routing equations were solved using different numerical methods. Further, governing equations of the TS model, when coupled with the flow routing equation increase the complexities in the solution procedures. The numerical solution procedure of the TS model used in the modelling framework, given by Runkel and Chapra (1993), failed to model the advective dominated dispersion phenomenon. Hence, there is need to evolve a model which integrates the parameters of flow transport and solute transport models, and allows simultaneous routing of both flow and solute.

7. The Muskingum method was used to model both the flow and the solute transport processes to study the dispersion under unsteady streamflow conditions, because of the similarities in model structures and parameters (Price, 1982; and Gabriele and Perkins, 1997). However, the relationships between the model parameters of flow and solute transport, such as U, D_f and D_L, have neither been clearly defined nor taken into account while dealing with solute transport studies under time-varying flows.

8. Flow routing in streams was modelled satisfactorily using the Variable Parameter Muskingum method (Perumal, 1994b; and Perumal et al., 2001) within the domain of its applicability. It may be worthwhile to explore the use of the logic of the VPM method for developing a solute

45

transport model for its applications under unsteady flow conditions. The parameters of the VPM method are varied form one time interval to the next time interval in a physically based manner, which may help in integration of parameters of flow and solute transport.

9. A model used to study the dispersion under unsteady flow conditions should be capable of simulating solute transport under steady flow conditions also, as steady flow is a particular case of unsteady flow. However, the Multilinear Discrete Lag Cascade-ADZ model (MDLC-ADZ model) proposed by Camacho (2000) fails to do so. Further, an application study of the model shows unnatural amplified routed peak concentration at downstream locations over and above the corresponding upstream peak concentrations. Therefore, a solute transport model, which consistently simulates the solute transport process under steady and unsteady flow conditions, is required to be developed.

governing equation describing the flow transport process as envisaged by Cunge (1969) and Koussis (1978) is not logically correct. Therefore, to overcome these logical errors, the present study attempts to develop an alternative approach, for developing the routing equation needed for studying the solute transport process. Moreover, as the steady flow is a special case of unsteady flow, the model based on VPM approach needs to be tested first for solute transport modelling under steady flow conditions for verifying its appropriateness.

This chapter presents (i) the development of an approximate AD equation, (ii) the formulation of the solute routing equation, based on this approximate AD equation, for studying longitudinal dispersion under steady flow condition, and (iii) the applicability of the proposed model. The suitability of the proposed model has been verified by testing it against a variety of available data.

3.2 DEVELOPMENT OF AN APPROXIMATE ADVECTION-DISPERSION EQUATION

One-dimensional solute transport under steady flow condition in a uniform channel is described by the AD equation expressed as (Rutherford, 1994).

$$\frac{\partial C}{\partial t} + U \frac{\partial C}{\partial x} = D_L \frac{\partial^2 C}{\partial x^2} \tag{3.1}$$

where, C is the cross-sectional average concentration of a conservative pollutant, U is the cross sectional average velocity of flow, and D_L is the longitudinal dispersion coefficient. The one-dimensional Convection-Diffusion (CD) equation proposed by Hayami (1951) to describe the movement of flood waves in open channel is expressed as

$$\frac{\partial Q}{\partial t} + c_k \frac{\partial Q}{\partial x} = D_f \frac{\partial^2 Q}{\partial x^2} \tag{3.2}$$

where, c_k is the wave celerity, and D_f is the flow diffusion coefficient given by

$$D_f = \frac{Q}{2S_0 B} \tag{3.3}$$

48

where Q is the discharge. S_0 is the bed slope and B is the top width of flow.

The similarity between Eqn. (3.1) and Eqn. (3.2) may be readily recognised and it enables one to consider that the solution approach adopted for solving the flow equation (Eqn. 3.2) may also be adopted for solving the AD equation governing the solute transport process.

Variable Parameter Muskingum (VPM) model advocated by Perumal (1994a) is an alternative to the physically based Muskingum methods proposed by Cunge (1969) and Koussis (1978). The VPM model has been developed using the Approximate Convection-Diffusion (ACD) equation (Perumal and Ranga Raju, 1999), which has been directly derived from the Saint-Venant equations. It has been shown by Perumal and Ranga Raju (1999) that though the ACD equation has the same form as that of the kinematic wave equation used in the development of the physically based Muskingum methods (Cunge, 1969; and Koussis, 1978), it is capable of accounting for physical dispersion directly without attributing to any numerical dispersion as has been done in the case of matched diffusivity based approaches. In the present study a concept analogous to the one used in the Approximate Convection-Diffusion (ACD) (Eqn. 2.34) equation is employed by replacing the discharge variable with that of the concentration in the development of a VPM type model for modelling the longitudinal dispersion of solute under steady flow conditions in uniform channels and rivers.

The following assumptions are made in the development of the approximate advection-dispersion equation considering steady flow conditions

1. The flow is steady and uniform.

2. Solute concentration is varying linearly with x over a small reach length Δx.

3. Longitudinal dispersion coefficient (D_L) is constant with reference to x and t.

For the development of the Approximate Advection-Dispersion equation, Eqn. (3.1) may be re-written as

$$\frac{\partial C}{\partial t} + U \frac{\partial C}{\partial x} - D_L \frac{\partial^2 C}{\partial x^2} = 0 \qquad (3.4)$$

Equation (3.4) may be modified by grouping the space differential terms together as

$$\frac{\partial(C)}{\partial t} + U \frac{\partial(C_M)}{\partial x} = 0 \qquad (3.5)$$

where, $C_M = C - \dfrac{D_L}{U} \dfrac{\partial C}{\partial x}$ \qquad (3.6)
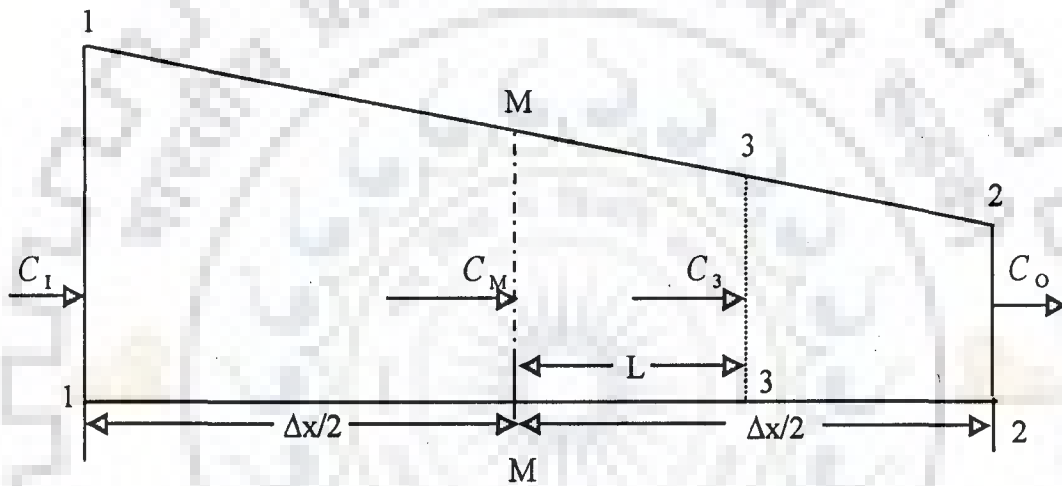
Figure 3.1 Definition sketch of the Muskingum solute routing reach

If C_M is considered as the concentration at the middle of the reach (at section M as shown in the definition sketch), (Fig. 3.1), and C_3 is the concentration at a section, which is located at a length L downstream of the mid-section of the reach, denoted as section-(3) in Fig. 3.1, then using assumption (2), C_M can be expressed as

$$C_M = C_3 - L \frac{\partial C_3}{\partial x} \qquad . \qquad (3.7)$$

and using the similarity between Eqns. (3.6) and (3.7), the dispersion coefficient D_L can be expressed as

$$D_L = L U \qquad (3.8)$$

50
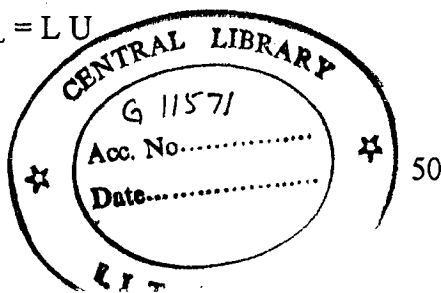
Eqn. (3.8) is in confirmation with the interpretation of Graf (1998) that the dispersion coefficient is the product of a characteristic length and velocity, and the choice of the characteristic length, L and the dispersion coefficient, D_L must be determined from relevant experiments. The assumption of linear variation of C with x over the reach length, Δx, enables one to write

$$\frac{\partial C_M}{\partial x} = \frac{\partial C}{\partial x} \tag{3.9}$$

Therefore, Eqn. (3.5) may be expressed as

$$\frac{\partial C}{\partial t} + U \frac{\partial C}{\partial x} = 0 \tag{3.10}$$

Equation (3.10) is termed as the Approximate Advection-Dispersion equation. The form of Eqn. (3.10) is similar to that of the ACD equation (Eqn. 2.34) proposed by Perumal and Ranga Raju (1999). Therefore, the solution algorithm of the VPM model for flow routing is equally applicable to solve Eqn. (3.10) using the solute concentration, C as a variable instead of discharge, Q. Perumal and Ranga Raju (1999) derived the Approximate Convection-Diffusion (ACD) equation, which has the inherent ability to model the physical diffusion of a flood wave directly without attributing the diffusion exhibited by it to any numerical scheme as theorized by Cunge(1969). Therefore, based on Eqns. (3.7) and (3.8), it can be interpreted that there exists a relationship between the concentration at mid-section and concentration at a distance L downstream from the mid-section in such a way that it satisfies Eqn. (3.5), and, thereby, implicitly accounting for dispersion analogous to the one that exists in the ACD equation. Though the form of Eqn. (3.10) is the same as that of the governing equation adopted by Koussis et al. (1983), it considers the presence of dispersion (i.e., $D_L \neq 0$) unlike that of the governing equation of Koussis et al. (1983) which assumes that dispersion is absent (i.e., $D_L = 0$). Hence, the proposed approach of arriving at the governing equation of

51

the solute transport process is devoid of the logical error involved in the corresponding approach of Koussis et al. (1983).

3.3 SOLUTE TRANSPORT MODEL FORMULATION

Applying Eqn. (3.10) at section (3) of Fig. 3.1 yields

$$\left.\frac{\partial C}{\partial t}\right|_3 + U \left.\frac{\partial C}{\partial x}\right|_3 = 0 \tag{3.11}$$

Due to the assumption of linear variation of concentration over the reach considered, $(\partial C/\partial x)|_3$ may be expressed as

$$\left.\frac{\partial C}{\partial x}\right|_3 = \left.\frac{\partial C}{\partial x}\right|_2 = \frac{C_o - C_I}{\Delta x} \tag{3.12}$$

where C_I and C_o denote the concentrations at the inlet and the outlet of the reach respectively. Again using the assumption of linear variation of concentration within the reach Δx, C_3 may be expressed as

$$C_3 = C_o + \frac{C_I - C_o}{\Delta x}\left(\frac{\Delta x}{2} - L\right) \tag{3.13}$$

Equation (3.13) may be rewritten in the form of weighted concentration by grouping the input and output concentration terms together, as

$$C_3 = \theta_c C_I + (1 - \theta_c) C_o \tag{3.14}$$

where, the weighting parameter θ_c is expressed as

$$\theta_c = \frac{1}{2} - \frac{L}{\Delta x} \tag{3.15}$$

in which, $L = \frac{D_L}{U}$ \hfill (3.16)

From Eqns. (3.15) and (3.16), θ_c is expressed as

$$\theta_c = \frac{1}{2} - \frac{D_L}{U\Delta x} \tag{3.17}$$

The ratio $\left(D_L/(U\Delta x)\right)$ is termed as dispersion number. Inverse of dispersion number

52

is termed as Peclet Number. Substituting Eqns (3.12) and (3.14) in Eqn. (3.11) and changing the partial differential notation to total differential notation yields

$$C_I - C_O = K_c \frac{d}{dt}[\theta_c \, C_I + (1 - \theta_c)C_O]$$
(3.18)

where, K_c denotes the average travel time of the solute cloud in moving from section (1) to section (2) of Fig. 3.1, and it is expressed as

$$K_c = \frac{\Delta x}{U}$$
(3.19)

The form of Eqn. (3.18) is the same as that of the governing equation of the Muskingum method with the term corresponding to the Muskingum storage expressed as:

$$S_c = K_c[\theta_c \, C_I + (1 - \theta_c)C_O]$$
(3.20)

where, S_c is the mass per unit discharge in the reach. Using the analogy of the governing equation of the Muskingum flow routing method, (Eqns. 2.30 to 2.33, in Chapter 2) the solute routing equation may be derived from Eqn. (3.18) as

$$C_{O,j} = \omega_1 C_{I,j} + \omega_2 C_{I,j-1} + \omega_3 C_{O,j-1}$$
(3.21)

where, $C_{I,j}$ and $C_{I,j-1}$ are the input concentrations at time $j\Delta t$ and $(j-1)\Delta t$ respectively; $C_{O,j}$ and $C_{O,j-1}$ are the output concentrations at time $j\Delta t$ and $(j-1)\Delta t$ respectively, and ω_1, ω_2, and ω_3 are the coefficients of the routing equation expressed as

$$\omega_1 = \frac{-K_c\theta_c + \Delta t/2}{K_c(1 - \theta_c) + \Delta t/2}$$
(3.22a)

$$\omega_2 = \frac{K_c\theta_c + \Delta t/2}{K_c(1 - \theta_c) + \Delta t/2}$$
(3.22b)

$$\omega_3 = \frac{K_c(1 - \theta_c) - \Delta t/2}{K_c(1 - \theta_c) + \Delta t/2}$$
(3.22c)

The output C-t curve for any given input C-t curve can be obtained by using the solute routing equation given by Eqn. (3.21) recursively. Since the approach

employed in the development of the VPM model (Perumal, 1994a) has been used in arriving at Eqn. (3.21), and considering that the VPM type model has been developed using the Approximate Advection-Dispersion equation (Eqn. 3.10), this model of solute routing may be called as AD-VPM model. Interestingly Cells-in-Series (CIS) model proposed to study the solute transport in rivers (Banks, 1974), also has the same dispersion concept as that of the proposed AD-VPM model. In CIS model, it is assumed that the output concentration is equal to the concentration in the cell or sub reach considered. However, in the AD-VPM model, the mass storage per unit volume in the reach is a linear function of both input and output concentrations (Eqn. 3.20). If $\theta_c = 0$, the AD-VPM model reduces to the CIS model. Hence, it can be concluded that the CIS model is a special case of the proposed model. Therefore, the dispersion built-in in the proposed model should not be attributed to any numerical dispersion as has been done in the approach adopted by Koussis et al. (1983).

The weighting parameter θ_c depends on the dispersion coefficient, D_L (Eqn. 3.17). Therefore, estimation of θ_c needs the estimation of D_L. Todate, even after four decades of research in this area there is no uniformly accepted equation to compute D_L without employing empiricism.

3.4 DETERMINATION OF THE DISPERSION COEFFICIENT

Dispersion coefficient, D_L depends on flow and channel reach characteristics. A number of empirical relationships are available to compute D_L based on the flow and channel reach characteristics (Table 2.1 in Chapter 2). All the empirical equations given in Table 2.1 link D_L only with flow and channel characteristics implying that the flow induces dispersion of the solute. The major objective of the present work is to study the dispersion of solute under unsteady flow conditions in rivers. Consequently, D_L is related to flow diffusion coefficient,

D_f as (McQuivey and Keefer, 1974)

$$D_L = \phi\, D_f \qquad\qquad (3.23)$$

in which D_f is given by Eqn. (3.3). ϕ is the relational constant. During steady flow, the discharge Q required to compute the value of D_f is constant and hence, D_L is constant. During unsteady streamflow conditions, D_f is a variable and, hence, D_L is a variable. Eqn. (3.23) has been developed based on the similarity between the diffusion equations governing the unsteady flow movement and the solute transport. Seo and Cheong (1998) compared the observed dispersion coefficients with the computed dispersion coefficients using the expressions presented by different researchers and for different rivers. They stated that the dispersion coefficient computed using Eqn. (3.23) proposed by McQuivey and Keefer (1974) gave relatively accurate values close to the observed D_L values. Hence, Eqn. (3.23) has been chosen to compute D_L in the proposed study.

The relational coefficient ϕ in Eqn. (3.23) has been determined using the D_L obtained from the observed C-t curves at two successive sections of the reach under consideration and using the hydro-geometric characteristics of the channel. The D_L required in Eqn. (3.23) has been calibrated by simulating the C-t curve observed at a downstream section of the reach using the input C-t curve at the upstream section and based on the close agreement between the observed and simulated C-t curves. The Nash-Sutcliffe's criterion (Nash and Sutcliffe, 1970), η in % has been used as a measure of agreement between the simulated and the observed C-t curves. ASCE task committee on definition of criteria for evaluation of the watershed models (1993) has also recommended this criterion. The D_L estimated based on the maximum value of Nash-Sutcliffe criterion has been used to arrive at the relational coefficient, ϕ. The value of the variance explained η is computed by

$$\eta = \frac{\sum_{i=1}^{n}(C_{Ob,i} - \overline{C_{Ob,i}})^2 - \sum_{i=1}^{n}(C_{Ob,i} - C_{C,i})^2}{\sum_{i=1}^{n}(C_{Ob,i} - \overline{C_{Ob,i}})^2} \times 100 \qquad (3.24)$$

where, n is the total observed concentration ordinates; $C_{Ob,i}$ is the ith observed concentration ordinate, $C_{C,i}$ is the ith computed concentration ordinate, $\overline{C_{Ob,i}}$ is the mean of the observed concentration ordinates. The value of ϕ (=0.116) suggested by McQuivey and Keefer (1974) may be used to estimate the solute dispersion coefficient, if observed C-t curves are not available.

3.5 ANALYSIS OF MODEL APPLICABILITY USING ANALYTICAL SOLUTIONS

The approximate AD equation (Eqn. 3.10) is obtained from the complete AD equation (Eqn. 3.1) using the assumption of linear variation of concentration over the reach Δx. Hence, the proposed approach considers the presence of D_L while approximating the AD equation in contrast to the existing method considering that the dispersion is absent (Koussis et al., 1983). In this section, the analysis of the applicability of the proposed AD-VPM model is presented. In the present study Nash-Sutcliffe criterion was used as the criterion for evaluating the AD-VPM model performance while verifying it against hypothetical, laboratory and field data.

3.5.1 Analysis of the Model Parameters

Given the physical dispersion coefficient, D_L solute routing can be performed through proper adjustment of the routing parameters K_c and θ_c. The advective velocity and the dispersion coefficient are sufficient to estimate the routing coefficients ω_1, ω_2 and ω_3. The C-t curves can be simulated using Eqns. (3.21) and (3.22) for specified values of Δx and Δt and for known average advective velocity and dispersion coefficient. As long as D_L and U remain constant for a given reach Δx, the value of K_c and θ_c would remain unchanged.

56

The reach travel time K_c is a physically based parameter and it can be determined using observed velocity and the reach length. As the reach travel time increases, the residence time of the solute increases, leading to increase in dispersion. The weighting parameter θ_c varies with the characteristic length, L. When the section (3) (Fig. 3.1) coincides with the outflow section, then L = $\Delta x/2$ and θ_c =0. If the section (3) coincides with the mid-section of the reach, then L =0 and θ_c =0.5, which leads to pure translation of C-t curve without any attenuation. Dispersion increases when θ_c decreases from the value of 0.5. The dispersion process has been termed as advection dominated when the dispersion number (= $D_L/(U\Delta x)$) is less than 0.2 (Koussis et al., 1983). The proposed AD-VPM model is suitable for advection dominated dispersion phenomena. The parameter θ_c assumes negative values when the dispersion number is more than 0.5 (Eqn. 3.17). In the proposed model, only D_L is to be calibrated from the measured C-t curves. In solute transport phenomenon, it is always necessary to calibrate one or more model parameters. There is no solute transport model that can be used without calibration of one or more model parameters unlike in flow routing where model parameters can be determined without any calibration process.

3.5.2 Applicability of the AD-VPM Model

The applicability of the model has been studied based on the analytical solution of the AD equation presented by Runkel (1996) for a given hypothetical uniform pulse input. The hypothetical analytical solution is considered as the bench mark solution with which the proposed approximate model solution is compared, because it will not exhibit any noise as observed in real life data arising due to conditions imposed on the system which are extraneous to the model assumptions.

Solute is, generally, disposed off into a river under three disposal or loading scenarios. First one is a slug of solute instantaneously disposed off at the upstream boundary, which generally happens during accidental spill of waste substances.

57

Second type is the one in which solute is disposed continuously and uniformly at the upstream boundary for a finite duration of time, (i.e., uniform pulse input loading case), which is the most general waste loading scenario. The third type of pollutant disposal is the one in which the solute is disposed continuously and uniformly over the cross-section of the channel at the upstream boundary (uniform step input case). As the second type of input loading is the most common and practically realizable scenario, the same is used in this study for evaluation of the AD-VPM model using hypothetical data. Moreover, use of uniform pulse input to obtain the analytical solution of the AD equation is preferred over that of the uniform step input as it allows one to know all the characteristics of the C-t curves such as magnitude of peak concentration, time to peak concentration, and the entire profile of the C-t curve including the rising and the receding limbs. This enables one to understand in a better way the capabilities of the proposed model in reproducing all the characteristics of the C-t curve. The use of the uniform step input for obtaining the analytical solution would not produce all the characteristics of C-t curve such as magnitude of peak concentration and its time of occurrence, and the receding limb profile. The agreement between the solutions using proposed model and the analytical method is measured using the Nash-Sutcliffe's criterion, (Nash and Sutcliffe, 1970) that is expressed using Eqn. (3.24).

It is considered that the AD-VPM model is able to closely reproduce the analytical solution, when $\eta > 99\%$. Such a criterion adopted in this work for evaluating the proposed model in reproducing the analytical solutions may be considered very stringent, when applied to field problems.

A hypothetical uniform pulse input of 100 mg/l for 2hrs duration is applied to arrive at the analytical solution of AD equation for the purpose of evaluating the applicability of the AD-VPM model. Solution of the AD-VPM model for this input is compared with the respective analytical solutions obtained for different combinations of velocities and dispersion coefficients. In these numerical

experiments, the flow velocities used are the characteristics of those observed in natural rivers as reported by Nordin and Sabol (1974) and Seo and Cheong (1998) and the velocity varies in the range of 0.2m/s-1.75m/s. The dispersion coefficient D_L used in these experiments varies in the range of insignificant dispersion to those values, which results in the values of $\eta \geq 98\%$. Typical results showing the comparison between the analytical solution and AD-VPM model solutions are presented in Fig. 3.2.

Based on these numerical experiments it is observed that

(i) For a given specified velocity of flow there exists a D_L, termed as limiting D_L. When D_L is greater than this limiting D_L, then the performance of the AD-VPM model in reproducing the analytical solution of AD model leads to poor agreement resulting in $\eta < 99\%$. It is observed that as the velocity increases the value of the limiting D_L increases. The velocities and their corresponding limiting dispersion coefficients are reported in Table 3.1.

Table 3.1 **Results showing the limiting D_L estimated from numerical experiments and determined using the applicability criterion equation**

Sl.No.	Velocity (m/s)	Limiting D_L estimated (m^2/s)	Limiting D_L (Eqn. 3.24) (m^2/s)
1	0.20	27	26.40
2	0.35	70	69.00
3	0.60	165	173.40
4	1.00	400	415.64
5	1.25	600	610.00
6	1.50	875	832.00
7	1.75	1100	1083.30
8	2.00	1555	1362.00
9	2.50	2100	2000.00
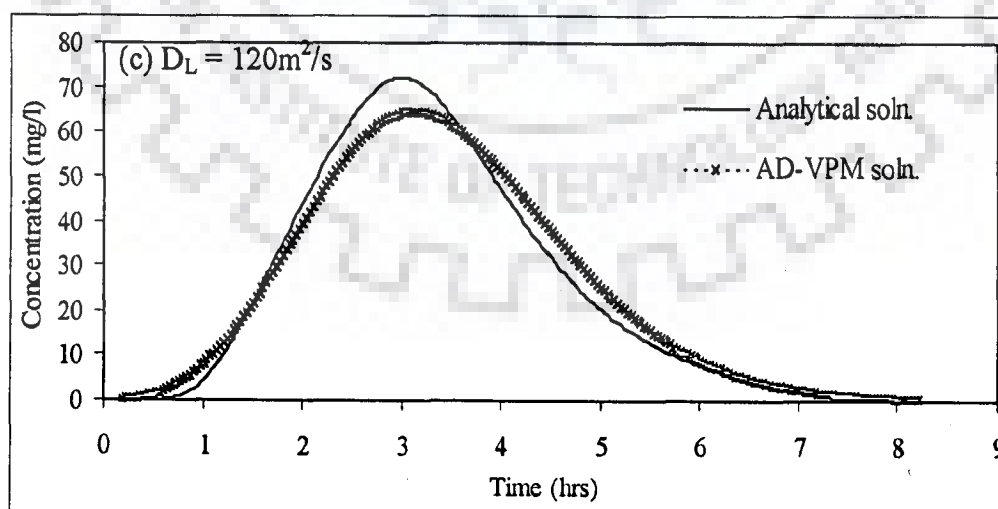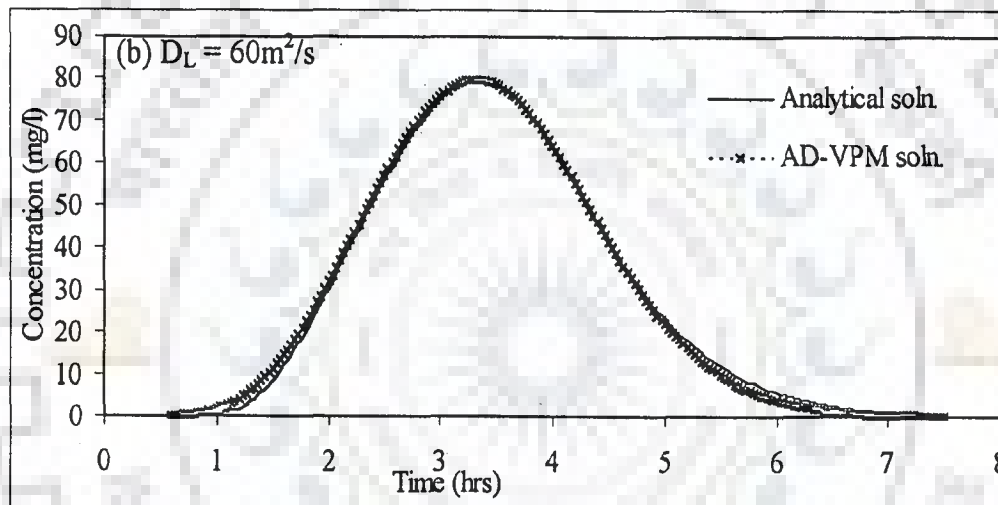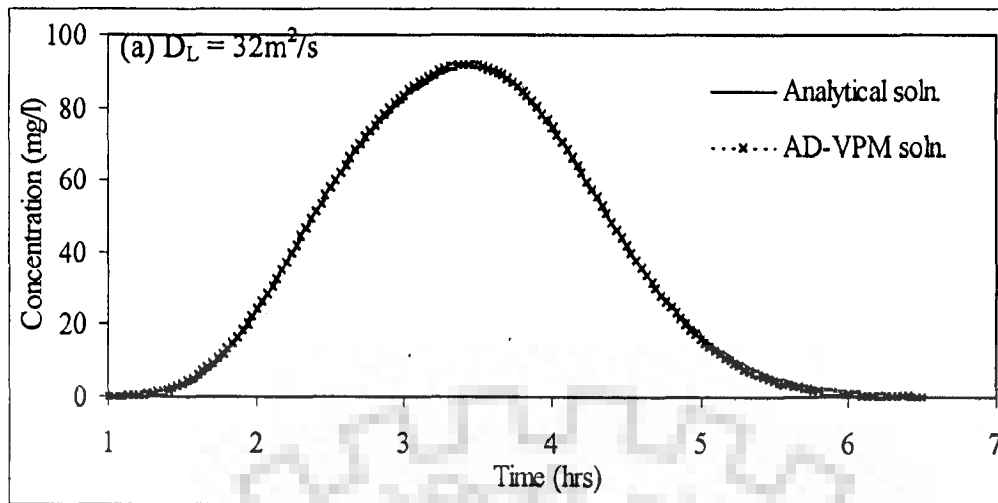
Figure 3.2(i) Analytical solution and AD-VPM solution for U=0.35m/s, X=3km,

Nr=15. (a) D_L=32m^2/s, (b) D_L=60m^2/s, and (c) D_L=120m^2/s
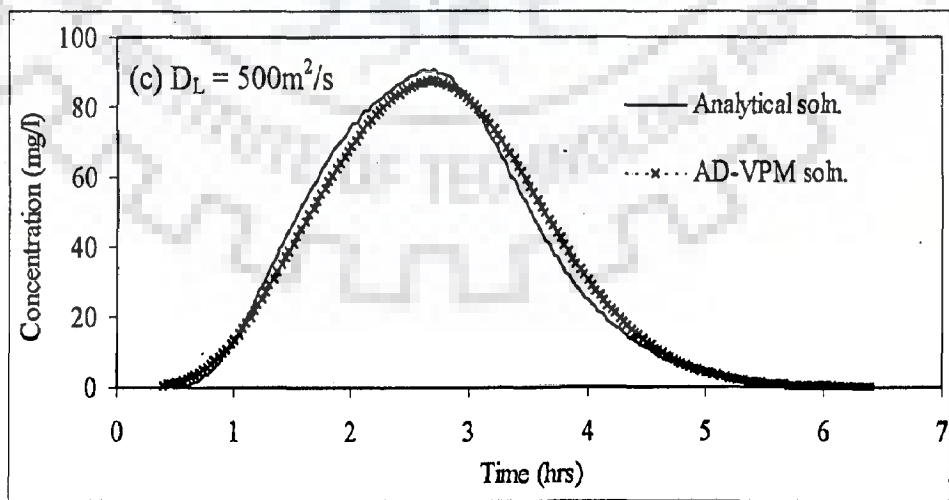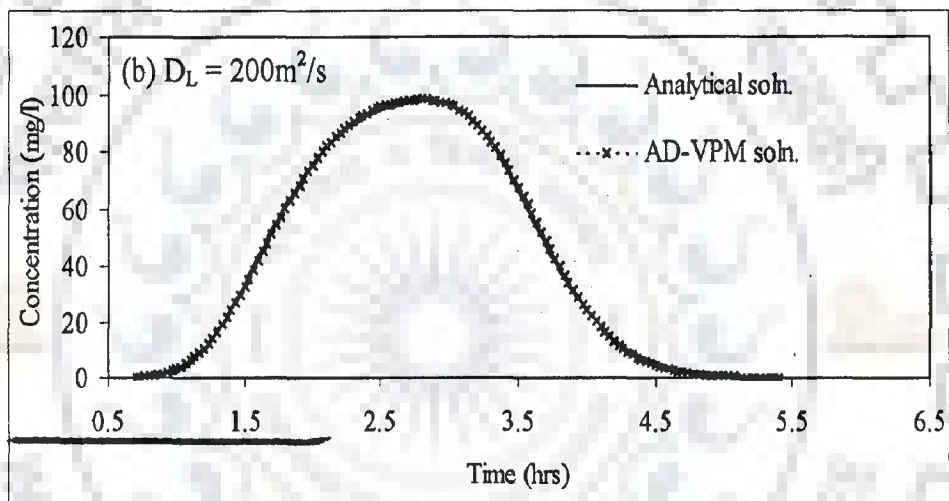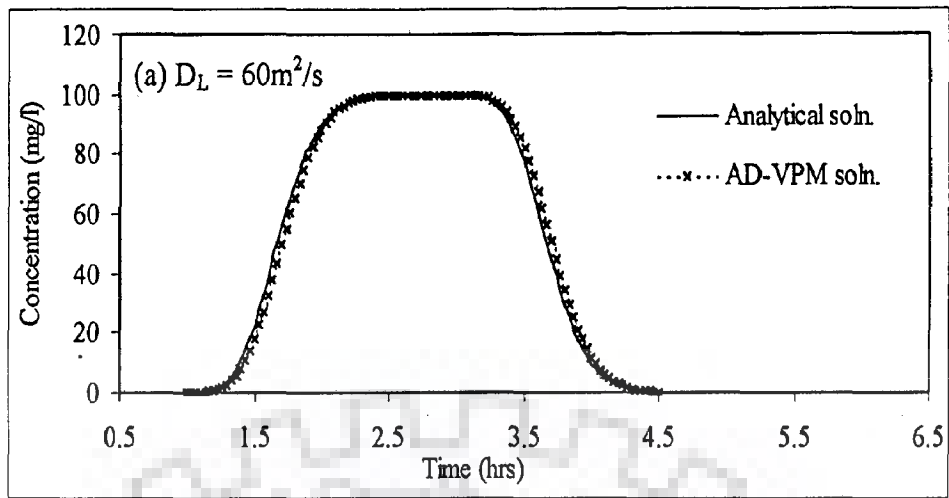
Figure 3.2(ii) Analytical solution and AD-VPM solution for U=1.0m/s, X=6km,
Nr=30. (a) D_L=60m^2/s, (b) D_L=200m^2/s, and (c) D_L=500m^2/s

61
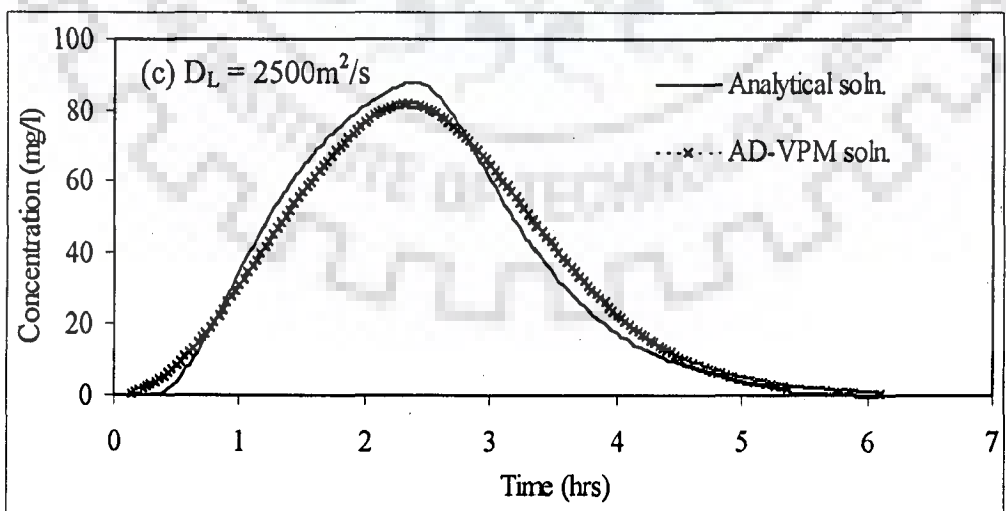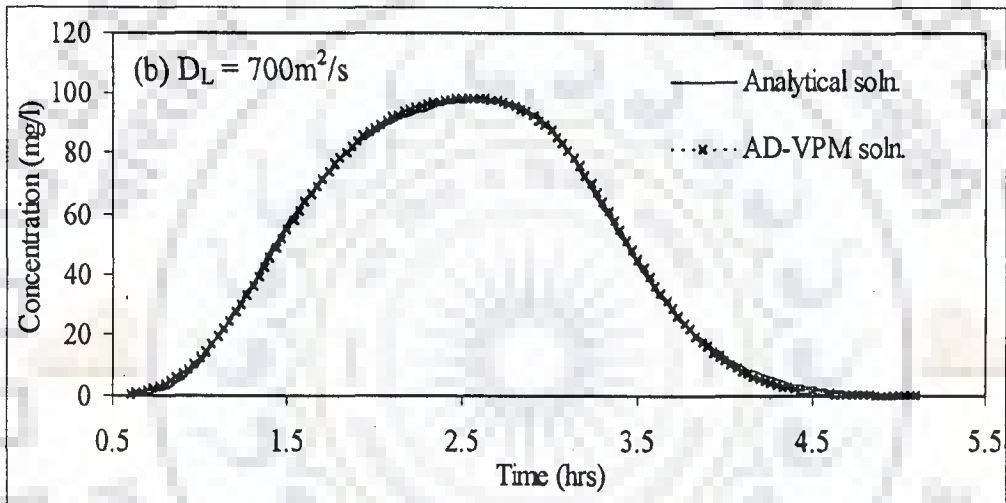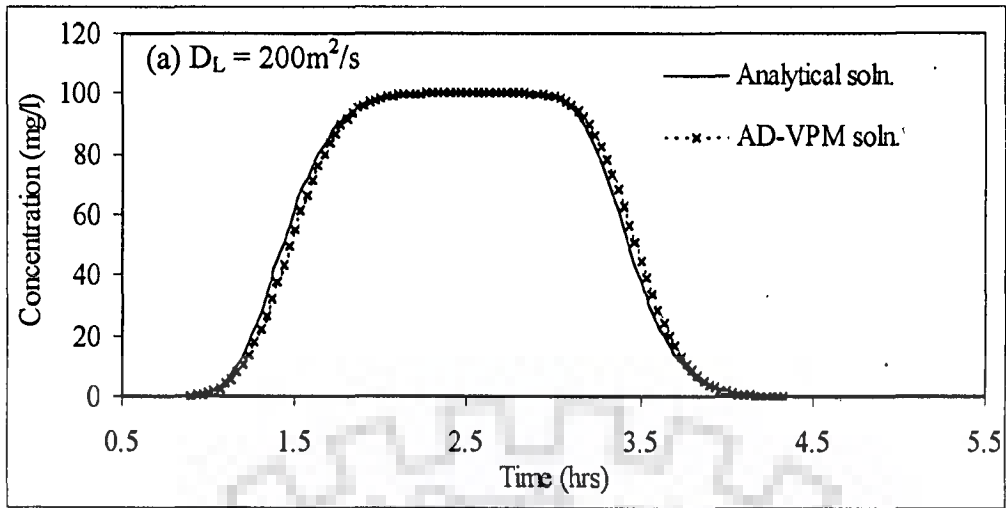
Figure 3.2(iii) Analytical solution and AD-VPM solution for U=1.75m/s, X=9km, Nr=45. (a) D_L=200m²/s, (b) D_L=700m²/s, and (c) D_L=2500m²/s

62
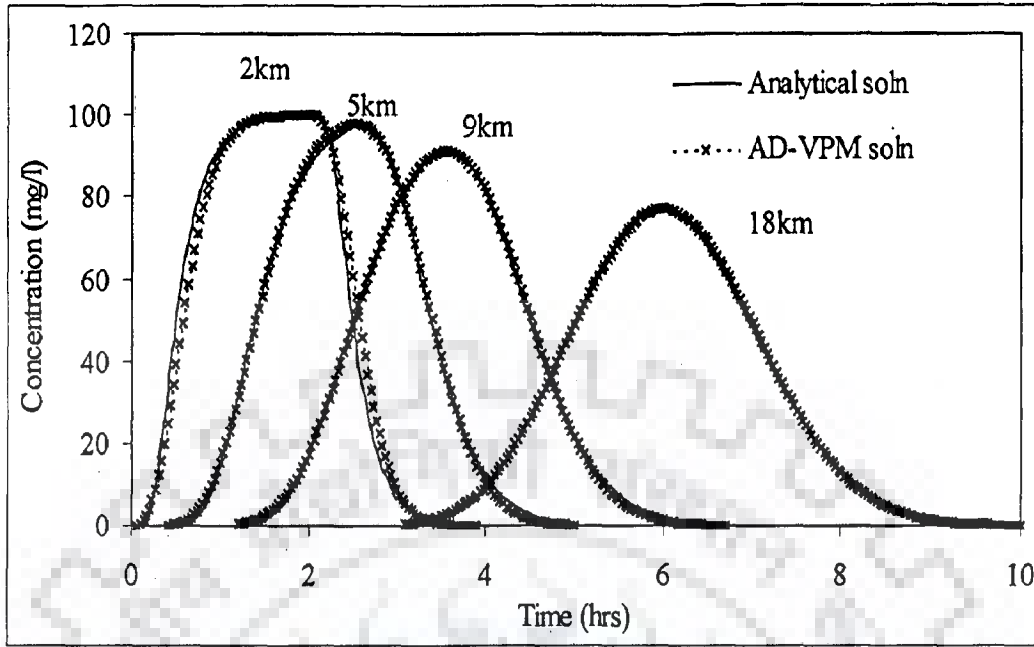
Figure 3.2(iv) Analytical solution and AD-VPM solution for pulse input at different downstream distances for U=1.0m/s and D_L=250m^2/s

(ii)   The relationship between the velocity and the limiting D_L is shown in Fig. 3.3 demarcating the applicability domain of the model within which the reproduction capability is measured with η> 99%. The demarcating curve is represented by the regression equation

$$D_L = 416.64 \, U^{1.71} \qquad\qquad\qquad (3.25)$$

It is noted that Eqn. (3.25) is not dimensionally homogeneous. While developing Eqn. (3.25), the objective was to get a better regression relationship to define the applicability domain. This equation allows one to know the limiting dispersion coefficient for an observed velocity, below which the performance of the proposed model in reproducing the analytical solution of AD equation is with η> 99%.

In addition, the relationship between the velocity and the limiting D_L is shown in Fig. 3.3 demarcating the applicability domain of the model within which the reproduction capability is measured with η>98%.

63
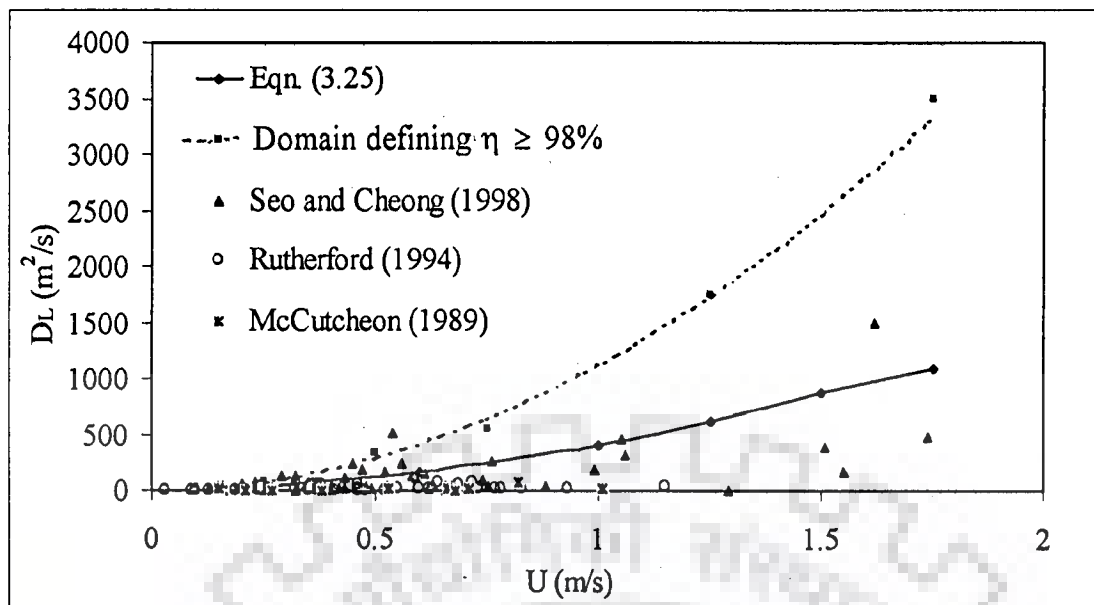
Figure 3.3 Applicability domain of the AD-VPM model

The velocities and their corresponding dispersion coefficients estimated from the observed C-t curves of a number of natural rivers as reported in the literature (McQuivey and Keefer, 1974; McCutcheon, 1989; Rutherford, 1994; and Seo and Cheong, 1998) are plotted in Fig.3.3. It is inferred from Fig. 3.3 that most of the estimated dispersion coefficients for different river reaches, corresponding to the observed velocities, are well within the applicable limits of the proposed AD-VPM model, i.e., within the domain defining the applicability criterion, $\eta > 99\%$ and a very few observed values fall within the demarcation curves of $\eta = 98\%$ and $\eta = 99\%$. Hence, it may be considered that the AD-VPM model is suitable for most of the practical cases.

The applicability of Eqn. (3.25) in the extrapolation range was tested by considering velocities beyond 1.75m/s, the upper limit of velocities used in developing Eqn. (3.25). Two velocities of 2.0m/s and 2.5m/s were used for different combinations of D_L to arrive at the respective limiting values of D_L similar to what was carried out in the numerical experiments used in the development of Eqn. (3.25). These experiments result in the limiting values of $D_L = 1555$ m^2/s and

$D_L=2100$ m^2/s respectively. The use of these velocities in Eqn. (3.25) yields the limiting values of $D_L=1362$ m^2/s and 2000m^2/s respectively, which may be considered as the close estimate of the observed limiting D_L. This experiment demonstrates the applicability of Eqn. (3.25) in the extrapolation range of the velocity. The results are shown in Table 3.1.

3.5.3 Sensitivity Analysis
3.5.3.1 Sensitivity analysis of dispersion coefficient

The parameter θ_C is a function of the spatial step size (Δx) and the dispersion coefficient (D_L). Therefore, it is necessary to study the sensitivity of the solution for the variations in spatial step size and dispersion coefficient. The D_L computed using Eqn. (3.23) has a standard error of estimate of approximately 30% based on comparative data over a wide range of flow conditions for 18 streams and 40 time-of- travel studies (McQuivey and Keefer, 1974). Hence, in the present study, the sensitivity of the solution of the AD-VPM model for the variation of D_L by an error less than 30% was studied. The sensitivity of the parameter D_L is studied by varying it by ± 20% from the true value. The numerical experiments show that ± 20% variation in the dispersion coefficient does not affect the simulation results of the AD-VPM model in reproducing the analytical solution. The results of the sensitivity analysis for different given velocities (viz., 0.25m/s, 0.5m/s, 1.0m/s, and 1.5m/s) and dispersion coefficients are presented in Table 3.2 and the comparison of the solutions are shown in Fig. 3.4.
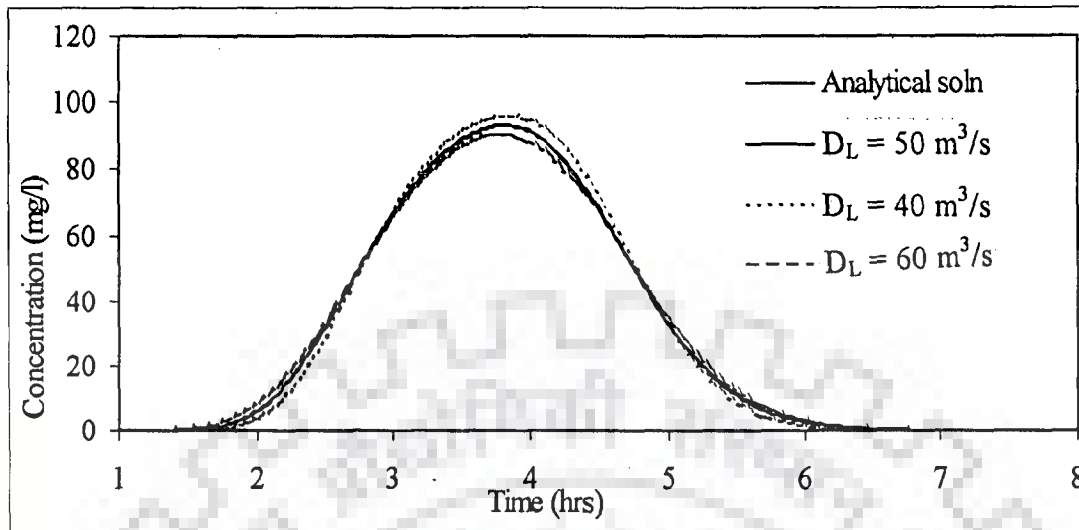
Figure 3.4(i) **Sensitivity of the AD-VPM solution for variations in D_L by $\pm 20\%$ in reproducing the analytical solution at X=5km for U=0.5m/s, D_L=50m²/s**
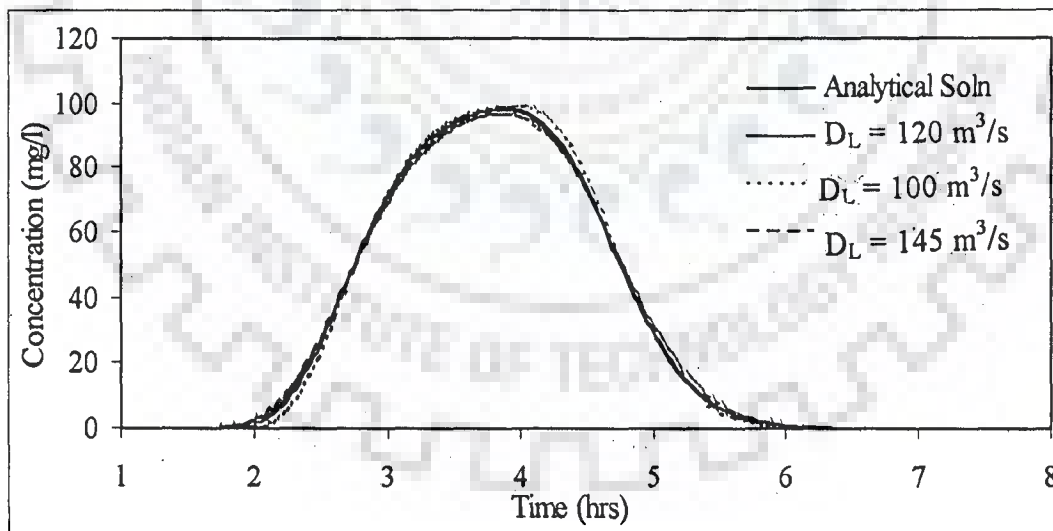
Figure 3.4(ii) **Sensitivity of the AD-VPM solution for variations in D_L by $\pm 20\%$ in reproducing the analytical solution at X=10km for U=1.0m/s, D_L=120m²/s**

Table 3.2 Results of the sensitivity analysis for the dispersion coefficient

Velocity (m/s)	D_L for analytical solution (m²/s)	Location form injection point (km)	D_L for the AD-VPM model (m²/s)	Variance explained (η) (%)
0.25	30	5	24	98.780
			30	99.835
			36	99.137
			40	98.090
0.5	50	5	30	98.875
			40	99.713
			50	99.990
			60	99.880
			70	99.500
1.0	120	15	100	99.747
			120	99.940
			140	99.896
			150	99.800
1.5	400	15	300	99.604
			400	99.972
			500	99.808
			600	99.293

3.5.3.2 Sensitivity analysis of spatial step size

The sensitivity of the AD-VPM model for change in number of reaches was studied for a given velocity U and dispersion coefficient D_L taking into account the applicability of the model governed by Eqn. (3.25). It was observed that the performance of the AD-VPM model in reproducing the analytical solution improves by using increased number of equal size sub-reaches in the given routing reach. This may be due to the reason that, for smaller sub-reaches the validity of the assumption of linear variation of concentration along x holds good. However, use of more number of sub-reaches beyond a certain limit would not improve the AD-VPM model capability in reproducing the analytical solution closely. The hypothetical numerical experiments were conducted at velocities equal to 0.25 m/s, 0.5 m/s, 1.0 m/s and 1.5 m/s and the dispersion coefficients of 30 m²/s, 80 m²/s,

200 m^2/s and 500 m^2/s respectively. The hypothetical numerical experimental results are summarised in Table 3.3. The comparison of the analytical solution and the AD-VPM model solution for different number of sub-reaches is shown in Fig. 3.5 and the Nash- Sutcliffe criterion are given in Table 3.3.

This is an advantage of the proposed model over the Cells-In-Series model, which is sensitive to the spatial step size.
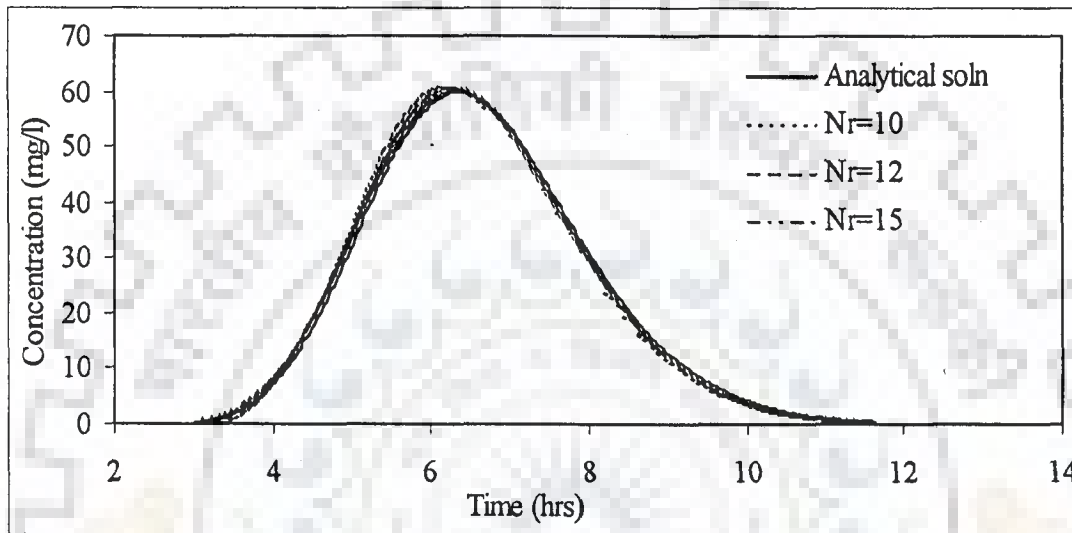
Figure 3.5(i) Analytical solution and AD-VPM solution for different number of reaches (Nr) at X=5km, U=0.25m/s and D$_L$=30m^2/s
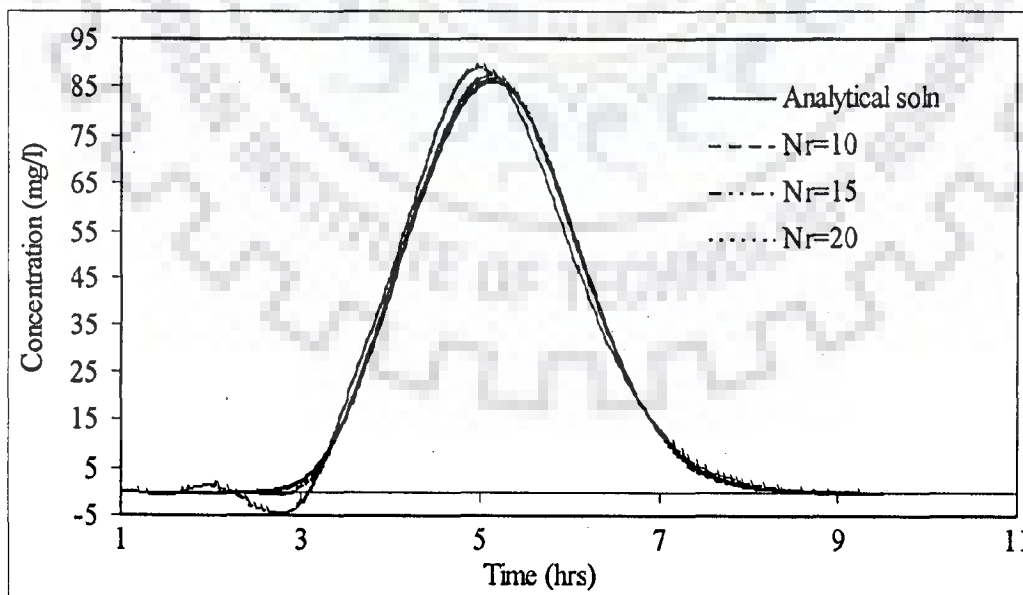
Figure 3.5(ii) Analytical solution and AD-VPM solution for different number of reaches (Nr) at X=15km, U=1.0m/s and D$_L$=200m^2/s

Table 3.3 The effect of variation of Δx on the solution of the AD-VPM model.

Velocity (m/s)	Dispersion coefficient (m²/s)	Location from injection point (km)	No. of sub-reaches	η (%)
0.25	30	5.0	5	84.313
			7	96.168
			8	97.892
			10	99.238
			12	99.655
			15	99.835
			20	99.879
0.50	80	5.0	3	88.048
			4	95.874
			5	98.397
			7	99.640
			10	99.911
			15	99.950
			20	99.951
			25	99.948
1.0	200	10.0	5	96.717
			7	99.251
			10	99.897
			15	99.990
			20	99.988
		15.0	30	99.970
			5	84.685
			7	95.590
			10	99.066
			12	99.627
			15	99.898
			20	99.989
			25	99.990
1.5	500	15.0	5	97.197
			7	99.391
			10	99.910
			15	99.989
			20	99.986
			30	99.974
			40	99.970

3.5.4 Negative Initial Response

In flood routing, negative initial response is obtained while using the Muskingum routing method, which is well documented in flood routing literature. Even though there is a dip in the initial outflow, Muskingum flow routing method has been used widely because of its simplicity. Perumal (1992) showed that the assumption of linear variation of discharge with reference to x over a given reach is responsible for the negative or reduced outflow at the beginning of the flood hydrograph.

The AD-VPM model also produces an negative initial response as the assumption of linear variation of concentration with x within a small reach Δx is used in the development of the solute routing equation, which has the same form as that of the Muskingum flow routing equation. One may accept the negative initial response, as long as it does not affect the practical utility of the results.

3.5.5 Mass Conservation

The AD-VPM model was tested for conservation of mass of solute based on hypothetical numerical experiments conducted for varying values of velocity ranging from 0.2m/s to 2.5m/s. The dispersion coefficient was varied for each velocity within the applicable range of the model as governed by Eqn. (3.25). In all cases, a hypothetical uniform pulse input with the concentration rate of 100 mg/l/sec for a duration of 2 hrs was used. Based on the numerical experiments it is found that the mass is conserved with an error of less than 1% for the cases studied.

3.6 APPLICATIONS OF THE AD-VPM MODEL IN FIELD AND LABORATORY TEST CASES

Any model proposed to simulate the solute transport process needs to be tested for its applications using a variety of data. Hence, the proposed model was tested for its applications using hypothetical data, laboratory data and field data.

Analysis of the model using hypothetical test cases was presented in section 3.5. However, the practical utility of the AD-VPM model can be demonstrated only if it is tested using laboratory data and data collected from the tracer experiments conducted in natural rivers. Two sets of laboratory experimental data (Fischer, 1966) and three sets of field experiments data (USGS Water Supply Paper, 1899-G, Tracer studies data on Colorado and Rhine Rivers) were used for validating the AD-VPM model.

Unlike the routing method of Koussis (1983), the AD-VPM model enables one to use the observed C-t curve measurements at unequal time intervals. However, to estimate the Nash-Sutcliffe criterion (η) by the AD-VPM model in simulating the observed C-t curves, it is necessary to have observed concentration values at the same time of the simulated concentration values. When this is not the case, it becomes necessary to arrive at the output C-t values by interpolating the observed C-t values so that the simulated and observed concentrations are available at the same time.

3.6.1 Laboratory Test Case

The data set of series 2600 and series 2700 from the laboratory experiments conducted by Fischer (1966) are used for this test case. The details of the observed data are presented in Appendix A.

3.6.1.1 Application to laboratory test case 1

Test case 1 refers to series 2600 containing C-t curves at four successive sections at a distance 7.0m apart; viz., at 7.06m (section 1), at 14.06m (section 2), at 21.06m (section 3), and at 28.06 m (section 4). The mean velocity in the channel was 0.269 m/s. The observed C-t data of series 2600 at section (2), (3), and (4) were adjusted for conservation of mass as suggested by Fischer (1966). These C-t curves, thus adjusted for mass conservation were used for calibration and verification of the AD-VPM model.

In the data set of 2600 series, observed input C-t measurements were available initially at 0.5 seconds time intervals (upto 26th second from the time of release of dye) and later on at 1.0 second time intervals. The observed timings of the concentration measurements of this data series are consistent with the requirements of simulation, (using the observed C-t measurements at unequal time intervals), as pointed out earlier. The D_L was determined by trial and error approach using the following procedure:

The C-t curve at section (1) was routed through the reach, for an assumed θ_c, to arrive at the computed C-t curve at section (2). The computed and observed C-t curves at section (2) were compared using the Nash- Sutcliffe criterion as given by Eqn. (3.24). This experiment was repeated for different θ_c values, and that θ_c which results in the maximum value of variance explained was considered as the best value. This θ_c was used in the estimation of the best D_L using Eqn. (3.17). The summary of the results obtained in estimating the D_L are shown in Table 3.4. The best D_L, thus obtained in this 2600 series laboratory test case using the above procedure is 0.0096 m²/s. This D_L obtained from the calibration of C-t curve at section (2) was used to simulate the C-t curves at section (3) and section (4) in the verification mode. Figure 3.6 shows the simulated C-t curves and the corresponding observed C-t curves, in which results at section (2) were obtained in calibration mode and that at sections (3) and (4) were obtained in verification mode. The AD-VPM model is able to simulate the observed C-t curves at sections (3) and (4) in verification mode, with Nash-Sutcliffe criterion (η) =99.395% and 99.651% respectively. It may be noted herein that the value of D_L =0.0096 m²/s estimated by the AD-VPM model is close to the value of D_L = 0.0117 m²/s obtained by Fischer (1966). It is also seen from Table 3.4 that a minimum $\Delta x \approx 0.40$m is required to be used for accurate reproduction of C-t curve at section (2).
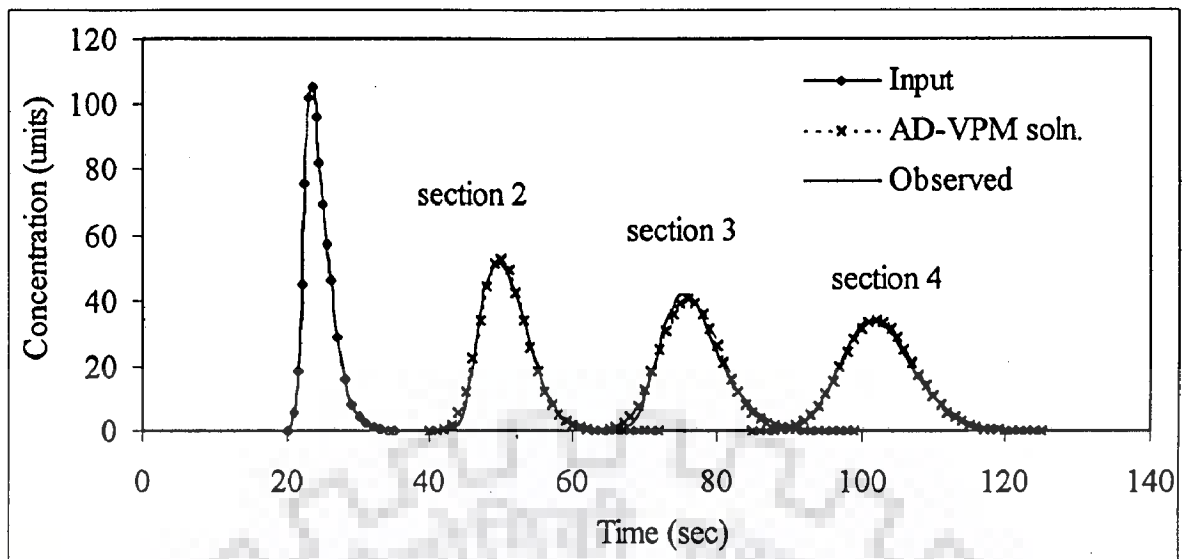
Figure 3.6 AD-VPM application to Fischer (1966) data series 2600

Table 3.4   Summary of the calibration results of D_L for the data series 2600 laboratory experiments

No. of sub-reaches	θ_c	D_L (m^2/s)	Maximum value of η (%)
7	0.3700	0.0350	68.48
10	0.3950	0.0198	84.27
14	0.4050	0.0128	95.20
18	0.4025	0.0102	99.04
21	0.3925	0.0096	99.61
22	0.3700	0.0111	99.42
23	0.3750	0.0102	99.56
24	0.3750	0.0098	99.52
28	0.3500	0.0100	99.21
30	0.3375	0.0102	99.06

3.6.1.2 Application to laboratory test case 2

Test case 1 refers to series 2700 containing C-t curves at two sections at a distance of 11.0m apart. The mean velocity of flow is 0.362m/s. The observed C-t data were adjusted for conservation of mass as suggested by Fischer (1966). The observed concentration measurements were available at unequal time intervals (0.5, 1.0 and 2.0 seconds). Even though, the AD-VPM model enables one to use the observed C-t curves at unequal time intervals, the observed concentration measurements at the output section were not available at the same time at which simulated concentrations were obtained. Hence, it is necessary to arrive at the input and output C-t values by interpolating the observed concentrations, so that simulated and observed concentrations at the output section are available at the same time.

The observed C-t curve at section (1) was considered as the input and the C-t curve at section (2) was simulated using the procedure described in the analyses of data set of series 2600 laboratory experiments. The summary of the results obtained in estimating the D_L are shown in Table 3.5. The best dispersion coefficient, thus obtained using the above procedure is 0.0225 m^2/s.

Table 3.5 Summary of the calibration results of D_L for the data series 2700 laboratory experiments

No. of sub-reaches	θ_c	D_L (m^2/s)	Maximum value of η (%)
10	0.400	0.0398	91.681
15	0.415	0.0225	98.948
20	0.390	0.0219	98.941
23	0.370	0.0225	98.365
24	0.365	0.0224	98.195
25	0.355	0.0231	98.039
30	0.325	0.0232	97.427

The simulated C-t curve could closely reproduce the corresponding observed C-t curve at section (2). It may be noted herein that the D_L estimated by the AD-VPM model is 0.0225 m²/s, which is close to the value of D_L = 0.0236 m²/s estimated by Fisher (1966). The comparison of simulated and observed C-t curves is shown in Fig. 3.7.
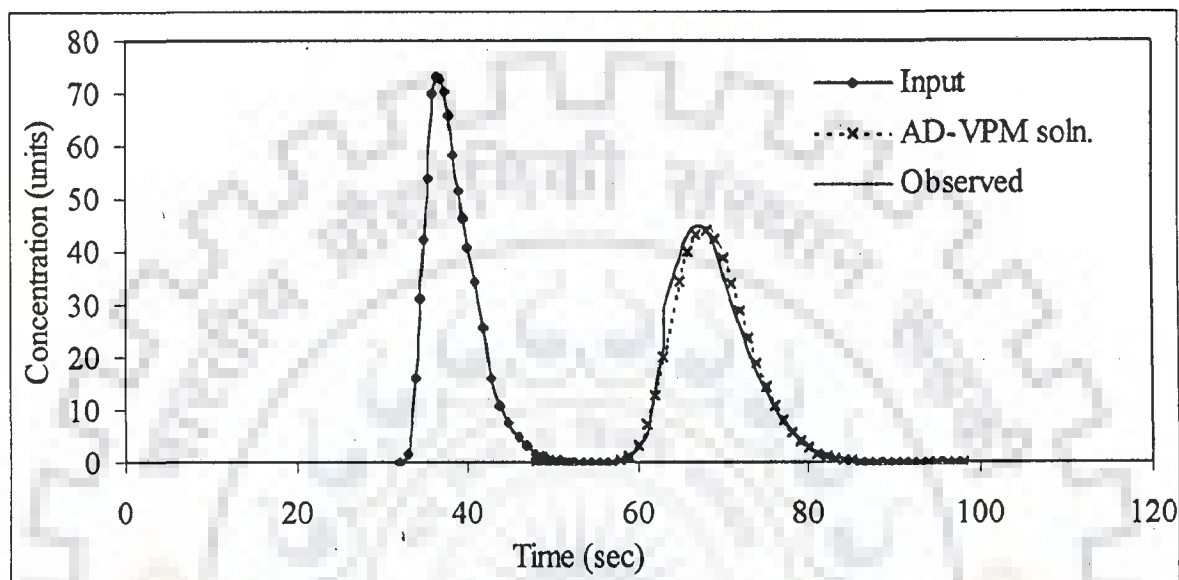
Figure 3.7 AD-VPM application to Fischer (1966) data series 2700

3.6.2 Field Test Cases

In the present study, the data of three sets of tracer experiments conducted on three rivers, viz., the Missouri River (Yotsukura et al., 1970), Colorado River (Graf, 1995) and the Rhine River (Van Mazijk, personnel communication) were used for evaluating the applicability of the AD-VPM model for studying solute transport in natural rivers.

The C-t curves recorded at each sampling station were tested for mass conservation against the input C-t curve. In all the cases, solute mass at each location was computed using a trapezoidal integration approximation (Camacho, 2000) of the mass evaluated for continuous distribution as

$$M = \int_0^\infty Q\,C\,dt \approx \sum_{i=1}^n (QC)_i\,\Delta t \tag{3.26}$$

The flow in each of these rivers was assumed to be steady during these tracer experiments. The steady-state-gain (SSG), defined as the ratio of the area under QC-t curve at a downstream location to the area under the input QC-t curve, is used as an indication of mass gain or loss. SSG>1 is an indication of mass gain and SSG<1 is an indication of mass loss (Camacho, 2000).

The above method is generally useful when the details about the injection of tracer are not available. If information about the amount of tracer injected, discharge during injection and type of injection are available, then recovery ratio method (Yotsukura et. al., 1970) may be used to determine mass loss or gain, thereby, the concentration-time distribution can be adjusted appropriately. Recovery Ratio (RR) is defined as the ratio of the amount of dye or tracer actually recovered at the cross-section to the total amount that was injected initially and is expressed as

$$RR = \frac{\int_0^\infty QC dt}{V_{IO} C_{IO}} \approx \frac{\sum_{i=1}^n (QC)_i \Delta t}{V_{IO} C_{IO}} \tag{3.27}$$

where V_{IO} and C_{IO} are the volume and the concentration of injected solution respectively.

3.6.2.1 Application to Missouri River

Yotsukura et al. (1970) conducted tracer experiments in a 227km reach of Missouri River between Sioux city and Plattsmouth (Fig. 3.8). The C-t measurement data are presented in Appendix B 1.1. Observed C-t curves of dye available at four down stream samples locations: Decatur Highway Bridge (RK 1112), Blair Highway Bridge (RK 1042.8), Ak-sar-ben Bridge in Omaha (RK 991.3) and Plattsmouth Highway Bridge (RK 951) were used in the present test case. The measured concentrations are compensated for dye loss that occurred in the stream at each down stream dye sampling station using recovery ratio given by Yotsukura et al. (1970). The recovery ratio at Blair Highway bridge, Ak-sar-ben bridge and Plattsmouth Highway bridge are 0.78, 0.775 and 0.775 respectively. Discharge in

the reach varies from 883.5 m³/s to 977m³/s and velocity varies from 1.19m/s to 1.84m/s. The slope of the entire reach is 0.0002. The observed hydraulic characteristics are presented in Table 3.6.
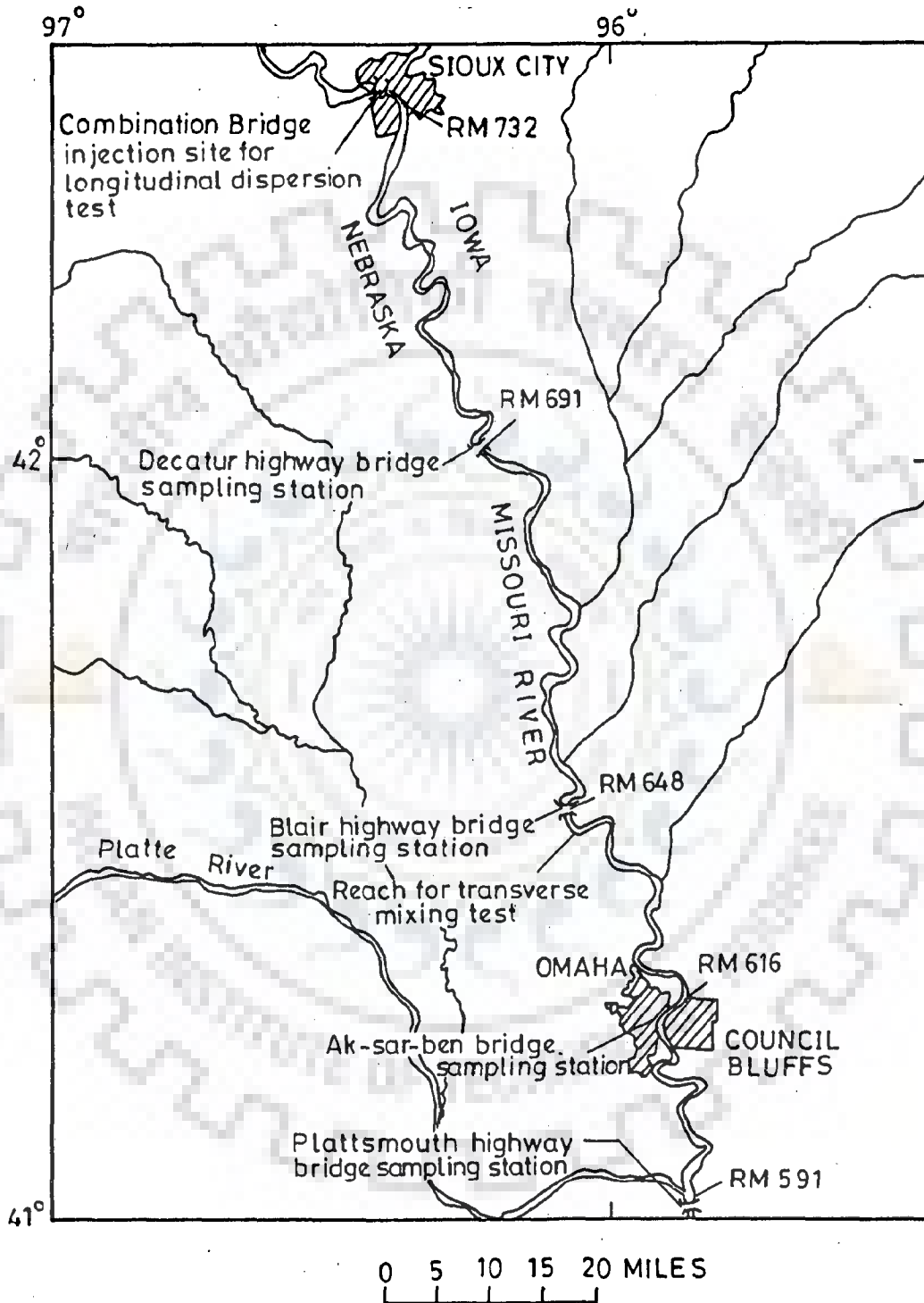
Figure 3.8 Schematic Study reach, Missouri River between Sioux City, Iowa, and Plattsmouth, Nebraska (Yotsukura et al., 1970)

Table 3.6   Hydro-geometric characteristics of the Missouri River reach (Yotsukura et al., 1970)

Station (distance from dye injection point)	Discharge (m^3/s)	Area (m^2)	Velocity (m/s)	Width (m)	Depth (m)
Decatur bridge, (65.658 km)	883.50	710.71	1.24	185.92	3.81
Blair Highway Bridge, (134.37 km)	976.35	558.35	1.75	182.90	3.05
Ak-sar-ben Bridge, (186.67km)	942.40	589.00	1.60	175.87	3.35
Plattsmouth bridge, (226.90 km)	962.20	523.41	1.84	178.30	2.93

The observed C-t curves available at Decatur Highway bridge, Blair Highway bridge, Ak-sar-ben Highway bridge in Omaha, and at Plattsmouth Highway bridge were used to test the AD-VPM model. The available observed concentration measurements at all the sampling stations are at irregular time intervals. Hence, the interpolated values were used in simulations without loosing the observed concentration measurements as far as possible. Therefore, a temporal time step of 900.0 seconds was used while simulating the observed C-t curve at Blair bridge sampling station and 1800 seconds was used while simulating the C-t curves at Ak-sar-ben bridge and Plattsmouth bridge sampling stations. The velocity was varying in the entire reach with a minimum of 1.243 m/s at Decatur bridge to 1.84 m/s at Plattsmouth bridge. Hence, in each sub-reach average values of hydraulic characteristics were computed and those were used in simulating the observed C-t curves. The average velocity computed in the sub-reach between

Decatur bridge and Blair bridge, sub-reach between Blair Highway bridge and Ak-sar-ben bridge in Omaha, and in the sub-reach between Ak-sar-ben bridge and Plattsmouth bridge were 1.496 m/s, 1.68 m/s and 1.72 m/s, respectively. Dispersion coefficient was calibrated by simulating the C-t curve observed at Blair Highway bridge using the AD-VPM model based on the procedure described in section 3.6.1.1 while analysing series 2600 laboratory test data. The D_L that gives the maximum Nash-Sutcliffe criterion (η) was considered as the appropriate dispersion coefficient. Based on the estimated D_L, and flow and channel characteristics of sub-reach Decatur bridge-Blair bridge, the relational coefficient ϕ was estimated using Eqn. (3.23) as 0.0651. The value of ϕ thus obtained was used to estimate the D_L for the subsequent reaches.

The C-t curves were simulated at Blair Highway bridge station in calibration mode, and at Ak-sar-ben Highway bridge and at Plattsmouth bridge in verification mode. The C-t curve observed at Blair Highway bridge was taken as input for the simulation of C-t curves at Ak-sar-ben Highway bridge and Plattsmouth bridge in verification mode. The comparison of observed and corresponding simulated C-t curves is shown in Fig. 3.9. Based on the studies it may be concluded that the AD-VPM model is able to simulate the observed C-t curves at all the sampling stations downstream of Decatur bridge satisfactorily as indicated by the values of Nash-Sutcliffe criterion (η) in Table 3.7. It is interesting to note that the variance explained (=96.97%) obtained in simulating the observed C-t curves at Balir Bridge in calibration model, is less in comparison with the variance explained in simulating the observed C-t curves at Ak-sar-ben and Plattsmouth bridge (=99.81% and 99.20% respectively) in verification.
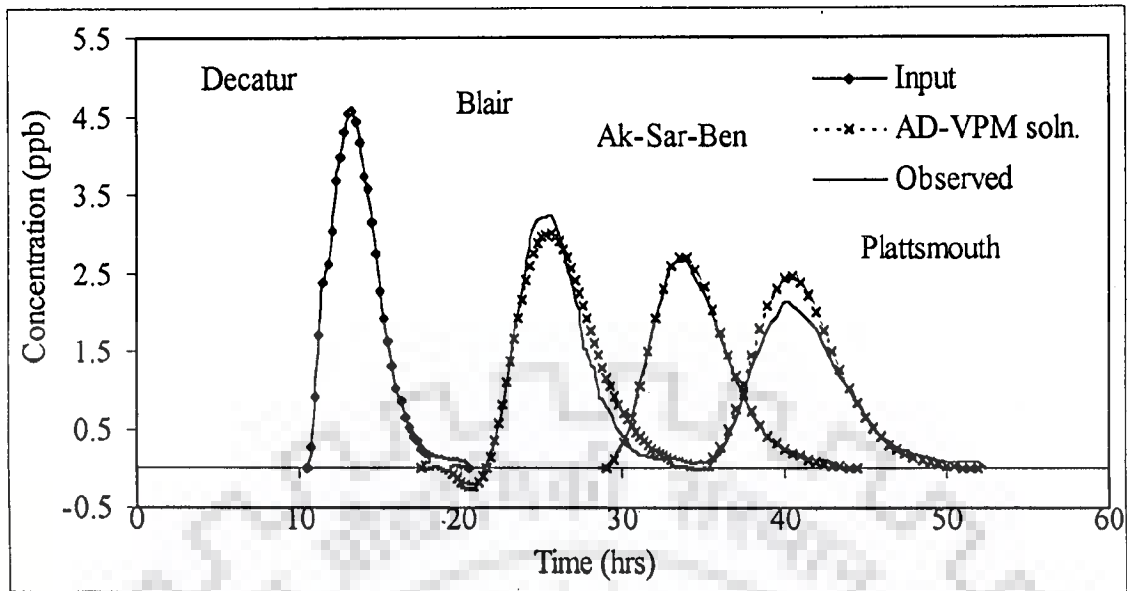
Figure 3.9 Observed and simulated C-t curves at different downstream stations in Missouri River

Table 3.7 Dispersion coefficient and Nash-Sutcliffe criterion for different sub-reaches of Missouri River

Sub-Reach	Reach length (m)	Number of sub-reaches	Reach length (m)	Average velocity (m/s)	Dispersion coefficient (m²/s)	η value (%)
Decatur bridge to Blair bridge	68716.0	12	68716.0	1.496	820.0	96.93
Blair bridge To Ak-sar-ben bridge	52292.5	12	52292.5	1.680	867.0	99.81
Ak-sar-ben bridge to Plattsmouth bridge	46707.5	12	46707.5	1.720	874.0	97.20

80

3.6.2.2 Application to Rhine River

Dispersion studies under relatively steady flow conditions were conducted extensively in the River Rhine (Van Mazijk, personnel communication). Figure 3.10 shows the schematic representation of the River Rhine along with locations of the sampling stations used in the tracer experiments. The data was supplied by Dr. Albert Van Mazijk of Delft University of Technology and the permission to use the data in the present work was given by Dr. Mr. M. Meulenberg of Commission International de L'Hydrologic du Bassion du Rhine (ICHR), The Netherlands.

Figure 3.10 **Schematic study area, channel discretisation and location of dye sampling sites (Source: Camacho, 2000)**

In the present work, the C-t curves available at the sampling stations between Koblenz (RK 590.35) and Lobith (RK 863.3) were taken for testing the applicability of the AD-VPM model. The C-t measurement data are presented in Appendix B 1.2. The hydraulic and geometrical characteristics are presented in Table 3.8 (Van Mazijk, personal communication).

81

Table 3.8 Hydro-geometric characteristics of the Rhine River reach (Van Mazijk, personnel communication)

Reach	Sub-Reach ID	Sub-Reach Length (m)	Q (m^3/s)	Velocity (m/s)	Area $(m^2/s$	Width (m)
Koblenz (RK590.35) To Bad Honnef (RK 640.0)	2205	2.15	2142	1.42	1511.25	280
	2301	12.5	2292	1.47	1359.39	330
	2401	9.0	2287	1.25	1594.09	315
	2402	20.0	2287	1.22	1629.09	310
	2501	6.0	2315	1.35	1711.42	310
Bad Honnef (RK 640.0) To Koeln (RK 689.5)	2501	7.5	2315	1.35	1711.42	310
	2502	12.5	2315	1.40	1652.71	445
	2503	11.0	2315	1.44	1611.36	450
	2601	17.0	2375	1.47	1612.17	390
	2602	1.5	2375	1.34	1771.06	410
Koeln (RK 689.5) To Dusseldorf (RK 759.60)	2602	13.0	2375	1.34	1771.06	410
	2603	13.5	2375	1.39	1709.8	395
	2701	20.0	2408	1.35	1778.23	365
	2702	5.2	2408	1.38	1743.82	325
	2703	15.4	2408	1.36	1775.96	425
Dusseldorf (RK 759.60) To Wesel (RK 814.0)	2703	2.4	2408	1.36	1775.96	425
	2801	18.8	2434	1.31	1863.66	300
	2802	16.2	2434	1.15	2114.09	300
	2901	17.0	2407	1.20	2011.12	300
Wesel (RK 814.0) To Lobith (RK 863.3)	2902	13.0	2407	1.15	2099.22	300
	3001	10.0	2409	1.08	2230.97	300
	3001	14.9	2409	1.08	2230.97	300
	3002	10.1	2409	1.08	2229.40	300
	3101	1.3	2383	1.16	2041.02	340

The observed C-t curves are available at Koblenz (RK 590.35), Bad Honnef (RK 640), Koeln (RK 689.5), Dusseldorf (RK 759.6), Wesel (RK 814), and at Lobith (RK 863.3). The observed concentration measurements were analysed for conservation of mass. The results of mass conservation analysis are summarised in Table 3.9. Based on the analysis for conservation of mass, the C-t curves at Wesel and Lobith were modified. The C-t measurements at Wesel and Lobith were divided by 0.7980 and 0.6711 to account for the loss of mass of the tracer.

Table 3.9 Steady State Gain at sampling stations on Rhine River

Measuring Station	Observed discharge (m^2/s)	Steady State Gain
Koblenz	2142	Reference mass
Bad Honnef	2315	0.9734
Koeln	2375	0.9771
Dusseldorf	2408	0.9554
Wesel	2407	0.7980
Lobith	2383	0.6711

The dispersion coefficient, D_L was estimated by the AD-VPM model as described in section 3.6.1.1 while testing the proposed model using 2600 series laboratory data. The D_L that gives the maximum value of Nash-Sutcliffe criterion (η) was considered as the appropriate dispersion coefficient. In this test case, the C-t curves at the station Koblenz and Bad Honnef were taken to estimate the dispersion coefficient. Based on the estimated reach averaged D_L and the average flow and flow and channel characteristics of the reach between Koblenz to Bad Honnef, the relational coefficient ϕ was estimated using Eqn.(3.23) as 0.116. The value of ϕ thus estimated was used to determine the D_L for the subsequent sub-

reaches using the Eqn. (3.23). The dispersion coefficients thus determined for different sub-reaches are presented in Table 3.10.

Table 3.10 Dispersion Coefficients for different reaches of River Rhine

Reach	Sub-Reach ID	Sub-Reach Length (km)	Dispersion Coefficient (m^2/s)
Koblenz (RK590.35) To Bad Honnef (RK 640.0)	-	49.65	1844.60
Bad Honnef (RK 640.0) To Koeln (RK 689.5)	2501	7.5	1883.17
	2502	12.5	1311.87
	2503	11.0	1297.29
	2601	17.0	1535.67
	2602	1.5	1460.76
Koeln (RK 689.5) To Dusseldorf (RK 759.60)	2602	13.0	1460.76
	2603	13.5	1516.24
	2701	20.0	1663.66
	2702	5.2	1868.41
	2703	15.4	2053.88
Dusseldorf (RK 759.60) To Wesel (RK 814.0)	2703	2.4	2053.88
	2801	18.8	2941.08
	2802	16.2	2941.08
	2901	17.0	2908.46
Wesel (RK 814.0) To Lobith (RK 863.3)	2902	13.0	2908.46
	3001	10.0	17249.63
	3001	14.9	17249.63
	3002	10.1	17249.63
	3101	1.3	15055.99

The C-t curves were simulated at Bad Honnef station (RK 640) in calibration mode, and at Koeln (RK 689.5), Dusseldorf (RK 759.6), Wesel (RK 814), and at Lobith (RK 863.3) stations in verification mode. The C-t curve at

station Koblenz (RK 590.35) was taken as the input for the simulations in the reach under consideration. Comparison of the observed and simulated C-t curves for Rhine River is shown in Fig. 3.11 and the results are summarised in Table 3.11. The AD-VPM model is able to simulate the observed C-t curves at all sampling stations downstream of Koblenz, except at Lobith, satisfactorily.
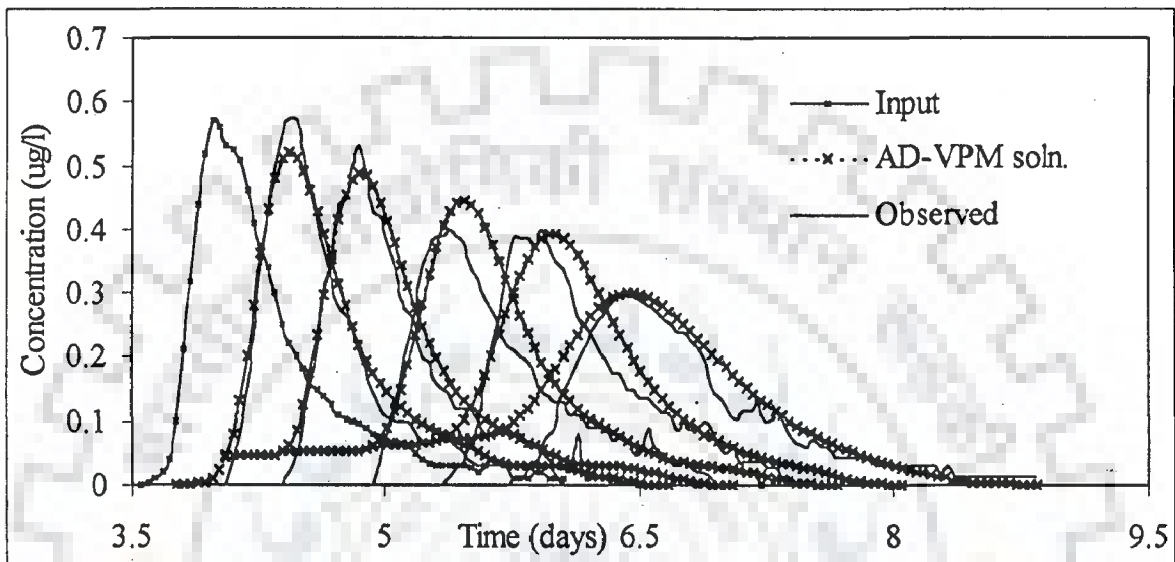
Figure 3.11 Observed and simulated C-t curves at different downstream stations in Rhine River

Table 3.11 Summary of the characteristics of the simulated and observed C-t curves of the Rhine River

Station at	Observed		Simulated by the AD-VPM model		Nash-Sutcliffe criterion (η) (%)
	Time to peak concentra tion (days)	Peak concentra tion (μg/l)	Time to peak concentra tion (days)	Peak concentra tion (μg/l)	
Bad Honnef	4.427	0.570	4.427	0.520	98.5
Koeln	4.844	0.530	4.844	0.489	98.2
Dusseldorf	5.386	0.400	5.469	0.446	92.0
Wesel	5.844	0.396	6.010	0.392	89.7
Lobith	6.407	0.296	6.428	0.301	65.0

3.6.2.3 Application to Colorado River

The data set of the tracer studies conducted on the Colorado River (Graf, 1995) were used to test the proposed AD-VPM model. Details of tracer experiments, the research inflow hydrographs controlled at Glen Canyon Dam, and available hydro-geometric channel characteristics for the sub-reaches of 380 km reach have been discussed by Graf (1995). The C-t data are presented in Appendix B 1. 3. The schematic diagram of the Colorado River reach is shown in Fig. 3.12.
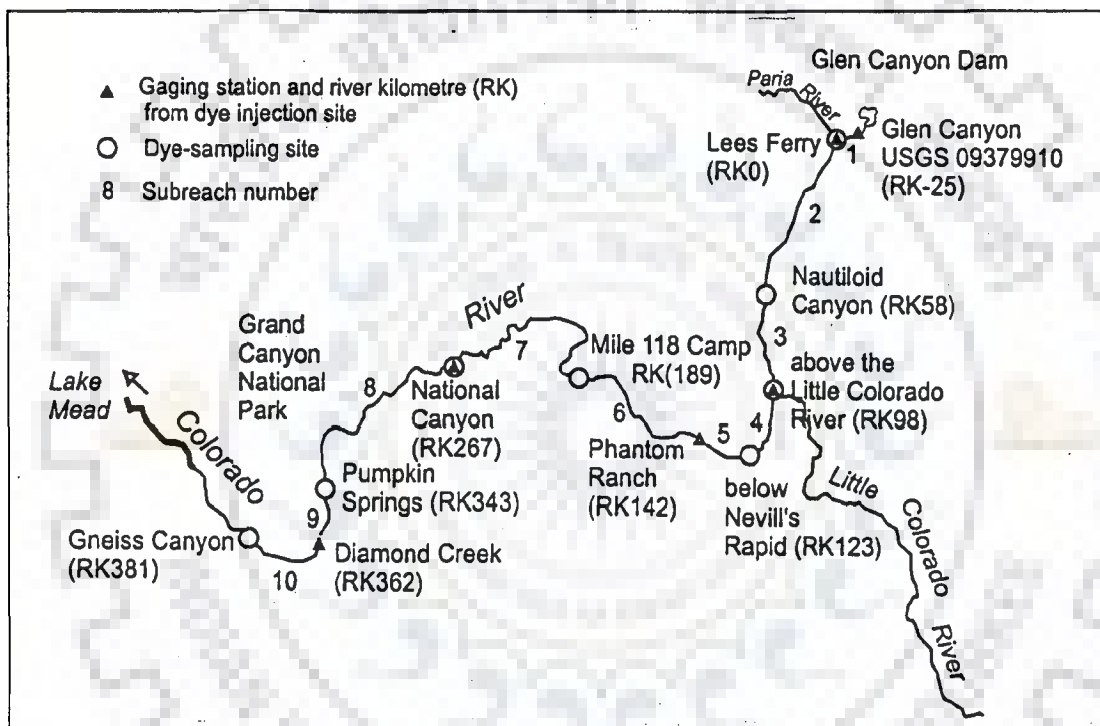
Figure 3.12 **Schematic study area, channel discretisation and location of dye sampling sites of Colorado River (Graf, 1995)**

During these experiments, under steady flow conditions, concentration measurements available at Nautiloid Canyon, above the Little Colorado, below Nevill's Rapid, Mile 118 camp, National canyon, Pumpkin spring, and at Gneiss Canyon located at a downstream distances of 58 km, 98 km, 123 km, 189 km, 267 km, 343 km, and 381 km from the tracer injection location respectively were used in this test case. The mass conservation analysis results showed that the dye loss was

insignificant at all the sampling stations (Graf, 1995). Hence, the observed C-t curves were used in the present study without any modification for mass conservation.

Reach averaged D_L was determined using the C-t curves at Nautiloid Canyon (input C-t curve) and at the station above Little Colorado River by the proposed AD-VPM model as described in section 3.6.1.1. This dispersion coefficient was used for the estimation of the relational coefficient ϕ using Eqn. (3.23) as 0.072. Using this value of $\phi=0.072$, the D_L for each of the subsequent sub-reaches used in the verification study was estimated from Eqn. (3.23). The observed reach length, the velocity, and the estimated dispersion coefficient of each of the sub-reaches are presented in Table 3.12.

Table 3.12 Dispersion coefficients for different sub-reaches of the Grand Canyon reach in the Colorado River during steady flow

Reach	Length of reach (m)	Average Velocity (m/s)	Dispersion Coefficient (m²/s)
Nautiloid - above Little Colorado	40600.0	0.75	154.40
Above Little Colorado.-Nevills rapid	24900.0	1.10	75.01
Nevill's rapid – M118 camp	66100.0	0.97	122.40
M118 camp – National Canyon	78600.0	1.10	135.56
National Canyon-Pumpkin spring	75700.0	1.10	204.86
Pumpkin spring - Gneiss Canyon	36900.0	1.00	132.31

The C-t curve observed at Nautiloid was routed using the dispersion coefficient D_L calibrated in the above manner to estimate the C-t curves at the downstream sampling stations in the Grand Canyon reach in verification mode. The comparison of observed and simulated C-t curves is presented in Fig. 3.13.
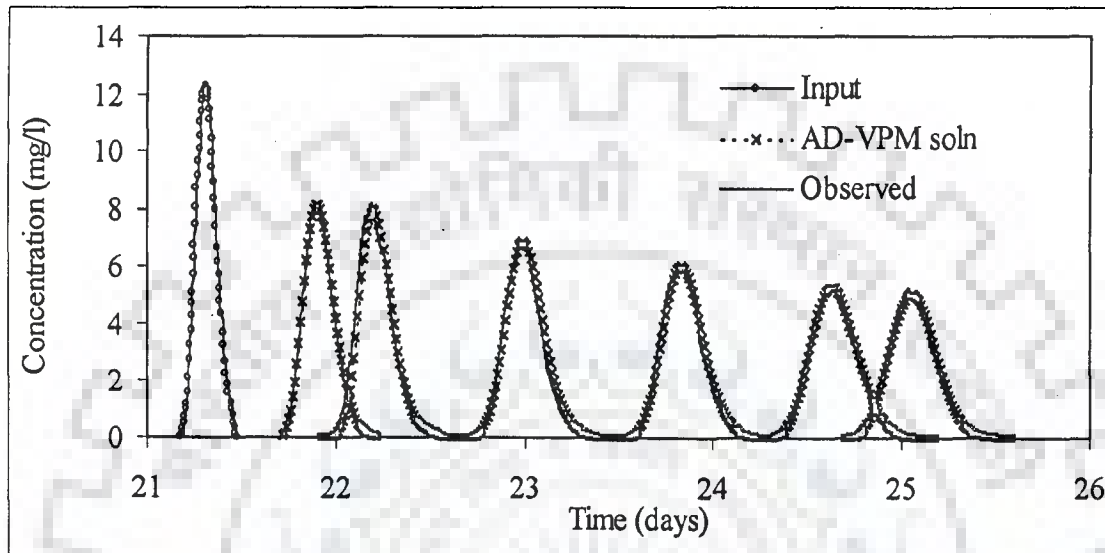
Figure 3.13 Observed and simulated C-t curves at different downstream stations in River Colorado

The Nash-Sutcliffe criterion, η value estimated at all the sampling stations were greater than 99% indicating the close reproduction of the observed C-t curves at each of these sampling stations. Such a good reproduction may be attributed to the quality of the experiments conducted under controlled environment, keeping the flow in the entire Grand Canyon reach as constant at approximately $428m^3/s$ by controlling the Glen Canyon dam releases. The following statement of Graf (1995) confirms this inference

"the C-t data under steady flow fit a simple one-dimensional mixing model ·without modification to account dead zone, better than data for many rivers for which measurements are available."

3.7 DISCUSSION OF RESULTS

The AD-VPM model is developed based on the concept (section 3.2 and 3.3) used in the development of the VPM model. It is appropriate to bring out the fact that the model formulated using Eqn. (3.19) to Eqn. (3.22) is the same as that proposed by Koussis et al. (1983). However, Koussis et al. (1983) obtained the parametric relationships for K_c and θ_c using the matched advective diffusivity approach advocated by Cunge (1969). Further, the matched diffusivity approach of Koussis et al. (1983) has been developed from the equation governing pure advection only, without considering dispersion process, which is contrary to the Fick's law governing the solute transport process in streams. Unlike in the case of flow routing wherein a one-to-one relationship between stage and discharge is possible, as postulated by Cunge (1969), implying absence of dispersion, the same logic is not applicable for solute transport in rivers. The proposed approach in the present study is devoid of these logical errors. The advantage of the proposed approach is that it enables to extend the use of Eqn. (3.19) to Eqn. (3.22) for solute transport modelling under unsteady flow conditions also, as discussed in Chapter 4. This is due to the reason that the AD-VPM model enables the integration of its parameters K_c and θ_c with K_f and θ_f of the VPM flow routing model.

In the Koussis et al. (1983) approach the weighting parameters θ_c is a function of Courant number $(= U\Delta t/\Delta x)$ and dispersion coefficient (Eqn. 2.13). Hence, to match the numerical dispersion generated in his model with a constant physical dispersion coefficient, it is necessary to keep Δx and Δt at constant values over the entire routing period (Eqn. 2.13). It is not possible to use unequal Δt values, which will lead to change in θ_c and, thereby, change in the dispersion coefficient. Therefore, it is not possible to use the observed concentration measurements, which are generally available at unequal time intervals. However, in

the AD-VPM model the weighting parameter θ_c is a function of the solute dispersion coefficient, velocity and spatial step size (Eqn. 3.17). The change in routing time interval Δt will not alter θ_c and thereby the dispersion coefficient. In the AD-VPM approach, the parameters K_c and θ_c can be kept at a constant values and the routing coefficients ω_1, ω_2 and ω_3 (Eqn. 3.22) can be varied for any change in the time interval Δt over the routing period. Hence, the AD-VPM model can handle situations where the observed concentration measurements are available at unequal time intervals. This has been proved while validating the AD-VPM model using series 2600 laboratory experimental data (section 3.6.1.1).

It is seen from Figs. 3.2 (i) to Fig. 3.2 (iii) that for a given velocity as the value of D_L increases, the solution of the AD-VPM model deviates from the analytical solution of AD equation. Proposed AD-VPM model reproduces the analytical solution of the AD equation (Eqn.2.2) satisfactorily, if the dispersion coefficient is within the applicability range of the proposed model (section 3.5.2). If the dispersion coefficient is higher than the limiting dispersion coefficient for a given velocity (Eqn. 3.25), then the proposed model fails to give satisfactory results as seen in Fig. 3.14.

In solute transport studies, when observed C-t curves are not available, the D_L has to be estimated using a suitable expression from among the expressions available in the literature (Table 2.1). Generally, it is not possible to determine the dispersion coefficient accurately in a river reach using any one of the empirical expressions developed for estimating the D_L as a function of the hydro-geometric characteristics of the river. When error in estimation of D_L is within $\pm$ 20% , the AD-VPM model can be used to simulate the downstream C-t curves satisfactorily, as explained in section 3.5.3 (Fig. 3.4).
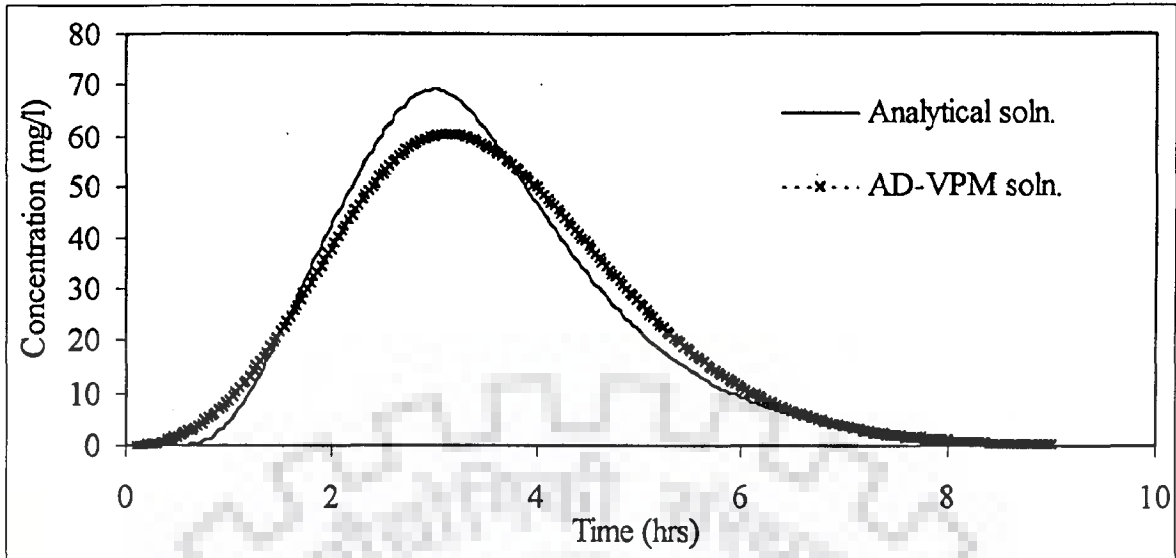
Figure 3.14(i) Analytical and AD-VPM solutions for U=0.45m/s, D_L=227.6m^2/s, X=4.0km
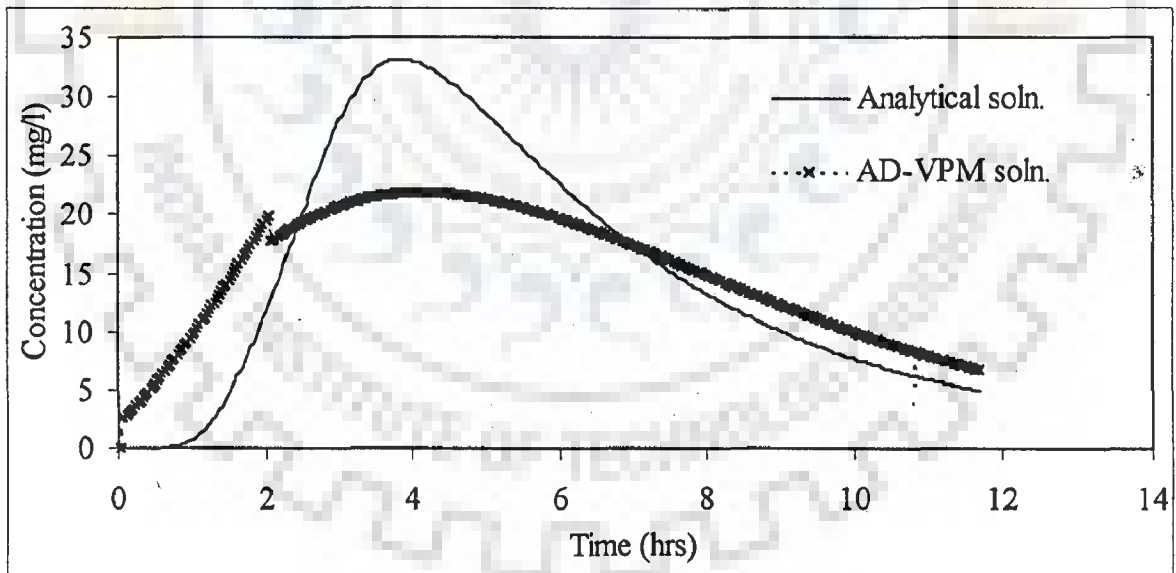
Figure 3.14(ii) Analytical and AD-VPM solutions for U=0.1m/s, D_L=54.7m^2/s, X=2.0km

The AD-VPM model produces initial negative response, particularly at high spatial step sizes. Reducing the spatial step size may reduce or eliminate this problem. However, one may accept the initial reduced response, as long as it does not affect the practical utility of the results.

The proposed AD-VPM model is verified under steady flow conditions by simulating (i) the analytical solutions obtained for an uniform pulse input (ii) using two laboratory test data (Fisher, 1966), and (iii) using three field experimental data sets. The satisfactory performance of the AD-VPM model in the above cases demonstrates the suitability of the proposed AD-VPM model for its application to longitudinal dispersion studies in rivers.

The performance of the AD-VPM model in the Missouri River test case (section 3.6.2.1) in reproducing the observed C-t curves in terms of Nash-Sutcliffe criterion, (η) is found to be greater than 96%. The flow and channel characteristics are not constant from one sampling station to another sampling station. Hence, the sub-reach averaged flow and channel characteristics in each-sub-reach were used in the simulations of the observed C-t curves. The satisfactory simulations of the observed C-t curves using the AD-VPM model implies that the sub-reach averaged hydro-geometric characteristics can be used as the representative values of the respective sub-reaches. It is worth noting that the parameter D_L obtained by the AD-VPM model for Fischer's laboratory data and Missouri river data (Yotsukura et al., 1970) closely correspond to the values of D_L obtained by Fischer (1966) and Yotsukura et al. (1970) respectively.

In the case of Rhine River, agreement between the simulated and observed C-t curves at Lobith in verification mode is not satisfactory (Fig. 3.11 and Table 3.11). This may be due to the fact that there is considerable loss of mass of solute at Lobith. The observed C-t curve at Lobith is modified using a dividing factor of 0.6771 based on the estimated loss of mass (Table 3.9), which is as high as 32%. Because of the considerable loss, there will be uncertainties involved in the

modified C-t curves (Nordin and Troutman, 1980). The observed loss of mass of solute at sampling station Wesel and Lobith may be due to some additional mechanism that is responsible for considerable loss of mass, which is to be actually accounted for while simulating the C-t curve at these sampling stations. Moreover, the dispersion coefficient is too high (Table 3.10). The large dispersion may be due to the presence of either dead zone or transient storage mechanism, or absorption or a combination of these processes. It was already stated that the proposed AD-VPM model might not simulate such dispersion dominated solute transport process satisfactorily (section 3.5.1).

In the Colorado River test case, the performance of the AD-VPM model in simulating the observed C-t curves is good. The following may be the possible reasons:

(i)   The dye loss was insignificant during each measurement, no adjustment of C-t curve for loss of mass was required.

(ii)   The flow from the dam is released under controlled condition to maintain a steady flow of approximately 428 m^3/s in channel during the entire period of experimentation.

In Colorado River tracer experiments, the loss of mass of dye was insignificant unlike in the case of tracer experiments in other rivers where the loss of mass was noted. The results demonstrate the ability of the AD-VPM model for practical solute transport applications. It is noteworthy that the approach followed in the present study allows one to extend it to the study of dispersion under unsteady flow conditions.

3.8   CONCLUSIONS

In this chapter an equation termed as Approximate Advection-Dispersion equation (Eqn. 3.10) has been developed, assuming linear variation of concentration with x within a small reach length Δx. Using the Approximate Advection-

Dispersion equation and adopting the concept used in the development of VPM flow routing model, a model termed as AD-VPM model for solute routing has been proposed (section 3.3). The proposed AD-VPM model is devoid of the logical inconsistencies that exist in the Koussis et al. (1983) approach. The concept of the VPM flow routing approach adopted in the development of the proposed AD-VPM model enables one to use the observed input C-t measurements at unequal time intervals in routing the solute concentration through a river reach. In the Koussis approach it is not possible to use solute concentrations at unequal time intervals as input, because the variation in time step size changes the dispersion coefficient (Eqn. 2.13). It is found that the proposed AD-VPM model is capable of reproducing the analytical solution of the AD equation for uniform pulse input with Nash-Sutcliffe criterion (η) > 99% when $D_L \leq 415.64\ U^{1.71}$ (section 3.5.2). The analysis of the model parameters is presented. It is observed that ±20% variation in D_L does not affect the simulation results obtained by the AD-VPM model in reproducing the analytical solution for a given dispersion coefficient. The sensitivity of the solution of the AD-VPM model for a change in number of reaches has also been studied (section 3.5.3.2). It is found that the decrease in size of sub-reach length below a particular Δx, in which the assumption of linear variation of concentration with x holds well, would not influence the solution of the AD-VPM model. The practical utility of this model is demonstrated by verifying its applicability, using laboratory data (Fischer, 1996) and three sets of field data from experiments conducted on Missouri River, Rhine River, and Colorado River. It is found that the proposed model works satisfactorily to simulate the solute transport in these rivers.

The similarity of both the VPM flow routing model and the AD-VPM solute transport model enables to integrate their parameters. This integration of parameters is important while using the AD-VPM model to simulate the solute transport under unsteady streamflow conditions. This extension is presented in the next chapter.

SOLUTE TRANSPORT MODELLING USING APPROXIMATE ADVECTION-DISPERSION EQUATION: UNSTEADY FLOW CASE

4.1 GENERAL

The solute transport under unsteady stream flow conditions is a combined process of unsteady flow and unsteady solute movement. The flow diffusion and the solute dispersion models need to be coupled properly for simultaneous routing of both the variables. In the past, attempts have been made to couple both flow and solute routing models (Keefer and Jobson, 1978; Price, 1982; and Gabriele and Perkins, 1997). However, deficiencies with the existing coupled models (Section 2.4.2 in Chapter 2) such as improper integration of flow and solute movement processes, use of complex solution approaches, and inability to link the model parameters of both the processes necessitate the development of an alternate approach that is reliable and less cumbersome. To overcome the above mentioned deficiencies, the mathematical similarity between the convection-diffusion equation (Eqn. 3.1, Hayami, 1951) governing the flood wave movement and the advection-dispersion equation (Eqn. 2.2) governing the solute dispersion process may be favourably employed to develop a common solution structure suitable for modelling both the processes. The AD-VPM model developed in Chapter 3 to study the solute transport process in rivers under steady flow conditions has a model structure similar to that of the VPM model used for flood routing. This AD-VPM model can be extended to study the longitudinal dispersion of solute under unsteady streamflow conditions.

This chapter presents (i) a brief description of the VPM model for flow routing, (ii) establishing the linkage of parameters of the AD-VPM and the VPM

models, and (iii) developing simultaneous routing procedure for flow and solute dispersion. The proposed model is tested using hypothetical and field data.

4.2 MODEL DEVELOPMENT

The AD model governing the solute transport process in rivers with uniform cross-section is described by equation (also see Eqn. 2.2)

$$\frac{\partial C}{\partial t} + U \frac{\partial C}{\partial x} = D_L \frac{\partial^2 C}{\partial x^2} \tag{4.1}$$

The flow routing model governing the flow movement in rivers with uniform cross-section has the same form as that of the solute transport model, given by (also see Eqn. 2.28)

$$\frac{\partial Q}{\partial t} + c_k \frac{\partial Q}{\partial x} = D_f \frac{\partial^2 Q}{\partial x^2} \tag{4.2}$$

The combined process of flow and solute movement in rivers under unsteady flow condition may be modelled either by solving the above two equations simultaneously or solving them one-by-one, first solving the flow equation to arrive at the entire discharge hydrograph, which is subsequently used to solve the solute transport equation to arrive at the C-t curve. The simultaneous solution of Eqns.(4.2) and (4.1) to solve for the variables Q and C respectively at any time using the numerical methods is cumbersome procedure. But the one-by-one sequential solution approach is used in the current practices (Keefer and jobson, 1978). However, simultaneous solution of Eqns (4.1) and (4.2) may be arrived at using the following approximate equations.

$$\frac{\partial C}{\partial t} + U \frac{\partial C}{\partial x} = 0 \tag{4.3}$$

and

$$\frac{\partial Q}{\partial t} + c_k \frac{\partial Q}{\partial x} = 0 \tag{4.4}$$

The solution of Eqn. (4.3) using the VPM type algorithm was demonstrated in Chapter-3 to model the solute dispersion process under steady flow conditions.

4.2.1 Solute Transport Simulation Under Unsteady Flow Conditions

The VPM method of flow routing is briefly described herein for the sake of bringing out the similarity in the solution procedures of flow routing and solute routing. Location of cross-sections referred in discharge routing may be seen from the definition sketch given in Fig. 4.1.
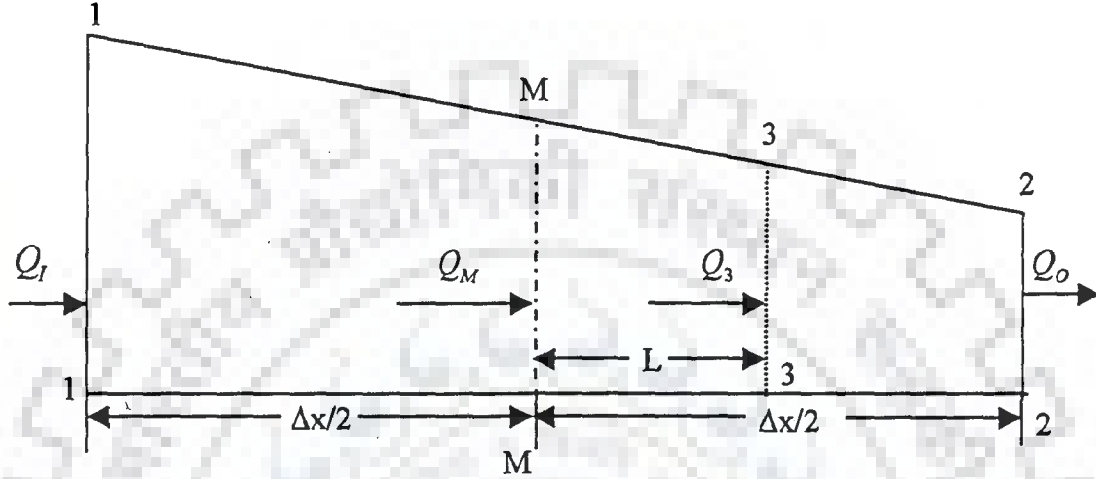
Figure 4.1 Definition sketch of the Muskingum flow routing reach

4.2.1.1 Flow Routing

The Variable Parameter Muskingum method proposed by Perumal (1994a) is used in the present study for flow routing:

The VPM flow routing parameters K_f and θ_f have been expressed in terms of physical properties of flow and channel geometry as

$$K_f = \frac{\Delta x}{\left[1 + m\left[\frac{P\,\partial R/\partial y}{\partial A/\partial y}\right]_3\right]U_3} \tag{4.5}$$

$$\theta_f = \frac{1}{2} - \frac{Q_3\left[1 - m^2 F_M^2\left[\frac{P\partial R/\partial y}{\partial A/\partial y}\right]_M^2\right]}{2S_0\frac{\partial A}{\partial y}\Big|_3\left[1 + m\left[\frac{P\partial R/\partial y}{\partial A/\partial y}\right]_3\right]U_3\Delta x} \tag{4.6}$$

where, R is the hydraulic radius, F_M is the Froude number at the middle of the reach Δx, P is the wetted perimeter, m is a constant (=2/3 for Manning's friction

law and =1/2 for Chezy friction law), and the suffix 3 refers to a section downstream from the mid-section of the routing reach Δx under consideration (Fig. 4.2). The above expressions of K_f and θ_f can be written as

$$K_f = \frac{\Delta x}{c_k} \tag{4.7}$$

in which c_k is the wave celerity, given by

$$c_k = \left[1 + m\left(\frac{P \partial R / \partial y}{\partial A / \partial y}\right)_3\right] U_3 \tag{4.8}$$

and

$$\theta_f = \frac{1}{2} - \frac{D_f}{c_k \Delta x} \tag{4.9}$$

in which D_f can be termed as the flow diffusion coefficient given by

$$D_f = \frac{Q_3 \left[1 - m^2 F_M^2 \left(P \frac{\partial R / \partial y}{\partial A / \partial y}\right)_M^2\right]}{2 S_0 \left(\frac{\partial A}{\partial y}\right)_3} \tag{4.10}$$

The flow routing equation is expressed as

$$(Q_o)_j = \varepsilon_1 (Q_I)_j + \varepsilon_2 (Q_I)_{j-1} + \varepsilon_3 (Q_o)_{j-1} \tag{4.11}$$

where $(Q_I)_j$ and $(Q_o)_j$ are the rate of inflow and outflow at time $j\Delta t$, respectively. $(Q_I)_{j-1}$ and $(Q_o)_{j-1}$ are the rate of inflow and outflow at time $(j-1)\Delta t$, respectively, where Δt is the routing time interval. The Muskingum coefficients ε_1, ε_2 and ε_3 are expressed as

$$\varepsilon_1 = \frac{-K_f \theta_f + \Delta t / 2}{K_f (1 - \theta_f) + \Delta t / 2} \tag{4.12a}$$

$$\varepsilon_1 = \frac{K_f \theta_f + \Delta t / 2}{K_f (1 - \theta_f) + \Delta t / 2} \tag{4.12b}$$

$$\varepsilon_3 = \frac{K_f (1 - \theta_f) - \Delta t / 2}{K_f (1 - \theta_f) + \Delta t / 2} \tag{4.12c}$$

98

In the VPM flow routing, the parameters K_f and θ_f are constant during a routing time interval Δt, but vary from one time interval to the next time interval in accordance with the variation of flow.

4.2.1.2 Solute Routing

The solute routing model (AD-VPM) has been developed in Chapter-3 for studying the solute movement in uniform channels and rivers under steady flow conditions. The routing equation and the associated parameter relationships are expressed as

$$C_{o,j} = \omega_1 C_{i,j} + \omega_2 C_{i,j-1} + \omega_3 C_{o,j-1} \qquad (4.13)$$

where, $C_{i,j}$ and $C_{i,j-1}$ are the inflow concentrations at time $j\Delta t$ and $(j-1)\Delta t$ respectively; $C_{o,j}$ and $C_{o,j-1}$ are the outflow concentrations at time $j\Delta t$ and $(j-1)\Delta t$ respectively; ω_1, ω_2, and ω_3 are the coefficients of the routing equation expressed as

$$\omega_1 = \frac{-K_c \theta_c + \Delta t/2}{K_c(1-\theta_c) + \Delta t/2} \qquad (4.14a)$$

$$\omega_2 = \frac{K_c \theta_c + \Delta t/2}{K_c(1-\theta_c) + \Delta t/2} \qquad (4.14b)$$

$$\omega_3 = \frac{K_c(1-\theta_c) - \Delta t/2}{K_c(1-\theta_c) + \Delta t/2} \qquad (4.14c)$$

in which

$$K_C = \frac{\Delta x}{U} \qquad (4.15)$$

and

$$\theta_C = \frac{1}{2} - \frac{D_L}{U\Delta x} \qquad (4.16)$$

The proposed AD-VPM model developed for steady flow conditions is extended to study longitudinal dispersion of solute under unsteady streamflow conditions. In extending this model, it is assumed that the stream flow in a river

99

reach, Δx, is steady and uniform over a routing time interval Δt, but varies from one time interval to the next time interval due to unsteady flow conditions. Based on this assumption, Eqn. (4.13) to (4.16) can be used to study the longitudinal dispersion of solute under unsteady streamflow conditions. The velocity at section 3, as shown in Fig. 3.1, is used to compute the characteristic reach length, L (Eqn. 3.16, section 3.3). Hence, during unsteady flow Eqn. (4.15) and Eqn. (4.16) are expressed as

$$K_c = \frac{\Delta x}{U_3} \tag{4.17}$$

and

$$\theta_c = \frac{1}{2} - \frac{D_L}{U_3 \Delta x} \tag{4.18}$$

The solute transport model parameters K_c and θ_c are kept constant during a routing time interval Δt. But K_c and θ_c are varied from one time interval to the next time interval in accordance with the variation of flow. Thus, a variable parameter solute routing model is developed which is similar to that adopted in VPM flow routing model, wherein the model parameters K_f and θ_f are constant during a routing time interval but vary from one time interval to the next time interval.

The model structure of the VPM flow routing and the AD-VPM solute routing being similar, it is now possible to simulate both the processes simultaneously. To achieve this, the parameters of flow routing (K_f and θ_f), and solute routing (K_c and θ_c) methods are interlinked. The reach travel time of flow (K_f), and that of solute cloud (K_c) are estimated using Eqn. (4.7) and Eqn. (4.17) respectively. The relationship between K_f and K_c is obtained using Eqns. (4.7), (4.8) and (4.17), as

$$K_c = K_f \left[1 + m \left(\frac{P \partial R / \partial y}{\partial A / \partial y} \right)_3 \right] \tag{4.19}$$

In a similar manner, the relationship between θ_f and θ_c may be obtained using Eqns. (4.9), (4.18) and (3.23) as

$$\theta_c = \frac{1}{2} - \phi \left[1 + m \left(\frac{P \partial R / \partial y}{\partial A / \partial y} \right)_3 \right] (0.5 - \theta_f) \tag{4.20}$$

Using Eqns. (3.23) and (4.10), the relationship between D_L and D_f can be expressed as

$$D_L = \phi \, \frac{Q_3 \left[1 - m^2 F_M^2 \left[\frac{P \partial R / \partial y}{\partial A / \partial y} \right]_M^2 \right]}{2 S_0 \left(\frac{\partial A}{\partial y} \right)_3} \tag{4.21}$$

Using Eqns. (4.18) and (4.21), the parameter θ_c can be expressed in terms of flow and channel characteristics as

$$\theta_c = \frac{1}{2} - \frac{\phi \, Q_3 \left[1 - m^2 F_M^2 \left[\frac{P \partial R / \partial y}{\partial A / \partial y} \right]_M^2 \right]}{2 S_0 \left. \frac{\partial A}{\partial y} \right|_3 U_3 \Delta x} \tag{4.22}$$

In the proposed solute dispersion studies under unsteady flow conditions, the necessary flow details such as c_k, U_3, and D_f were obtained from the VPM flow routing model and these are used to determine the solute routing parameters in a routing time interval, Δt. The solution algorithm is depicted in Fig. 4.2.

4.3 EVALUATION OF THE MODEL

The AD-VPM model has been described in Chapter-3 and it was meant for solute transport under steady flow conditions. The same is employed herein also, but for solute transport under unsteady flow conditions. The AD-VPM solute routing model is coupled with the VPM flow routing model for solute transport under unsteady flow conditions. Hence, for satisfactory application of the model, it should satisfy the applicability criteria of both the VPM flow routing model and the AD-VPM solute transport model.

$$\boxed{\text{Routing Step } J = 1}$$

Estimate initial K_f and θ_f and K_c and θ_c using Eqns. (4.5) & (4.6) and Eqns. (4.19) & (4.22) using initial values of flow

$$J = J + 1$$

$$\text{Iteration step } I = 1$$

Estimate ε_1, ε_2 & ε_3,

$$\varepsilon_1 = \frac{-K_f\theta_f + \Delta t/2}{K_f(1-\theta_f) + \Delta t/2}; \quad \varepsilon_2 = \frac{K_f\theta_f + \Delta t/2}{K_f(1-\theta_f) + \Delta t/2}; \quad \varepsilon_3 = \frac{K_f(1-\theta_f) - \Delta t/2}{K_f(1-\theta_f) + \Delta t/2}$$

and ω_1, ω_2 and ω_3 using Eqns. (4.14)

Estimate $(Q_O)_j = \varepsilon_1(Q_I)_j + \varepsilon_2(Q_I)_{j-1} + \varepsilon_3(Q_O)_{j-1}$

$C_{o,j} = \omega_1 C_{i,j} + \omega_2 C_{i,j-1} + \omega_3 C_{o,j-1}$

Estimate $Q_3 = \theta_f (Q_I)_j + (1-\theta_f)(Q_O)_j$

Estimate y_M using Newton-Raphson Method from $Q_3 = A_M C_f R_M^m S_0^{1/2}$

Estimate $Q_M = [(Q_I)_j + (Q_O)_j]/2$

Estimate $F_M = Q_M^2 (\partial A/\partial y)|_M / g (A_M)^3$

Estimate, $y_3 = y_M + (Q_3 - Q_M)/(\partial A/\partial y)|_M \{1 + m [(P\partial R/\partial y)/(\partial A/\partial y)|_M\} U_M$

Estimate A_3 corresponding to y_3

Estimate $U_3 = Q_3/A_3$

Estimate revised K_f and θ_f and K_c and θ_c for the present routing step using Eqns. (4.5) & (4.6) and Eqns. (4.19) & (4.22) respectively

$$I = I + 1$$

No ← IS $I > 2$?

yes

Estimate $y_J = y_M + (O_J - Q_M)/(\partial A/\partial y)|_M \{1 + m [(P\partial R/\partial y)/(\partial A/\partial y)]_M \} U_M$

No IS $J \geq N$ steps?

yes

$$\boxed{\text{STOP}}$$

Figure. 4.2 The solution algorithm for the AD-VPM model under unsteady streamflow conditions

102

The hydrograph to be routed should satisfy the criterion $|(1/S_0)(\partial y/\partial x)| < 1$ at any time for successful application of VPM flow routing model with S_0 and $\partial y/\partial x$ denoting channel bed slope and water surface slope respectively (Perumal, 1994b).

In the development of the AD-VPM solute routing model under unsteady flow conditions, it is assumed that the flow is steady during a routing time interval, but varies from one time interval to the next. Hence, the applicability criterion of the AD-VPM model evaluated in Chapter 3 under steady flow conditions is applicable here also. This applicability criterion is expressed as $D_L = 415.64 \ U^{1.71}$, Eqn. (3.25), and has been developed based on the ability of the AD-VPM model to closely reproduce the analytical solution of the AD equation for uniform pulse input. Accuracy of the AD-VPM model depends on the estimated dispersion coefficient for a given velocity. If the estimated D_L is less than the limiting value of D_L obtained using Eqn. (3.25), at any time during routing, the performance of the proposed AD-VPM model under unsteady flow conditions may be considered accurate.

The experimental studies of solute transport under unsteady streamflow conditions in rivers are very few, perhaps, due to the following difficulties in experimentation:

1. Controlling flow variation in the river to suit the experimental requirement,

2. Simultaneous monitoring, and recording of discharges and concentrations at regular time intervals at different downstream sections from the point of injection of solute or tracer.

Further, it is not possible to obtain an analytical solution of the system of partial differential equations governing coupled flow and solute transport processes. Hence, the proposed AD-VPM model for studying solute transport under unsteady flow conditions needs to be tested by simulating the numerical solution of the AD

103

equation coupled with the Saint- Venant Equations (SVE), termed herein as the SVE-AD solution for hypothetical data input.

4.3.1 Solution of the SVE-AD Model

To arrive at the benchmark solution of the SVE-AD model, the following procedure was used:

A given hydrograph at the input section of a uniform rectangular cross-section was routed to the desired location in the channel reach using the numerical solution procedure of the Saint-Venant equations (Viessman et al., 1977) expressed as:

$$\frac{\partial A}{\partial t} + \frac{\partial Q}{\partial x} = 0 \qquad \text{(continuity equation)} \qquad (4.23)$$

and

$$S_f = S_0 - \frac{\partial y}{\partial x} - \frac{Q}{gA}\frac{\partial U}{\partial x} - \frac{1}{g}\frac{\partial U}{\partial t} \qquad \text{(momentum equation)} \qquad (4.24)$$

The results obtained by solving the SVE were used in solving the AD equation to arrive at the benchmark SVE-AD solution using the following approach:

Runkel (1998) used the Crank-Nicolson numerical method to solve the Transient Storage (TS) model equations (Eqns. 2.29a and 2.29b). These equations converge to AD equation, if α and β are assumed to be zero. Hence, the algorithm suggested for solving the TS model can be used for AD model by assuming $\alpha = 0$ and $\beta = 0$. The oscillation problems associated with Runkel solution (1998) were avoided by maintaining the Peclet Number $(P_e = U\Delta x/D_L)$ sufficiently low, based on the numerical experiments carried out during the study. Thus, the stable solution obtained by solving the SVE-AD equations was considered as the benchmark solution needed for the evaluation of the solution of the AD-VPM model.

104

The agreement between the solutions of the AD-VPM model and the SVE-AD method is measured using the Nash-Sutcliffe criterion (η)(Nash and Sutcliffe, 1970) given by Eqn. (3.24).

4.3.2 Hypothetical Test Case

The numerical experiments were carried out by routing a given inflow hydrograph and a given C-t curve in uniform rectangular channels using the SVE-AD equations. The rectangular channels of 40km length with uniform width of 50 m and 100 m were considered for hypothetical tests. The configurations of the channels considered in the study are described in Table 4.1.

Table 4.1 Configurations of hypothetical channel

Channel ID	Width (m)	Bed Slope (S_o)	Manning's roughness (n)
C-1	50	0.0002	0.02
C-2	100	0.0002	0.02
C-3	50	0.0004	0.04
C-4	100	0.0004	0.04

The inflow hydrograph, defined by a four parameter Pearson Type-III distribution was used in these numerical experiments and it is expressed as

$$I(t) = I_b + (I_p - I_b)\left(\frac{t}{t_p}\right)^{\frac{1}{\gamma-1}} \exp\left(\frac{1-t/t_p}{\gamma-1}\right) \tag{4.25}$$

where, I_b is the initial steady flow (100 m^3/s), I_p is the peak flow (1000 m^3/s), t_p is the time to peak (10 hr), and γ is the skewness factor (1.15). Similarly, an input C-t curve having the form of Pearson Type-III distribution expressed by the following equation was used, as the input required for solute routing in the channel.

$$C(t) = C_b + (C_p - C_b)\left(\frac{t}{t_{cp}}\right)^{\frac{1}{\gamma_c-1}} \exp\left(\frac{t - t/t_{cp}}{\gamma_c - 1}\right) \qquad (4.26)$$

where, C_b is the initial concentration (0 mg/l), C_p is the peak concentration (50 mg/l), t_{cp} is the time to peak (10hrs), and γ_c is the skewness factor (1.15). The same form of input was used by Camacho (2000) while studying the solute transport in channels using the ADZ model under unsteady flow conditions. The inflow hydrograph and the C-t curve applied at the same input point were simultaneously routed through the channel using the proposed AD-VPM model. A routing time interval of 15 min. was used in the numerical experiments. A value of ϕ=0.116 was used in the hypothetical test cases as it is recommended by McQuivey and Keefer (1974) to compute the dispersion coefficient using Eqn. (3.23). An additional value of ϕ=0.058 was considered to evaluate the performance of the AD-VPM model during advection dominated solute transport process, as dispersion during unsteady flow is advection dominated phenomenon (Bedford et al., 1983). The accuracy of the reproduction of C-t curve shape and size was evaluated using the Nash-Sutcliffe criterion given by Eqn. (3.24). The results are shown in Table 4.2. The comparison of the solutions of the AD-VPM model with the corresponding benchmark solutions is shown in Figs. 4.3 to 4.6. Typical range of velocities, the estimated D_L values and the limiting D_L values computed using Eqn. (3.25) for these experiments are summarised in Table 4.3.
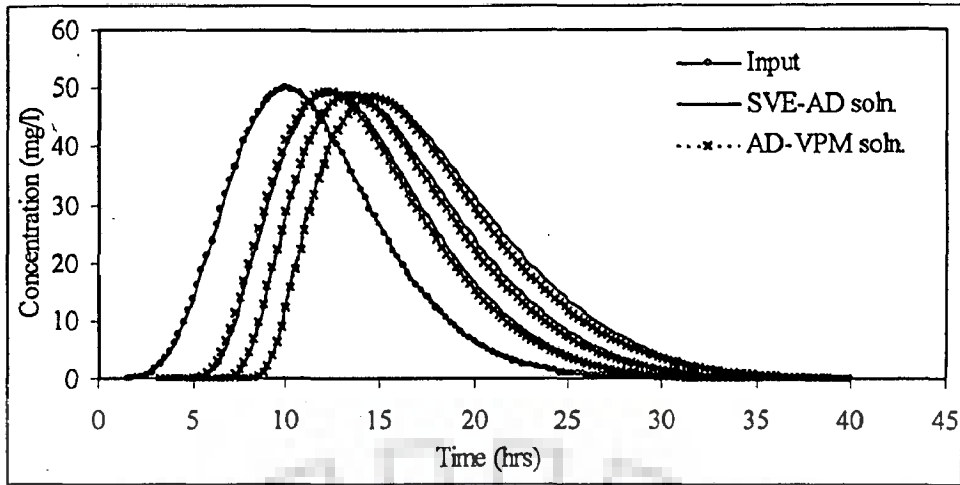
Figure 4.3(i)   SVE-AD and AD-VPM solutions for $\phi = 0.058$, channel type C-1 at 10, 20 and 30km downstream from source of solute.
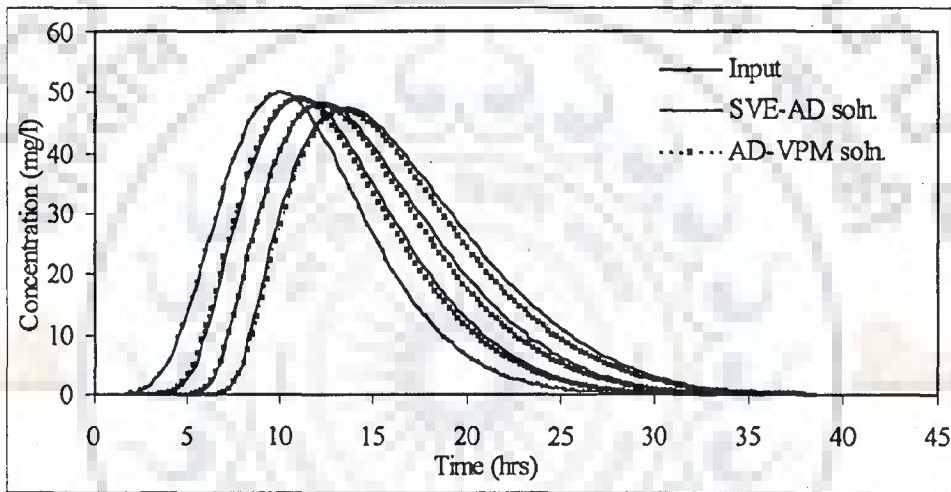
Figure 4.3(ii)   SVE-AD and AD-VPM solutions for $\phi = 0.116$, channel type C-1 at 10, 20 and 30km downstream from source of solute.
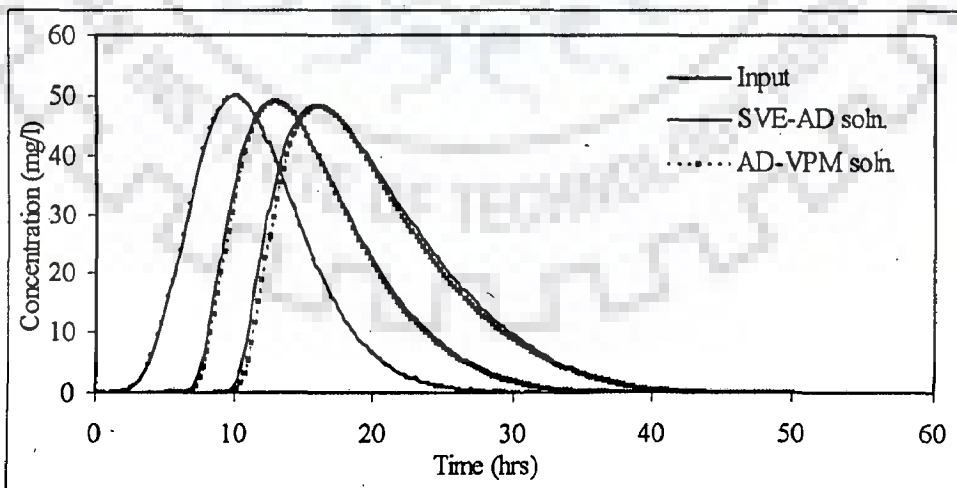
Figure 4.4(i)   SVE-AD and AD-VPM solutions for $\phi = 0.058$, channel type C-2 at 20 and 30km downstream from source of solute.
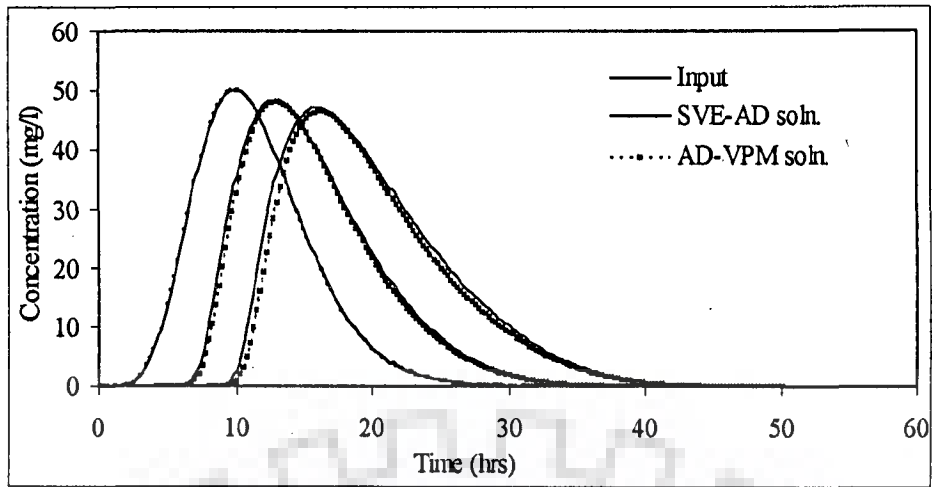
Figure 4.4(ii)   SVE-AD and AD-VPM solutions for $\phi = 0.116$, channel type C-2 at 20 and 30km downstream from source of solute.
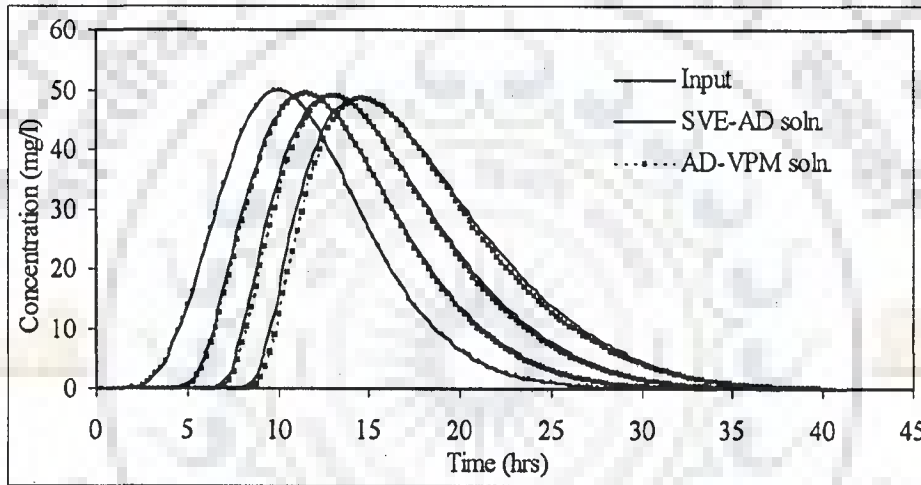
Figure 4.5(i)   SVE-AD and AD-VPM solutions for $\phi = 0.058$, channel type C-3 at 10, 20 and 30km downstream from source of solute.
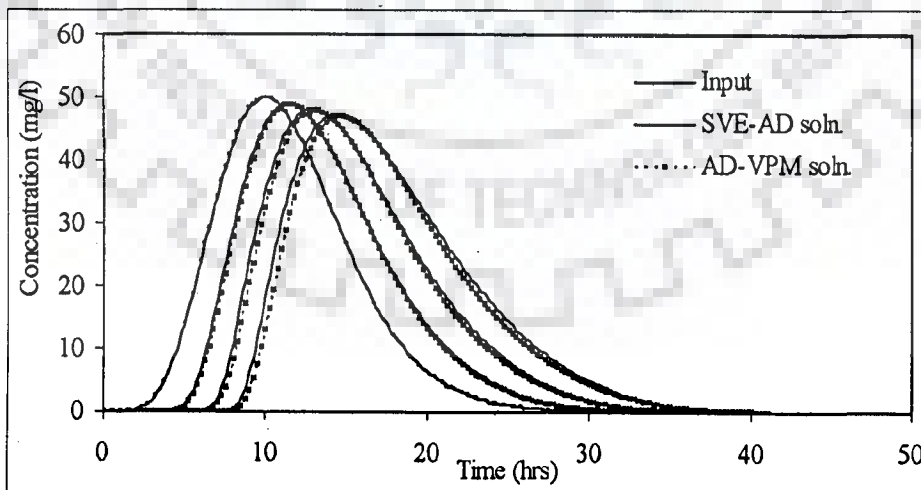
Figure 4.5(ii) SVE-AD and AD-VPM solutions for $\phi = 0.116$, channel type C-3 at 10, 20 and 30km downstream from source of solute.

108
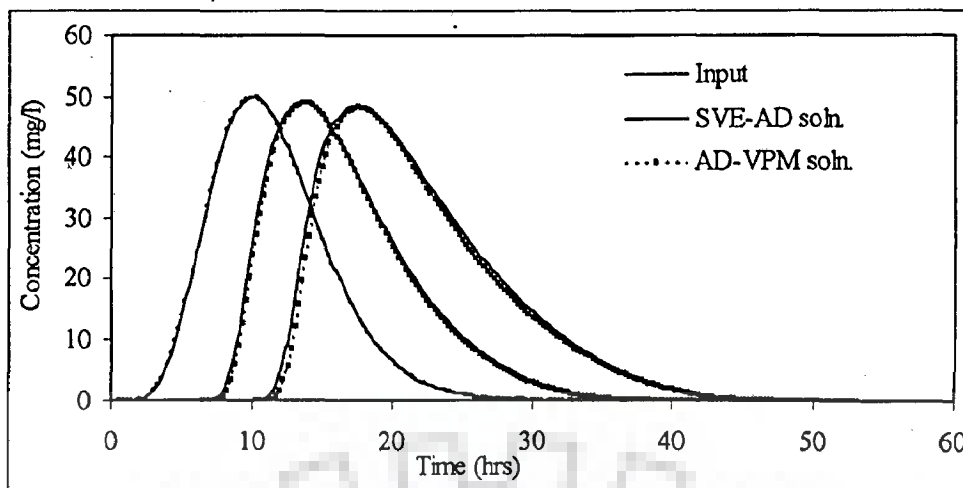
Figure 4.6(i) SVE-AD and AD-VPM solutions for ϕ = 0.058, channel type C-4 at 20 and 40km downstream from source of solute.
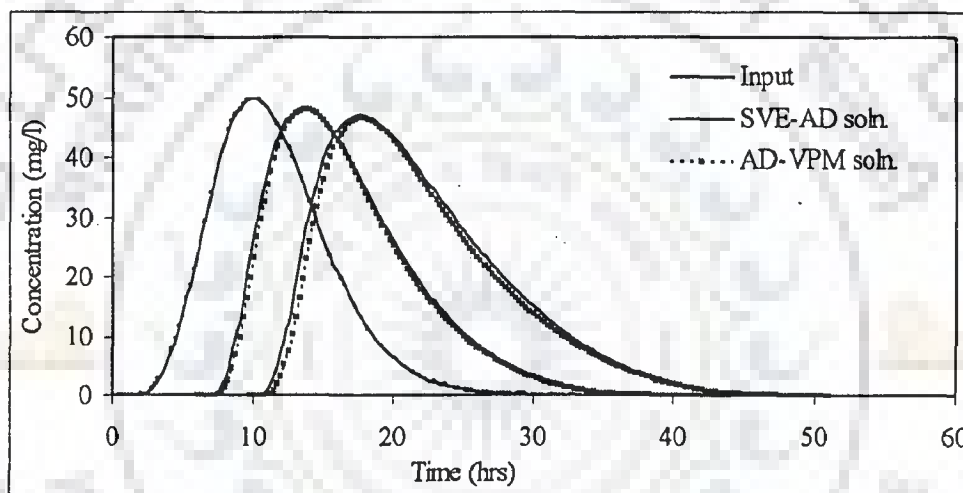
Figure 4.6(ii) SVE-AD and AD-VPM solutions for ϕ = 0.116, channel type C-4 at 20 and 40km downstream from source of solute.

Table 4.2 Results showing the reproduction of peak concentration and its time of occurrence for hypothetical test case

| Channel Type | ϕ | SVE-AD model | | AD-VPM model | | Nash-Sutcliffe Criterion (%) |
		Time to peak (hr)	Peak Concentra-tion (mg/l)	Tme to peak (hr)	Peak Concentra-tion (mg/l)	
C-1	0.058	14.75	48.40	14.75	48.13	99.22
	0.116	14.75	46.95	14.75	46.34	98.81
C-2	0.058	16.00	48.46	16.00	48.23	99.23
	0.116	16.00	46.46	16.00	46.51	98.90
C-3	0.058	16.00	48.40	16.00	48.18	99.22
	0.116	16.00	46.90	16.00	46.35	98.80
C-4	0.058	17.50	48.59	17.50	48.34	99.44
	0.116	17.50	47.07	17.50	46.73	99.04

Table 4.3 The range of velocities, D_L and limiting D_L for the hypothetical channels

Type of channel	Inflow velocity (m/s)		Outflow velocity (m/s)		ϕ	D_L (m²/s)		Limiting D_L (m²/s)	
	Min.	Max.	Min.	Max.		Min.	Max.	Min.	Max.
C-2	0.80	2.03	0.80	1.95	0.058	145	1450	286	1406
					0.116	290	2900		
C-4	0.65	1.62	0.65	1.55	0.058	72.5	725	199	952.6
					0.116	145	1450		

An inflow hydrograph defined by Eqn. (4.25) was used in the numerical experiments with the following characteristics: initial steady flow (I_b=100 m³/s), peak flow (I_f=500m³/s), time to peak (t_p=10hrs) and skewness factor (γ=1.15). The C-t curve defined by Eqn. (4.26) with an initial concentration, C_b=0 mg/l, peak concentration C_p = 50 mg/l, time to peak t_{cp} = 6hr, and, skewness factor γ_c = 1.15, was used as the input required for solute routing in the channels. These inflow hydrograph and input C-t curve applied at the same input point were simultaneously routed through the channels C-1 and C-3 using the proposed AD-VPM model for solute transport under unsteady flow condition. A routing time interval of 15 min. was used in the numerical experiments. The results are presented in Table 4.4 and the comparison of the solutions of the AD-VPM model with the corresponding benchmark SVE-AD solutions are shown in Figs. 4.7 and 4.8.

Table 4.4 Results showing the reproduction of peak concentration and its time of occurrence for hypothetical test case for peak flow of 500m³/s used in Eqn. (4.25)

Channel Type	ϕ	SVE-AD method		AD-VPM model		Nash-Sutcliffe Criterion (%)
		Time to peak (hr)	Peak Concentra-tion	Tme to peak (hr)	Peak Concentr-ation	
C-1	0.058	12.50	43.76	12.75	42.91	99.03
	0.116	12.50	38.98	12.75	38.12	98.80
C-3	0.058	14.25	43.85	14.25	42.43	99.67
	0.116	14.00	38.56	14.50	37.57	99.38
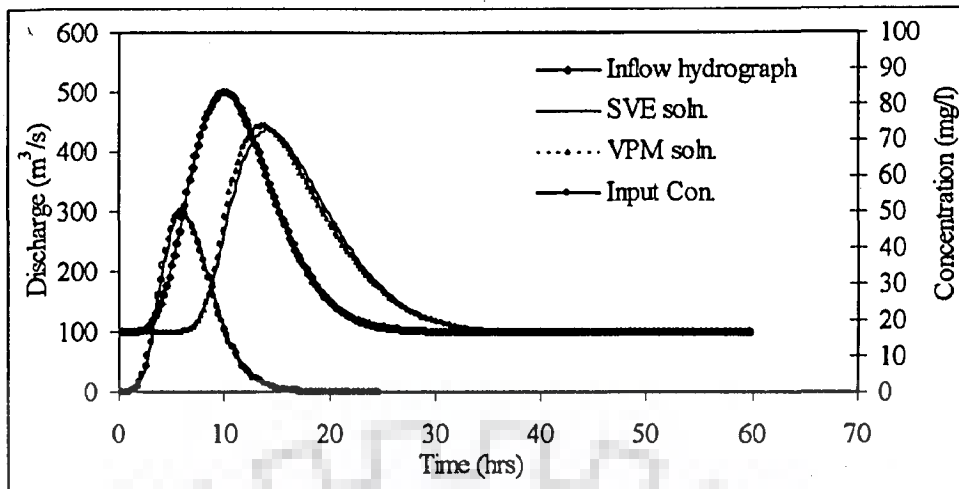
Figure 4.7(i)   Flow details for channel type C-1 for $I_f = 500 m^3/s$ along with input C-t curve
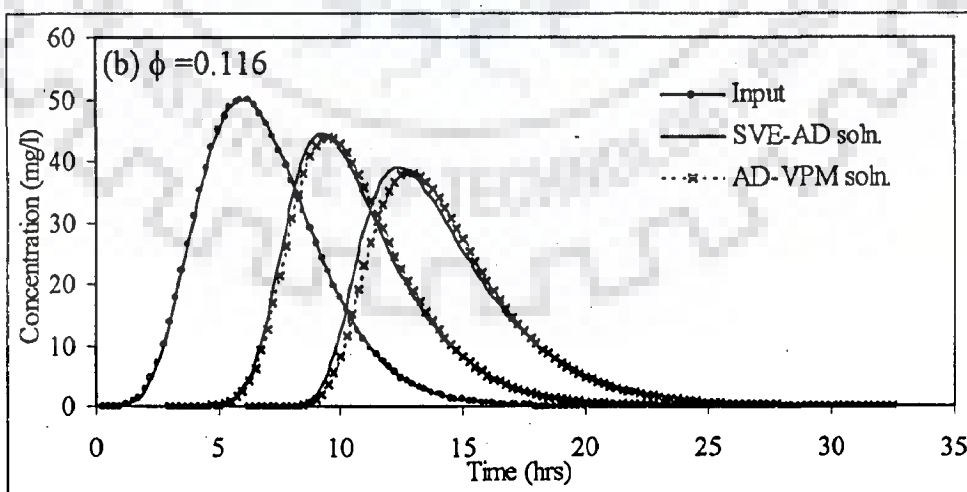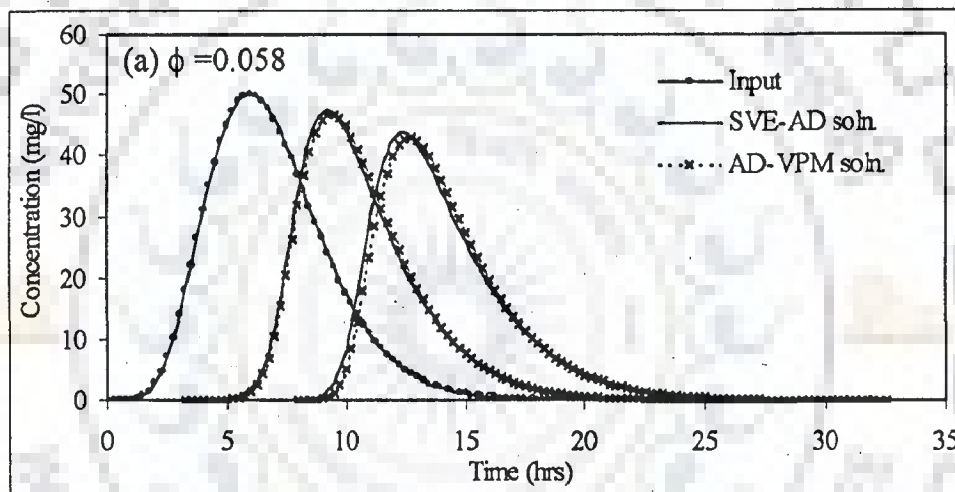
Figure 4.7(ii) SVE-AD and AD-VPM solutions at 20 and 40km downstream from source for channel type C-1 for the loading shown in Fig.4.7(i) (a) $\phi = 0.058$, (b) $\phi = 0.116$

111
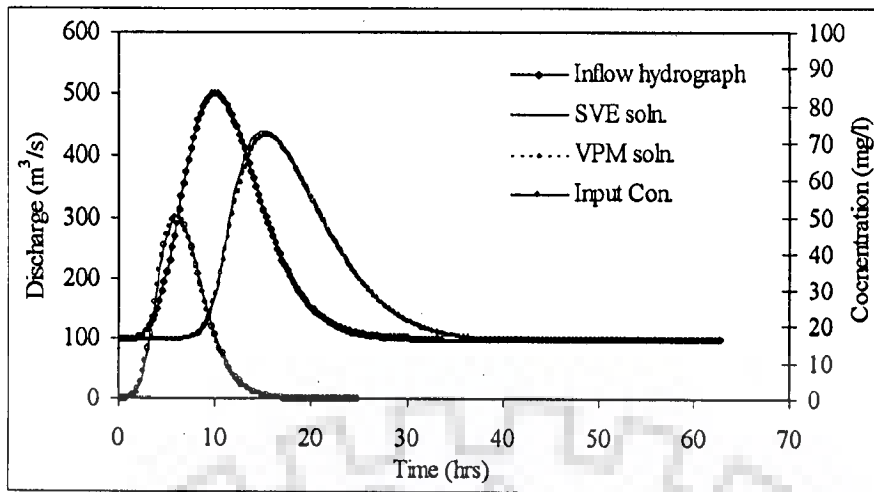
Figure 4.8(i) Flow details for channel type C-3 for $I_f = 500m^3/s$ along with input
C-t curve
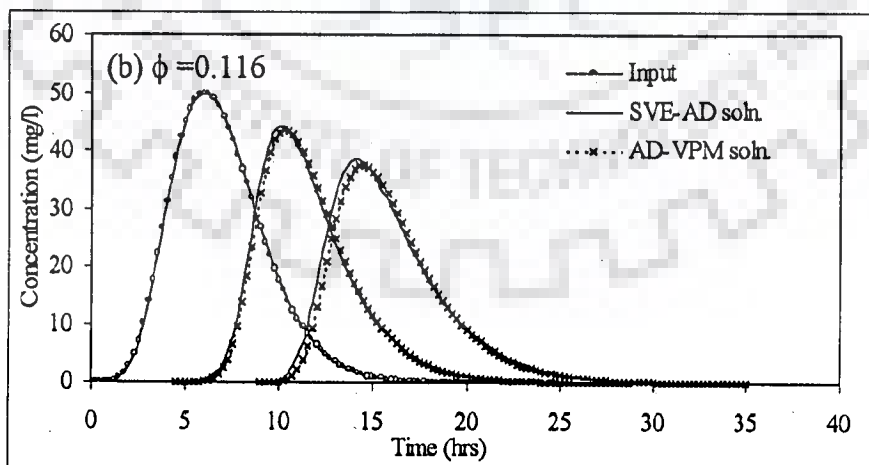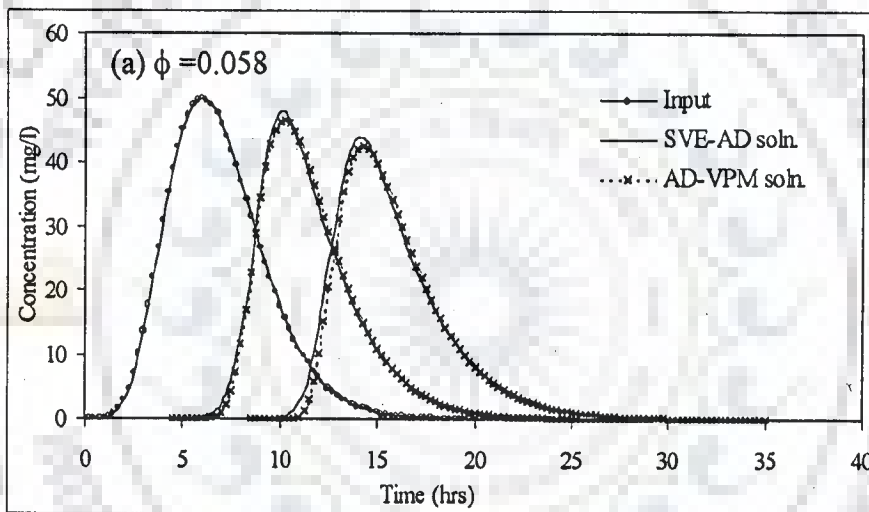
Figure 4.8(ii) SVE-AD and AD-VPM solutions at 20km and 40 km downstream
from source for channel type C-3 for the loading shown in Fig. 4.8(i).
(a) ϕ =0.058, (b) ϕ =0.116

112

4.3.3 Mass Conservation

The AD-VPM model was tested for conservation of mass of solute based on the hypothetical numerical experiments performed in rectangular channels with uniform width of 50m and 00 m and for different channel configurations. The configurations of the channels considered in the study are described in Table 4.1. In addition to the channel types given in Table 4.1, rectangular channels with a width of 100m and characterised by different bed slopes of 0.0006, 0.0008, and 0.002 and each having a Manning's roughness coefficient of 0.04 were also used in these mass conservation studies. In all the cases, a hypothetical input hydrograph and a C-t curve given by Eqn. (4.25) and Eqn.(4.26), respectively, were used. The value of peak flow equal to $1000m^3/s$ was used in the Eqn. (4.25). In order to estimate the dispersion coefficient required for solute transport studies the empirical relationship established by McQuivey and Keefer, (1974) linking the flow diffusion coefficient to the solute dispersion coefficient given in Eqn. (3.23) was used with a value of $\phi=0.116$. Additional experiments were carried out with values of $\phi=0.058$ and $\phi=0.025$. This was used to know the performance of the AD-VPM model under advection dominated dispersion, as dispersion during unsteady flow is advection dominated phenomenon (Bedford et al., 1982). The specific concern is that the numerical solution of the AD equation using a given C-t curve as the boundary condition may not conserve mass given an unsteady flow regime as shown in Figs. 4.11 to 4.13. To test the mass conservation, concentration-discharge profiles were integrated with respect to time to determine the mass passing a given sampling location (Runkel et al., 1998). The total solute mass was computed from the integration of mass flow rate over time. The total mass, M passing through the outflow section was estimated as

$$M = \int_0^\infty QC \, dt \quad = \sum_{i=1}^{n} (QC)_i \Delta t \qquad (4.27)$$

where i is the discretisation index.

The area under the mass flow rate-time curve was determined by numerical

113

integration using Eqn. (4.27). The results are summarised in Table 4.5. In all the test cases it was found that the AD-VPM model under unsteady flow conserved mass with a maximum error of 3.63% in channel type C-2. The loss of mass of solute is very less in case of channels with flow characterised by kinematic wave phenomenon. If a diffusive wave process governs the unsteady flow, the loss of mass is more compared to the corresponding one during kinematic wave unsteady flow process (Table 4.5). The complexities involved in the modelling of the longitudinal dispersion under unsteady flow condition, which is a highly non-linear process, and the approximations involved in the development of the AD-VPM model may be responsible for the loss of mass upto 3.63% (Table 4.5). However, the value is specific and applicable to this case (C-1) only. Based on the mass conservation analysis, it can be concluded that the proposed AD-VPM model conserves mass satisfactorily within its applicability range.

Table. 4.5 Mass conservation results for solute transport under unsteady flow conditions

Channel type	Relational parameter, ϕ	Conservation of Mass (% error)	
		Flow	Solute
C-1	0.025		1.87
	0.058	-0.10	2.51
	0.116		3.63
C-2	0.025		1.41
	0.058	-0.20	2.05
	0.116		3.14
C-3	0.025		1.61
	0.058	-0.13	2.27
	0.116		3.39
C-4	0.025		1.02
	0.058	-0.28	1.63
	0.116		2.69
C-5 (S_0=0.0006,n =0.04)	0.025		0.59
	0.058	-0.34	0.89
	0.116		1.41
C-6 (S_0=0.0008,n =0.04)	0.025		0.06
	0.058	-0.34	0.23
	0.116		0.54
C-7 (S_0=0.002,n=0.04)	0.025		-0.46
	0.058	-0.28	-0.42
	0.116		-0.37

4.3.4 Time of Release of Solute

The aspect of time of release of solute at different time points since the passing of the inflow hydrograph was investigated. The hypothetical channel of 100m width and the inflow hydrograph and input C-t curve used in section 4.3.2 were used in this case also. The studies have been made by injecting the hypothetical C-t curve i) during rising limb (case A: t_{cp}=7hr), ii) around the peak flow (Case B: t_{cp}=10hr), and iii) during receding limb (Case C: (i) t_{cp}=7hr (ii) t_{cp}=10hr), of the hydrograph. In Case A and Case B, both the input hydrograph and the input C-t curve start rising at the same time. In Case C, the input C-t curve starts rising after 7hrs from that of the input hydrograph. These studies help in deciding the time of disposal of stored or accumulated waste with less or no treatment so as to utilise the dilution capabilities of time varying flows in a river. It is found that the disposal during the rising limb would result in maximum dispersion and thereby reducing the concentration compared to the disposal around peak flow. Also, the residence time is less either in case A or case B loading conditions in comparison with case C loading conditions. If the disposal is around the peak flow of hydrograph, the flushing time will be less thereby carrying the solute at a faster rate in comparison with the disposal during rising limb or receding limb of the hydrograph. The input hydrograph along with input concentration distribution details are shown in Fig. 4.9. The solute transport simulation results are summarised in Table 4.6 and shown in Figs. 4.10 to 4.13.
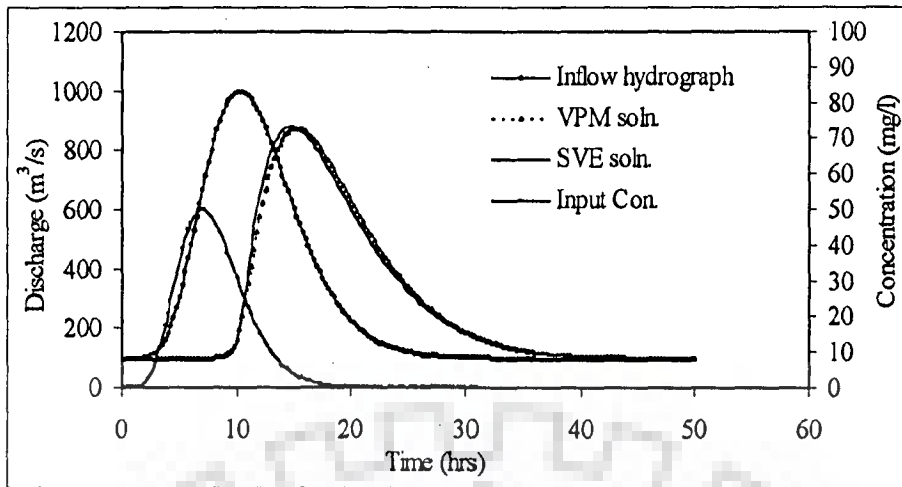
Figure 4.9(i)   Inflow and outflow hydrographs with input concentration distribution located in the rising limb of hydrograph (C-4, Case A)
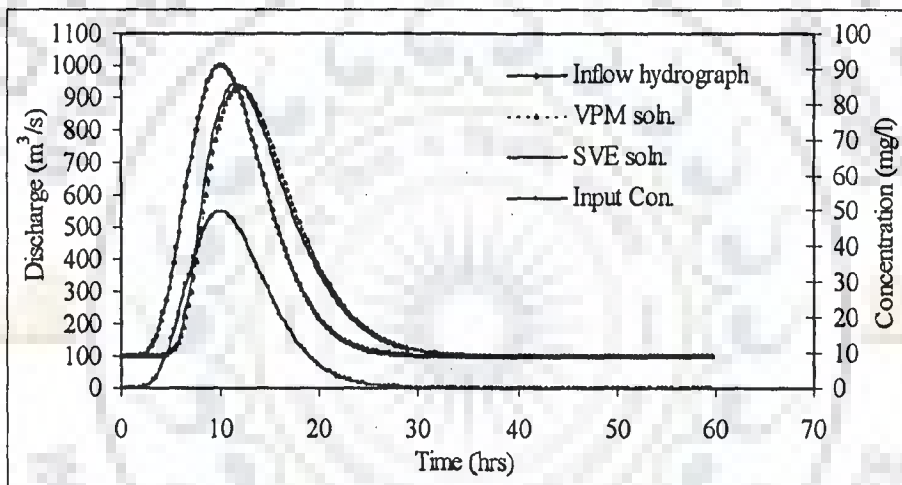
Figure 4.9(ii)   Inflow and outflow hydrographs with input concentration distribution located in the rising limb of hydrograph (C-2, Case B)
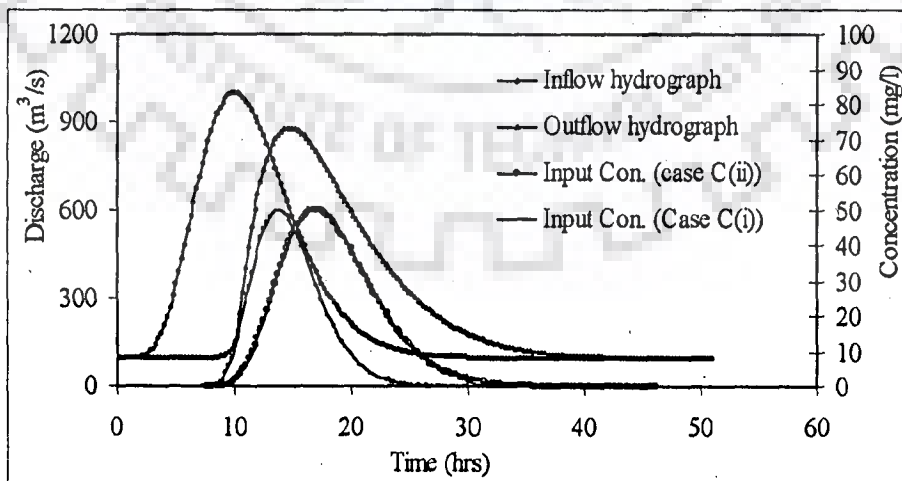
Figure 4.9(iii)   Inflow and outflow hydrographs with input concentration distribution located in the receding limb of hydrograph (C-4, Case C)

116
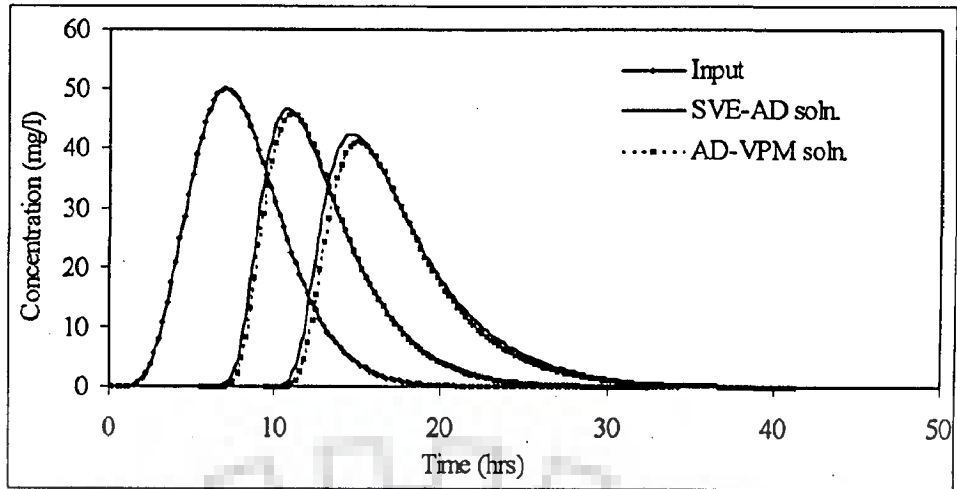
Figure 4.10 (i)   SVE-AD and AD-VPM solutions at 20km and 40km d/s from input of solute for channel type C-2, ϕ=0.058 (Case A)
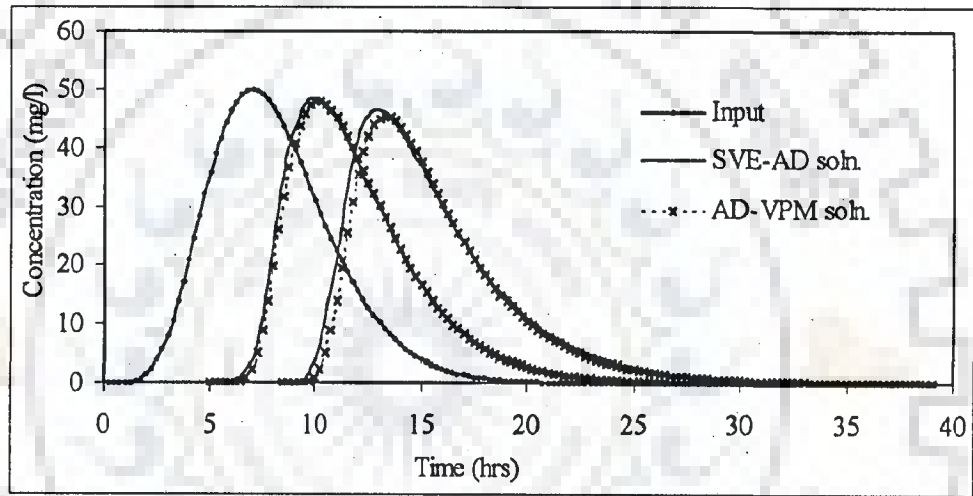
Figure 4.10(ii)   SVE-AD and AD-VPM solutions at 20km and 40km d/s from input of solute for channel type C-4, ϕ=0.116 (Case A).
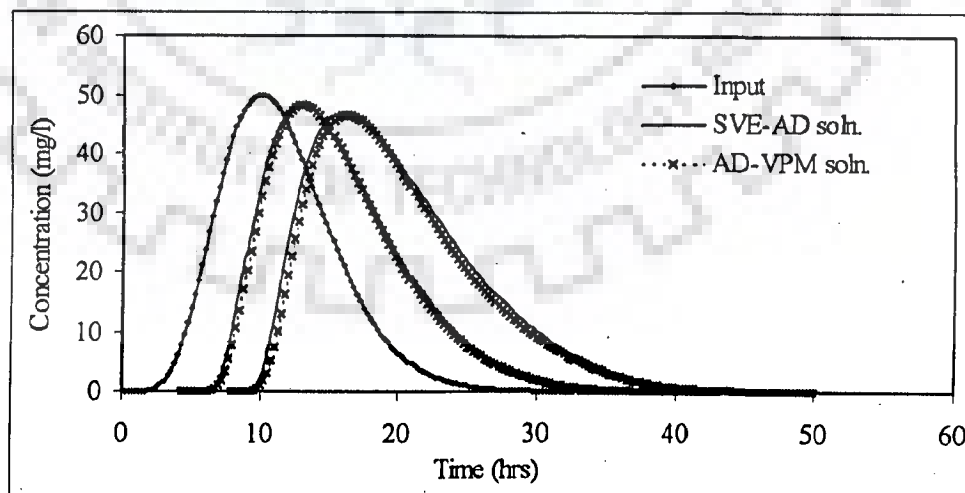
Figure 4.11(i)   SVE-AD and AD-VPM solutions at 20km and 40km d/s from input of solute for channel type C-2, ϕ=0.116 (Case B)
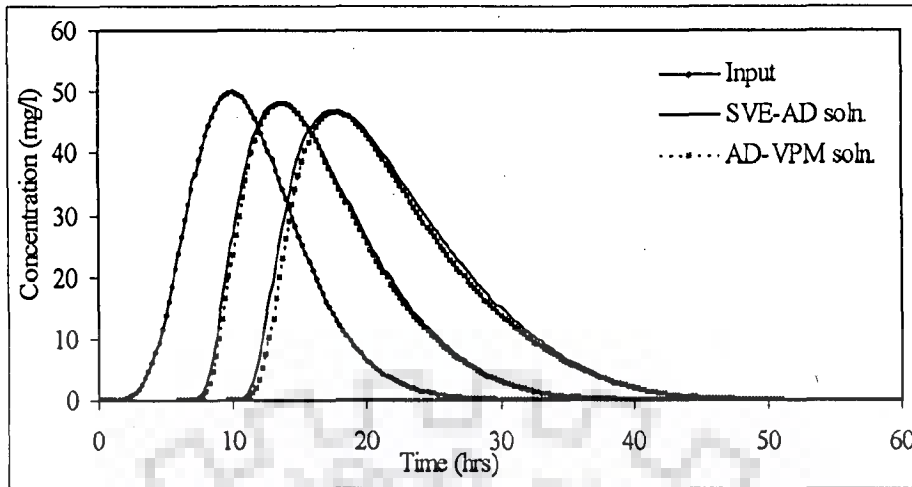
Figure 4.11(ii) SVE-AD and AD-VPM solutions at 20km and 40km d/s from input of solute for channel type C-4, ϕ=0.116 (Case B)
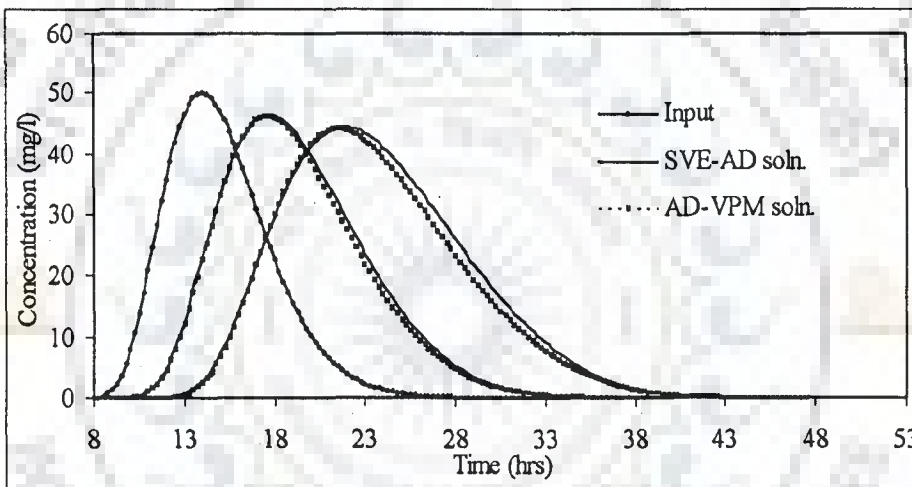
Figure 4.12(i) SVE-AD and AD-VPM solutions at 20km and 40km d/s from input of solute for channel type C-2, ϕ=0.116 (Case C(i))
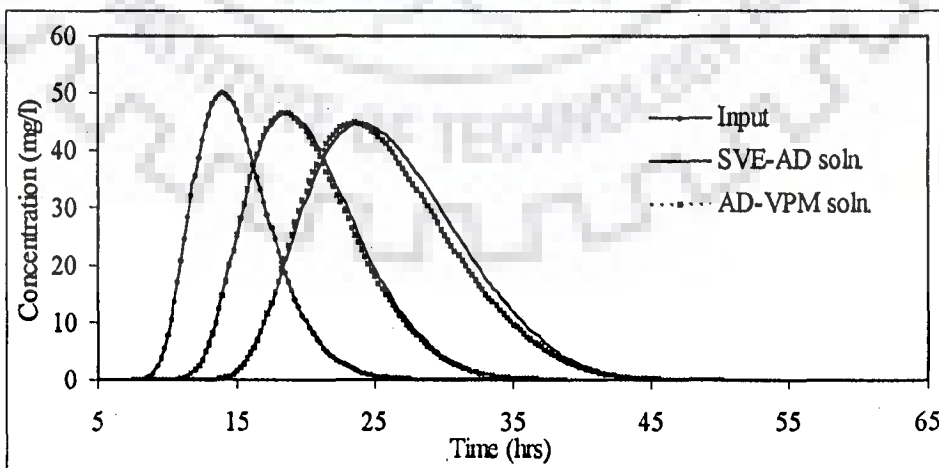
Figure 4.12(ii) SVE-AD and AD-VPM solutions at 20km and 40km d/s from input of solute for channel type C-4, ϕ=0.116 (Case C(i))
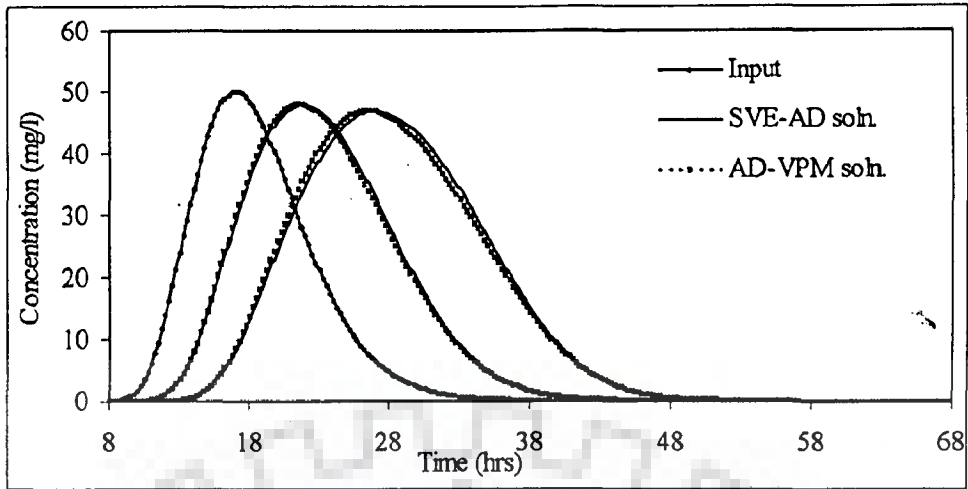
Figure 4.13(i) SVE-AD and AD-VPM solutions at 20km and 40km d/s from input of solute for channel type C-2, φ=0.116 (Case C(ii))
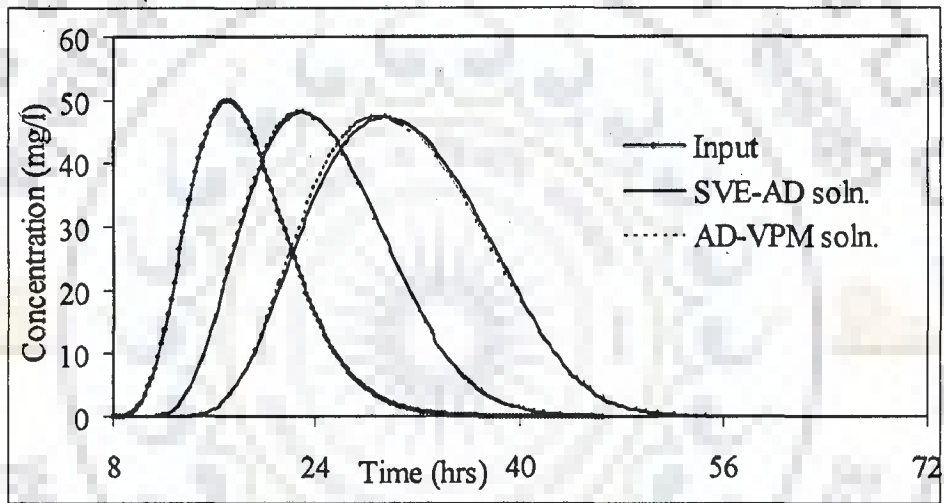
Figure 4.13(ii) SVE-AD and AD-VPM solutions at 20km and 40km d/s from input of solute for channel type C-4, φ=0.116 (Case C(ii))
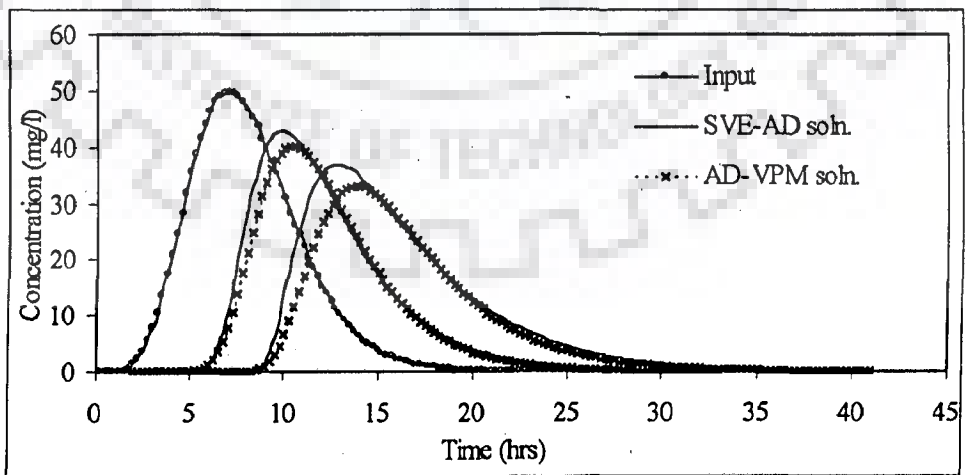
Figure 4.13(iii) SVE-AD and AD-VPM model solutions at 20km and 40km d/s from input of solute for channel type C-4, φ=0.3 (Case A)

119

Table 4.6 Results for the hypothetical channel with B=100m for different hypothetical loading cases

Loading case	Channel type	ϕ	SVE-AD solution		AD-VPM model	
			Time to peak concentration (hr)	Peak concentration (mg/l)	Time to peak concentration (hr)	Peak concentration (mg/l)
Case A	C-2	0.058	13.00	46.40	13.25	45.36
		0.116	13.00	42.73	13.50	41.40
	C-4	0.058	14.50	47.07	14.75	45.23
		0.116	14.75	42.45	15.00	41.24
Case B	C-2	0.058	16.00	48.46	16.00	48.23
		0.116	16.00	46.46	16.25	46.51
	C-4	0.058	17.50	48.59	17.50	48.34
		0.116	17.50	47.07	17.75	46.73
Case C(i)	C-2	0.058	21.75	46.91	21.50	46.81
		0.116	22.00	44.34	21.50	44.11
	C-4	0.058	23.75	47.30	23.50	47.25
		0.116	24.00	44.87	23.50	44.87
Case C(ii)	C-2	0.058	27.00	48.30	26.50	48.41
		0.116	27.00	46.77	26.75	46.95
	C-4	0.058	29.25	48.61	29.00	48.69
		0.116	29.25	47.20	29.00	47.45

4.4 COLORADO RIVER TEST CASE

The available data from the experiments conducted in a 380km long Grand Canyon reach of the Colorado River in May 1991 (Graf, 1995) was used to test the proposed AD-VPM model. Details of tracer experiments, the controlled inflow hydrographs released at Glen Canyon Dam, and available hydro-geometric channel characteristics for the sub-reaches of Grand Canyon reach have been discussed by Graf (1995). The experiments conducted in the Colorado River are useful for the present study as simultaneous measurements of hydrographs and the C-t curves enable the field testing of the proposed model. This unique experiment provides an opportunity to explore the dispersion mechanism and its relation with the flow in

120

rivers. The flow releases from Glen Canyon dam were controlled so as to provide two flow conditions for research viz., steady and unsteady flow conditions. The flow hydrographs during 5th to 19th May 1991 consist of variation of discharge ranging from 92 m^3/s to 754 m^3/s.

In Grand Canyon reach, observed hydrographs are available at Lees Ferry (RK 0;USGS 09380000), at above the Little Colorado river near Desert View (RK 98; USGS 0938100), at Phantom Ranch near Grand Canyon (RK 142; USGS 09402500), at National Canyon near Supai (RK 267; USGS 09404120) and at Diamond Creek near peach springs (RK 362; USGS 09404200). The hydrograph data were given in Appendix B 1.3. The schematic diagram is shown in Fig. 3.12. Discharge data at 15min. interval are available at all the above said sections.

The C-t curve measurements, during unsteady flow, available at Nautloid Canyon (RK 57.7), at the Little Colorado above Desert View (RK 98.3), at Nevill's rapid (RK 123), at Mile 118 camp (RK 189), at National Canyon (RK 267), and at Gneiss Canyon (RK 381) were used in the present test case. But the C-t curves at Mile 118 camp and at National canyon were incompletely observed during the unsteady flow resulting in absence of the leading edges. Simultaneous flow and dye concentration measurements are available only at Little Colorado and National canyon gauging stations. Figure 4.14 shows the observed flow hydrographs along with observed C-t curves. It is important to note that the observed C-t curves at sampling stations during unsteady flows do not have the long tails, and the same was observed under steady flow condition also (Chapter 3). The absence of long tails are indicative of the absence of the dead zone mechanism in the Grand Canyon reach of the Colorado River.
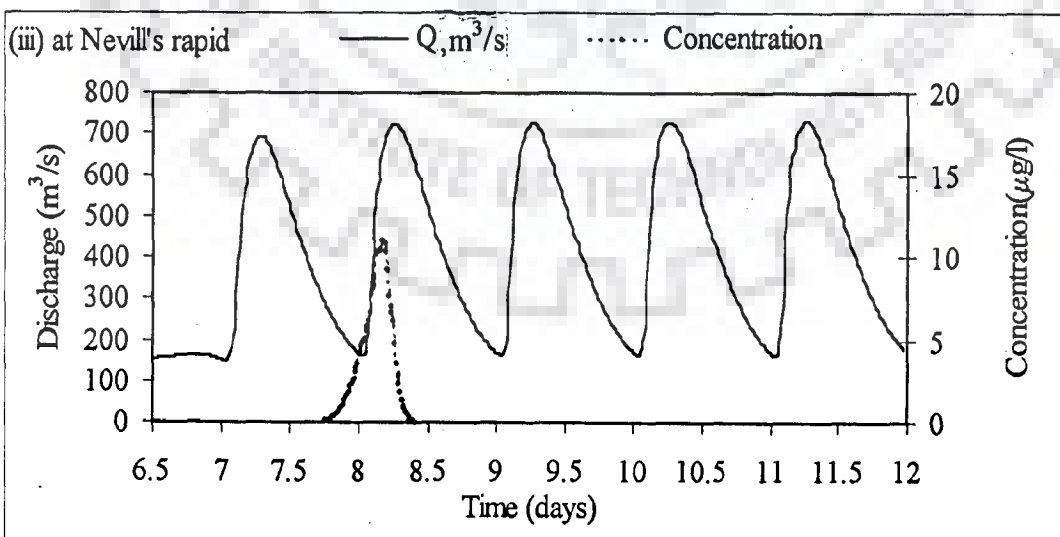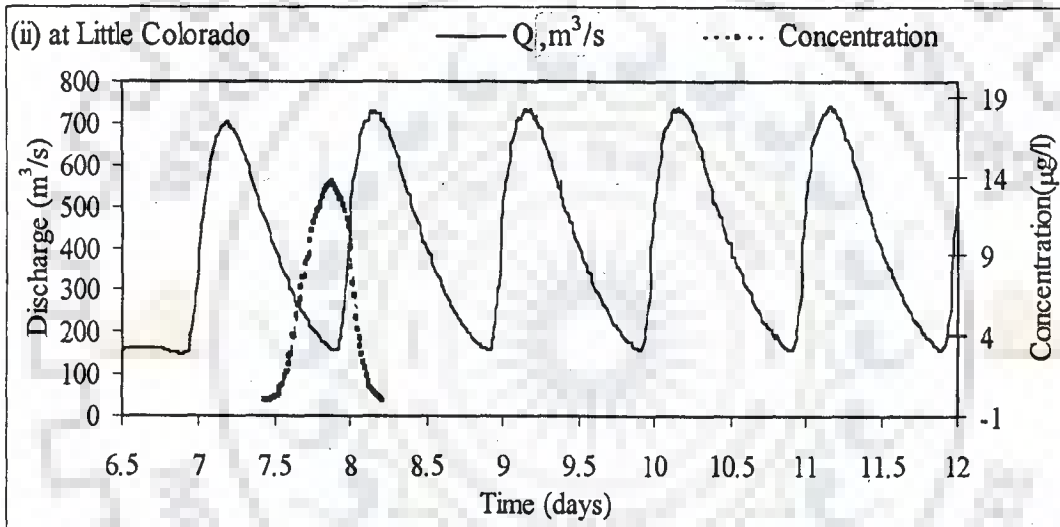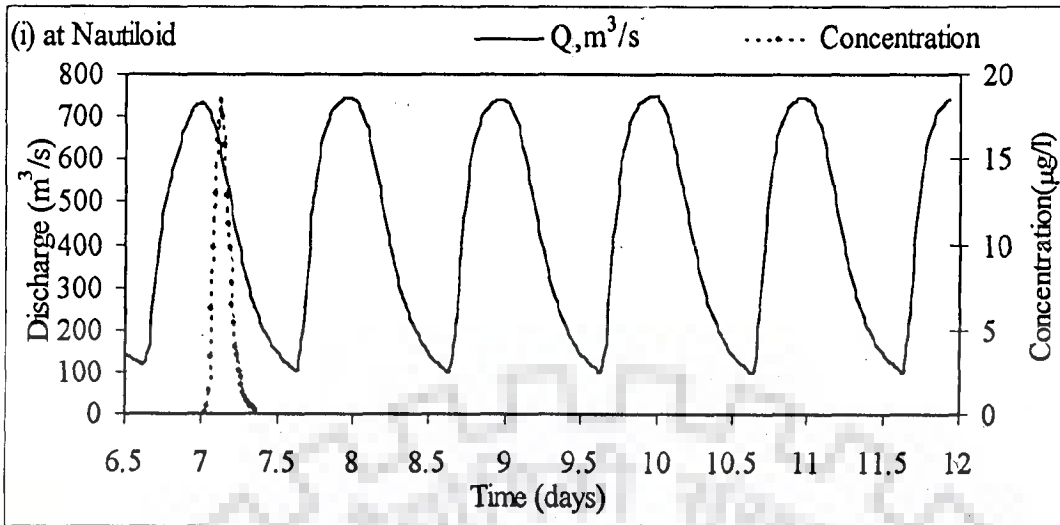
Figure 4.14 Observed hydrograph and the associated observed dye concentration at the sampling sites during unsteady flow.
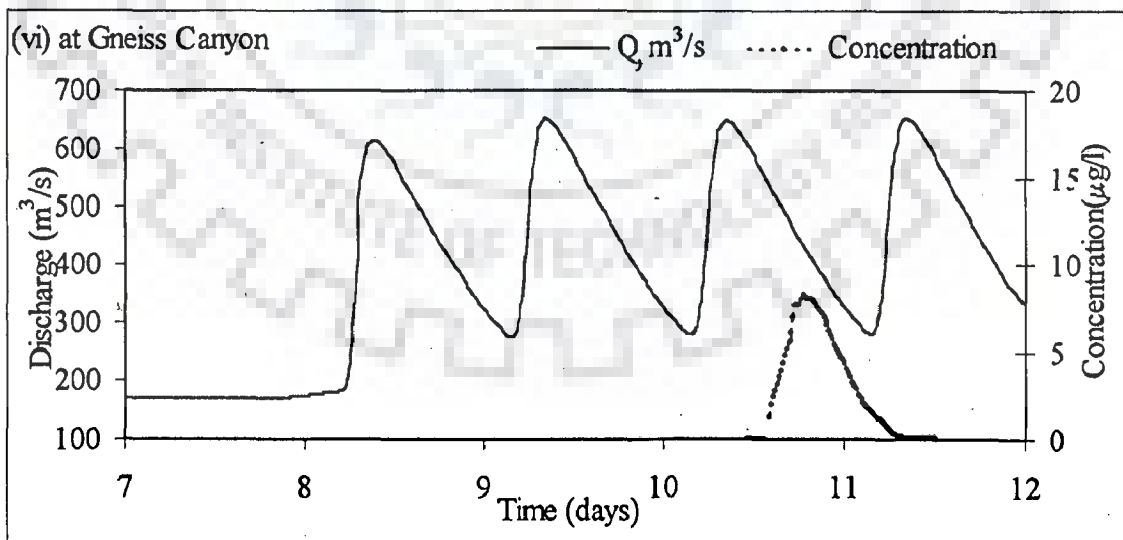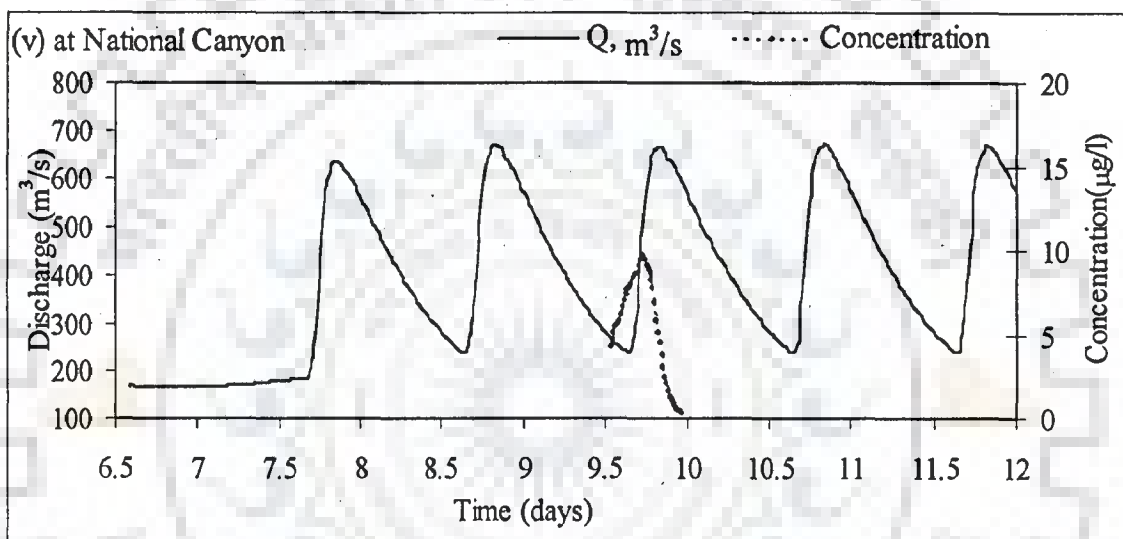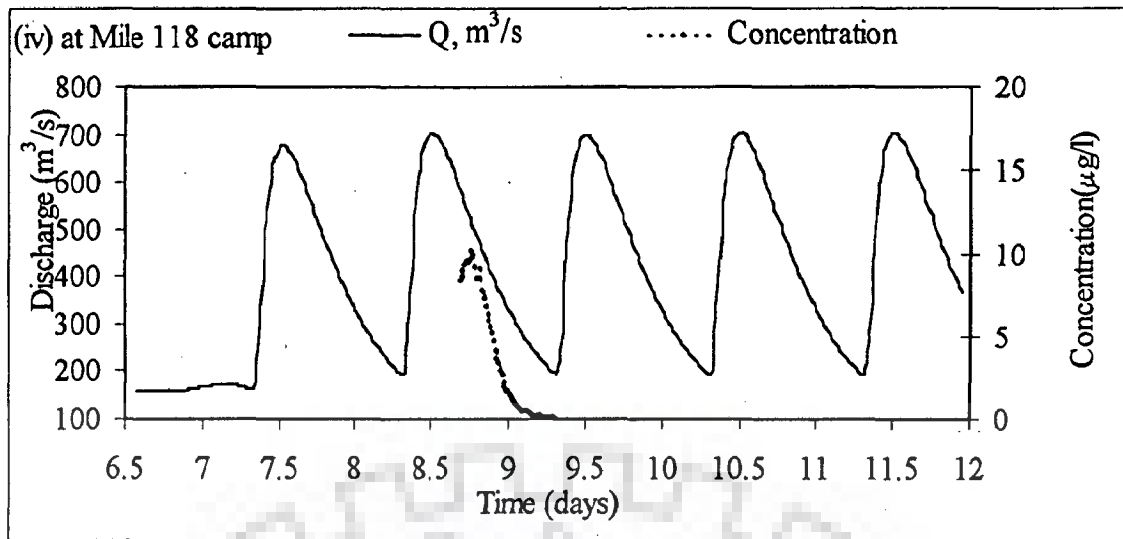
Figure 4.14 Observed hydrograph and the associated observed dye concentration at the sampling sites under unsteady flow

123

The channel characteristics of the Grand Canyon reach used in the analysis were estimated corresponding to a discharge of 680 m³/sec (Graf, 1995). Based on these characteristics, the Grand Canyon reach has been divided into 9 sub-reaches. The details are summarised in Table 4.7 and Table 4.8.

Wiele and Smith (1996) presented a procedure to compute the representative cross section using the observed cross-section measurements of Colorado River. The cross-section measurements on Colorado River consist of a distance from the left water edge and a corresponding depth. To average the cross-sections, each was first normalized in the cross-stream direction by dividing the cross-stream location by the water surface width so that the cross-stream dimension ranged from 0 to 1. The depths at corresponding cross-stream fractions were then averaged. The width was restored by multiplying the cross-stream fraction by the average channel width. Reach averaged representative trapezoidal sections (Camacho, 2000) are arrived at for the irregular natural channel adopting the procedure proposed by Wiele and Smith (1996) for the large range of discharges observed. In the present study, reach averaged trapezoidal sections arrived at by Camacho (2000) for the Grand Canyon reach has been taken. The bed width and side slopes of narrow channel are 35m and 1(horizontal) in 3.16 (vertical) respectively. The bed width and side slopes of wide channel are 48.75m and 1(horizontal) in 5.31(vertical) respectively. The representative trapezoidal cross-sections were arrived at by Camacho(2000) using the profiles measured at 199 sections along the Grand-Canyon reach. This may be additional reasons for the differences in velocities in the natural river section and assumed trapezoidal section of Camacho (2000).

Table 4.7 Channel characteristics corresponding to the discharge of 680m³/s (Graf, 1995)

Sub-reach ID	Length (Km)	Bed Slope	Width (m)	Depth (m)	Ratio of width to depth	Area (m²)
2	57.7	0.00141	71.6	8.2	8.7	573
3	40.6	0.00126	106.1	6.1	17.4	642
4	24.9	0.00274	119.2	5.2	22.9	613
5	18.8	0.00195	59.1	8.8	6.7	517
6	47.3	0.00195	59.1	8.8	6.7	517
7	78.6	0.00151	63.4	7.6	8.3	468
8	75.7	0.00134	94.2	6.7	14.1	609
9	18.4	0.00161	71.6	9.1	7.9	661
10	18.5	0.00161	71.6	9.1	7.9	661

Table 4.8 Classification of the Grand Canyon reach, Colorado River (Camacho, 2000)

Reach	Sub-reach	Classification based on width*	Sub-reach Identification No.
Lees Ferry – above Little Colorado river	Lees Ferry – Nautiloid Canyon	Narrow	2
	Nautiloid Canyon – above Little Colorado river	Wide	3
Above Little Colorado river – Grand Canyon	Above Little Colo.-Nevill's rapid	Wide	4
	Nevill's rapid – Grand Canyon	Narrow	5
Grand Canyon – National Canyon	Grand Canyon – Mile 118 camp	Narrow	6
	Mile 118 camp – National Canyon	Narrow	7
National Canyon-Diamond creek	National Canyon - Pumpkin spring	Wide	8
	Pumpkin spring-Diamond creek	Narrow	9
	Diamond creek- Gneiss	Narrow	10

*The sub-reaches are classified as wide, if the top width > 85m, and narrow, if top width < 85m

Flow and solute routing were carried out using the proposed AD-VPM model. The agreement between observed and simulated distributions (for both hydrographs and C-t curves) was measured using the Nash-Sutcliffe criterion (η). Flow details required in solute routing under unsteady flow conditions were arrived at from flow simulations. The hydrograph available for a longer duration is split into two parts: i) data set during 5th-11th May, 1991 and ii) data set during 13th-18th May, 1991. The first data set was used for calibrating the Manning's n using the VPM flow routing model and the second data set was used for verifying the same model using hydrograph simulations.

4.4.1 Flow Routing

In flow routing apart from the available channel characteristics and hydrographs, the Manning's roughness coefficient, n had to be calibrated from the available observed hydrographs.

4.4.1.1 Calibration and verification of roughness coefficient

The Variable Parameter Muskingum (VPM) model, was used to simulate the flow transport through the entire Grand Canyon reach from Lees Ferry to Diamond Creek to calibrate the roughness coefficient.

The observed hydrographs between 5th to 11th May 1991 were used to calibrate Manning's n for all the reaches considered. Manning's n was calibrated based on closest match between the observed and the simulated hydrographs at different downstream sections by routing the inflow hydrograph observed at immediate upstream section (Keefer and Jobson, 1978) for different values of Manning's n, varying from 0.03 to 0.08. The selected value of Manning's n for each reach is within the normal range, generally observed in natural channels (Chow et al., 1988). The hydrographs simulated in calibration mode are shown in Fig. 4.15. Using the calibrated Manning's n, the observed hydrographs between 13th to 18th May 1991 are simulated at downstream sections of each reach in verification mode. The hydrographs simulated in verification mode are shown in Fig. 4.16. The salient features of the calibration and verification results are presented in Table 4.9.

126
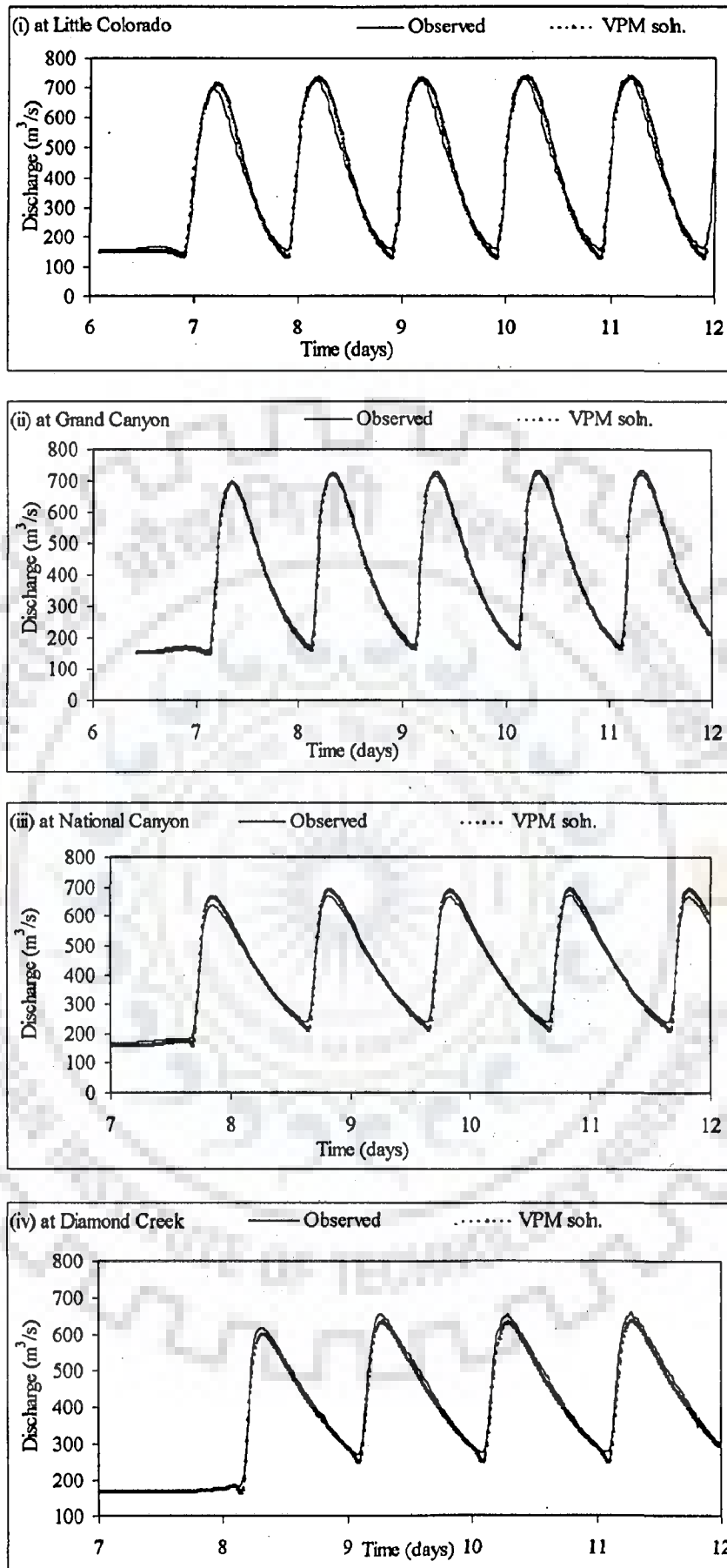
Figure 4.15 Observed and simulated (in calibrating Manning's n) hydrographs at the different streamflow gauging stations

127
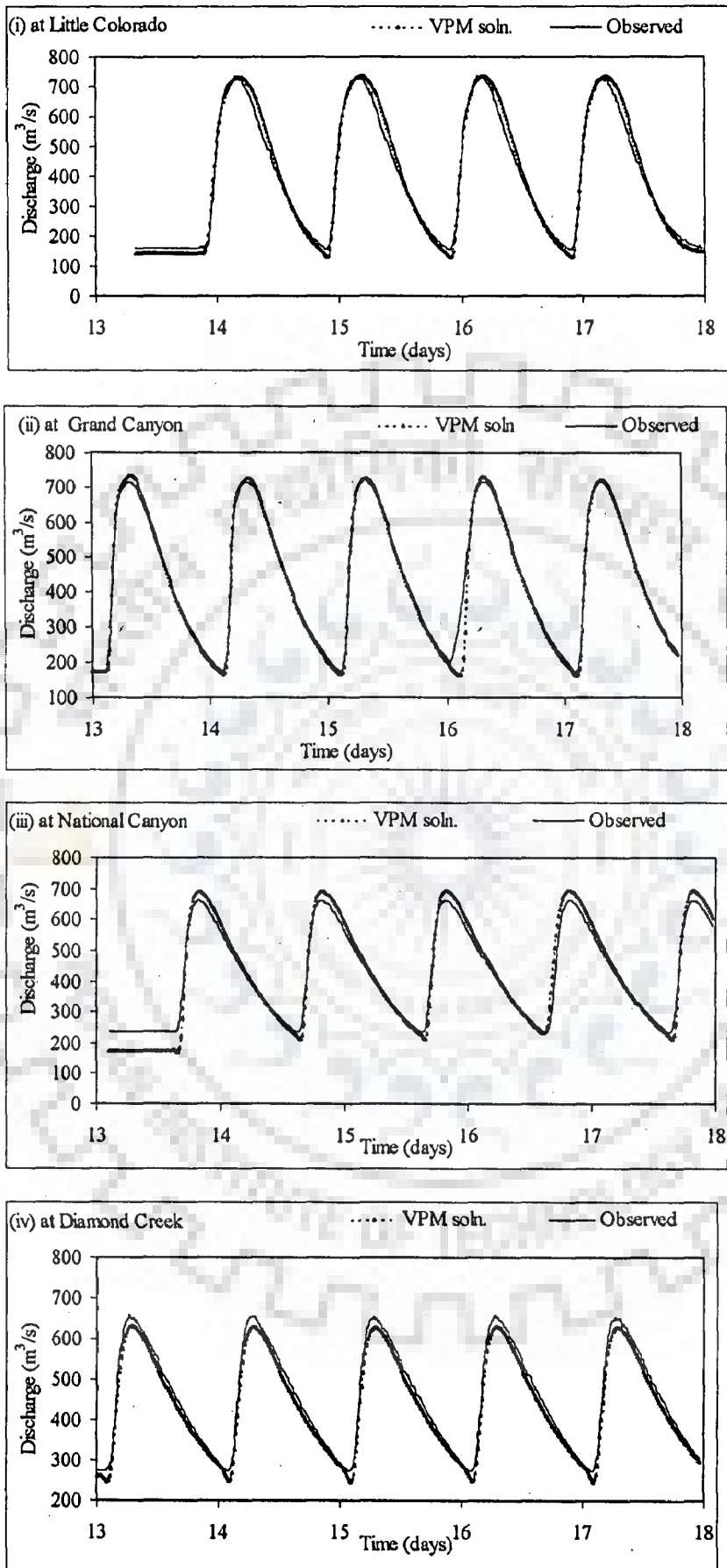
Figure 4.16   Observed and simulated (in verification of Manning's n) hydrographs at different streamflow gauging stations

Table 4.9. Manning's roughness coefficient Calibration and verification results

Reach	Sub-reach	Manning's n	Nash-Sutcliffe criterion, η (%)	
			Calibration	Verification
Lees Ferry-above Little Colo	2.Lees Ferry – Nautiloid	0.055	98.46	98.10
	3.Nautiloid- Little Colo.	0.064		
Above Little Colo.- Grand Canyon	4.above Little Colo-Nevill's rapid	0.062	99.79	98.43
	5.Nevill's rapid – Grand Canyon	0.042		
Grand Canyon – National Canyon	6. Grand Canyon – Mile 118	0.052	99.03	95.41
	7. Mile 118 – National Canyon	0.048		
National Canyon- Diamond creek	8.National Canyon-Pumpkin spring	0.048	99.34	97.69
	9. Pumpkin spring- Diamons creek	0.046		
	10. Diamond creek- Gneiss	0.046		

4.4.2 Solute Routing

In solute transport studies it is necessary to use the observed velocities in the natural river section. Hence, in solute transport studies under unsteady flow conditions, Runkel, et al. (1998) adjusted the widths of the channel so that the simulated velocities agreed with the observed velocities during single discharge measurements of the unsteady flow event. The calibration adopted by Runkel et al. (1998) resulted in differences between the observed and simulated discharges and cross-sectional areas.

In the present study, two representative trapezoidal cross-sections (one to represent the wide channel and another to represent the narrow channel of the Grand canyon reach as classified by Camacho (2000) and as shown in Table 4.7) were

129

used for flow routing in the Grand Canyon reach of the Colorado River. The observed hydrograph at a gauging location was used as inflow hydrograph for flow routing in each of the immediate sub-reach of the Grand Canyon reach. The Manning's n was calibrated so that the simulated discharge hydrographs agreed with the observed discharge hydrographs at downstream of each of the sub-reaches of the river. The usage of averaged trapezoidal cross-section representing the natural river cross-section, and the calibration of Manning's n to match the simulated hydrographs with observed hydrographs results in the velocity differences between those observed in natural river and that is estimated for the corresponding representative trapezoidal section reaches. This can be observed from the velocity in the trapezoidal section computed for each sub-reach at an approximate discharge of $425 m^3/s$ during steady flow conditions in comparison with the velocity in the respective sub-reach of the natural river section at a discharge of $425 m^3/s$ during steady flow given by Graf (1995) presented in Table 4.10. Based on the results presented in Table 4.10, it was observed that the velocity in the trapezoidal reach section at $425 m^3/s$ is higher than the velocity observed in the corresponding natural river reach.

Hence, a parameter ψ has been introduced to estimate the observed velocities in the actual river from the velocities computed from the reach averaged trapezoidal section using a relationship

$$U_a = \frac{U_r}{(1+\psi)} \qquad (4.28)$$

where U_a is the actual velocity measured in the river, U_r is the velocity estimated for the trapezoidal cross section representative reach. The velocity conversion coefficient (ψ) is calibrated using observed flow and concentration time series from the experiments conducted on Colorado river during controlled steady flow conditions from 20th May, 1991. The parameter ψ calibrated during simulation of dispersion under steady flow is summarised in Table 4.10.

Table 4.10 The summary of calibrated values of ψ

Reach	Velocities observed in natural channel at ≈ 425 m³/s (m/s)	Velocity estimated in reach averaged section at ≈ 425 m³/s (m/s)	Calibrated value of ψ
Nautiloid-Above Little Colorado	0.75	1.26	0.64
Above Little Colorado-Nevill rapid	1.00	1.69	0.57
Nevill rapid - Grand. Cany. Grand .Cany. - Mile 118	0.97	2.01	0.68 1.21
Mile118-National Canyon	1.10	1.87	0.74
Nat. Canyon to Pumpkin spring	1.10	1.58	0.45
Pumpkin spring to Gneiss canyon	1.00	1.96	0.86

The AD-VPM model, with parameter values of ψ thus obtained under steady flow condition, was used to simulate the C-t curves, in verification mode, for the period of unsteady flow tracer experiments between 5th and 13th May 1991. Both the computed hydrograph from VPM flow routing and the observed C-t curve at Nautiloid canyon were used as the inflow hydrograph and the input C-t curve for the VPM flow routing model and AD-VPM solute routing model respectively. Using the AD-VPM model coupled with the VPM flow routing model, the C-t curves at different downstream sampling stations were computed. The salient features of the results obtained are summarised in Table 4.11. The results of the MDLC-ADZ model (Camacho,2000) are also presented in Table 4.11. The comparison between the observed and computed C-t curves is shown in Fig. 4.17. The computed C-t curves using the MDLC-ADZ model are also presented for comparing the results with that of the AD-VPM model.
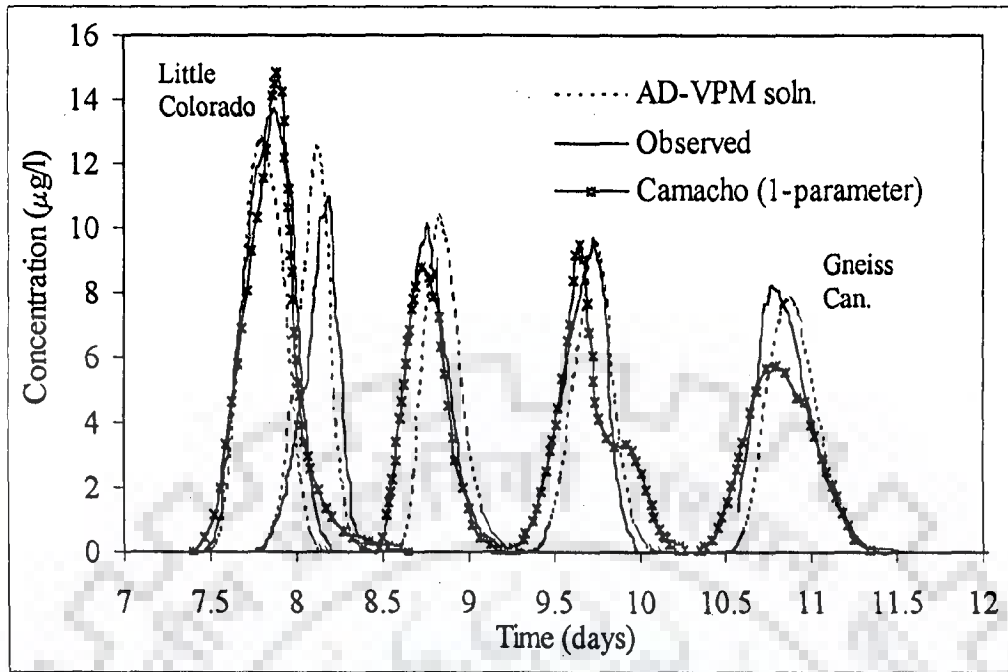
Figure 4.17 Observed and computed C-t curves at different sampling locations under unsteady flow conditions – Colorado River

The simulated results show that the AD-VPM model is able to reproduce the characteristics of the observed C-t curves such as shape, peak concentration, time of travel to peak concentration and η, and thus validating the proposed AD-VPM model. The Nash-Sutcliffe criterion, η estimated in simulating the C-t curves at Mile 118 camp and National Canyon are not actually representative because of the non-availability of the data in rising part of observed C-t curves. However, the Nash-Sutcliffe criterion values at Mile 118 camp and National Canyon are estimated to compare with the corresponding values arrived at using MDLC-ADZ model by Camacho (2000). The predicted peak concentrations and their time of occurrences are matching closely with those of the observed C-t curves in comparison to the simulation results of MDLC-ADZ model. The time of travel to peak concentration at above Mile 118 camp is well predicted by the MDLC-ADZ model in comparison with the AD-VPM model.

132

Table 4.11. Observed and predicted dispersion characteristics during unsteady streamflow in Colorado River

.Station	Observed		AD-VPM model			ADZ-MDLC model (Camacho, 2000)			
	Time to peak, (hr)	Peak concent-ration, (µg/l)	Time to peak, (hr)	Peak concent-ration, (µg/l)	η (%)	Time to peak, (hr)	Peak concent-ration, (µg/l)	η_1^{*} (%)	η_2^{*} (%)
Above Little Colo	32.00	13.40	30.25	12.75	86.7	30.95	14.45	70.0	46.3
Nevill's rapid	38.94	10.94	37.94	12.52	75.1	38.95	14.08	86.5	83.1
Mile118 camp	53.41	10.14	54.66	10.32	84.8	52.45	8.82	95.4	81.5
National Canyon	76.50	9.74	76.75	9.53	96.0	74.45	9.66	67.2	80.0
Gneiss Canyon	101.70	8.26	103.25	7.84	90.0	102.45	5.83	88.0	77.8

* η_1, η_2 are the Nash-Sutcliffe criterion for single and two-parameter MDLC-ADZ model (Camacho,2000)

4.5 DISCUSSION OF RESULTS

The proposed AD-VPM model for solute routing under unsteady flow conditions has the advantage of integration of the parameters of flow (K_f and θ_f) and solute transport (K_c and θ_c) models. Hence, it allows routing of the flow and solute concentration simultaneously. This integration and simultaneous routing is not possible in the approach suggested by Koussis et al. (1983), as (i) it is necessary to adjust the spatial and temporal step sizes with the variations in flow diffusion coefficient and transport dispersion coefficient accordingly, and (ii) the velocity that

is to be used in computing the solute routing model parameters (K_c and θ_c) under unsteady flow is not clearly identified. The AD-VPM model coupled with the VPM method enables to overcome these problems. Unlike in the procedure adopted by Gabriele and Perkins (1997), the AD-VPM model for solute transport coupled with the VPM model for flow routing considers the solute transport velocity and the solute dispersion coefficient while routing the solute through the channel. The proposed AD-VPM model provides the means to relate the solute transport parameters, i.e., K_c and D_L to the flow and hydro-geometric characteristics of the channel (Eqns. 4.19 and 4.21). The results shown in Fig. 4.3 to Fig. 4.8 illustrate that the proposed AD-VPM model with integrated parameters is able to reproduce the benchmark solution obtained using SVE-AD model satisfactorily within the applicability range of the AD-VPM model and the VPM method.

4.5.1 Differences in Velocities of Flood Wave and Solute Cloud

Equations (4.7) and (4.17) reveal that the reach travel time of solute cloud is more than that of flow. Therefore, the solute mass residence time in a reach is more compared to flood wave residence time for a given Δx. Based on these observations, it can be inferred that the C-t curve travels with a lesser velocity compared to the hydrograph during unsteady flow. Hence, C-t curves lag behind the corresponding flow hydrographs during unsteady flow. It is interesting to note that the same phenomenon has been observed in solute transport studies under unsteady streamflow conditions in rivers (Glover and Johnson, 1974; McCutcheon, 1989; Graf, 1995; Gabriele and Perkins, 1997; and Krien and Symander, 2000). Gabriele and Perkins (1997) state that "the contaminant mass-flux distribution and streamflow hydrograph do not travel at exactly the same speed through a channel reach".

4.5.2 Effect of Channel Type on Solute Transport

The solute transport under unsteady flow conditions has been studied using hypothetical inflow hydrographs and C-t curves in hypothetical channels as illustrated in section 4.3.2 and 4.3.4. Based on the results given in Table 4.2 and 4.4 and shown in Figs. 4.3 to 4.8, it can be stated that the percentage of attenuation of peak concentration is approximately the same in C-2 and C-4 type channels. The time of occurrence of peak concentration in channel type C-4 is delayed in case A, case B, case C(i) and case C(ii) loading conditions by 1.5 hrs, 1.5 hr 1.0 hr and 2.5 hrs respectively in comparison with the time of occurrences of peak concentrations in channel type C-2 (Table 4.6). This implies that the solute residence time in channel type C-4 is more than the solute residence time in channel type C-2. The velocities in the channel C-2 ranging, from 0.804 to 2.04 m/s, are higher in comparison with the velocities in channel C-4 ranging from, 0.652 m/s to 1.624 m/s. (Table 4.3). This might be the reason for the delayed occurrence of peak concentration at downstream distances in channel type C-4. It implies that if the velocity of flow is more the dispersion will be less and vice-versa. If the value of dispersion coefficient exceeds its limiting value given by Eqn. (3.25) at any time, then AD-VPM model solution starts deviating from the reference solution (Fig. 4.13(iii)).

4.5.3 Solute Transport in Colorado River

The AD-VPM model was used to simulate the observed C-t curves under unsteady flow conditions in the Grand Canyon reach of the Colorado River (Fig. 4.17). A constant value of Manning's n for each of the sub-reaches of the Grand Canyon reach was used in routing the hydrograph using the VPM flow routing method. Based on the calibration and verification results, it is concluded that the VPM method for flow routing gives good results for the calibrated Manning's n

values, which are within the practical range stated in the literature (Chow et al., 1988). Wiele and Smith (1996) proposed a variable roughness parameter in place of constant Manning's n, stating that a constant Manning's n will not predict the hydrographs satisfactorily. However, VPM flow routing model used in the present study simulates the observed hydrographs at different downstream stations using constant Manning's n values satisfactorily (section 4.4.1). Moreover, the observed hydrographs at different downstream stations in Grand Canyon reach were also simulated with a value of Nash-Sutcliffe criterion, η > 98%, using constant Mannign's n and Multilinear Discrete Lag Cascade (MLDC) method (Camacho, 2000). Hence, it may be concluded that the observations drawn by Wiele and Smith (1996) may be model specific and are not a generalised conclusion.

From the results obtained using the MDLC-ADZ model (Camacho, 2000) in solute routing under unsteady flow conditions, it is interesting to note that a model that gives satisfactory results in simulating dispersion under unsteady flow condition fails to simulate the C-t curves under steady flow, and vice-versa. Steady flow is a special case of unsteady flow, therefore a model applicable for solute transport under unsteady flow condition should be applicable for solute transport under steady flow condition also. MDLC-ADZ model presented by Camacho (2000) lacks this characterisation. However, the proposed AD-VPM model in the present study works well for simulation of solute transport under both steady as well as unsteady streamflow conditions.

Camacho (2000) used a parameter β to estimate the velocity in the natural channel from the velocity obtained using a reach averaged trapezoidal section (Eqn. 2.16) attributing the difference in these velocities to the transient storage solute transport mechanism. It is widely recognised that the observed C-t curves are

skewed particularly with long tails in streams in the presence of dead zones or transient storage zones (Day, 1975; Bencala and Walter, 1983; and Young and Wallis, 1992). However, the observed C-t curves in Colorado river do not show any long tails at any of the sampling stations, neither during steady flow nor during unsteady flow. Further, Graf (1995) stated that " If the dead zones are present that trap water for a significant length of time, then either their volume is small enough that they have no detectable effect on fluid transport in the main channel or they have sufficiently disconnected from the main flow that very little exchange takes place." Hence, it cannot be claimed that the differences, between observed velocities in river and computed velocities in reach averaged representative section, are because of the dead zone or transient storage zone mechanism, which is insignificant in the Grand Canyon reach under consideration (Graf, 1995).

Hence, the velocity conversion coefficient (ψ) used in the present study is a better representation to account for the velocity differences between observed in natural channel and reach averaged channel section (section 4.4.2).

4.5.3.1 Variability of the dispersion coefficient

The variations in D_L due to variations of rate of flow and flow diffusion process are well accounted for, because D_L is related to D_f that describes the flow diffusion process. The solute dispersion coefficient is estimated from flow diffusion coefficient using Eqn. (4.21). The relational coefficient ϕ in Eqn. (4.21) was calibrated using the observed C-t curves under steady flow condition and is kept constant for large variations of flow between 92 m^3/s to 754 m^3/s. Reasonably good predictions of solute transport process under unsteady flow conditions are obtained using a constant relational coefficient ϕ. This implies that the assumption of a constant relational coefficient ϕ is reasonable for the studied Grand Canyon reach.

The key to the demonstrated success of the suitability of the proposed AD-VPM model coupled with the VPM model for solute transport studies under unsteady flow conditions can be attributed to the integrated parameterisation that enables the computation of solute cloud travel time K_C and weighting factor θ_C from hydro-geometric channel characteristics and hydraulic variables.

4.6   CONCLUSIONS

In this chapter an integrated parameterisation of flow and solute transport is presented. This enables the simultaneous routing of both the flow and solute transport phenomena. The integration of parameters of flow and solute routing models has been made by exploiting the similarity in model structure and their parameters. The routing procedure was presented in Fig 4.2. The reach travel time K_C, and the weighting parameter θ_C are physically based parameters. The limiting conditions for the successful application of the AD-VPM model under unsteady flow condition was presented. The aspect of time of release of solute so as to take the advantage of dispersion capabilities of the varying river flow was studied. The proposed AD-VPM solute routing model coupled with VPM flow routing method was demonstrated for its applicability using hypothetical data and field data from experiments conducted on the Colorado River. However, Advection-Dispersion model cannot simulate the observed C-t curves in rivers in the presence of dead zone or transient storage mechanism. Therefore, the proposed AD-VPM model also cannot model the solute transport in the presence of the dead zone or transient storage mechanism. Hence, a simplified Transient Storage model to simulate the C-t curves observed in rivers in the presence of dead zone or transient storage zones is presented in the next chapter.

DEVELOPMENT OF AN APPROXIMATE TRANSIENT STORAGE MODEL

5.1 GENERAL

The bulk of the existing theories on solute dispersion in streams is based on a gradient transfer process. Since late 1960s, it has been realised that the classical AD equation, with constant dispersion coefficient, is not able to simulate the observed C-t curves, particularly with long tails. Hence, researchers (Thackston and Krenkel, 1967; Day, 1975; Sabol and Nordin, 1978; and Liu and Cheng, 1980) have been concerned with the development of a more appropriate theory for solute transport in rivers accounting for long tails. Various theories have been proposed to overcome the shortcomings of the AD model in simulating the observed C-t curves. One such theory considered that temporary entrapment of the solute mass in some pockets of the channel is primarily responsible for the C-t curves with long tails. In this theory, it was conceptualised that the solute transport process in a river reach takes place in two zones, viz., the main channel and a transient storage zone. The main channel is defined as that portion of the stream in which advection and dispersion are the dominant transport mechanisms. The transient storage zone encompasses those zones adjacent to the main channel, on stream bed and bank irregularities, representing relatively stagnant zones of water that are stationary in comparison to the fast moving water of the main channel. Solute transport in this transient storage zone is dominated by the mechanism of dispersion. In recent years, research has been focused to study the mechanism of solute transport in streams with transient storage zone. Mechanism of temporary solute mass trapping within the pockets, termed as dead zones or storage zones, of the channel has been thought

139

to be significantly affecting the longitudinal dispersion process in rivers. Initially, the transient storage zone acts as sink to reduce the solute concentration in main channel, as the concentration gradient is towards the transient storage zones. When the concentration of solute in the main channel becomes less than the concentration of solute in the transient storage zone, the solute mass from the transient storage zone starts entering into the main channel. This produces the observed long tail in the C-t curves. Based on this observation, Bencala and Walters (1983) inferred that " there is in fact a mechanism that presents itself as transient storage of solute mass along the length of the stream. Hence, we do not believe that a strict dead zone model is physically descriptive of the processes occurring in mountain streams, but rather that the observed ' transient storage' can be empirically simulated using the identical equations." Transient Storage model describing one-dimensional solute transport in a steady, uniform river reach with transient storage zone has been represented by the following governing equations (Bencala and Walters, 1983; and Seo and Cheong, 2001) as

$$\frac{\partial C}{\partial t} + U \frac{\partial C}{\partial x} = D_{ts} \frac{\partial^2 C}{\partial x^2} + \alpha \ (C_s - C) \qquad (5.1)$$

$$\frac{\partial C_s}{\partial t} = \alpha \frac{A}{A_s} (C - C_s) \qquad (5.2)$$

where, C is the solute concentration in the main channel, Q is the volumetric flow rate, A is the cross–sectional area of the channel, D_{ts} is the main channel dispersion coefficient of TS model, C_s is the solute concentration in the storage zone, A_s is the representative cross-sectional area of the storage zone, and α is the stream storage exchange coefficient. Eqn. (5.2) and the coupling term $\alpha(C_s - C)$ in Eqn. (5.1) are deceptively simple, for they embody several physical principles and constraints. Storage zones are assumed to be stagnant relative to the longitudinal flow of the stream and assumed to obey a first–order mass transfer exchange relationship. That

is, the exchange of solute between the main stream channel and the storage zone is proportional to the difference in concentration of solute between the main channel and the storage zone.

The TS model ideally describes a system with the following characteristics (Bencala and Walters, 1983):

i)   Solute concentration varies only in the longitudinal direction (i.e., concentration does not vary with depth or width).

ii)   There exists a storage zone that is not moving.

iii)   Within the storage zone, solute is instantaneously and uniformly mixed.

iv)   The difference in concentrations and an exchange coefficient simply determine the transport of solute between the storage zone and the main channel.

The effect of transient storage on solute transport has been included in longitudinal transport models using the first order mass transfer equation in which all underlying mechanism are arranged in model parameters, such as exchange coefficient (α) and ratio A_s/A.

The analytical solution of the transient storage model equations has not yet been derived. However, solution of the transformed Transient Storage model equations into the so called x-s image (Laplace) space using Laplace transform method is available, which is inadequate to solve the governing system of partial differential equations of TS model analytically in simple (x,t) plane (Nordin and Troutman, 1980; Czernuszenko and Rowinski, 1997). Numerical solutions of Eqns. (5.1) and (5.2) lack simplicity and require calibration of as many as three parameters. The TS model has not been widely used perhaps because of the complexities involved in the solution procedure and due to difficulties in estimating the parameters of the model.

Complexities increase further when the TS model is coupled with flow

routing model to study the solute transport under unsteady flow conditions. It is not possible to solve both the flow routing model and the TS model equations using a similar solution algorithm that enables simultaneous routing of flow and solute. So far, the flow and transport model equations have been solved using different numerical methods. The ADZ model, a simplified version of the Dead Zone model (Thackston and Krenkel, 1967; Valentine and Wood, 1977; and Sabol and Nordin 1978), has been developed to study the solute transport in rivers with transient storage (Beer and Young, 1983). The governing equation of the ADZ model resembles the governing equation of delayed Muskingum flow routing model (Strupczewski and Napiorkowski, 1990). In ADZ model identification and estimation of parameters is equally complicated. Hence, an attempt has been made in the present study to develop a simple TS model equation. The proposed equation allows one to solve it either analytically or using simple numerical methods.

This chapter presents (i) the development of an Approximate Transient Storage (ATS) model, (ii) the analytical solution of the developed ATS model equation for impulse, uniform step and pulse input boundary conditions, and (iii) Muskingum type solute routing formulation based on the ATS model under steady and unsteady streamflow conditions.

5.2 DEVELOPMENT OF AN APPROXIMATE TRANSIENT STORAGE MODEL

An Approximate Transient Storage model is developed using the governing equations (5.1) and (5.2) of the TS model. Eqn. (5.2) can be re-written as

$$\frac{\partial C_s}{\partial t} = \frac{\alpha}{\beta}(C - C_s) \tag{5.3}$$

in which, $\beta = A_s/A$

Using Eqn. (5.3), Eqn. (5.1) can be written as

142

$$\frac{\partial C}{\partial t} + U\frac{\partial C}{\partial x} = D_{ts}\frac{\partial^2 C}{\partial x^2} - \beta\frac{\partial C_s}{\partial t} \tag{5.4}$$

Differentiating Eqn. (5.1) with reference to t and rearranging the terms yields

$$\frac{\partial C_s}{\partial t} = \frac{1}{\alpha}\frac{\partial^2 C}{\partial t^2} + \frac{U}{\alpha}\frac{\partial^2 C}{\partial t\,\partial x} + \frac{\partial C}{\partial t} - \frac{D_{ts}}{\alpha}\frac{\partial^3 C}{\partial t\,\partial x^2} \tag{5.5}$$

Substituting Eqn. (5.5) in Eqn. (5.4) and rearranging the terms gives

$$\frac{\partial C}{\partial t} + \frac{U}{1+\beta}\cdot\frac{\partial C}{\partial x} = \frac{D_{ts}}{1+\beta}\frac{\partial^2 C}{\partial x^2} - \frac{\beta}{\alpha(1+\beta)}\left[\frac{\partial^2 C}{\partial t^2} + U\frac{\partial^2 C}{\partial t\,\partial x}\right] + \frac{\beta\,D_{ts}}{\alpha(1+\beta)}\frac{\partial^3 C}{\partial t\,\partial x^2} \tag{5.6}$$

The expressions for $\partial^2 C/\partial t^2$ and $\partial^2 C/\partial t\partial x$ in Eqn. (5.6) can be arrived at from the following steps:

Differentiating Eqn. (5.4) with reference to x and rearranging the terms results in

$$\frac{\partial^2 C}{\partial x\,\partial t} = -U\frac{\partial^2 C}{\partial x^2} + D_{ts}\frac{\partial^3 C}{\partial x^3} - \beta\frac{\partial^2 C_s}{\partial x\,\partial t} \tag{5.7}$$

Differentiating Eqn. (5.5) with reference to x gives an expression for $(\partial^2 C_s/\partial x\,\partial t)$ in Eqn. (5.7) as

$$\frac{\partial^2 C_s}{\partial x\,\partial t} = \frac{1}{\alpha}\frac{\partial^3 C}{\partial x\,\partial t^2} + \frac{U}{\alpha}\frac{\partial^3 C}{\partial t\,\partial x^2} + \frac{\partial^2 C}{\partial x\,\partial t} - \frac{D_{ts}}{\alpha}\frac{\partial^4 C}{\partial x\partial t\partial x^2} \tag{5.8}$$

Substituting Eqn. (5.8) into Eqn. (5.7) and rearranging the terms, yields

$$\frac{\partial^2 C}{\partial x\,\partial t} = -\frac{U}{1+\beta}\frac{\partial^2 C}{\partial x^2} - \frac{\beta}{\alpha(1+\beta)}\left[\frac{\partial^3 C}{\partial x\,\partial t^2} + U\frac{\partial^3 C}{\partial t\,\partial x^2}\right] + \frac{D_{ts}}{1+\beta}\frac{\partial^3 C}{\partial x^3} + \frac{D_{ts}}{\alpha}\frac{\beta}{(1+\beta)}\frac{\partial^4 C}{\partial x\partial t\partial x^2} \tag{5.9}$$

Differentiating Eqn. (5.4) with reference to t yields

$$\frac{\partial^2 C}{\partial t^2} = -U\frac{\partial^2 C}{\partial t\,\partial x} - \beta\frac{\partial^2 C_s}{\partial t^2} + D_{ts}\frac{\partial^3 C}{\partial t\,\partial x^2} \tag{5.10}$$

Differentiating Eqn. (5.5) with reference to t, gives

$$\frac{\partial^2 C_s}{\partial t^2} = \frac{1}{\alpha}\frac{\partial^3 C}{\partial t^3} + \frac{U}{\alpha}\frac{\partial^3 C}{\partial t^2\partial x} + \frac{\partial^2 C}{\partial t^2} - \frac{D_{ts}}{\alpha}\frac{\partial^4 C}{\partial t^2\partial x^2} \tag{5.11}$$

143

Substituting the expression for $\partial^2 C_s/\partial t^2$ from Eqn. (5.11) in Eqn. (5.10) and rearranging the terms gives

$$\frac{\partial^2 C}{\partial t^2} = -\frac{U}{1+\beta}\frac{\partial^2 C}{\partial t\,\partial x} - \frac{\beta}{\alpha(1+\beta)}\left[\frac{\partial^3 C}{\partial t^3} + U\frac{\partial^3 C}{\partial t^2\,\partial x}\right] + \frac{D_{ts}}{1+\beta}\frac{\partial^3 C}{\partial t\,\partial x^2} + \frac{D_{ts}}{\alpha}\frac{\beta}{(1+\beta)}\frac{\partial^4 C}{\partial t^2\,\partial x^2}$$

(5.12)

Substituting Eqn. (5.12) in Eqn. (5.6) and rearranging the terms, results in

$$\frac{\partial C}{\partial t} + \frac{U}{1+\beta}\frac{\partial C}{\partial x} =$$

$$\frac{D_{ts}}{1+\beta}\frac{\partial^2 C}{\partial x^2} - \frac{\beta^2}{\alpha(1+\beta)^2}U\frac{\partial^2 C}{\partial x\,\partial t} + \frac{\beta^2}{\alpha^2(1+\beta)^2}\left[\frac{\partial^3 C}{\partial t^3} + U\frac{\partial^3 C}{\partial t^2\partial x}\right] - \frac{\beta D_{ts}}{\alpha(1+\beta)^2}\frac{\partial^3 C}{\partial t\,\partial x^2} -$$

$$\frac{\beta^2 D_{ts}}{\alpha^2(1+\beta)^2}\frac{\partial^4 C}{\partial t^2\,\partial x^2}$$

(5.13)

Substituting the expression for $\partial^2 C/\partial x\,\partial t$ from Eqn. (5.9) into Eqn. (5.13), results in

$$\frac{\partial C}{\partial t} + \frac{U}{1+\beta}\frac{\partial C}{\partial x} =$$

$$\left[\frac{D_{ts}}{1+\beta} + \frac{U^2\beta^2}{\alpha(1+\beta)^3}\right]\frac{\partial^2 C}{\partial x^2} + \frac{\beta^2}{\alpha^2(1+\beta)^2}\left\{\left[\frac{\partial^3 C}{\partial t^3} + U\frac{\partial^3 C}{\partial t^2\partial x}\right] + \frac{U\beta}{(1+\beta)}\left[\frac{\partial^3 C}{\partial x\partial t^2} + U\frac{\partial^3 C}{\partial x\partial t\partial x}\right]\right\}$$

$$- \frac{U\beta^2 D_{ts}}{\alpha(1+\beta)^3}\frac{\partial^3 C}{\partial x^3} - \frac{\beta D_{ts}}{\alpha(1+\beta)^2}\frac{\partial^3 C}{\partial t\,\partial x^2} - \frac{\beta^2 D_{ts}}{\alpha^2(1+\beta)^2}\left[\frac{\partial^4 C}{\partial t^2\partial x^2} + \frac{U\beta}{(1+\beta)}\frac{\partial^4 C}{\partial x\partial t\partial x^2}\right]$$ (5.14)

Neglecting third and fourth order derivatives in Eqn. (5.14), gives an equation which is in a form similar to that of AD equation as

$$\frac{\partial C}{\partial t} + \frac{U}{1+\beta}\frac{\partial C}{\partial x} = \left[\frac{D_{ts}}{1+\beta} + \frac{U^2\beta^2}{\alpha(1+\beta)^3}\right]\frac{\partial^2 C}{\partial x^2}$$

(5.15)

Eqn. (5.15) can be written as

$$\frac{\partial C}{\partial t} + U_s\frac{\partial C}{\partial x} = D_{Lts}\frac{\partial^2 C}{\partial x^2}$$

(5.16)

where,

$$U_s = \frac{U}{1+\beta}$$

(5.17)

144

and

$$D_{Lts} = \left[\frac{D_{ts}}{1+\beta} + \frac{U^2 \beta^2}{\alpha(1+\beta)^3} \right] \qquad (5.18)$$

Equation (5.16) is termed as the Approximate Transient Storage (ATS) equation of the ATS model. This is an approximation of TS model as third and fourth order derivatives of concentration are negligible. The term $\beta^2/\alpha^2(1+\beta)^2$ appearing with third and fourth order derivatives in Eqn. (5.14) has been used subsequently to develop an applicability criterion of ATS model so that the simulations using this ATS model are in close agreement with the TS model.

5.3 CHARACTERISTICS OF THE APPROXIMATE TRANSIENT STORAGE MODEL

The ATS model is an approximation of the TS model. The assumptions used in the development of the TS model also hold good for the ATS model. The governing equation (Eqn. 5.16) of the ATS model is in a form similar to that of the AD equation (Eqn. 2.2). If β =0, and $D_{ts} = D_L$, then Eqn. (5.16) gets reduced to Eqn. (2.2). The ATS model enables one to distinguish the role of the transient storage model parameters β and α on solute transport process in rivers. When there is no exchange of solute between the main channel flow and transient storage zone $(\alpha \rightarrow 0)$, the effect of transient storage zones on solute transport will be absent. This situation was termed as frozen cloud phenomenon (Czernuszenko and Rowinski, 1997). Hence, β will influence the velocity of solute cloud U_s only in the presence of α, but α will not alter the value of U_S explicitly. In the ATS model, the relationship between the solute transport velocity and the flow velocity is obtained, as given by Eqn. (5.17), directly from the governing equation itself without involving the use of moment matching technique as has been done by Lees et al. (2000). Valentine and Wood (1977), Worman (2000), and Lees et al. (2000) suggested the same relationship between U and U_s as expressed by Eqn. (2.16) in which $\beta = A_s/A$.

145

In TS model, the dispersion is predominantly due to the rate of exchange of solute between the main flow and storage zone represented by the exchange coefficient α. It is seen from Eqn. (5.18) that the effect of D_{ts} on dispersion of solute may be incorporated in α and β so as to avoid the usage of D_{ts} explicitly. This concept is indirectly used in the development of the ADZ modelling which was conceptualized based on the Dead Zone model, where the effect of D_{ts}, α, and β were embodied in the dead zone residence time (Beer and Young, 1983) and advection is incorporated using a time delay parameter, τ_d (section 2.2.5). Similarly, the effects of α and β on dispersion of solute may be incorporated in D_{ts} enabling one to eliminate the theoretically less understood exchange coefficient α. This concept is used in the present study of developing the ATS model, where the effect of D_{ts}, α, and β is embodied in a parameter D_{Lts}, in a way similar to D_L of the AD model. The parameter D_{Lts} is termed as the ATS dispersion coefficient.

Unlike the ADZ model, which is conceptualised by neglecting the main channel dispersive characteristics, the governing equation of the ATS model has been derived directly from the TS model. The ATS model gives a greater insight into the dispersion mechanism of transient storage zone in comparison with the ADZ model. In the TS modelling approach there is yet a rather poor understanding of the role of exchange coefficient, α on the exchange of solute between the storage zone and the overlying water, and it is not feasible to estimate α theoretically (Rutherford, 1994). But the usage of α can be avoided In the ATS modelling by lumping the effects of D_{ts}, α, and β into the single parameter D_{Lts}. This also avoids the estimation of D_{ts} separately.

It may be inferred from Eqn. (5.18) that the parameters responsible for dispersion, viz., D_{ts}, β, and α are interrelated. Hence, it is possible to have different combinations of these parameters that can simulate the solute transport in rivers in the presence of transient storage. The same has been pointed out by Rutherford

146

(1994) stating that *"It is not easy to obtain a unique calibration of D_{ts}, β, and α from a set of tracer results."* As pointed out by Rutherford (1994), more research is still needed to interpret the physical significance of the model parameters, since comparatively few data sets have been analyzed and not enough information is available for practitioners.

5.3.1 Advantages of the model

The following are the advantages of the proposed ATS model (Eqn.5.16) over the TS model's system of partial differential equations in the TS model (Eqns. 5.1 and 5.2)

1.   The ATS equation (Eqn. 5.16) is in a form similar to that of the AD equation, which enables one to develop analytical solutions analogous to that of AD equation (Eqn. 2.2)

2.   The ATS equation can be solved using simple numerical methods, which have already been used and tested to solve the AD equation, unlike the complex numerical methods used to solve the governing equations of the TS model.

3.   The effect of individual parameters U, β, α, and D_{ts} on the overall dispersion of the ATS model can be investigated based on Eqn. (5.18).

4.   The number of parameters of the TS model can be reduced by replacing the combined effects of U, α, β, and D_{ts} on dispersion with a single representative parameter D_{Lts} analogous to the dispersion coefficient D_L of the AD equation. This reduces the problems associated with parametric uncertainty (because of the reduction in parameters) and estimation of a unique calibration set of D_{ts}, α, and β values of the TS model.

5.   The ATS equation using the parameter D_{Lts} avoids the usage of exchange coefficient α. This enables one to overcome the difficulty expressed by Rutherford (1994) in estimation of model parameter, α that there is yet no

147

clear understanding of the rate of exchange between transient storage zone and the overlying water and it is not feasible to theoretically estimate α from physical characteristics of flow and channel.

The disadvantage of the ATS model is that it cannot reproduce the TS model solution beyond a certain range of α and β because of the assumptions and approximations involved in its development from the TS model equations. The terms containing α and β, particularly α^2 in the denominator, associated with the 3rd and higher order derivatives of concentration restrict the applicability of the ATS model well within the applicability range of the TS model. In addition, further research is necessary to know the concentration of the solute in the transient storage zone using ATS model.

5.4 ANALYTICAL SOLUTION OF THE APPROXIMATE TRANSIENT STORAGE MODEL

The Transient Storage model cannot be solved to give an analytical solution for the concentration C(x,t), However, the form of the ATS model enables one to develop analytical solutions analogous to those corresponding to the AD equation developed for impulse input, step input, and pulse input boundary conditions under steady flow conditions assuming U and D_{Lts} as constant. The analytical solution of Eqn. (5.16), for steady and uniform flow conditions in a river, for uniform step input boundary condition ($C(x,0) = 0$, and $C(0,t) = C_I$), (known as Ogata and Banks (1961) solutions for the AD equation), has been given as

$$C(x,t) = \frac{C_I}{2}\left[erfc\left(\frac{x - U_s t}{2\sqrt{D_{Lts}t}}\right) + \exp\left(\frac{U_s x}{D_{Lts}}\right) erfc\left(\frac{x + U_s t}{2\sqrt{D_{Lts}t}}\right)\right] \quad (5.19)$$

where, $erfc(z)$ is complimentary error function given by Eqn.(2.5) U_s and D_{Lts} are given by Eqn. (5.17) and (5.18) respectively.

The analytical solution of the Eqn. (5.16) for an impulse input of conservative solute mass M is given as

148

$$C(x,t) = \frac{M}{A\sqrt{4\Pi D_{Lts}t}} \exp\left[\frac{-(x-U_s\,t)^2}{4D_{Lts}t}\right] \tag{5.20}$$

The analytical solution of Eqn. (5.16) for uniform pulse input of duration, τ, during $t \leq \tau$ is given by Eqn (5.19) and during $t > \tau$, it is given as

$$C(x,t) = \frac{C_I}{2}\left\{\begin{array}{l}\left[erfc\left(\frac{x-U_s t}{2\sqrt{D_{Lts}\,t}}\right) - erfc\left(\frac{x-U_s(t-\tau)}{2\sqrt{D_{Lts}(t-\tau)}}\right)\right] + \\ \exp\left[\frac{U_s\,x}{D_{Lts}t}\right]\left[erfc\left(\frac{x+U_s t}{2\sqrt{D_{Lts}t}}\right) - erfc\left(\frac{x+U_s(t-\tau)}{2\sqrt{D_{Lts}(t-\tau)}}\right)\right]\end{array}\right\} \tag{5.21}$$

Based on the AD equation, a simplified Muskingum type solute routing model (AD-VPM model) was developed in Chapter 3. In a similar way, a simplified Muskingum type solute routing model can be developed using the ATS model equation for modelling solute transport process in the presence of transient storage zone along the river reach.

5.5 DEVELOPMENT OF MUSKINGUM SOLUTE TRANSPORT MODEL

The Approximate Transient Storage model enables the development of Muskingum flow routing type solute transport model formulation based on the concept of the VPM method in a way as demonstrated for the case of the AD equation (sections 3.2 and 3.3)

5.5.1 Solute Transport Model Formulation- Steady Streamflow Conditions

The assumptions made and the procedure followed to develop an approximate AD equation (Eqn. 3.12) in section 3.2 of Chapter 3 can be adopted to develop a simplified ATS equation as described below:

Eqn. (5.16) can be written as

$$\frac{\partial C}{\partial t} + \frac{\partial(U_s C)}{\partial x} = \frac{\partial^2(D_{Lts}C)}{\partial x^2} \tag{5.22}$$
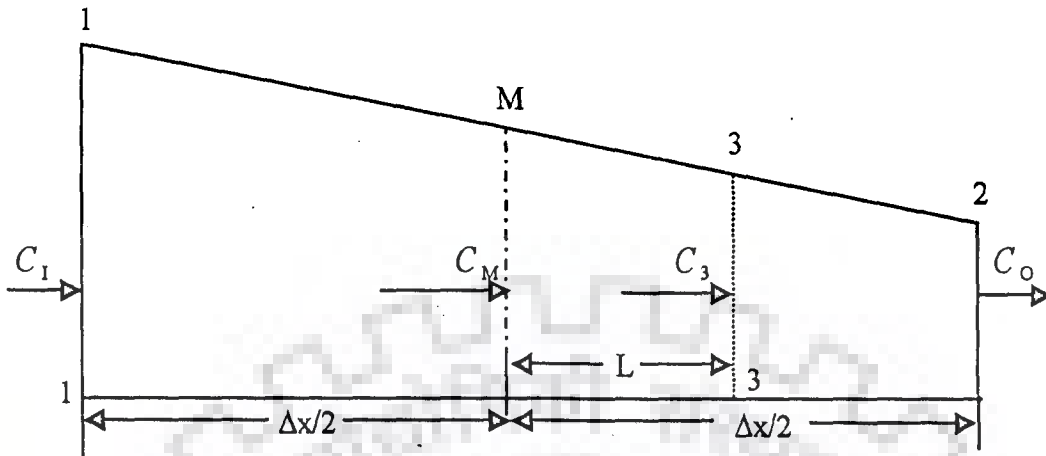
Figure 5.1 Definition sketch of the Muskingum solute routing reach

Assuming that the concentration varies linearly over a small reach length as shown in the definition sketch Fig. 5.1, Eqn. (5.22) can be written as

$$\frac{\partial C}{\partial t} + U_s \frac{\partial \left(C - \frac{D_{Lts}}{U_s} \frac{\partial C}{\partial x} \right)}{\partial x} = 0 \tag{5.23}$$

In a way similar to Eqn. (3.8), the concentration at the middle of the reach C_M is represented as

$$C_M = C - \frac{D_{Lts}}{U_s} \frac{\partial C}{\partial x} \tag{5.24}$$

using the Eqn. (5.24), Eqn. (5.23) is expressed as

$$\frac{\partial C}{\partial t} + U_s \frac{\partial C_M}{\partial x} = 0 \tag{5.25}$$

The linear variation of C over the small reach enables one to write $(\partial C_M / \partial x) = (\partial C / \partial x)$. Then Eqn. (5.25) can be written as

$$\frac{\partial C}{\partial t} + U_s \frac{\partial C}{\partial x} = 0 \tag{5.26}$$

The form of Eqn. (5.26) is similar to the approximate Advection-Dispersion

150

equation (Eqn.3.10) given in Chapter 3. The Muskingum type solute transport model can be formulated based on Eqn. (5.26), using the assumptions made in section 3.2 of Chapter 3, and adopting the procedure similar to that presented based on the approximate AD equation (Eqn. 3.10) in section 3.3 of Chapter 3. This formulation is presented below:

Assuming linear variation of the concentration (assumption 2, section 3.2) and applying Eqn. (5.26) at section 3, shown in Fig. 5.1, yields

$$\frac{dS_{cts}}{dt} = C_I - C_O \tag{5.27}$$

where C_I and C_O are the inflow and outflow concentrations, at a time step respectively and S_{cts} is the storage of mass per unit inflow rate analogous to the storage of flow and is given by

$$S_{cts} = K_{cts}\left[\theta_{cts}C_I + (1-\theta_{cts})C_O\right] \tag{5.28}$$

where, K_{cts} denotes the travel time and is expressed as

$$K_{cts} = \frac{\Delta x}{U_s} \tag{5.29}$$

θ_{cts} denotes the weighting parameter and is expressed as

$$\theta_{cts} = \frac{1}{2} - \frac{D_{Lts}}{U_s \Delta x} \tag{5.30}$$

Substituting the expression for U_s from Eqn. (5.17) and D_{Lts} from Eqn. (5.18), in Eqns. (5.29) and (5.30) respectively gives

$$K_{cts} = \frac{\Delta x}{U}(1+\beta) \tag{5.31}$$

and

$$\theta_{cts} = \frac{1}{2} - \left[\frac{D_{ts}}{(1+\beta)} + \frac{U^2\beta^2}{\alpha(1+\beta)^3}\right]\frac{(1+\beta)}{U\Delta x} \tag{5.32}$$

Eqn. (5.32) can also be written as

$$\theta_{cts} = \frac{1}{2} - \left[D_{ts} + \frac{U_s^2 \beta^2}{\alpha} \right] \frac{1}{U \Delta x} \qquad (5.33)$$

Using Eqn. (5.28) in Eqn. (5.27), the solute routing equation is expressed as

$$C_{o,j} = \omega_{ts1} C_{i,j} + \omega_{ts2} C_{i,j-1} + \omega_{ts3} C_{o,j-1} \qquad (5.34)$$

where, $C_{i,j}$ and $C_{i,j-1}$ are the inflow concentrations at time $j\Delta t$ and (j-1) Δt respectively; $C_{o,j}$ and $C_{o,j-1}$ are the outflow concentrations at time $j\Delta t$ and (j-1)Δt respectively; and $\omega_{ts1}, \omega_{ts2}$, and ω_{ts3} are the coefficients of the routing equation expressed as

$$\omega_{ts1} = \frac{-K_{cts}\theta_{cts} + \Delta t/2}{K_{cts}(1-\theta_{cts}) + \Delta t/2} \qquad (5.35a)$$

$$\omega_{ts2} = \frac{K_{cts}\theta_{cts} + \Delta t/2}{K_{cts}(1-\theta_{cts}) + \Delta t/2} \qquad (5.35b)$$

$$\omega_{ts3} = \frac{K_{cts}(1-\theta_{cts}) - \Delta t/2}{K_{cts}(1-\theta_{cts}) + \Delta t/2} \qquad (5.35c)$$

It is interesting to see that if $\beta = 0$, the expressions for K_{cts} and θ_{cts} get reduced to K_C (Eqn. 3.21) and θ_C (Eqn. 3.31). Eqns. (5.31) to (5.35) can be used to study the solute dispersion under steady flow condition. Since the approach employed in the development of the VPM method (Perumal, 1994a) has been used in arriving at Eqn. (5.34), and considering that the proposed method has been developed using the simplified Approximate Advection-Dispersion equation (Eqn. 5.26), this method of solute routing may be called as ATS-VPM method.

5.5.2 Solute Transport Model Formulation- Unsteady Streamflow Conditions

Simultaneous routing of flow and solute using the AD-VPM was envisaged in Chapter 4, based on the Approximate Advection-Dispersion equation of the respective process, to study the one-dimensional solute transport under unsteady flow conditions. The VPM method was used to model the flow diffusion process.

Similar assumptions and solution procedure can be adopted to study the solute transport in rivers under unsteady streamflow conditions in the presence of the transient storage mechanism affecting the solute transport. The parameters of the AD-VPM solute routing method (K_c and θ_c) were integrated with the parameters of the VPM flow routing method (K_f and θ_f) as described in section 4.2, Chapter 4. In a similar manner the parameters of the ATS-VPM method (K_{cts} and θ_{cts}) and the parameters of the VPM flow routing method (K_f and θ_f) may be integrated, and the parametric relationships thus obtained are expressed as (using Eqns. 5.31 and 4. 5)

$$K_{cts} = K_f \left[1 + m \frac{P(\partial R/\partial y)}{(\partial A/\partial y)} \right] (1+\beta) \tag{5.36}$$

and (using Eqns. 5.30 and 4.9)

$$\theta_{cts} = \theta_f + \frac{1}{U\Delta x} \left[\frac{D_f}{1 + m\left(\frac{P\partial R/\partial y}{\partial A/\partial y}\right)_3} - (1+\beta)D_{Lts} \right] \tag{5.37}$$

However, the integration of θ_{cts} with θ_f needs further studies, as unlike in the case of AD-VPM method where D_L is directly related to D_f, D_{Lts} is not directly related to D_f. The relationship between D_{Lts} and D_f is not yet established. D_{Lts} depends not only on the dispersion of the main channel flow, but also on the dispersion due to storage zone mechanism. Flow and solute can be routed simultaneously because of the similarity in the model structure and the integration of parameters of both the models. The algorithm of the ATS-VPM model coupled with the VPM flow routing method to simulate the solute transport under unsteady flow conditions in the presence of transient storage mechanism affecting dispersion process is presented in Fig. 5.2.

$$\boxed{\text{Routing Step J = 1}}$$

$$\downarrow$$

Estimate initial K_f and θ_f and K_{Cls} and θ_{Cls} using Eqns. (4.5) & (4.6) and Eqns. (5.31) & (5.32) and initial values of flow

$$\downarrow$$

$$\boxed{J = J + 1}$$

$$\downarrow$$

$$\boxed{\text{Iteration step I = 1}}$$

$$\downarrow$$

Estimate ε_1, ε_2 & ε_3,

$$\varepsilon_1 = \frac{-K_f\theta_f + \Delta t/2}{K_f(1-\theta_f) + \Delta t/2} \ ; \ \varepsilon_2 = \frac{K_f\theta_f + \Delta t/2}{K_f(1-\theta_f) + \Delta t/2} \ ; \ \varepsilon_3 = \frac{K_f(1-\theta_f) - \Delta t/2}{K_f(1-\theta_f) + \Delta t/2}$$

and $\omega_{ts1}, \omega_{ts2}$ and ω_{ts3} using Eqn. (5.35)

$$\downarrow$$

Estimate $(Q_O)_j = \varepsilon_1(Q_I)_j + \varepsilon_2(Q_I)_{j-1} + \varepsilon_3(Q_O)_{j-1}$

$C_{o,j} = \omega_{ts1}C_{i,j} + \omega_{ts2}C_{i,j-1} + \omega_{tc3}C_{o,j-1}$

$$\downarrow$$

Estimate $Q_3 = \theta_f (Q_I)_j + (1-\theta_f)(Q_O)_j$

$$\downarrow$$

Estimate y_M using Newton-Raphson Method from $Q_3 = A_M C_f (R_M)^m S_o^{1/2}$

$$\downarrow$$

Estimate $Q_M = [(Q_I)_j + (Q_o)_j]/2$

$$\downarrow$$

Estimate $F_M = Q_M^2 (\partial A/\partial y)|_M /g \ A_M^2$

$$\downarrow$$

Estimate, $y_3 = y_M + (Q_3 - Q_M) / (\partial A/\partial y)|_M \{1 + m [(P\partial R/\partial y)/(\partial A/\partial y)]_M\} U_M$

$$\downarrow$$

Estimate A_3 corresponding to y_3

$$\downarrow$$

Estimate $U_3 = Q_3/A_3$

$$\downarrow$$

Estimate revised K_f and θ_f and K_{Cls} and θ_{Cls} for the present routing step using Eqns. (4.5) & (4.6) and Eqns. (5.31) & (5.32) respectively

$$\downarrow$$

$$\boxed{I = I + 1}$$

$$\downarrow$$

No $\longleftarrow$ $\boxed{\text{IS } I > 2 \ ?}$

$\downarrow$ Yes

Estimate $y_I = y_M + ((Q_o)_j - Q_M)/(\partial A/\partial y)|_M \{1 + m [(P\partial R/\partial y)/(\partial A/\partial y)]_M\} U_M$

$$\downarrow$$

No $\longleftarrow$ $\boxed{\text{IS } J \geq N \text{ steps } ?}$

$\downarrow$ Yes

$$\boxed{\text{STOP}}$$

Figure 5.2 The solution algorithm of the ATS-VPM method under unsteady streamsflow conditions

154

5.6 CONCLUSIONS

Approximate Transient Storage (ATS) model has been developed from the governing equations of the TS model. The merits and demerits of the ATS model were discussed. The analytical solutions of the ATS model equation were presented for impulse, pulse, and step input boundary conditions. The ATS-VPM solute transport method was presented for studying the transport processes under steady and unsteady streamflow conditions.

The comparison of the ATS model and the TS model, the applicability criterion of the ATS-VPM method and the applications of the proposed ATS-VPM method are presented in the next chapter.
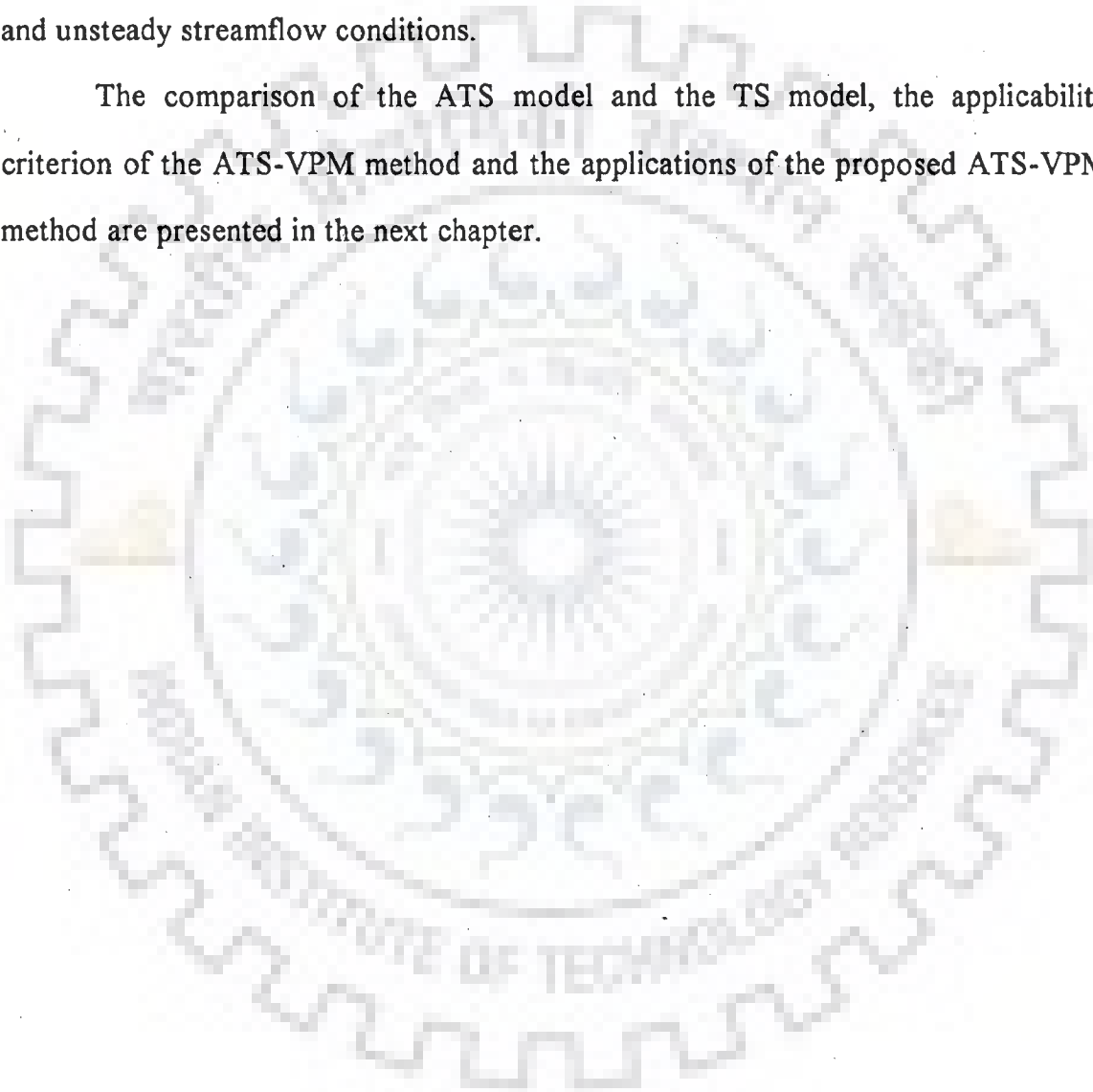
APPLICATIONS OF THE APPROXIMATE TRANSIENT STORAGE MODEL

6.1 GENERAL

Several researchers have suggested that the transient storage mechanism in natural channel is responsible for the skewed nature of solute concentration variation with time in rivers. Transient Storage (TS) model has been used to model the solute transport in rivers affected by transient storage mechanism. The TS model divides the flow into two zones viz., the main stream in which the one-dimensional equation given by Eqn. (5.1) governs the solute transport process, and the transient storage zone along the bed and banks, in which the solute is assumed to be thoroughly mixed and the concentration is assumed to be uniform. Exchange of solute takes place between the main channel flow and the transient storage zone. These two processes are described using a set of governing equations given by Eqns. (5.1) and (5.2) (Bencala and Walters, 1983).

In the present study, an Approximate Transient Storage (ATS) model described by the Eqn. (5.16), has been developed in Chapter 5 for studying solute transport process in rivers subjected to the TS process under steady as well as unsteady flow conditions. The governing equation of the ATS model was derived from the TS model equations (Eqns. 5.1 and 5.2). Equation (5.16) incorporates the effects of transient storage mechanism on flow velocity as Eqn. (5.17) and on dispersion coefficient as described by Eqn. (5.18). Based on the proposed ATS model, the ATS-VPM model was developed (section 5.4).

This chapter is intended to evaluate the ATS model and the ATS-VPM model in detail presenting (i) the comparison between the solutions of the TS model

and the ATS model (ii) the applicability of the ATS-VPM model, and (iii) the applications of the ATS-VPM model under steady and unsteady streamflow conditions.

6.2 COMPARISON OF THE TRANSIENT STORAGE AND THE APPROXIMATE TRANSIENT STORAGE MODELS

In the development of the ATS model from the governing equations of the TS model, it was assumed that the 3rd and higher order derivatives of concentrations are negligible. Hence, the ATS model is only an approximation to the TS model. It can be inferred from Eqn. (5.14) and the equation of the ATS model (Eqn. 5.16) that the parameter β used in the TS model is responsible for the difference between the velocity of solute cloud and that of the flow. The parameter β, defining the ratio of the transient storage zone area to the main channel area, influences the dispersive mechanism provided the exchange of solute between the main channel and the transient storage zone exists. The influence of D_{ts} on dispersion of solute depends on the rate of exchange of solute α, and β (Eqn. 5.18). In the TS modelling, the dispersion of a solute in a river is contributed by the main channel flow and by the transient storage zones. The parameters α and β governing the transient storage mechanism are mainly responsible for the dispersion of solute, particularly under low flow conditions. The rate of exchange represented by the parameter α ranges from a value as low as 10^{-6}/s (Seo and Cheong, 2001) to a value of 0.0162/s (Runkel et al., 1998). When α, is low, its effect on the dispersion of solute would be more in comparison with the corresponding effect of D_{ts} in the presence of transient storage mechanism. This may be explained using Eqn. (5.18) in, which α is present in the denominator of the second term of the right hand side of the equation.

6.2.1 Applicability Analysis of the ATS Model

As the ATS model is an approximation to the TS model, it is necessary to evaluate the applicability criterion under which the ATS model can reproduce the complete TS model solution. This has been studied based on the numerical solution of the complete TS model equations (Eqns. 5.1 and 5.2) for a given hypothetical uniform pulse input. The numerical solution of the TS model used in the present study was obtained using the Crank-Nicolson model suggested by Runkel and Chapra (1993). The numerical solution, thus obtained for the hypothetical input is considered as the benchmark solution with which the analytical solution of the proposed ATS model is compared. The analytical solution of the ATS model was obtained using Eqns. (5.19) and (5.21) for uniform pulse input. The agreement between the solutions of the ATS model and the TS model is measured using the Nash and Sutcliffe criterion, η given by Eqn. (3.24).

In general, the solutions of numerical models are compared with the analytical solutions so as to know the performance of a numerical model. However, in the present study the analytical solution of the ATS model is compared with the benchmark numerical solution of the TS model. Hence, it is considered that the ATS model is able to closely reproduce the numerical solution of the TS model, when $\eta>98\%$. However, criterion with $\eta<98\%$ may also be adopted for applying the model to field problems provided the results are acceptable under prevailing field conditions.

The term $[\beta/(\alpha(1+\beta))]^2$ that is associated with the 3rd order derivative of concentration (Eqn. 5.14) influences the close reproduction of the TS model by the ATS model. When, $[\beta/(\alpha(1+\beta))]^2$ is considered to be insignificant, then the solution of the TS model and that of the ATS model may not be significantly different from each other. Therefore, the magnitude of $[\beta/(\alpha(1+\beta))]^2$ may be

158

considered as the criterion for the applicability of the ATS model for the satisfactory approximation of the TS model. For further discussion on this chapter let it be expressed as λ, i.e.,

$$\lambda = \left[\frac{\beta}{\alpha(1+\beta)}\right]^2 \tag{6.1}$$

The λ is determined by reproducing the TS model results, obtained using hypothetical data, by the ATS model for the same data. In this study, it is considered that when the ATS model is able to closely reproduce the TS model results with Nash-Sutcliffe criterion, $\eta >98\%$, then the ATS model is an acceptable approximation of the TS model.

A hypothetical uniform pulse input of 50 mg/l for 2 hrs. duration is applied to arrive at the numerical solution of the TS model. The analytical solution of the ATS model for this input is compared with the respective numerical solutions of TS model obtained for different combinations of velocities, dispersion coefficients, exchange coefficients and different values of β. The value of U and β used in the numerical experiments vary in the range of 0.125m/s to 1.0m/s, and 0.1 to 0.75 respectively. The value of β, generally ranges from 0.01 to 0.50 (Seo and Cheong, 2001), but values as high as 3.0 (Bencala and Walters, 1983) and 15.9 to 34.3 (Runkel et al., 1998) have also been reported in literature. However, Runkel et al. (1998) stated that such high value of β might not be realistic. The value of α used in these numerical experiments ranges from 0.000025 /s to 0.0007/s. Since the magnitude of λ decides the closeness of the solution of the ATS model and the TS model, it is obvious from Eqn. (5.14) that the value of D_{ts} would have less or insignificant effect in reducing the TS model to the ATS model. This inference can be made from Eqn. (5.14) wherein D_{ts} is present in the terms $\left[U\beta^2 D_{ts}/(\alpha(1+\beta))^3\right]$ and $\left[\beta D_{ts}/(\alpha(1+\beta)^2)\right]$ associated with the 3rd order derivatives of C and these terms containing D_{ts} cannot magnify the 3rd order derivatives of C, because of the

presence of α in their denominator to an extent that influences the TS model solution. Hence, a constant value of D_{ts} =2.5 m^2/s was used in the numerical experiments. The comparison of both the ATS and TS models solutions are shown in Figs. 6.1 to 6.6. The results are summarised in Table 6.1. Based on the numerical experiments it is concluded that the ATS model can reproduce the TS model solution with a η>98%, when the value of $\lambda \leq 10^6$.
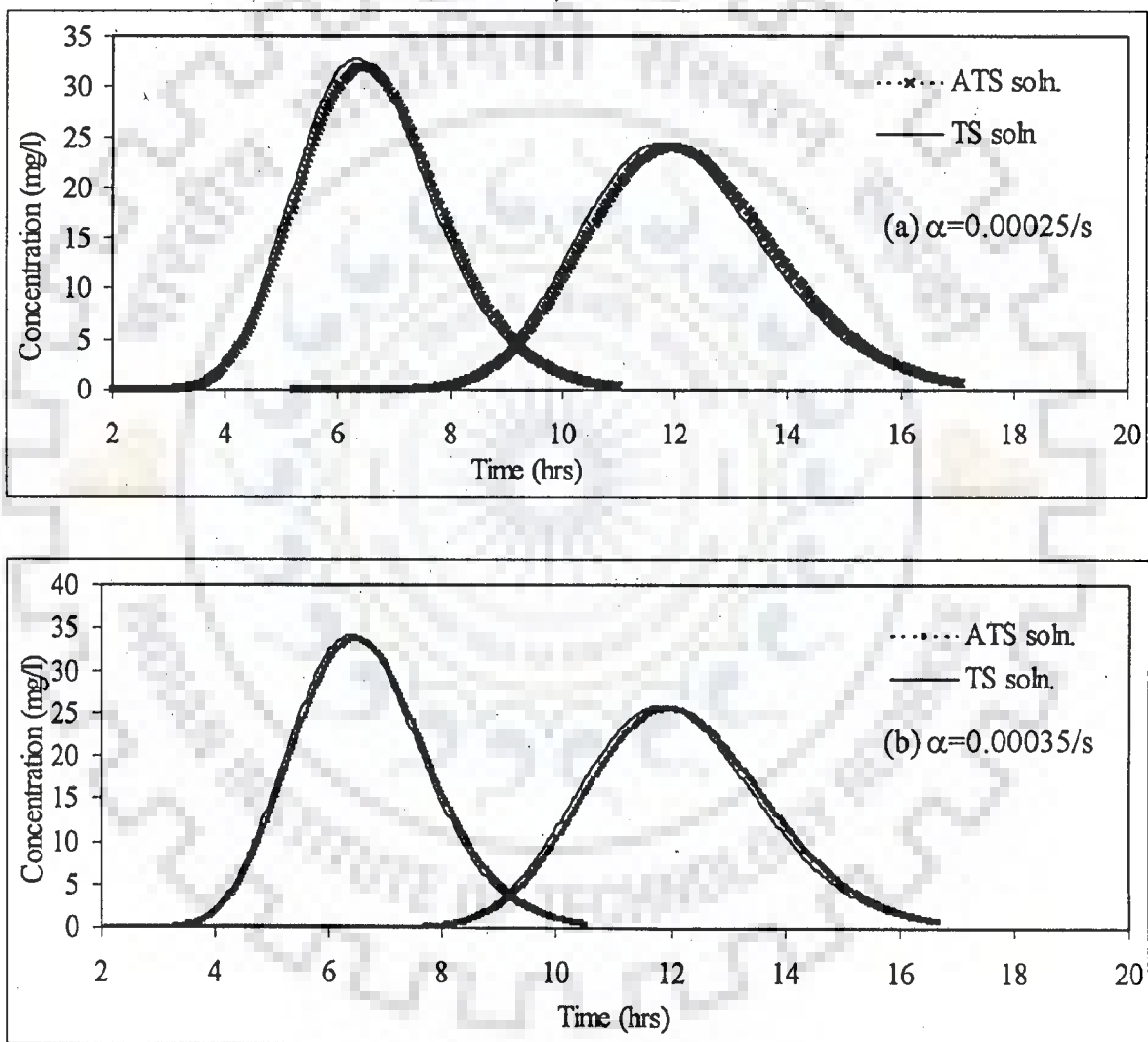
Figure 6.1 Solutions of ATS and TS models for U=0.125m/s, β=0.25 at x=2km and 4km, a) α = 0.00025/s, b) α= 0.00035/s
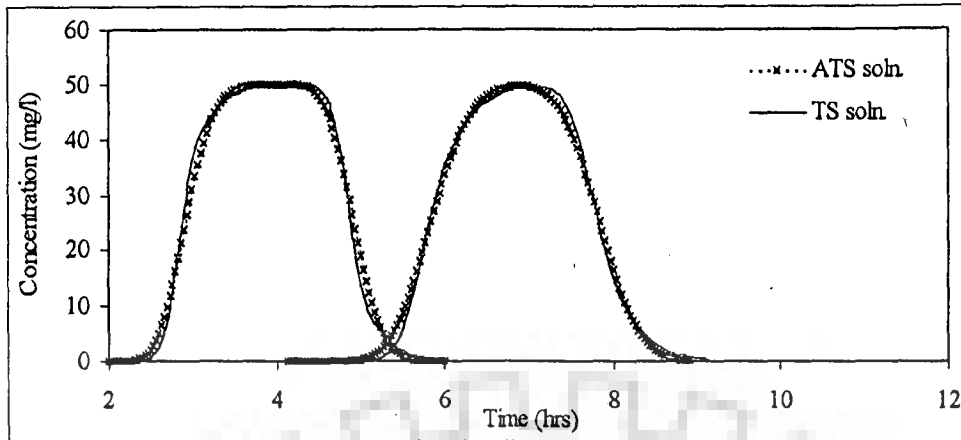
Figure 6.2 Solutions of ATS and TS models for α=0.000075/s, U=0.5m/s, β=0.05 at x=5 km and 10km.
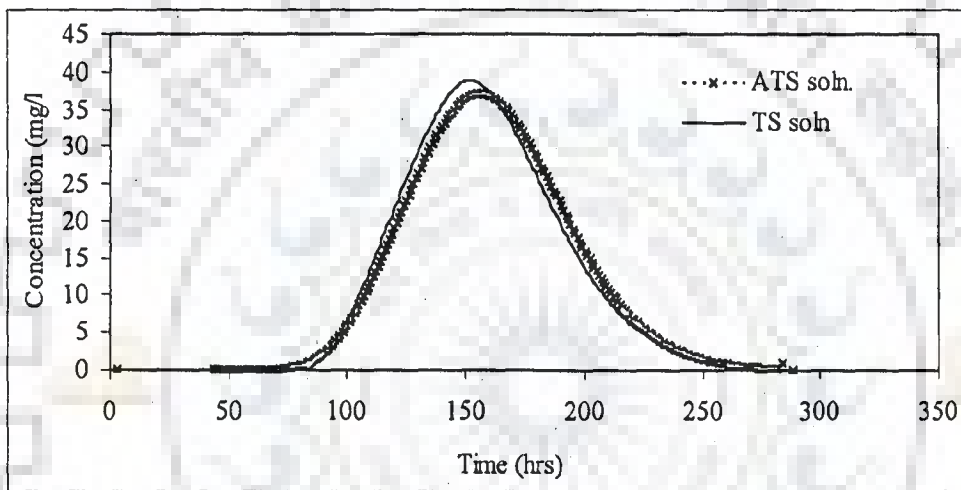
Figure 6.3 Solutions of ATS and TS models for α=0.0005/s, U=0.5m/s, β=0.5 at x=5 km
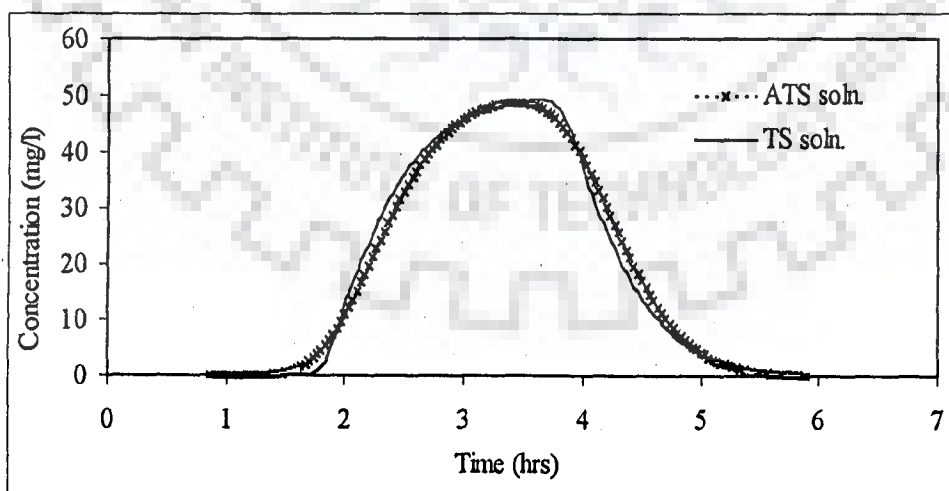
Figure 6.4 Solutions of ATS and TS models for α=0.00035/s, U=0.75m/s, β=0.25 at x=5 km

161
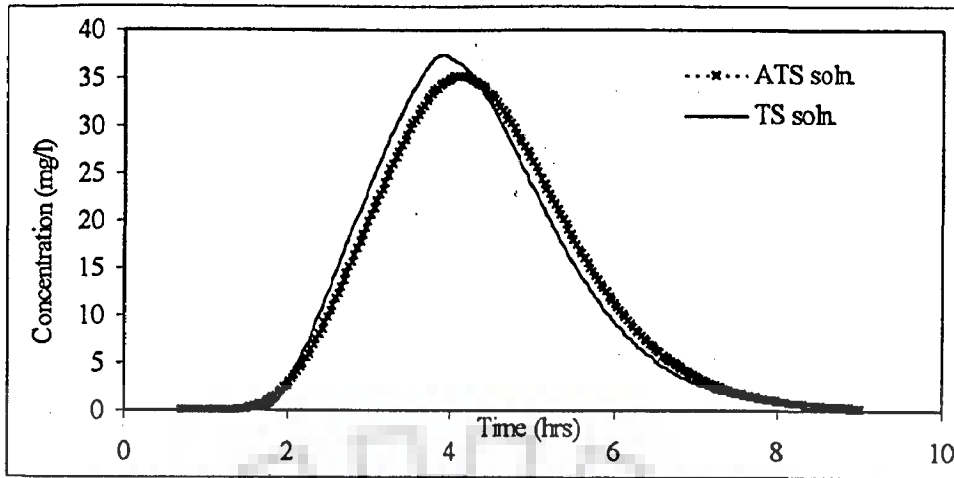
Figure 6.5 Solutions of ATS and TS models for α=0.0006/s, U=0.75m/s, β=0.75 at x=5 km
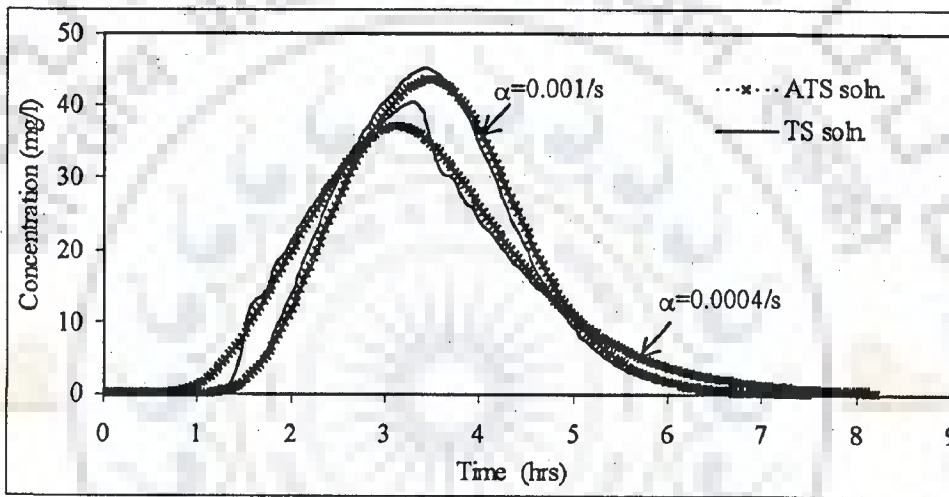
Figure 6.6 Effect of α on the solute transport in the presence of transient storage zone mechanism for U=1.0m/s, β=0.75 at x=5 km
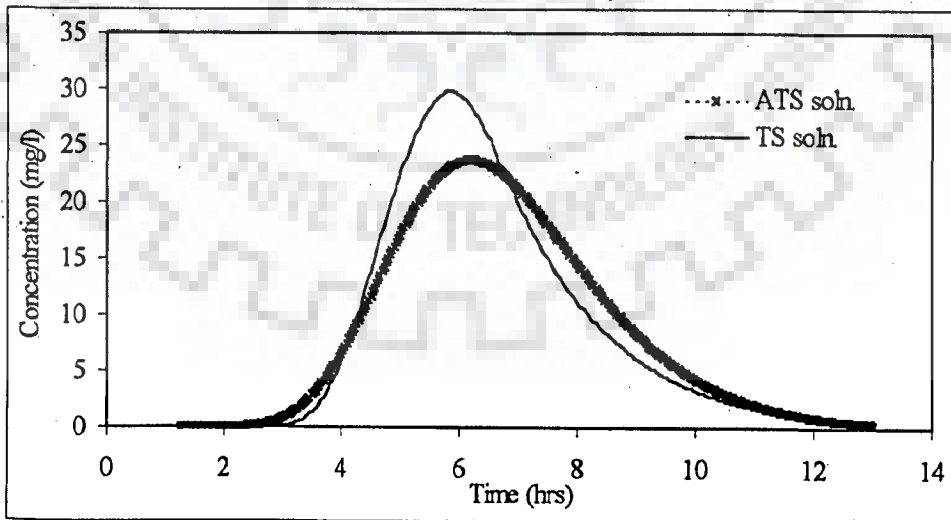
Figure 6.7 Solutions of ATS and TS models for α=0.000075/s, U=0.125m/s, β=0.25 at x=2 km

162

Table 6.1 Summary of the results for the determination of limiting criterion of ATS model to reproduce the TS model solution

Velocity (m/s)	β	α (s⁻¹)	λ	η (%)
0.125	0.1	0.000025	1.32E+07	0.94
		0.00005	3.31E+06	0.98
		0.000075	1.47E+06	0.99
		0.0001	8.26E+05	0.99
	0.25	0.00005	1.60E+07	0.89
		0.000075	7.11E+06	0.94
		0.0001	4.00E+06	0.97
		0.00025	6.40E+05	0.99
		0.00035	3.27E+05	0.99
0.25	0.1	0.00005	3.31E+06	0.96
		0.000075	1.47E+06	0.98
	0.25	0.000075	7.11E+06	0.89
		0.0001	4.00E+06	0.96
		0.00025	6.40E+06	0.99
	0.5	0.0001	1.11E+07	0.91
		0.00025	1.78E+06	0.96
		0.00035	9.07E+05	0.98
		0.0005	4.44E+05	0.99
0.5	0.05	0.00001	2.27E+07	0.92
		0.00003	2.52E+06	0.96
		0.00005	9.07E+05	0.98
		0.000075	4.03E+05	0.99
	0.25	0.00025	6.40E+05	0.98
	0.5	0.0003	1.23E+06	0.97
		0.0004	6.94E+05	0.99
		0.0005	4.44E+05	0.99
	0.75	0.0004	1.15E+06	0.97
		0.00055	6.07E+05	0.98
0.75	0.25	0.0001	4.00E+06	0.90
		0.00025	6.40E+05	0.98
		0.00035	3.27E+05	0.99
	0.5	0.00025	1.78E+06	0.98
		0.00035	9.07E+05	0.98
		0.0005	4.44E+05	0.99
	0.75	0.0004	1.15E+06	0.97
		0.0005	7.35E+05	0.97
		0.0006	5.10E+05	0.98
1	0.25	0.000075	7.11E+06	Oscillatory
		0.00025	6.40E+05	0.98
		0.0005	1.60E+05	0.99
	0.5	0.0003	1.23E+06	0.98
		0.0004	6.94E+05	0.98
		0.0005	4.44E+05	0.98
	0.75	0.00025	2.94E+06	0.96
		0.0004	1.15E+06	0.99
		0.0007	3.75E+05	0.99

6.3 APPLICABILITY ANALYSIS OF THE ATS-VPM MODEL

In order to enable the application of the ATS model to field problems, it is necessary to develop a solution algorithm based on the ATS equation. Using the similarity between the ATS equation (Eqn. 5.16) and the AD equation (Eqn. 3.1), it is considered appropriate to develop numerical solution algorithm using the approach employed in the development of the VPM model. Accordingly, the ATS-VPM model, an approximation of the ATS model was developed in a way similar to that of the AD-VPM model. The ATS model gets reduced to the AD model, if $\beta=0$. Hence, the applicability criterion arrived at for the AD-VPM model in reproducing the solution of AD equation (Section 3.5.2) can be adopted here also to arrive at the applicability criterion of the ATS-VPM model for the close reproduction of the analytical solution of the ATS model with Nash-Sutcliffe criterion, $\eta > 99\%$. Using Eqn. (3.25), and Eqns. (5.17) and (5.18), the relationship between the solute cloud velocity U_s, β and the limiting D_{Lts}, describing the boundary of the applicability domain expressed as

$$D_{Lts} = 416.64 \left[\frac{U}{1+\beta} \right]^{1.71} \tag{6.2}$$

For a given value of U and β the value of the limiting D_{Lts}, for the successful application of the ATS-VPM model, can be determined using the Eqn. (6.2). The limiting D_{Lts} obtained for a given velocity and β allows one to know the domain within which the performance of the ATS-VPM model in reproducing the analytical solution is satisfactory using the Nash-Sutcliffe criterion (η) greater than 99%. Using Eqn. (5.18) and Eqn. (6.2), the expression to compute the minimum value of α above which the ATS-VPM model can reproduce the solution of the ATS model can be arrived at, and is expressed as

$$\alpha = \frac{\beta^2 U^2}{D_{Lts}(1+\beta)^3 - D_{ts}(1+\beta)^2} \tag{6.3}$$

The validity of Eqn. (6.3) was tested by computing the minimum value of α and estimating the corresponding value of α by performing numerical experiments for a given set of U, β, and D_{ts}. The hypothetical uniform input of 100 mg/l for a duration of 2hrs was used in the numerical experiments to arrive at the analytical solution of the ATS model. The analytical solution of the ATS model was obtained for uniform pulse input using Eqns. (5.19) and (5.21). The agreement between the solutions of the ATS model and TS model is measured using the Nash and Sutcliffe's criterion. The value of α thus obtained was close to the value of α computed using Eqn. (6.3). The summary of the results is presented in Table 6.2. The comparison between the solutions of the ATS-VPM model and the ATS model is shown in Figs. 6.8 to 6.12. While conducting the numerical experiments based on the hypothetical data for varying values of U, β and α (Table 6.2), it is found that the ATS-VPM model conserves mass with an error of less than 1 % for all the cases studied.

Because of the similarity between the AD-VPM and the ATS-VPM models, the conclusions arrived from the studies of parameter sensitivity and the effect of using different number of sub-reaches in a given routing reach, as described in section 3.5 for the AD-VPM model are applicable for the ATS-VPM model also. Hence, when there is a variation of $\pm$ 20% in the value of D_{Lts}, the solution of the ATS-VPM model would not be affected significantly. This aspect can be observed in Mimram River experimental test case presented in the next section.

Table 6.2 Limiting value of α computed using Eqn. (6.3) and from Numerical experiments for given U, β, D$_{ts}$, and limiting D$_{Lts}$

β	Velocity (m/s)	D$_{ts}$ (m²/s)	Limiting D$_{Lts}$ (m²/s)	α from numerical Expt. (s⁻¹)	α from Eqn. (6.3) (s⁻¹)
0.1	0.1	1	6.85	0.000013	0.0000126
		5	6.85	0.000033	0.0000325
	0.25	5	32.90	0.00002	0.0000166
		15	32.90	0.000033	0.0000244
	0.5	15	107.78	0.000022	0.000020
		50	107.78	0.000031	0.0000301
		100	107.78	0.00011	0.000111
	0.75	50	215.76	0.000025	0.0000248
		150	215.76	0.000054	0.0000532
		200	215.76	0.00013	0.000125
	1	75	353.07	0.000027	0.0000264
		200	353.07	0.000044	0.0000439
		300	353.07	0.000095	0.0000935
	1.25	100	517.32	0.00003	0.0000275
	1.5	100	706.82	0.00003	0.0000274
		500	706.82	0.00007	0.000067
0.3	0.25	7.5	24.77	0.00014	0.000135
		20	24.77	0.00026	0.000274
	0.5	25	80.97	0.00017	0.000166
		75	80.97	0.0004	0.00044
	1	100	265.25	0.00022	0.000218
		200	265.25	0.00035	0.000368
	1.5	25	531.02	0.00013	0.00018
		75	531.02	0.00015	0.000195
0.5	0.25	7.5	19.35	0.00034	0.000323
		20	19.35	0.00085	0.00077
	0.5	10	63.38	0.00035	0.000327
		25	63.38	0.0004	0.000396
	0.75	25	126.88	0.00038	0.000378
		75	126.88	0.00055	0.000542
	1	50	207.62	0.0004	0.000425
		150	207.62	0.00065	0.000688
	1.5	50	415.64	0.0004	0.000436
		200	415.64	0.00075	0.00059
0.75	0.25	5	14.86	0.000575	0.000547
		10	14.86	0.00075	0.000717
	0.5	5	48.68	0.00057	0.000573
		25	48.68	0.00077	0.000763
	0.75	10	97.45	0.000625	0.000644
		50	97.45	0.00086	0.000857
	1	10	159.46	0.00065	0.000683
		50	159.46	0.0008	0.000802
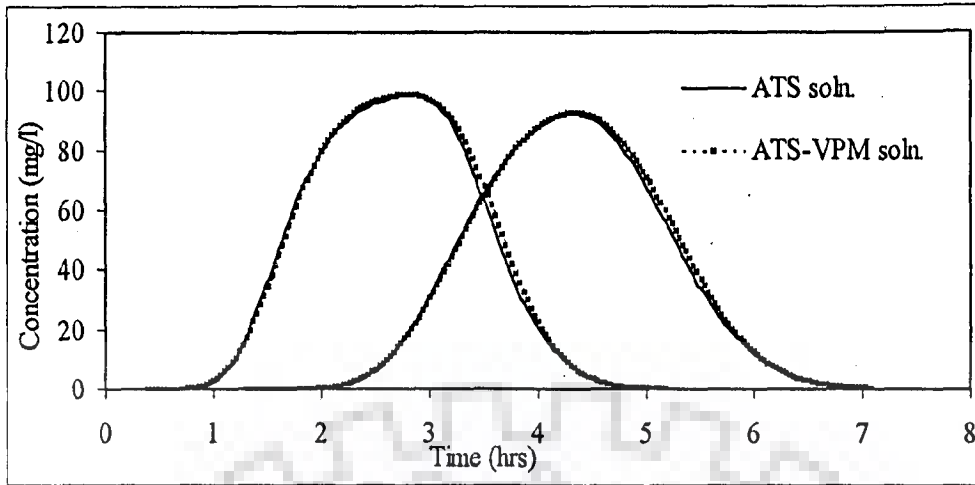
Figure 6.8   Solution of ATS model and ATS-VPM model for α=0.000075/s,
β = 0.1, U=0.75m/s, D_{ts}=30m²/s, at x=4km and 8km
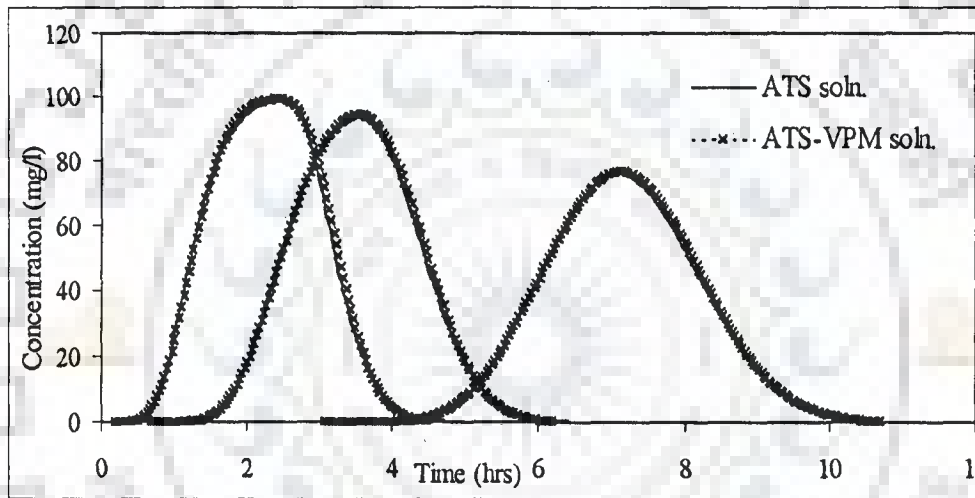
Figure 6.9   Solution of ATS model and ATS-VPM model for α=0.00005/s,
β = 0.1, U=0.5m/s, D_{ts}=7.5m²/s, at x=2km, 4km and 10km
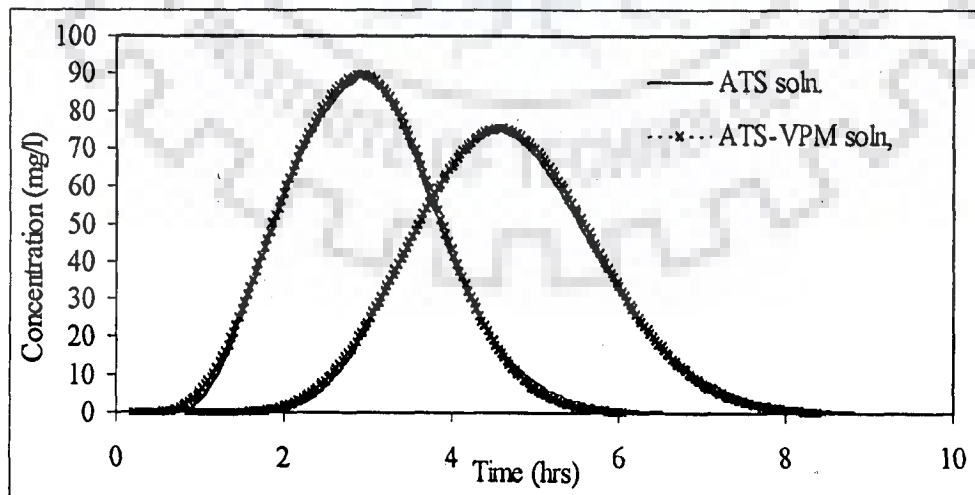
Figure 6.10 Solution of ATS model and ATS-VPM model for α=0.0002/s,
β=0.3, U=0.5m/s, D_{ts}=10m²/s, at x=2.6km and 5km
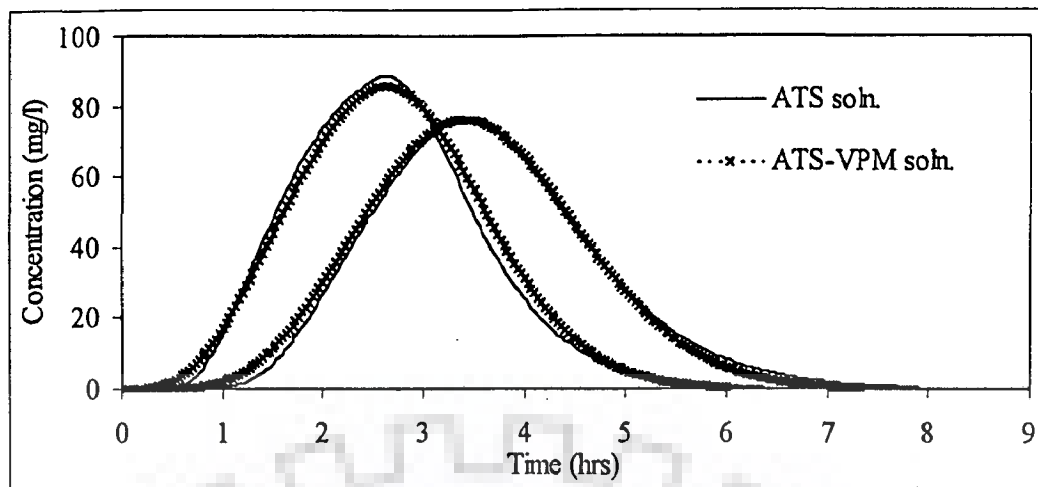
Figure 6.11 Solution of ATS model and ATS-VPM model for $\alpha=0.0003/s$, $\beta=0.5$, $U=1.0m/s$, $D_{ts}=2.5m^2/s$, at $x=4km$ and $6km$
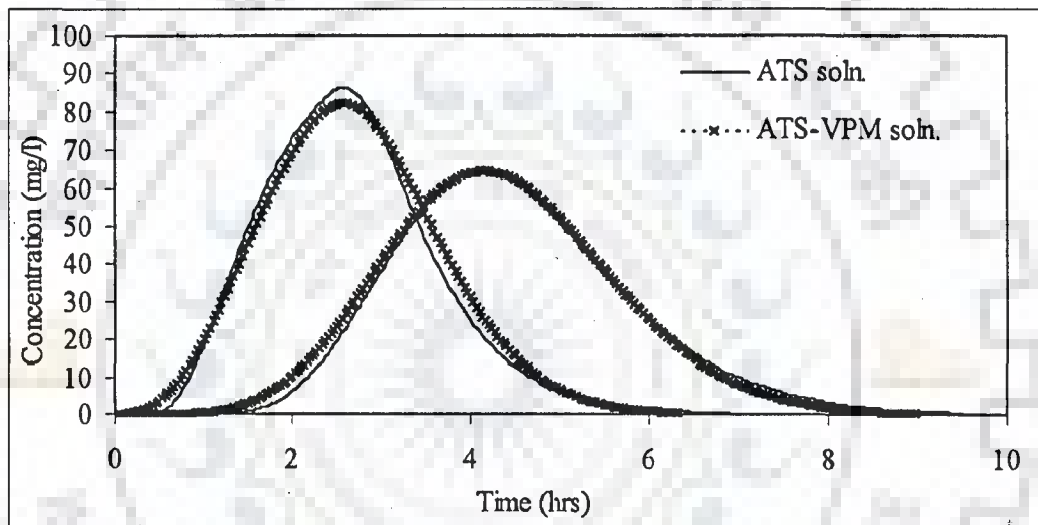
Figure 6.12 Solution of ATS model and ATS-VPM model for $\alpha=0.00025/s$, $\beta=0.5$, $U=0.5m/s$, $D_{ts}=2.5m^2/s$, at $x=2km$ and $4km$

6.4 APPLICATION OF THE ATS-VPM MODEL UNDER STEADY FLOW CONDITIONS

The applicability of the ATS-VPM model needs to be tested using hypothetical data, and data from tracer experiments conducted in rivers. Analysis of the model using hypothetical data was presented while conducting the numerical experiments in section 6.3. Two sets of solute dispersion experiments, one on the Mimram river (Lees et al., 1998) and another on the Uvas creek (Bencala and Walters, 1983), were used to test the applicability of the ATS-VPM model for field conditions.

168

6.4.1 Application to Mimram River Tracer Experiment

A tracer experiment was conducted by Lees et al. (1998) in a reach length of approximately 200 m on Mimram River near the Panshanger flow gauging flume in Hertfordshire, England. The experimental details are given in Appendix B 1.3. The available C-t measurements of this experiment at Site A at 100 m downstream from injection point; site B at 40 m downstream from site A; and Site C at 50 m downstream from site B were used in this test case. The observed hydro-geometric characteristics and the values of the parameters estimated by Lees et al. (2000) for the reaches between sampling stations A and B, and stations B and C are presented in Table 6.3.

Table 6.3 The hydro-geometric characteristics and the parameters for Mimram tracer experiment (Lees et al., 2000)

Reach	Reach Length (m)	Cross-section area (m^2)	Velocity (m/s)	D_{ts} (m^2/s)	β	α (s^{-1})
A-B	40	0.6798	0.3692	0.25	0.1896	0.0059
B-C	50	1.0150	0.2473	0.64	0.1785	0.0017

Using the parameter values estimated by Lees et al. (2000), the values of λ, D_{Lts}, and the limiting value of D_{Lts} were computed to know whether these values fall within the applicability domain of the ATS-VPM model. The computed values of λ and D_{Lts} and the limiting value of D_{Lts} for the observed velocity are shown in Table 6.4. It can be inferred from these values that the ATS-VPM model can be used to simulate the C-t curves observed from tracer experiments conducted on Mimram River.

Table 6.4 The magnitude of λ, D_{Lts} and Limiting D_{Lts} based on the parameter values given by Lees et al. (2000)- Mimram River

Reach	λ	D_{Lts} (m^2/s)	Limiting D_{Lts} (m^2/s)
A-B	0.73×10^3	0.70	56.0
B-C	7.94×10^3	1.24	28.8

Using the ATS-VPM model and the parameter values presented in Table 6.3, which were estimated by Lees et al. (2000), the C-t curves at site B and at site C were computed. The observed C-t curves at site A and B define the input C-t curves for the reaches A-B and B-C respectively (Lees et al., 2000). The ATS-VPM model was able to simulate the observed C-t curves at site B and at site C satisfactorily with a η equal to 97.303% and 90.843% respectively. The comparison of the observed and computed C-t curves at site B and site C are shown in Fig 6.13.
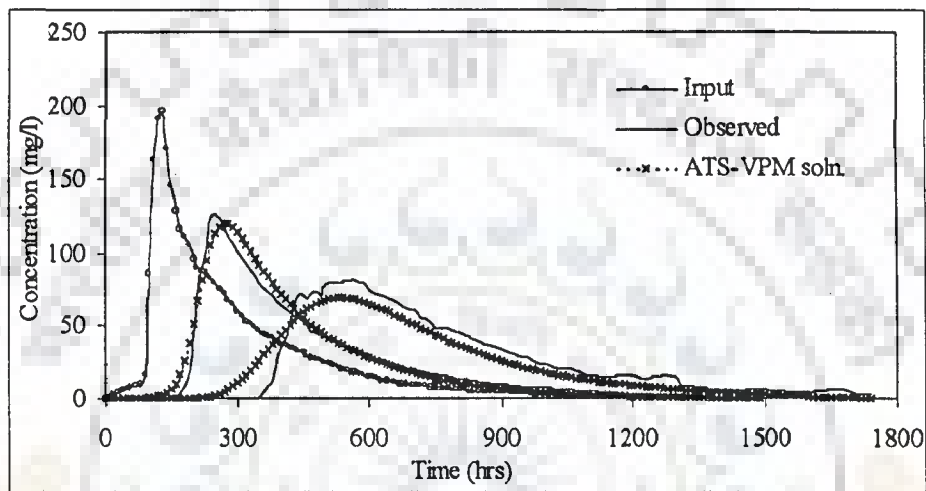
Figure 6.13 Observed and simulated concentration at sites B and C using ATS-VPM model and TS parameters given by Lees et al. (2000)-Mimram River

It is important to note that the values of the parameters, viz., α, β and D_{ts}, used for the simulations of the observed C-t curves were estimated by Lees et.al. (2000) for the TS model simulations.

Estimation of the parameter values by one model and use of these in another model of different structure may pose difficulties. Therefore, it seems prudent to apply the same model for identification and prediction of a system (Koussis et al., 1983). Hence, instead of using the parameter values estimated for the TS model by Lees et al. (2000), the parameter β and D_{Lts} were estimated using the ATS-VPM model. In estimating the values of parameters β and D_{Lts}, the C-t curves at sampling sites A and B define the input concentration for reaches A-B and B-C respectively.

The parameters were estimated by trial and error using the following procedure:

i) The value of β is varied from 0 to a value of 0.4, which is approximately more than twice the value given by Lees et al. (2000).

ii) For each value of β, the best D_{Lts} was determined using the following procedure, which is the same as that adopted in section 3.6.1 (Chapter-3) to estimate the dispersion coefficient, D_L:

The C-t curve at an input section is routed through the reach, for an assumed θ_{cts}, to arrive at the computed C-t curve at output section. The computed and observed C-t curves at output section are compared using the Nash-Sutcliffe criterion, η. This experiment is repeated for varying θ_{cts} values, and that θ_{cts} which results in the maximum value of Nash-Sutcliffe criterion, η, is considered as the best value. This θ_{cts} was used in the estimation of the best D_{Lts} using Eqn. (5.30).

iii) The step (ii) was repeated for varying values of β.

iv) The combination of β and D_{Lts} that result in maximum η was considered to be the best set of parameter values.

The calibrated values of β and D_{Lts} in simulating the C-t curves at site B and Site C are presented in Table 6.5. The best value of D_{Lts} for $\beta=0$ gives the D_L of the AD-VPM model. The C-t curves at sites B and C were computed for the estimated value of D_L using the AD-VPM model. Comparison of the observed and the simulated C-t curves using the AD-VPM model is shown in Fig 6.14. The C-t curves at site B and site C were simulated using the ATS-VPM model with the estimated values of the parameters β and D_{Lts}, and the comparison of the observed and simulated C-t curves is shown in Fig 6.15.
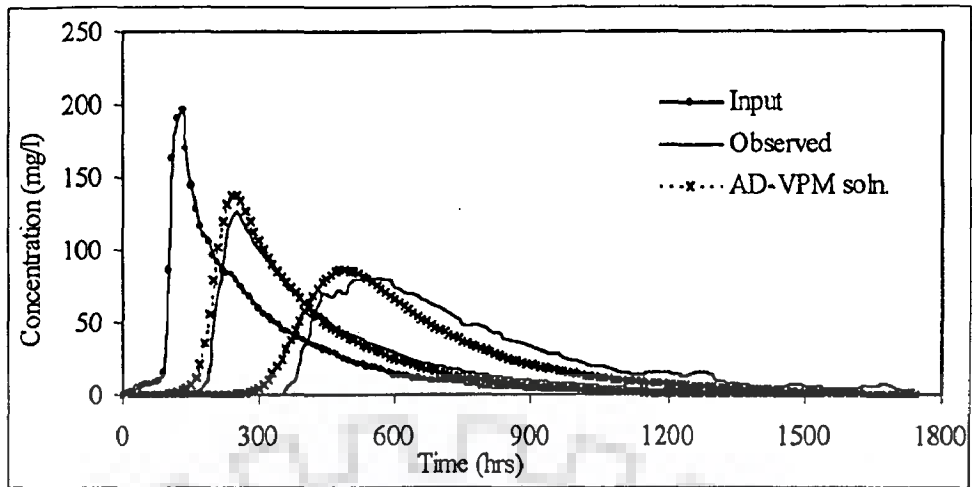
Figure 6.14 Observed and simulated concentration at sites B and C using AD-VPM model – Mimram River
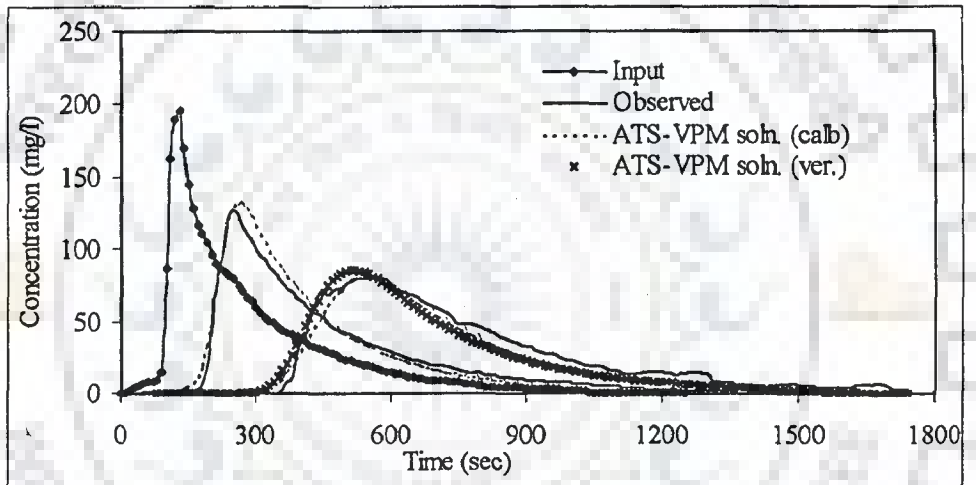
Figure 6.15 Observed and simulated concentration at sites B and C using ATS-VPM model – Mimram River

Table 6.5 Estimated values of the parameter using the ATS-VPM model and the values of η at site B and site C

Reach	β	D_{Lts} (m^2/s)	η (%)	Remarks
A-B	0	0.554	94.788	AD-VPM
	0.1375	0.487	98.098	ATS-VPM
B-C	0	0.696	85.275	AD-VPM
	0.2625	0.490	96.314	ATS-VPM

172

Using the ATS-VPM model and the value of $\beta=0.1375$ and $D_{Lts} = 0.4869$ m^2/s obtained for the reach A-B during calibration (of C-t curve at site B, Table 6.5), to simulate the observed C-t curve at site C with the C-t curve at site B defines the input concentration, gives a $\eta=94.005\%$. The simulated C-t curve at site C in verification mode is shown in Fig. 6.15.

6.4.2 Application to Uvas Creek Tracer Experiment

Bencala and Walter (1983) described the tracer experiments conducted in Uvas Creek, a mountain stream. The experiments were conducted during a period of low flow of 0.0125 m^3/s. The observed C-t curves at a distance of 38m (station 1), 105m (station 2), 281m (station 3) from the tracer injection point were used in the present test case. The C-t data used in this test case are presented in Appendix B 1.5.

The significant feature of the concentration data is the extent of the long tails present in the observed C-t curves. Bencala and Walters (1983) observed that the AD model would not explain the tracer transport in Uvas creek that is dominated by transient storage mechanism. Hence, they used the TS model to simulate the transport of chloride in Uvas Creek River. For the application of the TS model, the best fit model parameters were obtained in downstream sequence for each of the five reaches between successive sampling locations. Bencala and Walters (1983) selected the model parameters by visually determining the set of parameters, which yielded the best fit to the C-t curves. The parameter values thus estimated by Bencala and Walters (1983) are presented in Table 6.6. The effective storage zone area A_s for Uvas creek is greater than or equal to the main channel flow cross sectional area A. This may be due to very low velocities of flow in the Uvas Creek

(Table 6.7). Bencala and Walters (1983) stated that the following may be the plausible reason for the high value of storage area compared to main channel area.

1. turbulent eddies generated by large-scale bottom irregularities,

2. large, but slowly moving recirculating zones along the sides of pools, particularly located immediately downstream of the entrance to a pool from a riffle section,

3. small, but very rapidly mixing recirculating zones located behind flow obstruction, particularly located in riffle sections where cobble, small boulders, and vegetation commonly protrude through the flow,

4. side pockets of water effectively acting as dead ends for solute transport, and

5. flow into, out of, and through coarse gravel and cobble bed.

Table 6.6 The flow characteristics and simulation parameters of the experiments in the Uvas creek (Bencala and Walters, 1983).

Reach range (m)	Discharge (m^3/s)	Cross-sectional area, A (m^2)	D_{ts} (m^2/s)	Storage zone Area, A_s (m^2)	Exchange coefficient α (sec^{-1})
0-38	0.0125	0.3	0.12	0	0
38-105	0.0125	0.42	0.15	0	0
105-281	0.0133	0.36	0.24	0.36	0.3×10^{-4}
281-433	0.0136	0.41	0.31	0.41	0.1×10^{-4}
433-619	0.0140	0.52	0.40	1.56	0.45×10^{-4}

Using the parameters α, β, and D_{ts} (Table 6.6) estimated by Bencala and Walters (1983), the parameters of the ATS-VPM model, i.e., D_{Lts} and β, the applicability criterion given by λ (Eqn. 6.1) and the limiting value of D_{Lts} (Eqn. 6.2)

were computed to know whether these values are within the applicability domain of the ATS-VPM model. The computed values of these parameters for the observed velocity are shown in Table 6.7.

Table 6.7 ATS-VPM parameters and the limiting criterion values for Uvas Creek.

Reach range (m)	Velocity of flow (m/s)	β	D_{Lts} (m²/s)	Limiting D_{Lts} (m²/s)	$\dfrac{D_{Lts}}{\text{Limiting } D_{Lts}}$	λ
0-38	0.0417	0	0.121	1.8052	0.066	0
38-105	0.0298	0	0.150	1.0156	0.148	0
105-281	0.0369	1.0	5.806	0.4478	12.96	2.78×10^8
281-433	0.0332	1.0	13.908	0.3724	37.35	2.50×10^9
433-619	0.0269	3.0	2.365	0.0795	29.74	2.78×10^8

The values of λ computed for the Uvas creek reach after 105 m (station 2) from the point of injection of tracer are much greater than the limiting value ($\approx 10^6$) required for the successful application of the ATS model. Moreover, D_{Lts} values estimated using Eqn. (5.18) for the reaches after station (2) were also found to be higher than the values of limiting D_{Lts} required for the successful application of the ATS-VPM model.

Based on the values of the λ, D_{Lts}, and the limiting D_{Lts}, it can be inferred that the ATS-VPM model is applicable to simulate the observed C-t curves in tracer experiments conducted on Uvas creek upto a distance of 105m. Hence, the ATS-VPM model is not applicable to simulate the solute transport after station (2), i.e., for simulating the observed C-t curves at station (3), (4) and (5). To demonstrate this, the ATS-VPM model, with the parameter values estimated by Bencala and

175

Walters (1983), was used to simulate the C-t curves at station (1), (2) and (3). In these tracer experiments, performed for an uniform input of solute with a concentration of 11.4 mg/l for duration of 3 hours was made. The same was used as the input to the ATS-VPM model. The comparison of observed and simulated C-t curves at stations (1), (2) and (3) are shown in Fig 6.16.
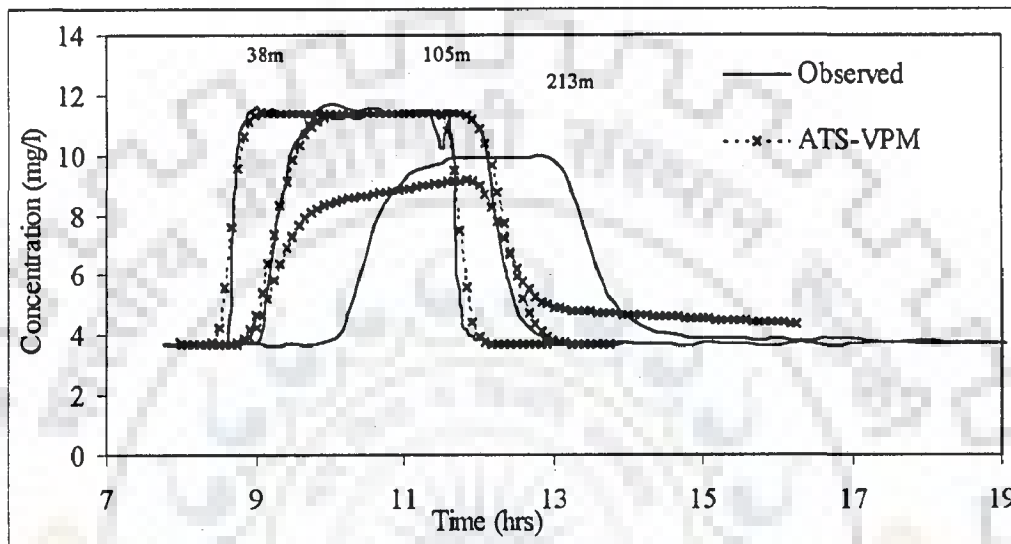
Figure 6.16 Observed and simulated concentration-time profiles at different sections d/s of the pulse injection-Uvas Creek

The results show that the ATS-VPM model can reproduce the observed C-t curves at section (1) and (2) successfully with Nash-Sutcliffe criterion, $\eta > 98\%$. As stated earlier, the ATS-VPM model failed to simulate the observed C-t curve at station (3) because the solute transport process in the reach after 105m from the point of injection of dye is not within the applicability range of the ATS model. Hence, the ATS-VPM model, which is an approximation of the ATS model, is applicable to simulate the solute transport upto the section located at 105m from the injection point of solute. It is noted that the value of β in the reach upto 105m is 0, which implies the absence of TS mechanism. It was already stated that the

176

ATS-VPM model get reduced to AD-VPM model for β=0. Hence, the AD-VPM model is also applicable for the reach upto 105m.

6.5 APPLICATION OF THE ATS-VPM MODEL UNDER UNSTEADY FLOW CONDITIONS

The ATS-VPM model developed in section 5.5 is meant for solute transport under steady flow conditions. The same may be suitably adopted for modelling solute transport under unsteady flow conditions also (section 5.6). This is achieved by using the assumption that the flow remains steady within a given routing time interval, but varies from one time interval to the next. The ATS-VPM model is coupled with the VPM flow routing model for solute transport under unsteady flow conditions. Hence, for the satisfactory application of the model, it should satisfy the applicability criteria of both the VPM flow routing model and the ATS-VPM solute transport model.

The hydrograph to be routed should satisfy the criterion $\left|(1/S_o)\partial y/\partial x\right| < 1$ at any time for successful application of VPM flow routing model (Perumal, 1994b). In the development of the ATS-VPM model under unsteady flow conditions, it is assumed that the flow is steady during a routing time interval, but varies from one time interval to the next. Hence, the applicability criterion of the ATS-VPM model evaluated in section 6.3 (Eqn. 6.2) under steady flow condition is applicable here also.

Accuracy of the ATS-VPM model depends on the estimated dispersion coefficient for a given velocity of flow and the parameter β. If the estimated D_{Lts} is less than the limiting value of D_{Lts} obtained using Eqn. (6.2) at any time during the

177

routing, the performance of the proposed ATS-VPM model may be considered accurate.

The experimental studies on solute transport under unsteady streamflow conditions in rivers are very few, perhaps, due to difficulties in experimentation as discussed in section 4.3. Further, it is not possible to obtain an analytical solution of the system of partial differential equations governing the coupled flow (Saint-Venant Equations) and solute transport processes (TS model). Hence, the application of the proposed ATS-VPM model for solute transport studies under unsteady flow conditions needs to be tested by simulating the numerical solution of the TS model coupled with the Saint-Venant Equations (SVE), termed herein as the SVE-TS model for hypothetical data input.

6.5.1 Solution of the SVE-TS Model

To arrive at the benchmark solution of the SVE-TS model, the following procedure was used:

A given hydrograph at the input section of a uniform rectangular cross-section was routed to the desired location in the channel reach using the numerical solution procedure of the Saint-Venant equations (Viessman et al., 1977) given by Eqns. (4.23) and (4.24). The results obtained by solving the SVE were used in solving the TS equation, to arrive at the benchmark SVE-TS solution.

The algorithm of Runkel (1998) was used for solving the TS model in the present study. The oscillation problems associated with Runkel solution (1998) have been avoided by maintaining the Peclet Number $(P_e = U\Delta x/D_L)$ sufficiently low, based on numerical experiments carried out during the study. Thus, the stable solution obtained by solving the SVE-TS model was considered as benchmark

178

solution needed for the evaluation of the solution of the ATS-VPM model. The agreement between the solutions of the ATS-VPM model and the SVE-TS model was measured using the Nash-Sutcliffe criterion, η (Eqn. 3.24).

6.5.2 Hypothetical Test Studies

Rectangular channels having different channel configurations, but with a uniform width of 100 m are considered for the hypothetical tests. The slope and Manning's n of the channels used in these numerical experiments are given in Table 6.8.

Table 6.8 Configurations of hypothetical channel

Channel Type	Bed Slope (S_o)	Manning's roughness (n)
1	0.0002	0.02
2	0.0004	0.04
3	0.0004	0.02

The inflow hydrograph and C-t curve used in these numerical experiments was defined by Eqns (4.25) and (4.26) respectively with the same values of I_b (=100 m^3/s), I_p (=1000 m^3/s), t_p (=10 hr.), and γ (=1.15) for hydrograph, and C_b (= 0 units), C_p (= 50 units), t_{cp} (=10 hr.), and γ (= 1.15) for C-t curve. The inflow hydrograph and the C-t curve are routed through the channel for a reach length of 40km using the proposed ATS-VPM model. A routing time interval of 15 min. was used in the numerical experiments. The accuracy in the reproduction of C-t curve shape and size has been evaluated using the Nash-Sutcliffe criterion, η. The results are given in Table 6.9 and the solutions of the SVE-TS and the ATS-VPM model are compared in Figs. 6.17 to 6.23.

179

Table 6.9 Peak concentration and it's time of occurrence for hypothetical test studies

β	φ	Channel Type	α (s^{-1})	SVE-TS model		ATS-VPM model	
				Time to peak (hr)	Peak Concentration	Time to peak (hr)	Peak Concentration
0.3	0.025	1	0.00005	18.00	42.670	18.75	41.738
			0.000075	18.25	44.212	18.50	43.819
			0.0001	18.25	45.244	18.50	44.965
			0.0003	18.25	47.772	18.25	47.455
		2	0.00005	20.25	41.758	21.00	40.382
			0.000075	20.50	43.632	20.75	43.140
			0.0001	20.75	44.871	20.75	44.442
			0.0003	20.75	47.916	20.25	47.315
		3	0.00005	16.25	44.175	16.75	43.301
			0.000075	16.25	45.550	16.75	45.239
			0.0001	16.50	46.529	16.50	46.299
			0.0003	16.25	49.007	16.25	48.494
	0.05	1	0.00005	18.00	41.940	18.75	40.870
			0.000075	18.25	43.370	18.50	42.826
			0.0001	18.25	44.319	18.50	43.916
			0.0003	18.25	46.661	18.25	46.286
		2	0.00005	20.50	40.978	21.00	40.080
			0.000075	20.75	42.724	21.00	42.287
			0.0001	20.75	43.867	20.75	43.524
			0.0003	20.50	46.677	20.50	46.280
		3	0.00005	16.25	43.750	16.75	43.032
			0.000075	16.50	45.690	16.75	44.943
			0.0001	16.50	46.003	16.50	45.981
			0.0003	16.50	48.322	16.50	48.155
0.5	0.025	1	0.000075	19.50	39.030	20.50	37.731
			0.0001	20.00	40.584	20.50	39.795
			0.0003	20.00	45.209	20.00	45.105
			0.0005	20.00	46.819	19.75	46.380
		2	0.000075	22.50	37.839	23.50	36.649
			0.0001	23.00	39.673	23.25	38.880
			0.0003	23.00	45.386	22.75	44.757
			0.0005	23.00	46.941	22.50	46.220
		3	0.000075	17.25	40.742	18.00	39.472
			0.0001	17.50	42.139	18.00	41.500
			0.0003	17.75	46.901	17.75	46.534
	0.05	1	0.000075	19.50	38.366	20.50	36.900
			0.0001	20.00	39.783	20.50	38.840
			0.0003	20.25	44.282	20.25	43.776
			0.0005	20.00	45.470	20.00	44.986
		2	0.000075	22.75	37.133	23.50	35.982
			0.0001	23.00	38.846	23.50	38.090
			0.0003	23.25	44.079	23.00	43.568
			0.0005	23.00	45.501	22.75	44.932
		3	0.000075	17.25	40.340	18.00	39.209
			0.0001	17.50	41.676	18.00	41.196
			0.0003	17.75	46.266	17.75	46.162
			0.0005	17.75	47.500	17.50	47.291

0.75	0.025	1	0.000075	20.75	33.526	22.50	31.160
			0.0002	22.75	39.916	22.75	39.219
			0.0003	22.75	42.241	22.50	41.664
			0.0005	22.50	44.505	22.25	43.950
		2	0.000075	25.00	31.913	26.50	29.955
			0.0002	26.75	39.249	26.50	38.480
			0.0003	26.75	41.861	26.25	41.106
			0.0005	26.75	44.457	26.25	44.007
		3	0.000075	17.75	35.632	19.50	32.898
			0.0002	19.50	41.436	19.75	40.981
			0.0003	19.50	43.805	19.50	43.408
			0.0005	19.50	46.007	19.25	45.612
	0.05	1	0.000075	20.75	32.994	22.50	30.527
			0.0002	22.75	38.915	22.75	38.071
			0.0003	22.75	41.014	22.75	40.311
			0.0005	22.75	43.033	22.50	42.404
		2	0.000075	25.00	31.395	26.50	29.462
			0.0002	27.00	38.236	26.75	37.551
			0.0003	27.00	40.612	26.50	40.025
			0.0005	26.75	42.941	26.25	42.363
		3	0.000075	17.75	35.300	19.50	32.698
			0.0002	19.50	40.876	19.75	40.612
			0.0003	19.50	43.123	19.50	42.974
			0.0005	19.50	45.341	19.25	45.121
1	0.025	1	0.0001	23.75	30.936	25.00	28.968
			0.0002	25.50	36.205	25.50	35.218
			0.0003	25.75	39.083	25.25	38.298
			0.0005	25.75	42.093	25.25	41.395
		2	0.0001	29.25	29.600	30.25	27.894
			0.0002	31.00	35.419	30.50	34.423
			0.0003	31.25	38.567	30.50	37.696
			0.0005	31.25	41.914	30.00	41.041
		3	0.0001	19.50	32.761	21.25	30.601
			0.0002	21.25	37.661	21.50	36.967
			0.0003	21.50	40.661	21.50	40.107
			0.0005	21.50	43.787	21.25	43.249
	0.05	1	0.0001	23.75	30.421	25.00	28.335
			0.0002	25.50	35.309	25.50	34.183
			0.0003	25.75	37.916	25.50	37.015
			0.0005	25.75	40.588	25.25	39.821
		2	0.0001	29.25	29.097	30.25	27.409
			0.0002	31.00	34.539	30.50	33.614
			0.0003	31.25	37.419	30.75	36.667
			0.0005	31.25	40.426	30.25	39.758
		3	0.0001	19.50	32.444	21.25	30.400
			0.0002	21.25	37.164	21.50	36.630
			0.0003	21.50	39.974	21.50	39.684
			0.0005	21.50	42.968	21.25	42.726
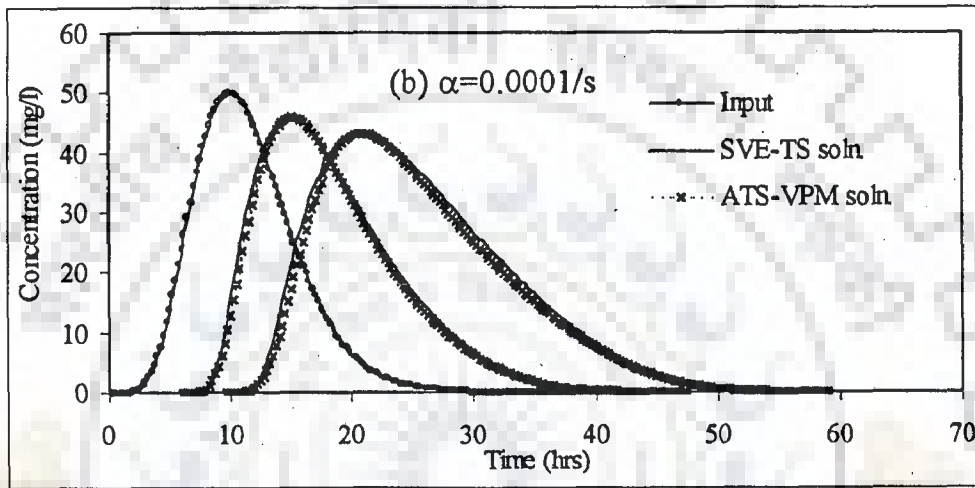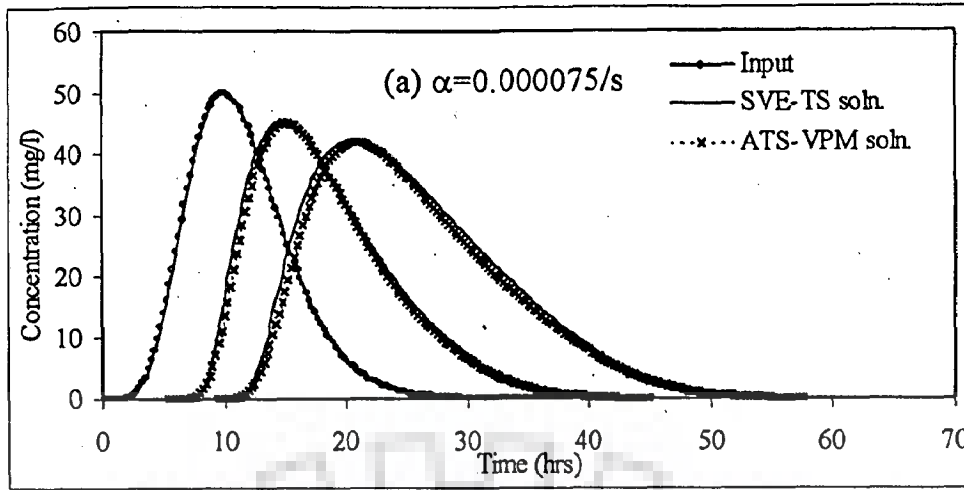
Figure 6.17   Solutions of SVE-TS and ATS-VPM model for φ=0.058, β=0.3, at x=20km and 40km d/s from solute source (Channel type-2)
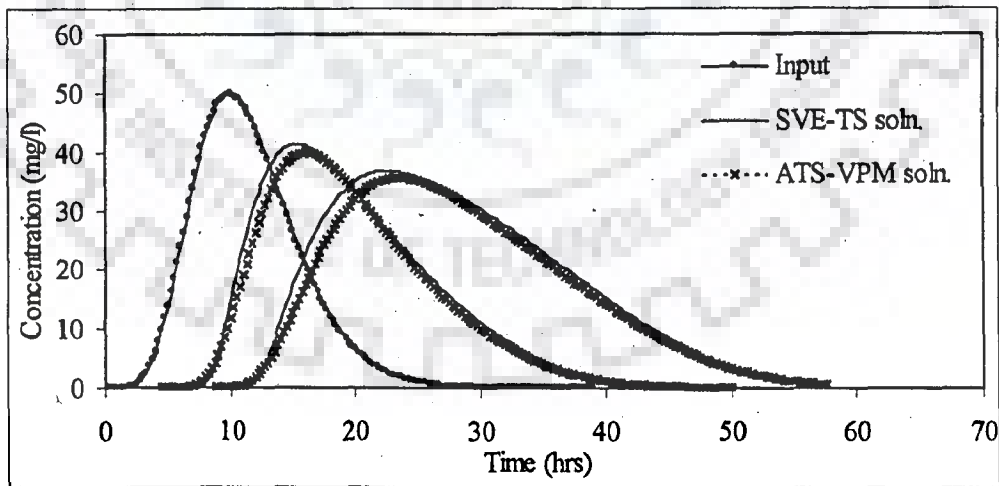
Figure 6.18   Solutions of SVE-TS and ATS-VPM model for α=0.000075/s, φ=0.058, β=0.5, at x=20km and 40km d/s from solute source (Channel type-2)
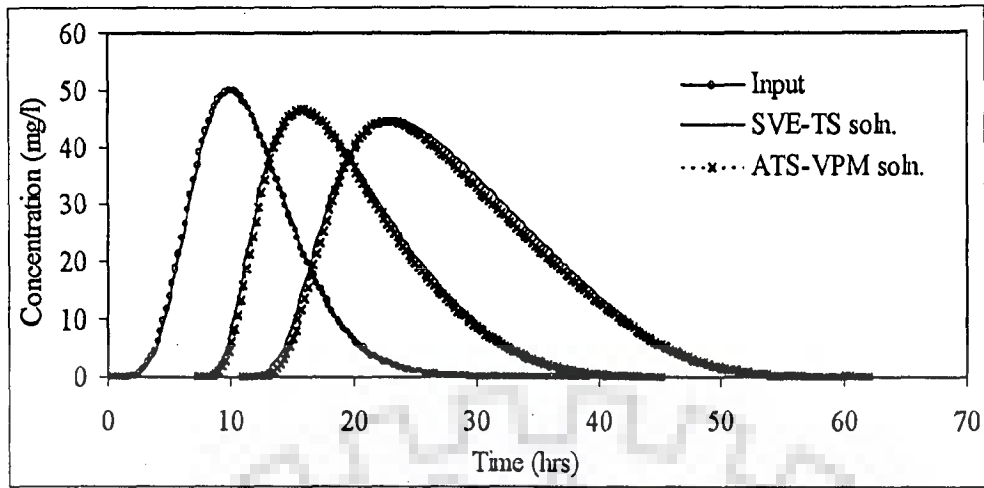
Figure 6.19 Solutions of SVE-TS and ATS-VPM model for α=0.0005/s, ϕ=0.058, β=0.5, at x=20km and 40km d/s from solute source (Channel type-2)
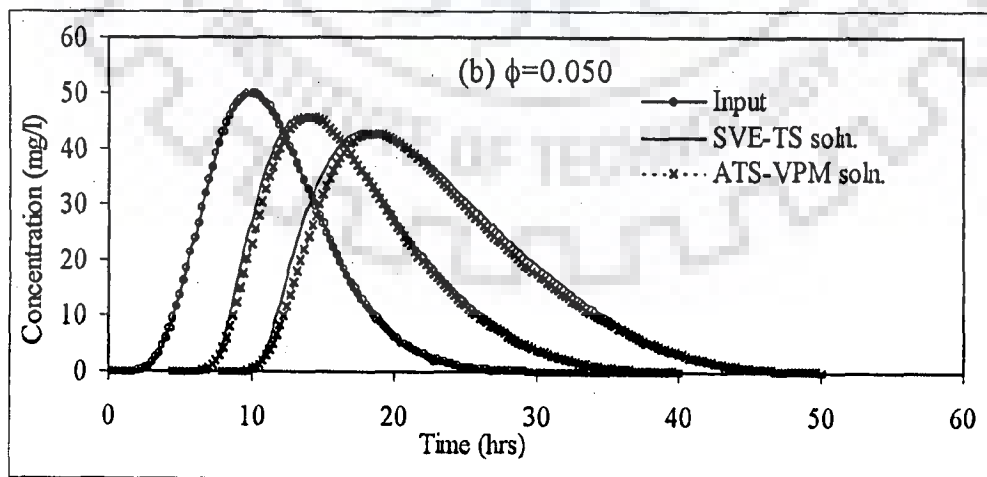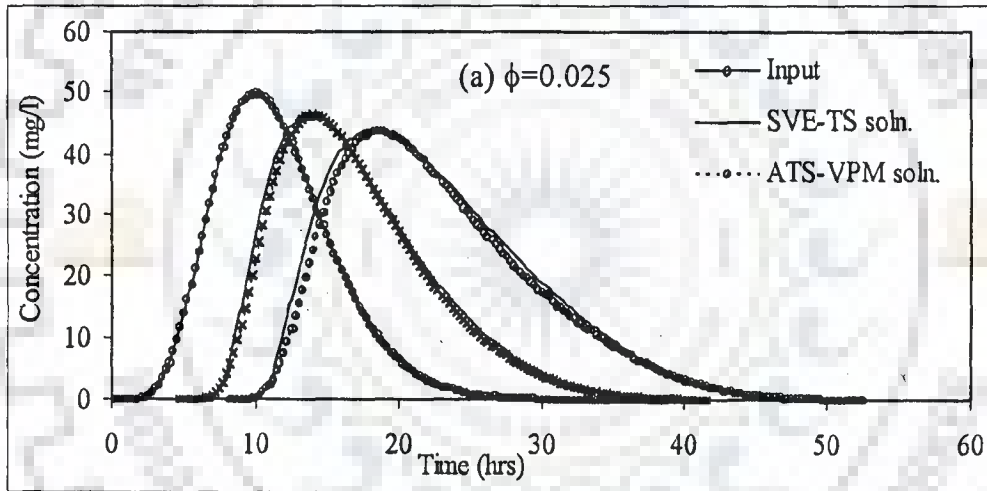
Figure 6.20 Solutions of SVE-TS and ATS-VPM model for α=0.000075/s, β=0.3, at x=20km and 40km d/s from solute source (Channel type-1)
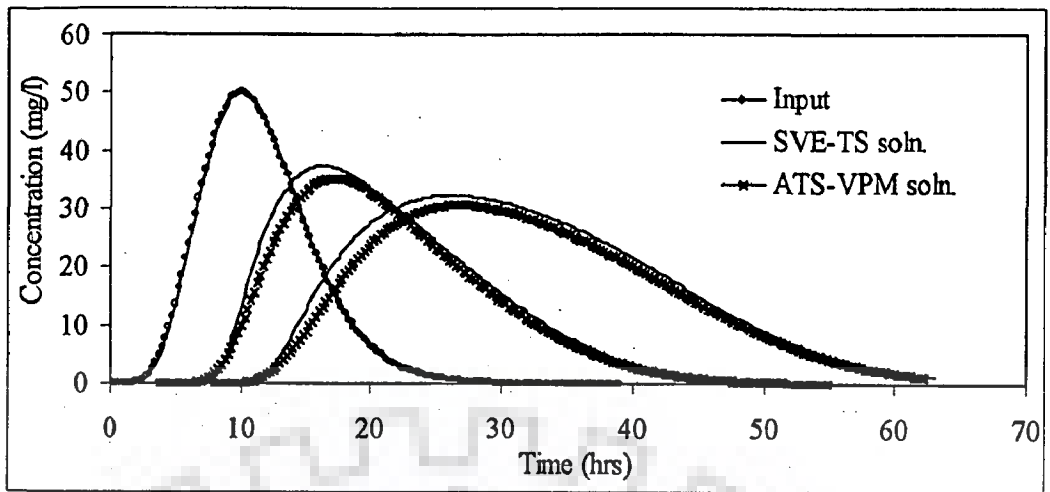
Figure 6.21 Solutions of SVE-TS and ATS-VPM model for α=0.0001/s, φ=0.116, β=0.75, at x=20km and 40km d/s from solute source (Channel type-2)
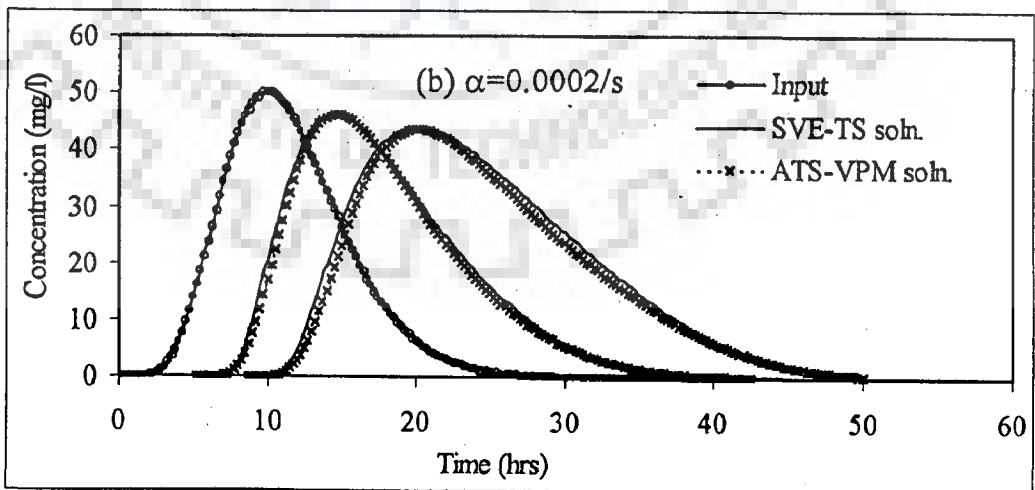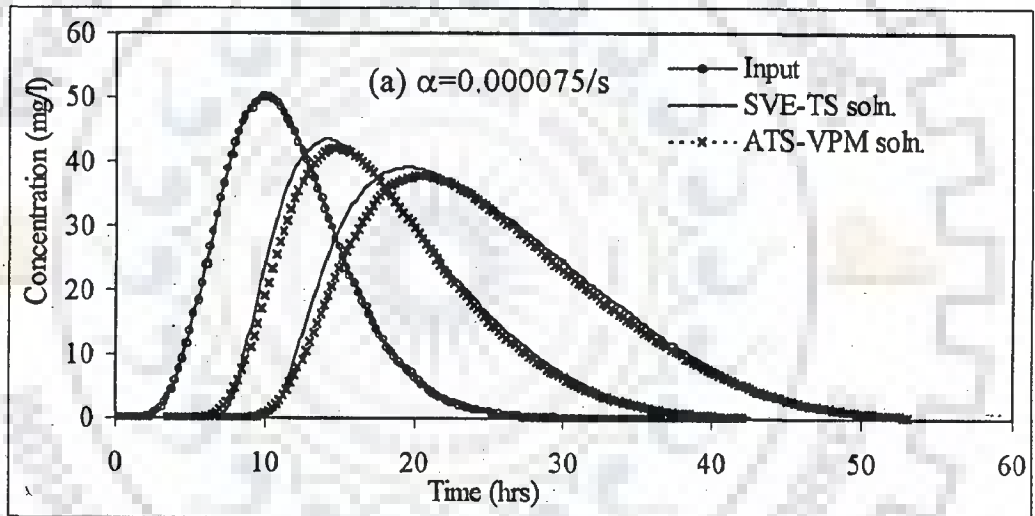
Figure 6.22 Solutions of SVE-TS and ATS-VPM model for φ=0.025, β=0.5, at x=20km and 40km d/s from solute source (Channel type-1)
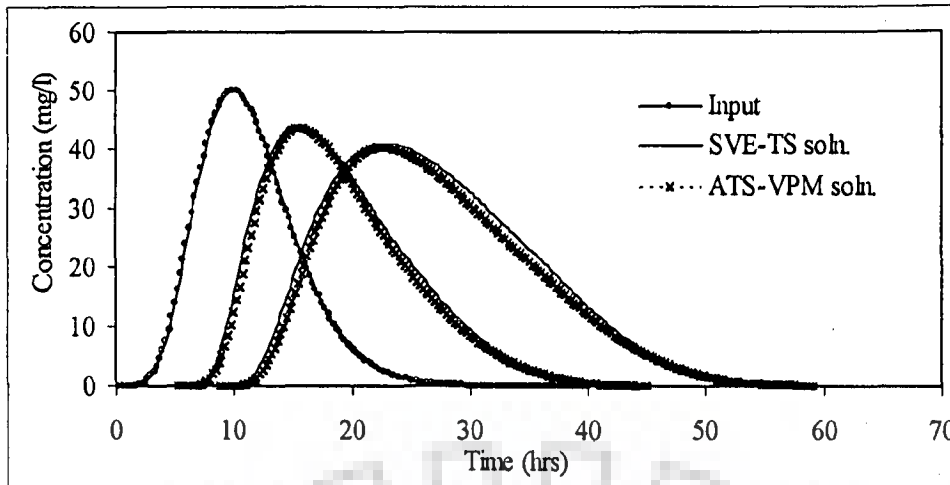
Figure 6.23 Solutions of SVE-TS and ATS-VPM model for α=0.0003/s, φ=0.05, β=0.75, at x=20km and 40km d/s from solute source (Channel type-1)

6.5.3 Application to Huey Creek Tracer Experiment

A tracer-dilution experiment conducted in Huey Creek, in January 1992, to determine the extent and rate of hyporheic exchange was described by Runkel et al. (1998). The details are given in Appendix B 1.6. The C-t measurements available at downstream distances of 9m (location 1), 213m (location 2), 457m (location 3), 762m (location 4), and at 1052m (location 4) from the point of injection of the LiCl injectate were used in the present test case (Fig. 6.24).
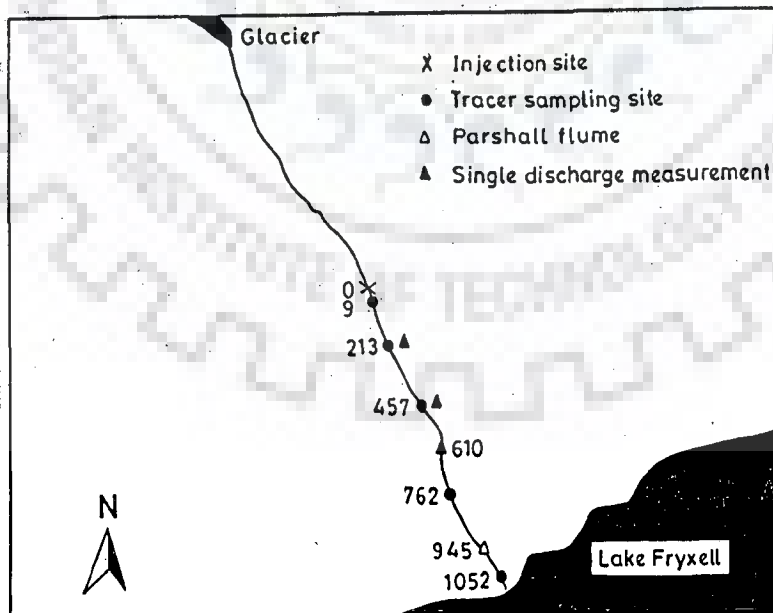
Figure 6.24 Map of Huey Creek showing tracer sampling and streamflow measurement stations (Runkel et al., 1998)

185

A Parshall flume provided a continuous stream flow record of Huey Creek above the outlet to Lake Fryxell at 945 m. Stream flow measurements of this site were fair to poor, with measurement errors potentially > 15% (von Guerard et al. (1995) as referred in Runkel et al., 1998). Flume estimates of stream flow varied from 50 to 120 l/s during the tracer addition. In addition to this, discharge data measured and used by Runkel et al. (1998) at sites 213m, 457m and 610m (Fig. 6.24) was used in the present study also. Field observations of Huey creek indicated that the channel was approximately rectangular (Runkel et al., 1998). Channel widths were available from the discharge measurements at sites 213m, 457m, and 610m (1.0, 1.2, and 1.2 m, respectively). Average channel widths used in the routing model were adjusted upward from 0.4 to 0.6m as part of the calibration process. Widths were adjusted such that simulated velocities agreed with velocities observed during the given discharges at sites 213m, 457m, and 610m. The discharge, flow area and velocity are shown in Table 6.10.

Table 6.10 Area and velocity at different locations given by Runkel et al. (1998)

Gauging Location (m)	Time (hrs)	Flow (l/s)	Area (m^2)	Velocity (m/s)
213	11.8	93.4	0.13	0.73
457	12.3	101.9	0.12	0.85
610	12.7	96.3	0.12	0.79

Runkel et al. (1998) used surveyed cross-sections, bed-slopes and reach lengths together with the point velocity measurements to back-calculate reach estimates of the Manning's n required for the routing model. The bed slope, channel width and the Manning's n for the various flow routing reaches given by Runkel et al. (1998) are presented in Table 6.11.

Table 6.11 Parameters used for flow routing (Runkel et al., 1998)

Reach range (m)	Bed Slope (%)	Channel width (m)	Manning's roughness (n)
0-9	9.1	1.4	0.100
9-213	12.3	1.4	0.100
213-457	6.9	1.6	0.061
457-610	5.0	1.8	0.054
610-762	5.2	1.8	0.054
792-945	4.0	1.8	0.054
945-1006	1.9	1.8	0.054
1006-1052	1.1	1.8	0.054

In the study, flow estimates from the Parshall flume indicated substantial variation in flow rate during the tracer addition. Failure to consider stream flow variability would result in a flat concentration profile (plateau) during this period (Runkel et al., 1998). Therefore, in the present study, the ATS-VPM model, coupled with the VPM flow routing model as described in section 5.5 was used to simulate the solute transport in the Huey creek. In this modelling framework, The VPM flow routing and ATS-VPM solute routing are carried out simultaneously within each routing time interval. Runkel et al. (1998) developed an inflow hydrograph at the upstream boundary (the injection point, at site 0km) using the observed downstream hydrograph at site 945m.

Runkel et al. (1998) calibrated the TS model parameters for each reach using the observed C-t measurements. The values of the parameters thus estimated are presented in Table 6.12. Using these values of α, A_s, and D_{ts} (Table 6.13), the parameters values of the ATS-VPM model, i.e., D_{Lts} and β are obtained. The applicability criterion λ (Eqn. 6.1) and the value of limiting D_{Lts} (Eqn. 6.2) were computed to know whether these values are within the applicability domain of

187

the ATS-VPM model. The computed values of λ and D_{Lts} and the value of limiting D_{Lts} (Eqn. 6.2) for the observed velocity are shown in Table 6.12 and Table 6.13.

Table 6.12 The TS model parameter values of the reaches of Huey Creek given by Runkel et al., (1998)

Reach Range (m)	Storage zone area, A_s (m)	β ($= A_s/A$)		Exchange coefficient α (s^{-1})	λ	
		Min	Max		Min	Max
0-213	0.20	1.1	1.8	1.07×10^{-3}	2.37×10^5	3.61×10^5
213-457	0.25	1.5	2.4	5.43×10^{-4}	1.22×10^6	1.69×10^6
457-762	0.14	0.8	1.4	1.62×10^{-2}	0.75×10^3	1.30×10^3
762-1052	3.07	15.9	34.3	4.67×10^{-4}	4.04×10^6	4.33×10^6

Table 6.13 The computed values of D_{Lts} (Eqn. 5.18) and limiting D_{Lts} (Eqn. 6.2) values for the reaches of Huey creek

Gauging Location (m)	Velocity (m^2/s)	α (s^{-1})	β		D_{Lts} (m^2/s)		Limiting D_{Lts} (m^2/s)	
			Min	Max	Min	Max	Max	Min
213	0.73	0.001070	1.1	1.8	65.31	73.69	68.26	41.71
457	0.85	0.000543	1.5	2.4	191.80	195.14	65.72	38.82
610	0.79	0.016200	0.8	1.4	4.51	5.67	101.74	62.18

Based on the computed values of λ, D_{Lts}, and the limiting D_{Lts}, it can be concluded that the ATS-VPM model is applicable for the reach upto a distance of 762.0m from the point of injection of solute in Huey Creek. Using the ATS-VPM model for solute routing coupled with the VPM model for flow routing and the values of parameters given by Runkel et al. (1998), the C-t curves at 213m, 457m, 762m, and at 1052m were computed. The inflow hydrograph estimated by Runkel et al. (1998), was used as the input for flow routing (Fig. 6.25). The observed C-t curve at 9m (location 1) was used as the input for the computation of C-t curves. The results comparing the observed and simulated C-t curves at downstream sampling locations are shown in Fig. 6.26.
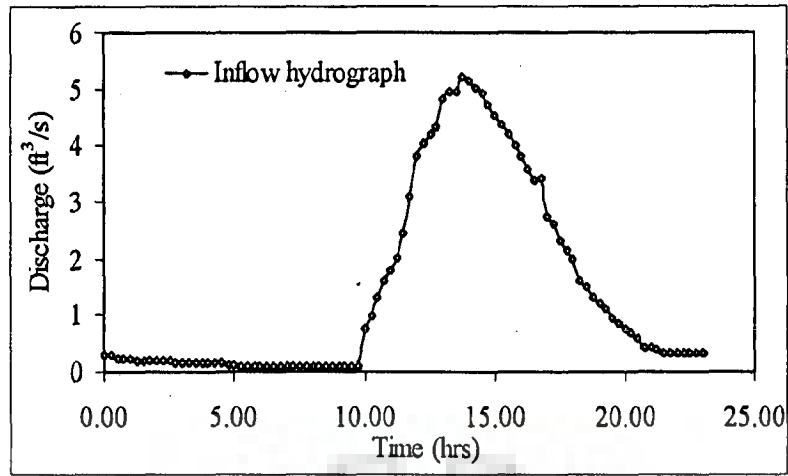
Figure 6.25 Inflow hydrograph for Huey creek at x=0m computed by Runkel et al., (1998)
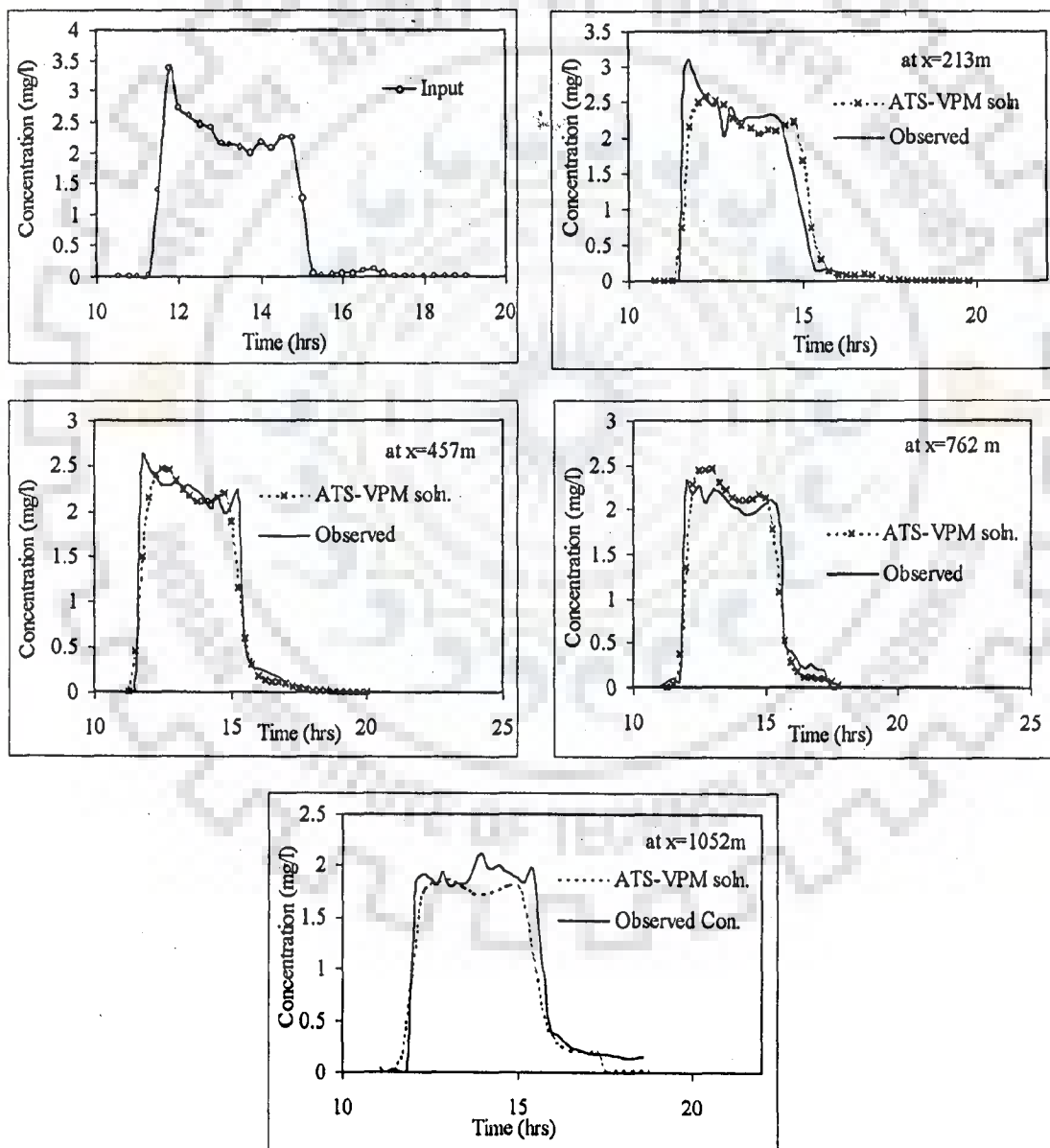
Figure 6.26 Simulated and observed Li concentrations at d/s sampling locations – Huey Creek

189

6.6   DISCUSSION OF RESULTS

6.6.1   Solute Transport Under Steady Flow Conditions

The ATS model is a simplified approximation of the TS model. Hence, if the assumptions made in its development are not satisfied, the ATS model fails to reproduce the TS model solution satisfactorily. This can be observed from the results of numerical experiments presented in Table 6.1 and Figs. 6.1 to 6.6 that, if the magnitude of the applicability criterion, the λ is within the approximate limiting value of 10^6, the ATS model can reproduce the numerical solution of the TS model satisfactorily with Nash-Sutcliffe criterion being greater than 98%. When this criterion is not satisfied, the analytical solution of the ATS model fails to reproduce the numerical solution of the TS model as seen in Fig. 6.7. The comparison between the solutions of the ATS and TS models was not made for cases such as one shown in Fig. 6.27, because the numerical method proposed by Runkel and Chapra (1993) to solve the TS model produces oscillatory results.
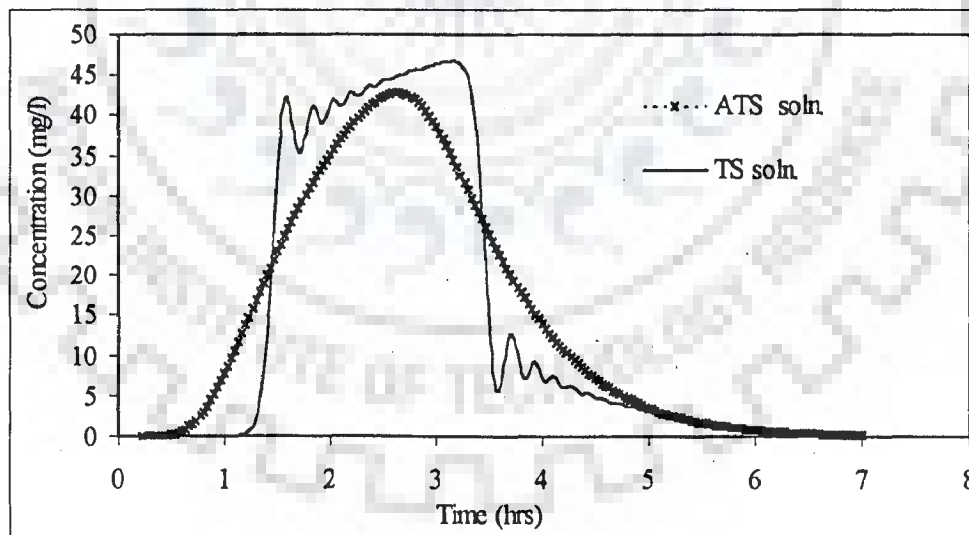
Figure 6.27   Numerical solution of TS model showing oscillations during advection dominated solute transport at x=5km for U=0.5m/s, α=0.000075/s, β=0.25

190

It is seen from Fig. 6.28 that (i) the value of D_{Lts} increases with increase in β for given values of U, D_{ts} and α, and (ii) the value of D_{Lts} decreases as the value of α increases for given values of U, D_{ts}, and β. It implies that for higher values of α the effect of TS zones on the dispersion is less. This may be attributed to the phenomenon that at higher value of α the TS zones act as active part of the main channel.
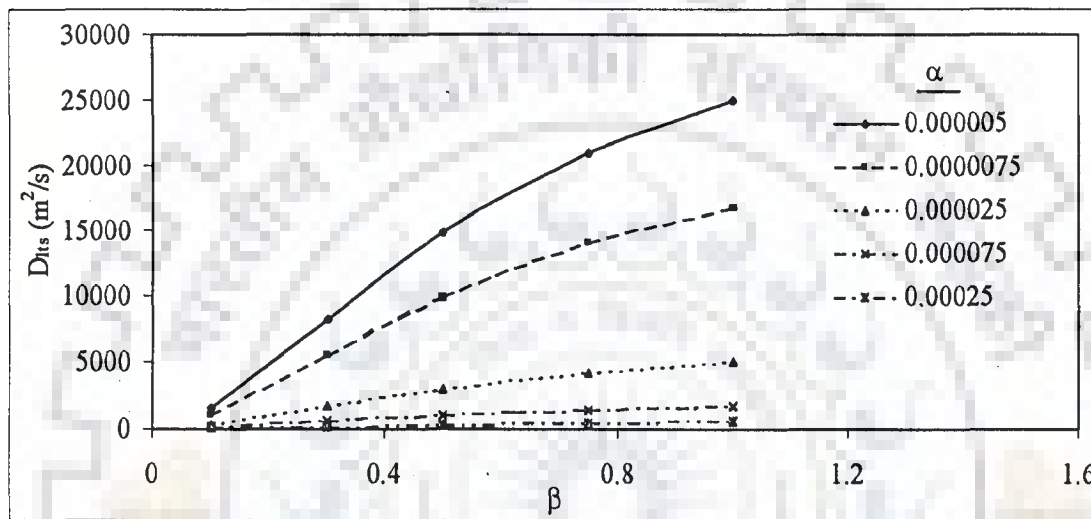
Figure 6.28 Variation of D_{Lts} with the variation of β for different values of α for a given value of U=1m/s, and $D_{ts}=10m^2/s$

Based on the results from numerical experiments presented in Table 6.2 and Figs. 6.8 to 6.12, it can be observed that the ATS-VPM model reproduces the solution of the ATS model when the value of D_{Lts} is less than the value of the limiting D_{Lts} given by Eqn. (6.2). It is seen from Fig. 6.29 that the ATS-VPM model fails to reproduce the solution of the ATS model as the value of D_{Lts} is more than the value of limiting D_{Lts}. For a given set of values of U, α, and D_{ts}, as the value of β increases, the velocity of solute cloud decreases and D_{Lts} increases with decrease in the magnitude of limiting D_{Lts}. It implies that for a given U, α, and D_{ts} as β increases the applicability range of the ATS-VPM model in reproducing the solution of ATS model decreases. Also for a given U and β, the magnitude of the limiting

191

dispersion coefficient of the ATS-VPM model is less than that of the corresponding AD-VPM model.
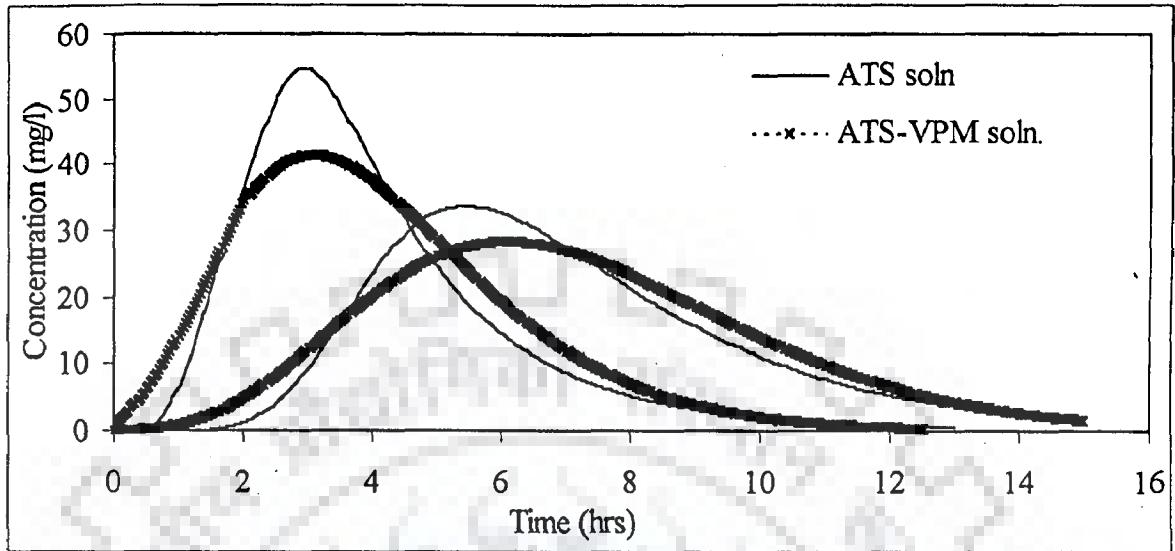
Fig. 6.29(i) Solutions of ATS and ATS-VPM models for α=0.00001/s, β=0.1, U=0.1m/s, and D_{ts}=15.0m^2/s at a distance of x=1km and 2km
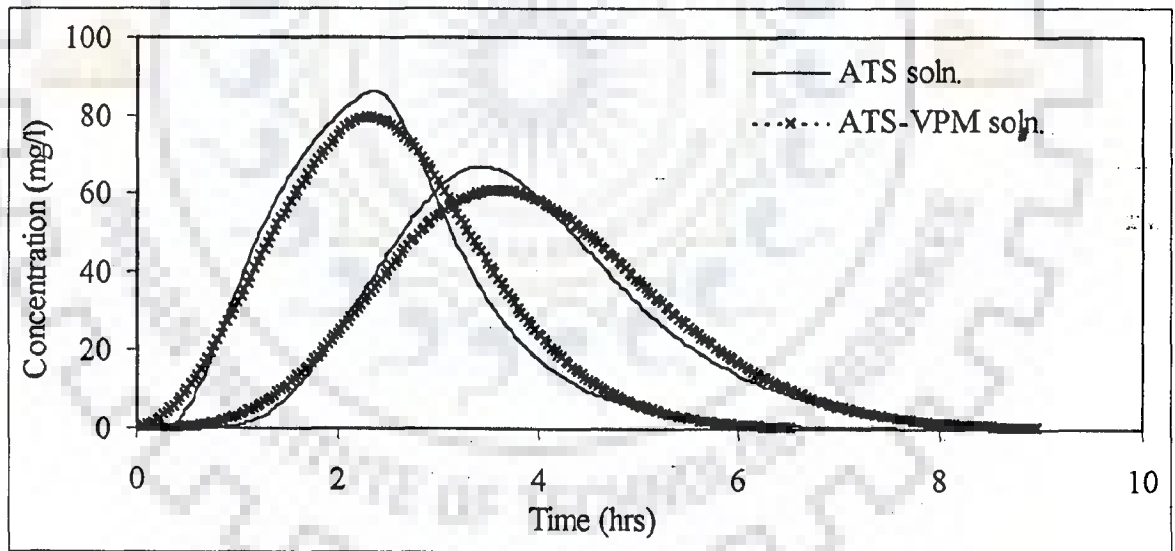
Fig. 6.29(ii) Solutions of ATS and ATS-VPM models for α=0.000075/s, β=0.3, U=0.5m/s, and D_{ts}=5.0m^2/s at a distance of x=2km and 4km

The Mimram River tracer experimental test case demonstrates the applicability of the ATS-VPM model to simulate the solute transport in rivers in the presence of transient storage zones (Fig. 6.15). In Mimram river tracer experimental

test case, the results show that the parameter values estimated using the observed C-t curves for the reach A-B, when used in simulating the C-t curve at site C in verification mode, closely reproduces the observed C-t curve at site C satisfactory with η=94.005%. Failure to consider the effect of transient storage zones would results in relatively poor simulation results in comparison with those obtained considering the transient storage zone effects (Table 6.5). The Mimram tracer experimental test case demonstrates that the usage of α can be avoided in using the ATS-VPM model.

The AD-VPM model results obtained using the calibrated values of D_L show an agreement with the observed data at sites B and C with the η values of 94.79% and 85.275% respectively. The ATS-VPM model results obtained using the values of β and D_{Lts} estimated using the parameter values given by Lees et al. (2000) show an agreement with the observed data at sites B and C with η values of 97.303% and 90.843% respectively. The ATS-VPM model results obtained using the calibrated values of β and D_{Lts} (Table 6.5) show an agreement with the observed data at sites B and C with η values of 98.10% and 96.319% respectively. This reveals that the ATS-VPM model gives better results in comparison with the AD-VPM model for the observations of Mimram experiments. The usage of parameters β and D_{Lts} calibrated using the ATS-VPM model in the simulations of C-t curves gives good results particularly at site C with a η value of 96.319% in comparison with that obtained using the values of β, and D_{Lts} which is estimated from the values of U, α, β and D_{ts} given by Lees et al. (2000).

In Uvas Creek dye experimental test case, it was observed that the solute transport phenomenon upto a distance of 105m from the injection point is not affected by the transient storage mechanism. Hence, the C-t curves computed at station (1) and (2) by the ATS-VPM model with β=0 are in good agreement with the

observed C-t curves at the corresponding stations (Fig. 6.16). The C-t curves at section (1) and (2) are arrived at using the values of the parameters given by Bencala and Walters (1983). It is noted that the C-t curve computed by the ATS-VPM model at section (3) fails to reproduce the observed C-t curve at the same section (3). This is due to the reason that the applicability criterion estimated for the reaches after 105m from the point of injection indicate the applicability of the ATS model and Table 6.7 brings out this aspect. The low velocity (0.02692 m/s to 0.03694 m/s), high values of β (1 to 3), and the low value of exchange coefficient (1×10^{-5} /s to 4.5×10^{-5}/s) may be responsible for the failure of the ATS-VPM model to simulate the solute transport in the reach after 105m from the point of injection of tracer. The low exchange results in large dispersion because of higher solute residence time in transient storage zones. As the value of α is low, the solute gets trapped in the transient storage zone for larger time and it will be released very slowly into the main channel (Fig.6.6). These low values of α associated with high values of β may be responsible for substantially low interaction of solute between main channel and the storage zone. This low interaction may be the reason for the presence of considerable long tail concentration in C-t curves observed in tracer experiments conducted on Uvas creek.

6.6.2 Solute Transport Under Unsteady Flow Conditions

Based on the results of the numerical experiments (Table 6.9 and Fig. 6 17 to 6.23), it was observed that the ATS-VPM model coupled with the VPM model of flow routing is capable of reproducing the numerical solution of SVE-TS model within the applicability range of the ATS-VPM model and the VPM flow routing model as specified in section 6.5. The results of the numerical experiments carried out (Table 6.9) reveal the following:

1. For a given value of β and ϕ, as the value of α increases, the accuracy of the ATS-VPM model under unsteady flow condition in reproducing the solution of the SVE-TS model increases (Figs. 6.17, 6.18, 6.19). Similarly, for a given value of α and ϕ, as the value of β increases, the accuracy of the ATS-VPM model in reproducing the solution of the SVE-TS model decreases (Figs. 6.17(a) and 6.18). This may be due to the fact that an increase in β decreases the solute velocity. This leads to the increase in residence time, which in turn increases the dispersion of solute cloud.

2. In channel type 3, the peak concentrations at the location of 40km are realised earlier in comparison with those realised in channel types 1 and 2 at the same location. It implies that the solute mass is getting flushed out quickly in channel type 3. This may be due to higher velocities of flow in channel type 3 in comparison with the velocities observed in channel types 1 and 1. The realisation of shorter travel time of peak concentration at the location of 40km in different channels used in the numerical experiments follows, in general, the order, channel type 3, 1 and 2.

3. For a given value of bed slope S_0, as the Manning's roughness n increases, the velocity decreases, thereby, the residence time of solute cloud increases. Residence time of solute in a reach should be as less as possible so as to reduce the effects of polluting solute on the ecosystem of a river reach. The realisation of longer residence time of solute cloud in channels follows, in general, the order channel type 2, 1 and 3.

4. Based on the solutions of SVE-TS model, it can be inferred that the attenuation of peak concentration in rivers affected by transient storage mechanism increases with increase in the value of α upto a limiting value of peak concentration. Any further increase in the value of α results in decrease in the % attenuation of peak concentration (Fig. 6.30)
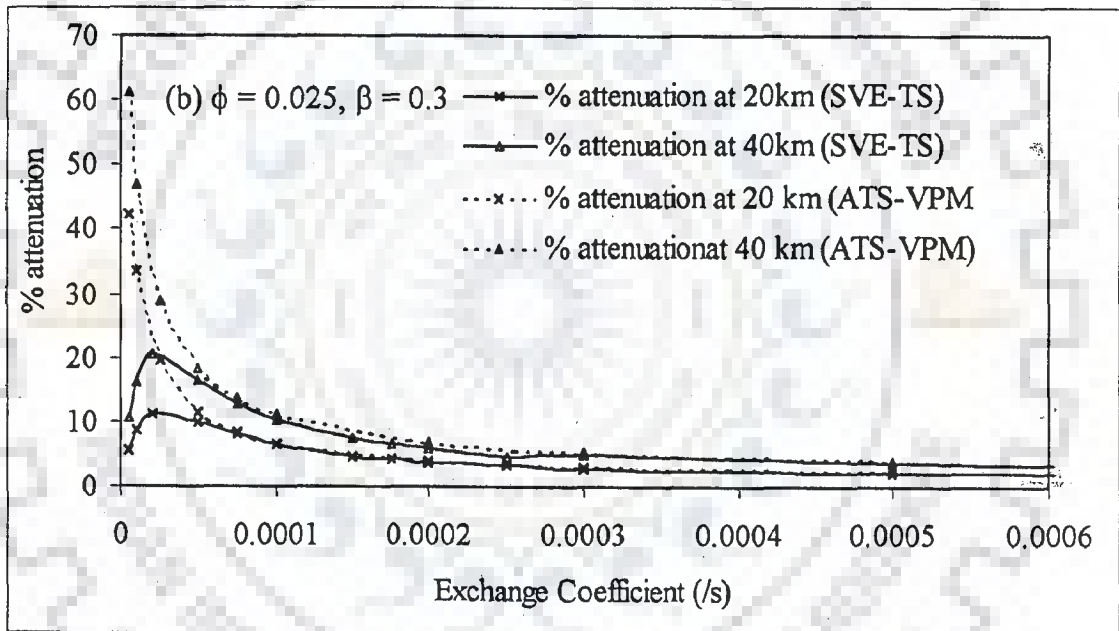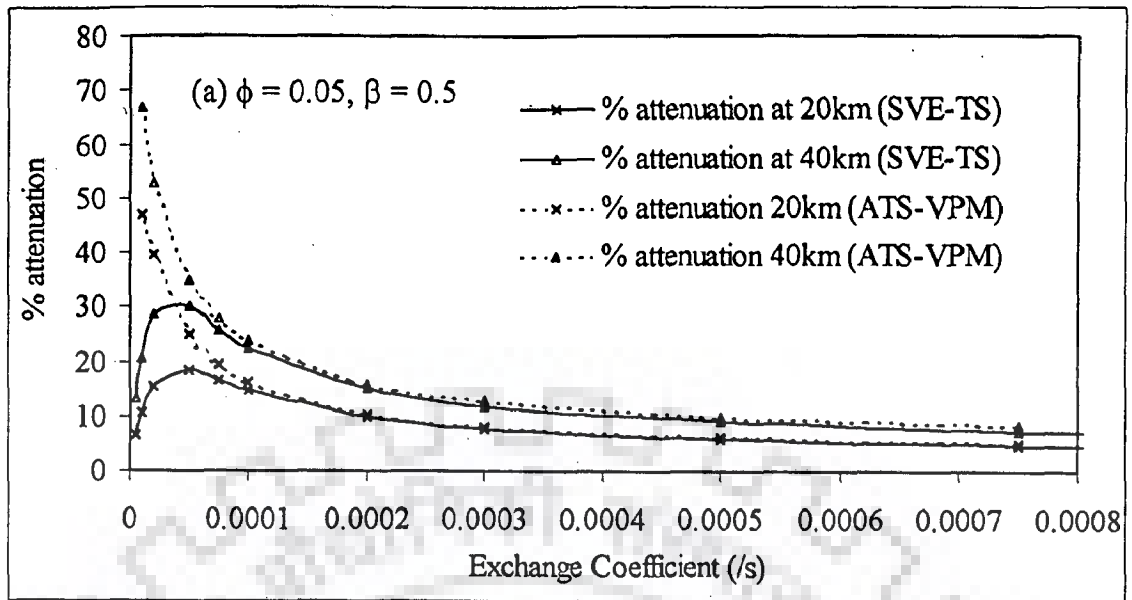
Figure 6.30 Relation between the % attenuation and exchange coefficient (α)
(a) φ = 0.05, β = 0.5, (b) φ = 0.025, β = 0.3

The ATS-VPM model can reproduce the benchmark SVE-TS model solution for values of α greater than that produces maximum attenuation of peak concentration (Fig. 6.30). Within the applicability range of the ATS-VPM model, as α increases the attenuation of peak concentration decreases. This characteristic may be attributed to the retention time of solute in the transient storage zone. There

exists an α beyond which the transient storage zone acts as active part of the main channel. The same is observed in Fig. 6.30, as attenuation is approximately constant or the attenuation curve is asymptotic to the horizontal axis beyond a value of α, making the effect of transient storage mechanism on dispersion is to be negligible.

Related to the aspect of conservation of mass, it can be observed from Figs. 6.17 and 6.21 that there is some gain in concentration. However, there is no gain in mass even though it appears that there is some gain of concentration. Runkel et al. (1998) stated that "*The specific concern is that the numerical solution of the TS equations using the concentration boundary condition may not conserve mass given an unsteady flow regime. To test the mass conservation, concentration-discharge profiles were integrated with respect to time to determine the mass passing a given sampling location. These integrated values agreed closely with the mass introduced via the upstream condition* ". The conservation of mass was tested by Runkel et al. (1998) for the modelling frame work suggested by him and it was found that it conserves mass with a maximum error of 0.074%. (Runkel et al., 1998). As the numerical solution of the TS model suggested by Runkel (1998) under unsteady flow conditions is being reproduced by the ATS-VPM model within its applicability range, it can be concluded that the proposed ATS-VPM model also conserves mass satisfactorily.

The Huey creek experimental test case results show that there is close agreement between the observed and computed C-t curves at 213m, 451m, and 762m. The agreement between the observed and computed C-t curves at 1052m is relatively poor because the ATS-VPM model is applicable in the reach upto 762m only. The β in the last reach of Huey creek, varying between 15.9 to 34.3, is very large. The actual storage zone area for the final reach might have been considerably lower than the estimated value (Runkel et al., 1998). In the Huey Creek experimental data (Runkel et al., 1998), the inflow hydrograph at the upstream

boundary was developed based on the observed downstream flow data at site 945m. This was required because a continuous record of the hydrograph at the upstream boundary was not available. Errors might have been associated with the development of inflow hydrograph based on the downstream data (Runkel et al., 1998). Because of the errors in the estimated input flow hydrograph, the routed hydrograph may have associated errors, which in turn affects the solute transport estimates. To avoid any such errors, it is necessary to have simultaneous flow and C-t measurements.

In computing the C-t curves using the ATS-VPM model for Huey Creek experimental data, the parameter α was used. The value of D_{Lts} was calculated using Eqn. (5.18) and the available value of α, β and D_{ts} estimated by Runkel et al. (1998) so as to demonstrate the validity of the model proposed in the present study for the field conditions.

Future efforts could consider modifications in the model that express the transient storage parameters as a function of the flow regime. Several researchers have noted that the value of the exchange coefficient increases with increasing streamflow (Harvey et al., 1986, and Morrice et al., 1997). The physical reason for the increase in α with discharge may be due to the increase in stream velocity. At higher stream velocities the exchange between the active channel and the transient storage zone may be significant (Runkel et al., 1998). Harvey et al. (1996) and Morrice et al. (1997) indicate that a decrease in the transient storage zone area and, consequently the magnitude of β decreases with increasing streamflow (Runkel et al., 1998). This decrease may be due to the reason that the storage zones at low flow may become active parts of the main channel at high flow. Comparatively few data sets are available and not enough information is available for practitioners (Lees et al., 2000) to test these inferences. Hence, more research is needed to understand and interpret the physical significance of the model parameters of TS and ATS models.

6.7 CONCLUSIONS

In this chapter the comparison of the TS and ATS models was made. The effect of α, β and D_{ts} on solute transport in rivers affected by transient storage mechanism was analysed based on the ATS model. The applicability criterion for the ATS model to reproduce the TS model solution was presented. It was found that the ATS model is capable of reproducing the numerical solution of the TS model with a variance explained using Nash-Sutcliffe criterion, η >98% when $\lambda \leq 10^6$. The applicability of the ATS-VPM model to reproduce the solution of the ATS model under steady flow conditions was also presented. It was found that the ATS-VPM model is capable of reproducing the ATS model solution with a Nash-Sutcliffe criterion, $\eta > 99\%$, when the value of D_{Lts} is less than $416.64 \left[U/(1+\beta) \right]^{1.71}$. An equation (Eqn. 6.3) to compute the exchange coefficient α, for a given value of U, β, and D_{ts} above which the ATS-VPM model can reproduce the ATS model solution was presented. The practical utility of the ATS-VPM model under steady flow conditions was demonstrated by verifying its applicability using field data from experiments performed on Mimram River and Uvas Creek. It was also demonstrated that when the applicability criterion is not satisfied, the model would fail to model the solute transport in rivers affected by transient storage mechanism. The performance of the ATS-VPM model for solute routing coupled with the VPM model for flow routing for solute transport under unsteady flow was evaluated using SVE-TS model solutions obtained using hypothetical data. From the numerical experiments, it was found that the ATS-VPM model under unsteady flow conditions can reproduce the SVE-TS model solution for values of α greater than that produces maximum attenuation of peak concentration (Fig. 6.30). The practical utility of the ATS-VPM model under unsteady flow conditions subjected to the satisfaction of its applicability criterion, was demonstrated by using the data from experiments performed on Huey Creek, an Antarctic stream.

CONCLUSIONS AND RECOMMENDATIONS

7.1 CONCLUSIONS

The present study stems from the recognition of the need for the development of longitudinal solute dispersion models that adequately consider the governing flow regime, and yet require cumbersome solution algorithms. Accordingly, the problem of solute transport process in rivers and streams under unsteady flow conditions is studied by developing coupled flow routing and solute routing models based on simplified governing equations of these processes. The simplification of the governing equations sought in this study are those of the well known Advection-Dispersion model, and the Transient Storage model which combinedly consider the solute dispersion due to main channel flow, and due to the presence of storage zones in rivers. The modelling approach proposed in this study is to develop first the simplified solute transport model under steady flow conditions and then extend it to study the same process under unsteady flow conditions. The capabilities of the developed models for studying longitudinal solute dispersion process under unsteady flow conditions are demonstrated using hypothetical, laboratory and field experimental data. The main findings of the present study are as follows:

1. The evaluation of the existing model proposed by Koussis et al. (1983) for solute transport modelling under steady flow conditions brings out certain logical inconsistencies in his approach. To overcome these inconsistencies, an approximate Advection-Dispersion equation, based on the assumption of linear variation of concentration along a small river reach length Δx, is developed. Using this equation and the concept used in the development of the Variable Parameter Muskingum (VPM) flow routing model, a model termed as AD-VPM

model is developed. The suitability of the AD-VPM model is first studied for dispersion under steady flow conditions against analytical solution of the AD model, and for variety of data from laboratory experiments and field experiments. It is found that the model is capable of reproducing observed C-t profiles satisfactorily within the applicability range governed by the criterion $D_L \leq 415.64\ U^{1.71}$.

2. A methodology for solute routing under unsteady flow conditions is presented by integrating the parameters of the AD-VPM model and the VPM model. The advantage of the proposed method is that it allows simultaneous routing of flow and solute, as the model structure is similar for both the processes. The appropriateness of the application of the AD-VPM model under unsteady flow conditions has been then tested using hypothetical data obtained by solving the Saint-Venant's equations coupled with the AD equation (SVE-AD model). It was found that AD-VPM model could closely reproduce the results obtained from numerical solutions of the SVE-AD model and also could reproduce the field experimental data of the Colorado River. Based on the proposed method's performance in the reproduction of the SVE-AD solutions and the observed C-t curves in field experiments, it can be concluded that the proposed method is suitable for simulation of solute transport under unsteady flow conditions within the applicability range defined previously.

3. An Approximate Transient Storage (ATS) model is developed from the TS model equations which incorporate solute transport due to transient storage. The ATS model has a form similar to that of the AD model, but incorporates the transient storage parameters. Based on the developed governing equation of the ATS model, analytical solution is presented in analogy to the analytical solution of the AD model under steady flow conditions.

4. The appropriateness of the ATS model under steady flow conditions is tested by comparing the numerical solution of the TS model with the corresponding analytical solution of the ATS model. It is found from the analysis that the ATS model is able to closely simulate the TS model solution when magnitude of $\beta^2/(\alpha\,(1+\beta))^2 \leq 10^6$, where α and β are the model parameters.

5. Using the similarity of the ATS model and the AD model, a model termed as the ATS-VPM model is developed on the same lines as that of the AD-VPM model. The appropriateness of the ATS-VPM model has been demonstrated under steady flow conditions using the analytical solution of the ATS model and a criterion (chapter 6) has been developed for the successful application of the ATS-VPM model similar to that of the AD-VPM model, in reproducing the analytical solution of the ATS model. The suitability of the ATS-VPM model was also demonstrated for field applications.

6. The procedure for the application of the ATS-VPM model for simulating solute transport process under unsteady streamflow conditions was presented by integrating its parameters with the VPM flow routing model. The suitability of the ATS-VPM model for simulating solute transport process under unsteady streamflow conditions was demonstrated by reproducing the benchmark solutions obtained from the numerical solutions of the Saint-Venant Equations coupled with the TS model equations (SVE-TS model) and, subsequently, the observed data from field experiments. The results of this study suggest the suitability of the ATS-VPM model for its application to solute transport modelling under unsteady streamflow conditions in the presence of transient storage zones in the river reach.

Based on the study it can be concluded that the proposed AD-VPM and ATS-VPM models simulate the solute transport in rivers and streams under steady as well as unsteady flow conditions satisfactorily within their applicability ranges.

7.2 RECOMMENDATIONS FOR FURTHER STUDY

Based on the present study, the following recommendations are made for further studies:

1. The AD-VPM and ATS-VPM models proposed in the present study may be extended to the simulation of non-conservative solute transport by properly incorporating the first order decay phenomenon.

2. Expressions to compute β and D_{Ls} using hydro-geometric characteristics of rivers may be developed, which need the analysis of many experimental data sets conducted on rivers.
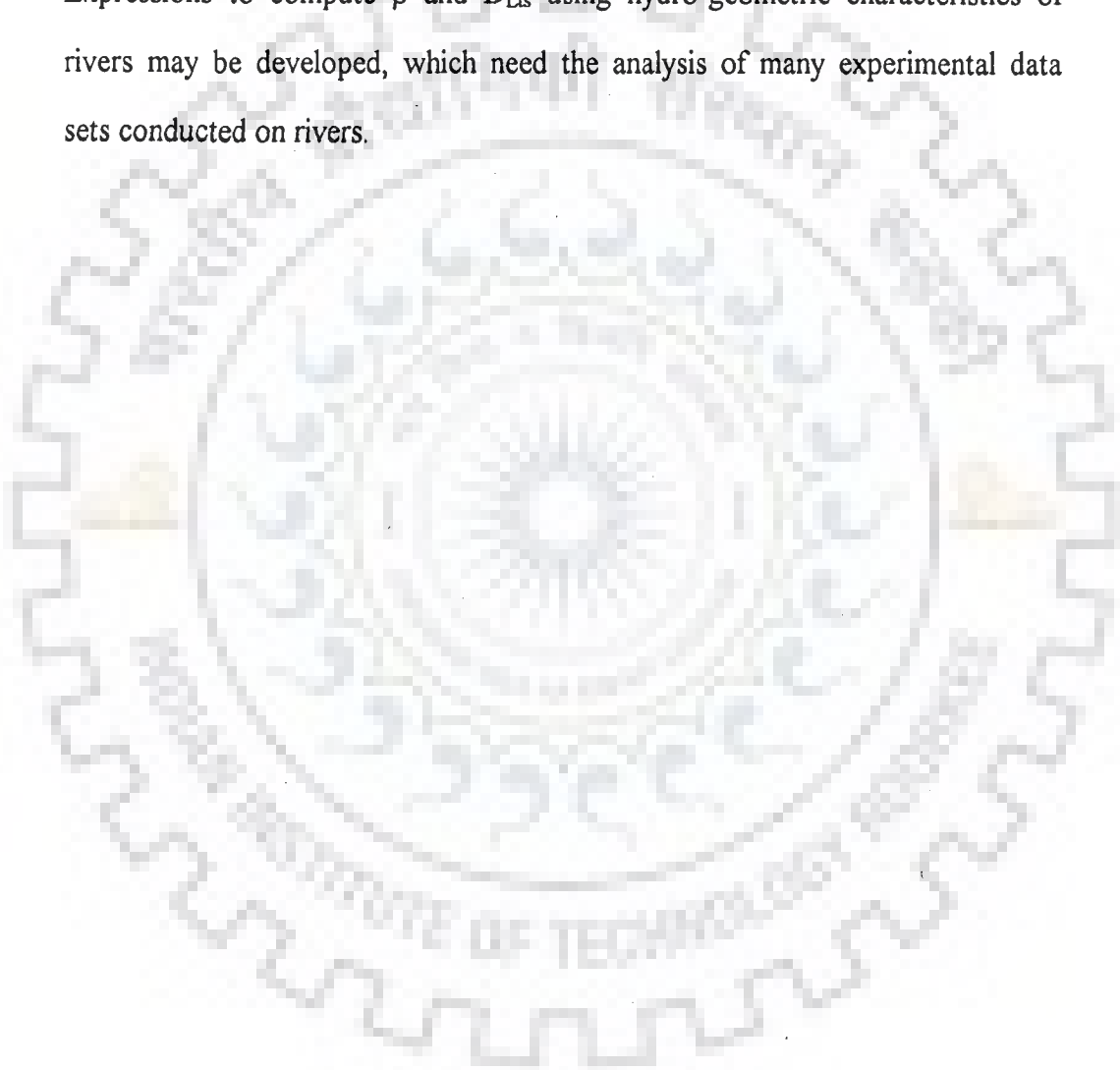
REFERENCES

1. Alley, W. M., and Smith, P. E. (1982). "Distributed routing rainfall-runoff model." Version II, Computer Program Documentation, User's Manual, US Geological Survey, Open-File Report 82-344, NTSL Station, Mississippi.

2. Amein, M. M., and Fang, C. S. (1970). "Implicit flood routing in natural channels." J. of Hydraul. Div., ASCE, 96(12), 2481-2500.

3. Asai, K., Fujisaki, K., and Awaya, Y. (1991). "Effect of aspect ratio on longitudinal dispersion coefficient." in Environmental Hydraulics, Lee and Cheung (Ed.), Vol.2, Balkema, Rotterdam, The Netherlands. 493-498.

4. ASCE task committee on Definition of Criterion for Evaluation of Watershed Models of the Watershed management, Irrigation and Drainage Division, (1993). "Criteria for evaluation of watershed models." J. of Irrig. and Drain. Engrg., ASCE, 119(3), 429-442.

5. Banks, R.B. (1974). "A mixing cell model for longitudinal dispersion in open channel." Water Resour. Res., 10(2), 357-358.

6. Bedford, K.W., Sykes, R.M., and Libicki, C. (1983). "Dynamic advective water quality model for rivers." J. of Envir. Engrg., ASCE, 109(3), 535-554.

7. Beer, T. and Young, P.C. (1983). "Longitudinal dispersion in natural streams." J. of Envir. Eng., ASCE, 109(5), 1049-1067.

8. Bella, D.A., and Dobbins, W.E. (1968). "Difference modeling of stream pollution." J. of Sanit. Engrg. Div., ASCE, 94(5), 995-1016.

9. Beltaos, S. (1978). "An interpretation of longitudinal dispersion data in rivers." Report no. SER 78-3, Transportation and Surface Water Div., Alberta, Research Council, Edmonton, Canada.

10. Beltaos, S. (1980). "Longitudinal dispersion in rivers." J. of Hydraul. Div., ASCE, 106(1), 151-172.

11. Beltaos, S. (1982). "Dispersion in tumbling flow." J. of Hydraul. Div., ASCE, 108(1), 591-612.

12. Bencala, K.E. (1983). "Simulation of solute transport in a mountain pool-and-riffle stream: with a kinetic mass transfer model for sorption." Water Resour. Res., 19(3), 732-738.

13. Bencala, K.E. and Walters, R.A. (1983). "Simulation of solute transport in a mountain pool-and-riffle stream: A transient storage model." Water Resour. Res., 19(3), 718-724.

14. Camacho, L. A. (2000). "Development of a hierarchical modelling framework for solute transport under unsteady flow conditions in rivers." Ph.D. thesis submitted to University of London, Dept. of Civil and Envir. Engrg. Imperial College of Science and Technology and Medicine, London.

15. Chatwin, P.C. (1980). "Presentation of longitudinal dispersion data." J. of Hydraul. Engrg. Div., ASCE, 106(1), 71-82.

16. Chatwin, P.C. and Allen, C. M. (1985). "Mathematical models of dispersion in rivers and estuaries." Annual Review of Fluid Mech., 17, 119-149.

17. Chow, V.T., Maidment, D.R., and Mays, L.W. (1988). Applied Hydrology. McGraw-Hill Book Co., New york.

18. Cunge, J.A. (1969). "On the subject of a flood propagation computation method (Muskingum method)." J. of Hydraul. Res., IAHR, 7(2), 205-230.

19. Czernuszenko, W., and Rowinski, P. M. (1997). "Properties of the dead zone model of longitudinal dispersion in rivers." J. of Hydraul. Res., 35 (4), 491-504.

20. Day, T. J. (1975). "Longitudinal dispersion in natural channels." Water Resour. Res., 11(6), 909-918.

21. Elder, J. W. (1959). "The dispersion of marked fluid in turbulent shear flow." J. of Fluid Mech., 5(4), 544-560.

22. Fischer, H.B. (1966). "Longitudinal dispersion in laboratory and natural streams." Report No. KH-R-12, W.M.Keck Laboratory of Hydraul. and Water Resour., California Institute of Technology, California.

23. Fischer, H.B. (1967). "The mechanics of dispersion in natural streams." J. of Hydraul. Engrg. Div., ASCE, 93(6), 187-216.

24. Fischer, H.B. (1968). "Dispersion predictions in natural streams." J. of Sanit. Engrg. Div., ASCE, 94(5), 927-943.

25. Fischer, H.B., List, E.J., Koh, R.C.Y., Imberger, J. and Brooks, N.H. (1979). Mixing in inland and coastal waters. Academic Press Inc., New York, NY.

26. Fukuoka, S., and Sayre, W. W. (1973). "Longitudinal dispersion in sinuous channels." J. of Hydraul. Div., ASCE, 99(1), 195-218.

27. Gabriele, H.M.S., and Perkins, F.E. (1997). "Watershed-specific model for stream flow, sediment, and metal transport." J. of Envir. Engrg., ASCE, 123(1), 61-70.

28. Glover, B. J., and Johnson, P. (1974). "Variations in the natural chemical concentration of river water during flood flows and the lag effect." J. of Hydrology. 22, 303-316.

29. Godfrey, R.G., and Frederick,B.J. (1970). "Stream dispersion at selected sites." Professional paper 433K, U.S.Geological Survey, Washington, D.C.

30. Graf, J.B. (1995). "Measured and predicted velocity and longitudinal dispersion at steady and unsteady flow, Colorado river, Glen Canyon Dam to Lake Mead." Water Resour. Bulletin, AWRA, 31 (2), 265-281.

31. Graf, W.H. (1998). Fluvial Hydraulics. John-Wiley & Sons, Chichester

32. Guymer, I. (1998). "Longitudinal dispersion in sinuous channel with changes in shape." J. of Hydraul. Engrg., ASCE,124(1), 33-40.

33. Harvey, J.W., Wagner, B.J., and Bencala, K.E. (1996). "Evaluating the reliability of the stream tracer approach to characterize stream-subsurface water exchange." Water Resour. Res., 32(8), 2441-2451.

34. Hayami, S. (1951). "On the propagation of flood waves." Bull.no.1, Disaster Prevention Research Institute, Kyoto, Japan.

35. Holly, F. M., and Preissmann, A. (1977). "Accurate calculation of transport in two dimensions." J. of Hydraul. Div., ASCE, 103 (11),1259-1277.

36. Islam, M.R., and Chaudhry, M. H. (1997). "Numerical solution of transport equation for applications in environmental hydraulics and hydrology." J. of Hydrology, 191,106-121.

37. Jain, S.C., (1976)."Longitudinal dispersion coefficient for streams." J. of Envir. Engrg., ASCE, 102(2), 465-474.

38. Jaque, D.T., and Ball, J.E. (1994). "Numerical simulation of advection-diffusion mass transport." J. of Hydroscience and Hydraul. Engrg., 11(2),.

39. Jirka, G.H. (1982). "Multiport diffusers for heat disposal: A summary." J. of Hydraul. Div., ASCE, 108(12), 1425-1468.

40. Jobson, H. E. (1980). "Comment on 'A new collocation method for the solution of the convection-dominated transport equation' by George E. Pinder and Allen Shapiro." Water Resour. Res., 16(6) 1135-1136.

41. Karolewski, M. (2001). "Tracer 1.5." http://www.ualberta.ca/~mkarol.

42. Keefer, T. N., and Jobson, H. E. (1978). "River transport modeling for unsteady flow." J. of Hydraul. Div., ASCE, 104(5), 635-647.

43. Kezhong, H., and Yu, H. (2000). "A new empirical equation of longitudinal dispersion coefficient." in Stochastic Hydraulics 2000, Wang and Hu (Eds), Balkema, Rotterdam.

44. Komatsu, T. Ohgushi, K., and Asai, K. (1997)."Refined numerical scheme for advective transport in diffusion simulation." J. of Hydraul. Engrg., ASCE, 123(1), 41-50.

45. Koussis, A. D. (1978). "Theoretical estimation of flood routing parameters." J. of Hydraul. Div., ASCE, 104(1), 109-115.

46. Koussis, A.D., Saenz, M. A. and Tollis, I.G. (1983). "Pollution routing in streams." J. of Hydraul. Engrg., ASCE, 109(12), 1636-1651.

47. Koussis, A.D. (1983). "Unified theory of flood and pollution routing in streams." J. of Hydraul. Engrg., ASCE, 109(12), 1652-1664.

48. Koussis, A. D., and Rodriguez-Mirasol, J. (1998)."Hydraulic estimation of dispersion coefficient for streams." J. of Hydraul. Engrg., ASCE,124(3), 317-320.

49. Krein, A., and Symader, W. (2000). "Pollutant sources and transport patterns during natural and artificial flood events in the Olewiger Back and Kartel borns-bach basins, Germany." Proceedings of symposium on the Role of Erosion and

Sediment Transport in nutrient and contaminant transfer held at Waterloo, Canada, July 2000, IAHS publ. 263,167-173.

50. Lees, M. J., Camacho, L. A., and Chapra, S.C. (2000). "On the relationship of transient storage and aggregated dead zone models of longitudinal solute transport in streams." Water Resour. Res., 36(1), 213-224.

51. Lees, M. J., Camacho, L., and Whitehead, P. (1998). "Extension of the QUASAR river water quality model to incorporate dead-zone mixing." Hydrology and Earth System Sciences, 2, (2-3), 353-365.

52. Li, C.W. (1990). "Advection simulation by minimax-characteristics method." J. of Hydraul. Div., ASCE,116(9), 1138-1143.

53. Li, S. G., and Zhou, X. (1997). "Stochastic theory for irregular stream modelling. II: solute transport." J. of Hydraul. Engrg., ASCE, 123(7), 610-616.

54. Liu, H. (1978). "Closure of 'Discussion on predicting dispersion coefficient of streams." J. of Envir. Engrg. Div., ASCE, 104(4), 825-828.

55. Liu, H., and Cheng, A.H.D. (1980)."Modified Fickian model for prediction dispersion." J. of Hydraul. Engrg. Div., ASCE, 106(6), 1021-1040.

56. Manson, J. R., Wallis, S.G., and Hope, D. (2001)."A conservative semi-lagrangian transport model for rivers with transient storage zones." Water Resour. Res., 37(12), 3321-3329.

57. Marivoet, J. L., and Craenenbroeck, W.V. (1986)."Longitudinal dispersion in ship canals." J. of Hydraul. Res., 24(2), 123-133.

58. McCutcheon, S.C. (1989). Water quality modeling: Volume I transport and surface exchange in rivers. CRC press, Inc. Boca Raton, Florida.

59. McQuivey, R.S., and Keefer, T.N. (1974). "Simple method for predicting dispersion in streams." J. of Envir. Engrg. Div., ASCE, 100(4), 997-1011.

60. Morrice, J. A., Valett, H. M., Dahm, C. N., and Campana, M.E. (1997). "Alluvial characteristics, groundwater-surfacewater exchange and hydrological retention in headwater streams." Hydrological Processes, 11, 253-267.

61. Nash, J.E., and Sutcliffe, J.V. (1970). "River flow forecasting through conceptual models. Part I- a discussion of principles." J. of Hydrology, 10, 282-290.

62. Natural Environment Research Council (1975). Flood studies report, Volume III-Flood routing studies. London, U.K.

63. Nordin, C. F., and Sabol, G. V. (1974). "Empirical data on longitudinal dispersion in rivers." U.S Geological Survey Water Resources Investigations 20-74, Washington, D.C.

64. Nordin, C. F., and Troutman, B.M. (1980)."Longitudinal dispersion in rivers: The persistence of skewness in observed data." Water Resour. Res., 16(1), 123-128.

65. Ogata, A., and Banks, R.B. (1961)."A solution of the differential equation of longitudinal dispersion in porous media." Professional Paper no. 411-A, U.S. Geological Survey.

66. Orlob, G.T. (Ed.) (1983). Mathematical modeling of water quality: streams, lakes and reservoirs. John-Wiley & Sons, Chichester.

67. Perumal, M. (1992), "The cause of negative initial outflow with the Muskingum method." Hydrological Sci. J., IAHS, 37(4), 391-401.

68. Perumal, M. (1994a). "Hydrodynamic derivation of a variable parameter Muskingum method: 1. Theory and solution procedure." Hydrological Sci. J., IAHS, 39(5), 431-442.

69. Perumal, M. (1994b). "Hydrodynamic derivation of a variable parameter Muskingum method: 2.Verification." Hydrological Sci. J., IAHS, 39(5), 443-458.

70. Perumal, M., and Ranga Raju, K.G. (1999). "Approximate Convection-Diffusion equations." J. of Hydrol. Engrg., ASCE, 4(2), 160-164.

71. Perumal, M, O'Connell, P.E., and Ranga Raju, K.G. (2001). " Field applications of a Variable Parameter Muskingum method." J. of Hydrolog. Engrg., ASCE, 6(3), 196-207.

72. Ponce, V. M., and Yevjevich, V. (1978). "Muskingum-Cunge method with variable parameters." J. of Hydraul. Div., ASCE, 104 (12), 1663-1667.

73. Price, R.K. (1982). "Flow routing for river regulation." in Gravel-bed rivers, by Hey, R.D., Bathurst, J.C., and Thorne, C.R.(Eds.) John Wiley & Sons Ltd., 603-632.

74. Ranga Raju, K.G., Kothyari, U.C., and Ahmad, Z. (1997). "Dispersion of conservative pollutant." Dept. of Civil Engrg. Univ. of Roorkee, Roorkee, India.

75. Runkel, R. L., and Chapra, S. C. (1993). "An efficient numerical solution of the transient storage equations for solute transport in small streams." Water Resour. Res., 29(1), 211-215.

76. Runkel, R.L. (1996)."Solution of the advection–dispersion equation: continuous load of finite duration." J. of Envir. Engrg., ASCE, 122 (9), 830-832.

77. Runkel, R. L. (1998). "One dimensional transport with inflow and storage (OTIS): A solute transport model for streams and rivers." USGS Water Resour. Invest. Report No. 98-4018., Denver, Colorado.

78. Runkel, R. L., McKnight, D. M., and Andrews, E. D. (1998). "Analysis of transient storage subject to unsteady flow: diel flow variation in an Antarctic stream." J. N. Am. Benthol. Soc., 17(2), 143-154.

79. Rutherford, J.C. (1994). River Mixing, John-Wiley & Sons, Chichester

80. Sabol, G.V. and Nordin, C.F. (1978). "Dispersion in rivers as related to storage zones." J. of Hydraul. Engrg. Div., ASCE, 104(5), 695-708.

81. Sayre, W.W. (1968). "Dispersion of Mass in open channel flow." Hydraulic papers No.3, Colorado State Univ., Fort Collins, Co.

82. Schohl, G.A., and Holly, Jr. F.M. (1991). "Cubic-spline interpolation in lagrangian advection computation." J. of Hydraul. Engrg., ASCE, 117(2), 248-253.

83. Seo, I. W., and Cheong, T.S. (1998). "Predicting longitudinal dispersion coefficient in Natural Streams." J. of Hydraul. Engrg., ASCE, 124 (1), 25-32.

84. Seo, I. W., and Cheong, T.S. (2001). "Moment-based calculation of parameters for the storage zone model for river dispersion." J. of Hydraul. Engrg., ASCE, 127 (6), 453-465.

85. Sooky, A.A. (1969). " Longitudinal dispersion in open channels." J. of Hydraul. Div., ASCE, 95(4), 1327-1345.

86. Stefan, H.G., and Demetracopoulos, A.C. (1981)."Cells-in-series simulation of riverine transport." J. of Hydraul. Div., ASCE, 107(6), 675-697.

87. Stone, H. L., and Brian, P.L.T. (1963)."Numerical solution of convective transport problems." J. of American Institute of Chemical Engineers, 9(5), 681-688.

88. Strupczewski, W.G., and Napiorkowski, J.J. (1990). "What is the distributed delayed Muskingum model?." Hydrological Sci. J., IAHS, 35(1), 65-78.

89. Sumer, M. (1969). "On the longitudinal dispersion coefficient for a broad open channel." J. of Hydraul. Res., 7(1), 129-135.

90. Taylor, G.I. (1921)."Diffusion by continuous movement." Proc. of the London Mathematical Society, Series A, 196-211.

91. Taylor, G.I. (1953). "Dispersion of soluble matter in solvent flowing slowly through a tube." Proc. Royal Society, London, series A, 219, 186-203.

92. Taylor, G.I. (1954). "The dispersion of matter in turbulent flow through a pipe." Proc. Royal Society, London, series A, 223, 446-468.

93. Thackston, E. L., and Krenkel, P. A. (1967)."Longitudinal mixing in natural streams." J. of Sanit. Engrg. Div., ASCE, 93(5), 67-90.

94. Thackston, E. L., and Schnelle, K. B. Jr. (1970)."Predicting effects of dead zones on stram mixing." J. of Sanit. Engrg. Div., ASCE, 96(2), 319-331.

95. Thomann, R.V., and Mueller, J.A. (1987). Principles of Surface Water Quality Modelling and Control. Harper & Row Publishers, NewYork.

96. Valentine, E.M. and Wood, I.R. (1977). "Longitudinal dispersion with dead zones." J. of Hydraul. Div., ASCE, 103(9), 975-990.

97. Viessmann Jr W., Knapp, J.W., Lewis, G, L., and Harbaugh, T.E. (1977). Introduction to Hydrology. IEP A Dun-Donnelley Publ., NewYork.

98. Von Guerard, P., McKnight, D. M., Harnish, R. A., Gartner, J. W. and Andrews, E. D. (1995). "Streamflow, water-temperature, and specific-conductance data for selected streams draining into Lake Fryxell, Lower Taylor Valley, Victoria Land, Antarctica, 1990-92. USGS, Open File Report 94-545, Denver, Colorado.

99. Wallis, S.G. (1994). "Simulation of solute transport in open channel flow." in Mixing and Transport in the Environment, Ed. By K. J. Beven, P. C. Chatwin and J. H. Millbank., John Wiley & Sons Ltd. NewYork, 89-110.

100. Whitehead, P., Young, P.C., and Hornberger, G. (1979). "A systems model of streamflow and water quality in the Bedford Ouse river system-I. Stream flow modelling." Water Research, 13, 1155-1169.

101. Whitehead, P., Beck, B., and O'Connell, E. (1981). "A systems model of streamflow and water quality in the Bedford Ouse river system-II. water quality modelling." Water Research, 15, 1157-1171.

102. Wiele, S.M., and Smith, J.D. (1996). "A reach-averaged model of diurnal discharge wave propagation down the Colorado river through the Grand Canyon." Water Resour. Res., 32 (5), 1375-1386.

103. Worman, A. (2000). "Comparison of models for transient storage of solutes in small streams." Water Resour. Res., 36(2), 455-468.

104. Yotsukura, N., Fischer, H.B., and Sayre, W.W. (1970). "Measurement of mixing characteristics of the Missouri river between Sioux City, Iowa and Plattsmouth, Nebraska." Water Supply paper 1899-G, U.S.Geological Survey, Washington.

105. Young, P. C., and Wallis, S. G. (1993). "Solute transport and dispersion on channels." in Channel Network Hydrology. Beven, K., and Kirkby, M. J.(Eds)., John Wiley & Sons Ltd.

106. Zoppou, C., and Knight, J. H., (1997). "Analytical solutions for advection and advection- diffusion equations with spatially variable coefficients." J. of Hydraul. Engrg., ASCE, 123 (2),144-148.

DISPERSION DATA OF TESTS CONDUCTED IN LABORATORY CHANNELS

This appendix contains the data of the series 2600 and series 2700 experiments conducted in laboratory flume by Fischer (1966). These experiments were conducted in a 40m long rectangular laboratory flume having a width of 1.10m. Conservative Rhodamine WT was used as the tracer for the experiments.

A 1.1 Laboratory Experiment Data-Series 2600

Series 2600 data of time-concentration measurements at four successive sections at a distance 7.0m apart are given in Table A1.1.

Table A 1.1 Time-Concentration data -Series 2600

Distance from source = 7.06m		Distance from source = 14.06m		Distance from source = 21.06m		Distance from source = 28.06m	
Section-1		Section-2		Section-3		Section-4	
Time from release (sec)	Mean Concentration (CU)*	Time from release (sec)	Mean Concentration (CU)*	Time from release (sec)	Mean Concentration (CU)*	Time from release (sec)	Mean Concentration (CU)*
20.0	0.1	41	0.0	64	0.0	88	0.2
21.0	5.6	42	0.2	65	0.3	90	1.7
21.5	18.8	43	0.8	66	1.0	92	6.6
22.0	44.9	44	4.0	67	2.1	94	20.3
22.5	75.7	45	14.8	68	5.6	96	45.5
23.0	102.1	46	36.9	69	13.2	98	74.8
23.5	105.4	47	66.3	70	26.9	100	95.0
24.0	96.3	48	83.9	71	43.5	102	98.4
24.5	82.0	49	94.0	72	63.5	104	87.2
25.0	69.5	50	94.4	73	83.7	106	68.7
25.5	57.4	51	87.3	74	97.0	108	48.0
26.0	46.0	52	76.9	75	104.2	110	31.6
27.0	28.9	53	63.4	76	104.9	112	19.0
28.0	16.3	54	49.2	77	99.2	114	10.5

Table A 1.1 (Contd....)

Distance from source = 7.06m		Distance from source = 14.06m		Distance from source = 21.06m		Distance from source = 28.06m	
Section-1		Section-2		Section-3		Section-4	
Time from release (sec)	Mean Concentration (CU)*	Time from release (sec)	Mean Concentration (CU)*	Time from release (sec)	Mean Concentration (CU)*	Time from release (sec)	Mean Concentration (CU)*
29.0	8.3	55	36.6	78	87.9	116	5.7
30.0	4.7	56	25.0	79	73.4	118	3.7
31.0	2.7	57	16.9	80	60.6	120	2.3
32.0	1.4	58	11.0	82	39.2	122	1.3
33.0	0.5	59	7.1	84	23.6	124	1.0
34.0	0.2	60	4.4	86	13.0	128	0.3
35.0	0.0	62	2.0	88	6.1	132	0.2
36.0	0.0	64	0.9	90	3.2		
		66	0.4	92	1.5		
		68	0.2	95	0.7		
		72	0.0	100	0.1		
				105	0.0		

* concentration units as measured by Fischer (1966).

A 1.2 Laboratory Experiment Data-Series 2700

Series 2700 data of time- concentration measurements at two sections at a distance of 11.0m apart are given in Table A 1.2.

Table A 1.2 Time-Concentration data -Series 2700

Distance from source =14.06m		Distance from source = 25.06m	
Section-1		Section-2	
Time from release (sec)	Mean Concentration (CU)*	Time from release (sec)	Mean Concentration (CU)*
32	0	57	0
33	1.5	59	0.7
34	16.2	61	13.4
34.5	31.2	62	31.4
35	42.4	63	52.4
35.5	54	64	72.5
36	70	65	91.5
36.5	73.3	66	102.1
37	72.9	67	106.6
37.5	70.6	68	105.3
38	66	69	97.1
38.5	58.4	70	84.3
39	51.7	71	71.6
39.5	46.3	72	61.4
40	41	73	50.6
41	34.3	74	41.1
42	25.6	75	32.1
43	16.1	76	25
44	10.9	77	18.4
46	4.7	79	10.3
48	1.7	81	4.9
50	0.5	83	2
52	0.2	85	1
		87	0.5
		89	0.2

* concentration units as measured by Fischer (1966).

DISPERSION DATA OF TESTS CONDUCTED IN RIVER

In this appendix details of the data used in the present study from experiments conducted on Missouri River (Yotsukura et al., 1970), Rhine River (Van Mazijk, personnel communication), Colorado River (Graf, 1995), Mimram River (Lees et al., 1998), Uvas Creek (Bencala and Walters, 1983) and Huey Creek (Runkel et al., 1998) are presented.

B 1.1   Missouri River Experiment Data

Yotsukura et al., (1970) conducted tracer experiments in a 227km reach of Missouri River between Sioux city and Plattsmouth A total of 272.16 kg. of Rhodamine WT 20 percent solution was injected downstream from Combination Bridge at Sioux City at about 17 hrs. November 13, 1967. Time-concentration measurements of dye are available at four down stream sampling locations: Decatur Highway Bridge (RK 1112), Blair Highway Bridge (RK 1042.8), Ak-sar-ben Bridge in Omaha (RK 991.3) and Plattsmouth Highway Bridge (RK 951). The data consists of cross-sectional average dye concentration as a function of time at each sampling cross-section and are given in Table B 1.1.

B 1.2   Rhine River Experiment Data

Dye experiments were conducted, in June 1991,(Van Mazijk, personnel communication) in a relatively normal discharge range from 2140 m³/s to 2290 m³/s. The sampling stations, where the time-concentration measurements were taken are located in a reach length of 273 km (Fig. 3.10). The observed data available at the sampling stations between Koblenz (RK 590.35) and Lobith (RK 863.3) are given in Table B 1.2. The bed slope in different sub-reaches is given in Table B 1.3. (Note. The data of these experiments have been used in the present study with prior permission from Dr. Mr. M. Meulenberg of Commission International de L'Hydrologic du Bassion du Rhine (ICHR), The Netherlands.)

Table B 1.1 Distribution of cross-sectional average dye concentration with time, Missouri River, November 1967

Decatur Bridge (RR=0.882)		Blair Bridge (RR=0.780)		Ak-sar-ben Bridge (RR=0.775)		Plattsmouth Bridge (RR=0.775)	
Time after injection (hr:min)	Dye Concentration (ppb)	Time after injection (hr:min)	Dye Concentration (ppb)	Time after injection (hr:min)	Dye Concentration (ppb)	Time after injection (hr:min)	Dye Concentration (ppb)
10:30	0	20:59	0.01	28:33	0	34:02	0
10:45	0.25	21:27	0.02	29:06	0.04	35:02	0.03
11:00	0.80	21:51	0.22	29:32	0.11	36:02	0.15
11:25	1.89	22:10	0.35	30:03	0.29	37:01	0.49
11:36	2.32	22:30	0.60	30:33	0.53	38:02	1.00
11:49	2.84	22:47	0.88	31:03	0.88	39:00	1.37
11:58	3.21	23:01	1.09	31:32	1.16	40:00	1.64
12:16	3.55	23:16	1.38	32:02	1.52	41:02	1.57
12:35	3.92	23:52	1.88	32:33	1.79	42:02	1.39
12:47	4.05	24:12	2.23	33:02	2.01	43:00	1.07
13:03	4.03	24:34	2.45	34:02	2.09	44:30	0.62
13:17	3.88	24:55	2.50	34:35	1.84	46:11	0.29
13:33	3.64	25:27	2.52	35:05	1.73	47:58	0.15
13:47	3.36	25:55	2.39	36:05	1.28	50:03	0.08
14:03	3.10	26:24	2.10	37:03	0.88	52:05	0.06
14:18	2.70	26:53	1.78	38:00	0.54	55:12	0.03
14:33	2.38	27:46	1.20	39:01	0.32	59:06	0.02
14:47	2.07	28:02	1.01	40:01	0.20	63:10	0.01
15:02	1.64	28:33	0.74	41:01	0.13	66:58	0.01
15:17	1.39	29:02	0.61	42:01	0.09		
15:32	1.12	29:35	0.42	43:02	0.07		
15:48	0.86	30:02	0.30	45:00	0.05		
16:03	0.72	30:32	0.21	47:10	0.03		
16:23	0.49	31:02	0.14				
16:43	0.37	32:03	0.09				
17:03	0.28	33:01	0.09				
17:22	0.19	34:04	0.06				
17:42	0.14	35:06	0.07				
18:04	0.11	36:03	0.05				
18:37	0.09	38:03	0.03				
19:02	0.08	40:02	0.02				
19:35	0.06	43:05	0.02				
20:02	0.06						

Table B 1.2 Distribution of cross-sectional average dye concentration with time, River Rhine, June, 1991

(Van Mazijk, personnel communication).

Measuring station Koblenz Rhine-km 590.35 (left bank)		Measuring station Bad Honnef Rhine-km 640.0 (right bank)		Measuring station Koeln(Cologne) Rhine-km 689.5 (left bank)		Measuring station Dusseldorf Rhine-km 759.6 (right bank)		Measuring station Wesel Rhine-km 814.0 (right bank)		Measuring station Lobith Rhine-km 863.3 (right bank)	
Time after release days	Conc. µg/l	Time after release days	Conc. µg/l	Time after release days	Conc. µg/l	Time after release days	Conc. µg/l	Time after release days	Conc. µg/l	Time after release days	Conc. µg/l
3.5104	0	4.0521	0	4.3438	0	4.8854	0	5.3021	0	5.6563	0
3.5521	0	4.1354	0.08	4.3854	0	4.9271	0	5.3438	0	5.6979	0
3.6354	0.01	4.2188	0.23	4.4271	0.02	4.9688	0.04	5.3854	0.01	5.7396	0
3.7188	0.04	4.3021	0.43	4.4688	0.05	5.0104	0.08	5.4271	0.02	5.7813	0.01
3.8021	0.21	4.3854	0.55	4.5104	0.1	5.0521	0.13	5.4688	0.03	5.8229	0.01
3.8854	0.44	4.4688	0.57	4.5521	0.15	5.0938	0.17	5.5104	0.05	5.8646	0.02
3.9688	0.57	4.5521	0.47	4.5938	0.21	5.1354	0.22	5.5521	0.08	5.9063	0.03
4.0521	0.53	4.6354	0.37	4.6354	0.31	5.1771	0.27	5.5938	0.13	5.9479	0.05
4.1354	0.51	4.7188	0.28	4.6771	0.34	5.2188	0.34	5.6354	0.17	5.9896	0.06
4.2188	0.41	4.8021	0.25	4.7188	0.44	5.2604	0.37	5.6771	0.21	6.0104	0.09
4.3021	0.34	4.8854	0.18	4.7604	0.45	5.3021	0.39	5.7188	0.26	6.3438	0.20
4.3854	0.25	4.9688	0.12	4.8021	0.5	5.3438	0.39	5.7604	0.31	6.6771	0.17
4.4688	0.20	5.0521	0.10	4.8438	0.53	5.3854	0.4	5.8021	0.31	6.8646	0.14
4.5521	0.16	5.1354	0.10	4.8854	0.49	5.4271	0.39	5.8438	0.31	6.9063	0.12
4.6354	0.14	5.2188	0.07	4.9271	0.43	5.4688	0.38	5.8854	0.3	6.9479	0.10
4.7188	0.11	5.3021	0.07	4.9688	0.42	5.5104	0.34	5.9271	0.32	6.9896	0.09
4.8021	0.10	5.3854	0.05	5.0104	0.38	5.5521	0.32	6.0104	0.28	7.0313	0.08
4.8854	0.09	5.4688	0.03	5.0521	0.34	5.5938	0.29	6.0521	0.27	7.0729	0.07
4.9688	0.07	5.5521	0.03	5.0938	0.29	5.6354	0.27	6.0938	0.25	7.1146	0.08
5.0521	0.07	5.6354	0.03	5.1354	0.27	5.6771	0.24	6.1354	0.21	7.1563	0.08
5.1354	0.06	5.7188	0.03	5.1771	0.25	5.7188	0.22	6.1771	0.2	7.1979	0.09
5.2188	0.04	5.8021	0.03	5.2188	0.2	5.7604	0.21	6.2188	0.19	7.2396	0.07

Table B 1.2 (Contd…)

Time after release days	Conc. µg/l	Time after release days	Conc. µg/l	Time after release days	Conc. µg/l	Time after release days	Conc. µg/l	Time after release days	Conc. µg/l	Time after release days	Conc. µg/l
5.3021	0.03	5.8854	0.03	5.2604	0.19	5.8021	0.2	6.2604	0.17	7.2813	0.07
5.3854	0.03	5.9688	0.03	5.3021	0.16	5.8438	0.19	6.3021	0.16	7.3229	0.08
5.4688	0.03	6.0521	0	5.3438	0.15	5.8854	0.17	6.3438	0.14	7.3646	0.06
5.5521	0.02			5.3854	0.14	5.9271	0.15	6.3854	0.14	7.4063	0.05
5.6354	0.04			5.4271	0.12	5.9688	0.14	6.4271	0.12	7.4896	0.04
5.7188	0.03			5.4688	0.12	6.0104	0.13	6.4688	0.12	7.5313	0.05
5.8021	0.01			5.5104	0.12	6.0521	0.13	6.5104	0.11	7.5729	0.04
5.8854	0.01			5.5521	0.10	6.0938	0.11	6.5521	0.11	7.6146	0.04
5.9688	0.01			5.5938	0.08	6.1354	0.11	6.5938	0.1	7.6563	0.03
6.0521	0.02			5.6354	0.08	6.1771	0.10	6.6354	0.09	7.6979	0.03
6.1354	0.02			5.6771	0.08	6.2188	0.09	6.6771	0.09	7.7396	0.03
6.2188	0.01			5.7188	0.08	6.2604	0.09	6.7188	0.07	7.7813	0.03
6.3021	0.01			5.7604	0.08	6.3021	0.09	6.7604	0.08	7.8229	0.03
6.3854	0.01			5.8021	0.08	6.3438	0.07	6.8021	0.07	7.8646	0.03
6.4688	0			5.8438	0.06	6.3854	0.08	6.8438	0.07	7.9063	0.02
				5.8854	0.06	6.4271	0.07	6.8854	0.08	7.9479	0.02
				5.9271	0.05	6.4688	0.05	6.9271	0.07	7.9896	0.02
				5.9688	0.04	6.5104	0.05	6.9688	0.05	8.0313	0.02
				6.0104	0.03	6.5521	0.09	7.0104	0.04	8.0729	0.02
				6.0521	0.03	6.5938	0.06	7.0521	0.05	8.1146	0.02
				6.0938	0.02	6.6354	0.05	7.0938	0.03	8.1563	0.02
				6.1354	0.08	6.6771	0.04	7.1354	0.03	8.1979	0.02
				6.1771	0.01	6.7188	0.03	7.1771	0.03	8.2396	0.02
				6.2188	0.01	6.7604	0.04	7.2188	0.03	8.2813	0.01
				6.2604	0.01	6.8021	0.03	7.2604	0.02	8.3229	0.02
				6.3021	0.01	6.8438	0.02	7.3021	0.02	8.3646	0.01
				6.3438	0	6.8854	0.02	7.3438	0.01	8.4063	0.01

Table B 1.2 (Contd...)

Time after release days	Conc. µg/l	Time after release days	Conc. µg/l	Time after release days	Conc. µg/l	Time after release days	Conc. µg/l	Time after release days	Conc. µg/l
		6.3854	0	6.9271	0.01	7.3854	0.01	8.4479	0.01
				6.9688	0	7.4271	0	8.4896	0.01
						7.4688	0	8.5313	0.01
								8.5729	0.01
								8.6146	0.01
								8.6563	0.01
								8.6979	0.01
								8.7396	0.01
								8.7813	0.01
								8.8229	0.01
								8.8646	0.01
								8.9063	0.01
								8.9896	0.01
								9.0313	0.01
								9.0729	0.01
								9.1146	0.01
								9.1563	0
								9.1979	0
								9.2396	0
								9.2813	0
								9.3229	0.01
								9.3646	0.01
								9.4063	0
								9.4479	0

Table B 1.3 The bed slope in different sub-reaches

Rhine reach (km)	Bottom slope
496.8-744	2.3×10^{-4}
744-837	1.6×10^{-4}
837-863	2.7×10^{-5}

B 1.3   Colorado River Experiment Data

The dispersion data of this experiment conducted during steady and unsteady flow conditions have been obtained from, USGS, WRD, Tucson, AZ 85719. Graf (1995) has described the dye experiments conducted in the Grand Canyon reach, the Colorado River, during controlled steady and unsteady flow conditions, in May 1991. At Lees Ferry gauging station, on 20th May 1991 at 11:35hrs, 63.5kg of Rhodamine WT dye was injected for the experiments conducted during steady streamflow. During these experiments, under steady flow conditions, concentration measurements were taken at Nautiloid Canyon, above the Little Colorado, below Nevill's Rapid, Mile 118 camp, National canyon, Pumpkin spring, and at Gneiss Canyon located at a downstream distances of 58 km, 98 km, 123 km, 189 km, 267 km, 343 km, and 381 km from the tracer injection location respectively. The flow in Colorado River was maintained at an average rate of 428 m^3/s by controlling the flow from the Glen canyon dam.

During controlled unsteady flow conditions, Rhodamine WT dye was injected at Lees Ferry gauging station, on 6th May 1991 at 13:05 hrs, 127kg.for the measurements of dispersion during unsteady flow. The time-concentration measurements are available at Nautloid Canyon (RK 57.7), at the Little Colorado above Desert View (RK 98.3), at Nevill's rapid (RK 123), at Mile 118 camp (RK 189), at National Canyon (RK 267), and at Gneiss Canyon (RK 381) during unsteady flow.

In Grand Canyon reach, observed hydrographs are available at Lees Ferry (RK 0;USGS 09380000), at above the Little Colorado river near Desert View (RK

98; USGS 0938100), at Phantom Ranch near Grand Canyon (RK 142; USGS 09402500), at National Canyon near Supai (RK 267; RK 09404120) and at Diamond Creek near peach springs (RK 362; USGS 09404200).

The flow and dispersion data during steady and unsteady flow conditions are presented in floppy diskette attached. Files contain dispersion data collected at each site and have time, in decimal days, and dye concentration, in microgram per litre. Files are:

Dispersion data during steady flow:

nautsdy.dat, lcrsdy.dat, nevsdy.dat, m118sdy.dat, natusdy.dat, pumpsdy.dat, and gnssdy.dat, in downstream order.

Dispersion data during steady flow:

nautusdy.dat, lcrusdy.dat, nevusdy.dat, m118usdy.dat, natusdy.dat, and gnssdy.dat, in downstream order.

Files (named with gauging station number) containing the hydrographs data at gauging station, in down stream order, are:

9380000.txt, 9381000.txt, 9402500.txt, 9404120.txt, and 9404200.txt

In the hydrograph data the first column specifies year, second column specifies the month number, third column specifies date, fourth column specifies time in min and the fourth column specifies the discharge in ft^3/s.

B 1.4 Mimram River Experiment Data

A tracer experiment was conducted by Lees et al., (1998) on Mimram River near the Panshanger flow gauging flume in Hertfordshire, England. The reach is approximately 200 m long and is characterised by non-uniform cross-sections of sandy pebbled bed with heavy weed growth. A constant discharge of 0.251 m^3/s was measured at the gauging flume during the tracer experiment. Approximately 10 kg of sodium chloride (NaCl) was gulp injected into the river upstream of the flume's hydraulic jump and the resulting tracer cloud was measured over time at three

sampling stations downstream as follows: Site A at 100 m downstream from injection point; site B at 40 m downstream from site A; and Site C at 50 m downstream from site B. Measurements of conductivity were taken at irregular time intervals at each section, and the concentration of NaCl was computed from the conductivity calibration curves. The recorded concentrations, interpolated over an uniform sampling interval of 10 seconds were plotted by Lees et al. (1998). The plotted C-t curves were digitized using Tracer software (Karolewski, 2001) and the data thus digitized were used in the present study. The data is given in the diskette with file name Mimram.dat

B 1.5 Uvas Creek Experiment Data

Bencala and Walter (1983) described the tracer experiments conducted in Uvas Creek, a mountain stream, by injecting chloride at a constant rate for three hours duration. A maximum concentration of 11.9 mg/L was reached at a short distance below injection point. The experiments were conducted in late summer during a period of low flow of 0.0125 m^3/s. The overall slope is 0.03 m/m. Background concentration was measured to be 3.7 mg/l. The channel is highly irregular, composed of alternating pools and riffles. In riffle sections, the water is in contact with gravel and cobble bed and solute can easily enter the accessible void spaces. The observed C-t curves are available at a distance of 38m (station 1), 105m (station 2), 281m (station 3), 433m (Station 4), and 619m (station 5) from the tracer injection point. The time- concentration data used in the present study are given in Table B 1.4.

Table B 1.4 Time-concentration data from experiments on the Uvas Creek (Bencala and Walters, 1983)

Distance from source = 38km		Distance from source = 105km		Distance from source = 281km	
Time (hrs)	Concentration (mg/l)	Time (hrs)	Concentration (mg/l)	Time (hrs)	Concentration (mg/l)
7.933333	3.87	7.766667	3.72	7.8	3.69
8.016667	3.76	8	3.66	8.333333	3.67
8.5	3.67	8.083333	3.63	8.5	3.71
8.533333	3.73	8.333333	3.72	8.666667	3.77
8.566667	3.66	8.5	3.65	8.833333	3.7
8.6	3.69	8.666667	3.65	9	3.73
8.633333	3.73	8.75	3.79	9.166667	3.65
8.666667	5.58	8.833333	3.91	9.333333	3.65
8.7	8.44	8.916667	3.75	9.5	3.73
8.766667	10.61	9	3.75	9.666667	3.68
8.8	10.91	9.083333	4.16	9.833333	3.7
8.833333	11.14	9.166667	5.49	10	3.83
8.866667	11.22	9.25	7.15	10.16667	4.15
8.9	11.41	9.333333	8.21	10.33333	5.36
8.933333	11.49	9.416667	9.39	10.5	6.75
8.966667	11.49	9.5	10.2	10.66667	8.03
9	11.61	9.583333	10.57	10.83333	8.71
9.033333	11.49	9.666667	10.87	11	9.18
9.066667	11.47	9.75	11.03	11.16667	9.49
9.1	11.59	9.833333	11.22	11.33333	9.64
9.133333	11.47	9.916667	11.22	11.5	9.74
9.166667	11.47	10	11.26	11.66667	9.94
9.233333	11.55	10.08333	11.22	11.83333	9.91
9.3	11.47	10.16667	11.18	12	9.91
9.366667	11.47	10.25	11.28	12.16667	9.95
9.433333	11.43	10.33333	11.23	12.33333	9.94
9.5	11.47	10.41667	11.24	12.5	9.94
9.566667	11.47	10.5	11.4	12.66667	9.91
9.633333	11.43	10.66667	11.4	12.83333	9.96
9.7	10.99	10.83333	11.38	13	9.81
9.766667	11.41	11	11.38	13.16667	9.36
9.833333	11.48	11.16667	11.48	13.33333	8.29
10	11.68	11.33333	11.51	13.5	7.02
10.16667	11.63	11.5	11.4	13.66667	5.81
10.33333	11.52	11.58333	11.51	13.83333	5.06
10.5	11.54	11.66667	11.44	14	4.61
10.66667	11.56	11.75	11.4	14.16667	4.33
10.83333	11.37	11.83333	11.34	14.33333	4.15
11	11.46	11.91667	11.16	14.5	4.07
11.16667	11.4	12	10.95	14.66667	4
11.33333	11.44	12.08333	10.45	14.83333	3.92
11.5	10.23	12.16667	8.97	15	3.92
11.53333	10.51	12.25	7.68	15.16667	3.9

Table B 1.4 (Contd....)

Distance from source = 38km		Distance from source = 105km		Distance from source = 281km	
Time (hrs)	Concentration (mg/l)	Time (hrs)	Concentration (mg/l)	Time (hrs)	Concentration (mg/l)
11.56667	10.99	12.33333	6.31	15.33333	3.88
11.6	11.22	12.41667	5.66	15.5	3.89
11.63333	11.21	12.5	4.89	15.66667	3.85
11.66667	9.05	12.58333	4.53	15.83333	3.83
11.7	6.47	12.66667	4.24	16	3.91
11.73333	5.22	12.75	4.1	16.16667	3.86
11.76667	4.6	12.83333	3.94	16.33333	3.86
11.8	4.28	12.91667	3.84	16.5	3.86
11.83333	4.18	13	3.81	16.66667	3.91
11.86667	4.01	13.08333	3.79	16.83333	3.88
11.9	3.95	13.16667	3.75	17	3.87
11.93333	3.93	13.25	3.75	17.36667	3.8
11.96667	3.86	13.33333	3.78	17.86667	3.82
12	3.85	13.41667	3.74	18.36667	3.75
12.03333	3.96	13.5	3.74	19.36667	3.73
12.06667	3.81	13.58333	3.77	20.36667	3.73
12.1	3.79	13.66667	3.72	21.36667	3.75
12.13333	3.76	13.75	3.72	22.36667	3.73
12.16667	3.73	13.91667	3.75	23.36667	3.72
12.23333	3.72	14.08333	3.71	24.36667	3.83
12.3	3.71	14.25	3.71	25.36667	4
12.36667	3.71	14.41667	3.72	26.36667	4
12.43333	3.72	14.58333	3.73	27.36667	4.06
12.5	3.71	14.75	3.68	28.36667	4.22
12.56667	3.67	14.91667	3.7	29.36667	4.14
12.63333	3.67	15.08333	3.76	30.36667	4.2
12.7	3.7	15.25	3.7	31.36667	4.29
12.76667	3.71	15.5	3.7	32.36667	4.24
12.83333	3.71	15.75	3.68	33.36667	4.31
13	3.67	16	3.68	34.36667	4.33
13.16667	3.64	16.25	3.75	35.36667	4.22
13.33333	3.66	16.5	3.69	36.36667	4.24
13.5	3.64	16.75	3.66	37.36667	4.24
13.66667	3.66	17	3.71	38.36667	4.2
13.83333	3.64	17.5	3.79		
14	3.75	18.06667	3.72		
14.16667	3.68	19.06667	3.72		
14.33333	3.7	20.06667	3.7		
15.16667	3.7	21.06667	3.71		
15.68333	3.83	22.06667	3.71		
16.16667	3.74	23.06667	3.77		
16.68333	3.88				
17.16667	3.66				
17.68333	3.72				

223

Table B 1.4 (Contd...)

Distance from source = 38km		Distance from source = 105km		Distance from source = 281km	
Time (hrs)	Concentration (mg/l)	Time (hrs)	Concentration (mg/l)	Time (hrs)	Concentration (mg/l)
18.68333	3.76				
19.68333	3.72				
20.68333	3.74				
21.68333	3.83				
22.68333	3.8				
23.68333	3.93				
24.68333	4.06				
25.68333	4.1				
26.68333	4.11				
27.68333	4.08				
28.68333	4.16				
29.68333	4.5				
30.68333	4.46				
31.68333	4.28				
32.68333	4.41				
33.68333	4.38				
34.68333	4.51				
35.68333	4.39				

B 1.6 Huey Creek Experiment Data

A tracer-dilution experiment conducted in Huey Creek, in January 1992, to determine the extent and rate of hyporheic exchange was described by Runkel et al., (1998). A solution containing Lithium Chloride (LiCl) was injected into Huey Creek beginning at 11:25 hrs on 7th January. The injection continued at a rate of 8.7 ml/s for ≈3.75 h. Injectate concentration of Lithium (Li) was 34 g/l. The C-t measurements are available at downstream distances of 9m (location 1), 213m (location 2), 457m (location 3), 762m (location 4), and at 1052m (location 4) from the point of injection of the LiCl injectate (Fig. 6.24). The inflow hydrograph data given by Runkel et al., (1998) are given in Table B 1.5. The time concentration data used in the present study are given in Table B 1.6.

Table B 1.5 Inflow Hydrograph for Huey creek (Runkel et al., 1998)

Time (hrs)	Discharge (ft^3/s)	Time (hrs)	Discharge (ft^3/s)
0.00	0.28	18.25	1.6
0.25	0.28	18.50	1.5
0.50	0.24	18.75	1.3
0.75	0.24	19.00	1.2
1.00	0.22	19.25	1.1
1.25	0.2	19.50	0.96
1.50	0.2	19.75	0.84
1.75	0.2	20.00	0.76
2.00	0.2	20.25	0.7
2.25	0.2	20.50	0.59
2.50	0.19	20.75	0.42
2.75	0.17	21.00	0.41
3.00	0.17	21.25	0.38
3.25	0.15	21.50	0.34
3.50	0.15	21.75	0.34
3.75	0.15	22.00	0.34
4.00	0.15	22.25	0.34
4.25	0.15	22.50	0.32
4.50	0.15	22.75	0.32
18.00	1.9769	23.00	0.32

Table B 1.6 Distribution of cross-sectional average Li concentration with time, Huey creek (Runkel et al., 1998)

Distance from source = 9m		Distance from source =213 m		Distance from source = 457 m		Distance from source = 762.0m		Distance from source =1 052.0m	
Time (hr,m)	Concentration (mg/l)	Time (hr,m)	Concentration (mg/l)	Time (hr,m)	Concentration (mg/l)	Time (hr,m)	Concentration (mg/l)	Time (hr,m)	Concentration (mg/l)
11:17	0.012	11:15	0.046	11:15	0.042	10:50	0.037	11:04	0.036
11:20	0.052	11:25	0.02	11:30	0.011	11:10	0.037	11:15	0.004
11:45	3.366	11:35	2.968	11:45	2.617	11:30	0.091	11:25	0.023
11:55	2.807	11:45	3.093	12:00	2.500	11:45	0.067	11:35	0.011
12:05	2.708	11:55	2.844	12:15	2.382	12:00	2.323	11:51	0.03
12:15	2.596	12:05	2.67	12:30	2.289	12:15	2.174	12:05	1.843
12:25	2.509	12:25	2.447	12:45	2.289	12:30	2.273	12:20	1.913
12:45	2.404	12:35	2.496	13:00	2.312	12:45	2.078	12:33	1.867
13:00	2.16	12:45	2.025	13:15	2.265	13:00	2.223	12:43	1.813
13:30	2.11	12:55	2.422	13:30	2.289	13:15	2.198	12:52	1.937

Table B 1.6 Contd...)

Distance from source = 9m		Distance from source =213 m		Distance from source = 457 m		Distance from source = 762.0m		Distance from source =1 052.0m	
Time (hr,m)	Concentration (mg/l)	Time (hr,m)	Concentration (mg/l)	Time (hr,m)	Concentration (mg/l)	Time (hr,m)	Concentration (mg/l)	Time (hr,m)	Concentration (mg/l)
13:55	2.135	13:10	2.248	13:45	2.218	13:30	2.124	13:03	1.796
14:10	2.248	13:25	2.273	14:00	2.148	13:45	2.031	13:13	1.82
14:15	2.085	13:45	2.273	14:15	2.031	14:00	2.000	13:32	1.843
14:30	2.248	14:05	2.323	14:30	2.171	14:15	1.937	13:43	1.937
14:50	2.248	14:25	2.198	14:45	1.984	14:30	1.960	13:57	2.125
15:12	0.097	15:20	0.172	15:00	2.054	14:45	2.007	14:12	1.96
15:27	0.012	15:35	0.168	15:15	2.218	15:00	2.074	14:27	2.007
15:55	0.06	15:45	0.162	15:30	0.511	15:15	2.099	14:42	1.937
16:20	0.078	16:05	0.107	15:45	0.281	15:30	1.917	14:57	1.89
16:35	0.084	16:25	0.054	16:00	0.254	15:45	0.493	15:12	1.843
16:41	0.11	17:00	0.083	16:15	0.228	16:00	0.400	15:27	1.96
16:52	0.072		0	16:30	0.188	16:15	0.289	15:42	1.08
				16:45	0.156	16:30	0.209	15:57	0.434
				17:07	0.112	16:45	0.256	16:12	0.358
						17:00	0.191	16:27	0.264
						17:15	0.184	16:42	0.228
						17:30	0.166	16:57	0.198
						17:45	0.135	17:12	0.181
						18:00	0.141	17:27	0.178
						18:15	0.121	17:42	0.175
								17:57	0.15
								18:13	0.137
								18:33	0.156

FORTRAN PROGRAM LISTING

```
C***********************************************************************
C PROGRAM FOR SIMULTANEOUS FLOOD AND SOLUTE ROUTING BY AD-VPM   METHOD
C***********************************************************************
C   DESCRIPTION OF VARIABLE NOTATIONS USED IN THE PROGRAM
C   AI          INFLOW HYDROGRAPH ORDINATES AT THE INLET OF EACH SUB-REACH
C   QOBS        OBSERVED OUTFLOW HYDROGRAPH ORDINATE.
C   QCOM        COMPUTED OUTFLOW HYDROGRAPH ORDINATE
C   YM          COMPUTED STAGE AT THE MIDDLE OF THE SUB-REACH.
C   YOBS        OBSERVED STAGE AT THE OUTLET OF THE REACH
C   YCOM        COMPUTED STAGE AT THE OUTLET OF THE REACH
C   AIN1        ORDINATE OF THE GIVEN INFLOW HYDROGRAPH
C   Y1          COMPUTED STAGE CORRESPONDING TO AI
C   SIN1        STAGE CORRESPONDING TO GIVEN INFLOW AIN1
C   DYDXUP      NON-DIMENSIONALISED WATER SURFACE SLOPE COMPUTED AT
C               THE INLET OF THE REACH
C   DYDX1       NON-DIMENSIONALISED WATER SURFACE SLOPE GIVEN AT THE C
C               INLET OF THE REACH (COMPUTED USING ST. VENANT'S EQNS.)
C   CI          INPUT C-t CURVE ORDINATES AT INLET OF EACH SUB-REACH
C   COBS        OBSERVED OUTPUT C-t CURVE ORDINATES
C   CINT        ORDINATES OF THE INPUT C-t CURVE
C   CCOM        COMPUTED OUTPUT C-t CURVE ORDINATE
C   DL          DISPERSION COEFFICIENT
C   N           TOTAL NUMBER OF INFLOW AND OUTFLOW VARIABLE
C   NP          TOTAL NUMBER OF INPUT AND OUTPUT C-t ORDINATES (optional)
C   DT          ROUTING INTERVAL
C   YIN         INTIAL STAGE
C   Z           SIDE SLOPES
C   B           WIDTH OF THE CHANNEL
C   G           ACCELERATION DUE TO GRAVITY
C   SO          BED SLOPE
C   PI          RELATIONAL COEFFICIENT
C   AN          MANNING'S ROUGHNESS COEFFICIENT
C   NREACH      NUMBER OF SUBREACHES USED IN THE GIVEN ROUTING REACH
C   FSQ         SQUARE OF FROUDE NUMBER
C   R           HYDRAULIC RADIUS
C   THETA       WEIGHTING PARAMETER FOR FLOW ROUTING
C   AK          REACH TRAVEL TIME FOR FLOW ROUTING
C   AKP         REACH TRAVEL TIME FOR SOLUTE ROUTING
C   TETAM       WEIGHTING PARAMETER FOR SOLUTE ROUTING
C   Psi         Velocity conversion coefficient (optional)
C***********************************************************************
      REAL      AIN1(1000),Y1(1000),AI(1000),YM(200),DYDX(1000), YOBS(1000)
      REAL      QCOM(995),YCOM(995),FUNC(200),DYDX1(995),QOBS(995),YOUT(200)
      REAL      YCOM1(1000), QCOM1(1000),SIN1(1000),DYDX1(1000),FUNC2(200)
      REAL      DYDXUP(1000), aift(1000),SF(100),RI(100)
      REAL      CI (1000), CINT (1000),COBS (1000),CCOM (1000),A3(1000), disp (1000)
C
C   FILE 'dybydx.dat' IS AN OUTPUT FILE AND IT DISPLAYS GIVEN INFLOW, COR
C   RESPONDING COMPUTED AND ST. VENANT'S SOLUTION NON- DIMENSIONAL
C   ISED WATER SURFACE SLOPES
C
      OPEN (1,FILE='DYBYDX. DAT')
```

```
C   FILE 'vpm.dat' IS INPUT FILE AND IT STORES GIVEN INFLOW AND OUTFLOW
C   CORRESPONDING STAGE HYDROGRAPHS, INPUT AND OUTPUT CONCENTRATION
C   DISTRIBUTIONS, THE VALUES OF N, DT,YIN, B,G, SO, AN, TTL, NREACH, JUMP, PI, Z, and NP
C
    OPEN (2,FILE='VPM.DAT')
C
C   FILE 'vpm.out' IS AN OUTPUT FILE WHICH DISPLAYS GIVEN INPUT VALUES
C   OF N, DT,YIN, B,G, SO, AN, TTL, NREACH, JUMP, PI, Z, AND NP, IT ALSO
C   DISPLAYS    GIVEN    INFLOW    AND    OUTLFOW    HYDROGRAPH    AND    THE
C   CORESPONDING COMPUTED INFLOW AND OUTFLOW STAGE HYDROGRAPHS,
C   INPUT    AND    OUTPUT    CONCENTRATIONS,    COMPUTED    AND    OBSERVED
C   STAGE    HYDROGRAPHS. SUM OF INFLOW, SUM OF OUTFLOW AND SUM OF
C   COMPUTED OUTFLOW ALONG WITH MEASURES FOR VARIANCE EXPLAINED AND ERROR
C   IN VOLUME ARE DISPLAYED.
C
        OPEN (3,FILE='VPM.OUT')
C
C   FILE ' akth.out' IS AN OUTPUT FILE WHICH DISPLAYS THE LAST SUBREACH
C   INFLOW    AND    THE    CORRESPONDING    COMPUTED    MUSKINGUM    WEIGHTING
C   PARAMETER.
C
    OPEN (4,FILE='AKTH.OUT')
C
C   FILE 'dydx.dat' IS AN INPUT FILE WHICH STORES NON-DIMENSIONALISED WATER SURFACE
C   SLOP COMPUTED USING ST. VENANT'S SOLUTION AT THE
C   INLET OF THE REACH
C
    OPEN (7, FILE='DYDX.DAT')
C
C   FILE 'advpm.out' IS OUTPUT FILE WHICH GIVES THE VELOCITY AT SECTION
C   3, DISPERSION COEFFICIENT AND THE WEIGHTING PARAMETER OF SOLUTE
C   ROUTING AD-VPM MODEL
C
        OPEN (8,FILE='ADVPM.OUT')
C
        G=9.81
        READ(2,*)N,DT,YIN,B,SO,TTL,NREACH,Z, PI, NP,AN, Psi
        WRITE(3,99) N,DT,YIN,B,SO,AN,TTL,NREACH,G,Z,PI,NR1,NP
99      FORMAT(15X,'NO. OF ORDIANTES=',I6/15X,'ROUTING TIME INTERVAL
1       (Sec)=',F8.2/15X,'INTIAL DEPTH(mts)=',F8.4/15X,'CHANNEL WIDTH
2       (mts)=',F8.2/15X,'BED SLOPE(m/m)=',F6.4/15X,'MANNINGS ROUGHNESS
3       COEFF=',F6.3/15X,'TOTAL LENGTH OF THE REACH(m)=',F10.1/15X,'NO.
4       OF SUB REACHES =', I5 /15X,'ACC.DUE TO GRA=', F6.3/15X,'Z=',F8.4/
5       14X,'RELATIONAL PARA.=',F7.4/15X,'NO.OF REACHES=',I4/10X,'NP=',I4)

        READ(2,*) (AI(I),I=1,N+1)
        READ(2,*)(QOBS(I),I=1,N)

        READ(2,* )(CI(I),I=1,NP)
        READ(2,*)(COBS(I),I=1,NP)
        READ(7,890)(DYDX1(I),I=2,N+1)
890     FORMAT(10F8.5)
        Z1=SQRT(1.0+Z*Z)
C   STORING OF ORIGINAL AI AND CI VALUES IN AIN1 AND CINT ARRAYS
        DO 6 I=1,N
        CINT(I)=CI(I)
6       AIN1(I)=AI(I)
```

```
C   DO 8 I=1,NP
C   8    CINT(I)=CI(I)
        DXP=TTL/NR1
        DX=TTL/NREACH
        WRITE(*,*)DX,DXP
        DX1=0.0
        WRITE (3, *)' MANNING'S n =', AN

C  DX1- LENGTH OF CUMULATIVE ROUTING REACH

7       DX1=DX1+DX
        IF((DX1-1).GT.TTL)GOTO 26
95      FORMAT (15X,'SUB-REACH LENGTH=',F12.2,',',F12.2)
        Y1(1)=YIN
        QIN=AI(1)
        CIN=CI(1)
        DADY=B+2*Z*YIN
        DL=PI*QIN/(2.*SO*DADY)
        PRA=(B*(B+2.0*Z*YIN)+2.0*Z1*Z*YIN*YIN)/((B+2.*Z*YIN)*
     1  (B+2.0*Z1*YIN))
        VIN=QIN/((B+Z*YIN)*YIN)
        AK = DX/((1+2./3.*PRA)*VIN)
        AKP=DXP/VIN
        FSQ = QIN*QIN*(B+2.*Z*YIN)/(G*((B+Z*YIN)*YIN)**3)
        R=(B+Z*YIN)*YIN/(B+2.*YIN*Z1)
        THETAN=QIN*(1-(4./9.)*FSQ*PRA*PRA)
        THETAD=2.*SO*(B+2.*Z*YIN)*(1+2./3.*PRA)*VIN*DX
        THETA = 0.5-(THETAN/THETAD)
        TETAM=0.5-DL/(VIN*DXP)
        CONST=(1./AN)*SQRT(SO)
        QCOM(1)=QIN
        YCOM(1)=YIN
        CCOM(1)=CIN
        J=1
        YMID=YIN
C   COUNTER M IS USED FOR UPDATING THE PARAMETERS AT ANY TIME.
5       M=0
        J=J+1
9       CDIN=AK*(1.-THETA)+DT/2.
C   C1, C2 AND C3 ARE COEFFICIENTS OF THE MUSKINGUM FLOW ROUTING  EQUATION

        C1=(-AK*THETA+DT/2.)/CDIN
        C2=(AK*THETA+DT/2.)/CDIN
        C3=(AK*(1.0 - THETA)-DT/2.)/CDIN
        PDIN=AKP*(1.-TETAM)+DT/2.
C   PK1, PK2 AND PK3 ARE THE COEFFICIENTS OF THE MUSKINGUM SOLUTE
C   ROUTING EQUATION
        PK1=(-AKP*TETAM+DT/2.)/PDIN
        PK2=(AKP*TETAM+DT/2.)/PDIN
        PK3=(AKP*(1.0 - TETAM)-DT/2.)/PDIN
        M=M+1
C   COMPUTATION OF OUTFLOW
        QCOM (J)=C1*AI (J)+C2*AI (J-1)+C3*QCOM(J-1)
C   COMPUTATION OF OUTPUT CONCENTRATION
        CCOM(J)=PK1*CI(J)+ PK2*CI(J-1)+ PK3*CCOM(J-1)
C   COMPUTATION OF WEIGHTED OUTFLOW
        Q3 = QCOM(J)+THETA*(AI(J)-QCOM(J))
        I=1
```

229

```fortran
         YM(I)=YMID
C    FINDING THE STAGE AT THE MIDDLE OF THE REACH
         R=(B+Z*YM(I))*YM(I)/(B+2.*YM(I)*Z1)
         FUNC(I)=Q3-CONST*R**(2./3.)*(B+Z*YM(I))*YM(I)
         I=2
         YM(I)=YMID+0.2*YMID
10       R=(B+Z*YM(I))*YM(I)/(B+2.*YM(I)*Z1)
         FUNC(I)=Q3-CONST*R**(2./3.)*(B+Z*YM(I))*YM(I)
         DYM=-FUNC(I)*(YM(I)-YM(I-1))/(FUNC(I)-FUNC(I-1))
         YM(I+1)=YM(I)+DYM
         IF(ABS((YM(I+1)-YM(I))/YM(I+1)) .LT. 0.01) GOTO 30
         I=I+1
         GO TO 10
30       YMID=YM(I+1)
C    COMPUTATION OF THE DISCHARGE AT THE MIDDLE OF THE REACH
         QMID=(AI(J)+QCOM(J))/2.0
         VM=QMID/((B+Z*YMID)*YMID)
         VNORM=Q3/((B+Z*YMID)*YMID)
         PRA=(B*(B+2.0*Z*YMID)+2.0*Z1*Z*YMID*YMID)/((B+2.*Z*YMID)*
     1   (B+2.0*Z1*YMID))

C    COMPUTATION OF THE SQUARE OF THE FROUDE NUMBER
         FSQ = QMID*QMID*(B+2.*Z*YMID)/(G*((B+Z*YMID)*YMID)**3)
         YCOM(J)=YMID+(QCOM(J)-QMID)/((B+2.*Z*YMID)*(1.+ 2./3.*PRA)*VM)
         Y3 = YMID+(Q3-QMID)/((B+2.*Z*YMID)*(1.+ 2./3.*PRA)*VM)
C        A3(j)=(B+Z*Y3)*Y3
C    COMPUTATION OF THE VELOCITY AT THE WIGHTED OUTFLOW SECTION
         V3=Q3/((B+Z*Y3)*Y3)
C 23     FORMAT (1X,'VELOCITY3=',F15.6)
         PRA=(B*(B+2.0*Z*Y3)+2.0*Z1*Z*Y3*Y3)/((B+2.*Z*Y3)*
     1   (B+2.0*Z1*Y3))
         DADY=B+2*Z*Y3
C    COMPUTATION OF DISPERSION COEFFICIENT USING WEIGHTED DISCHARGE
         DL=PI*Q3/(2.*SO*DADY)
C    disp(j)=dl
C    alfa=(a3(j)*disp(j)-a3(j-1)*disp(j-1))/(dx*a3(j))
C    COMPUTATION OF VECLOCITY OF SOLUTE CLOUD
         V3M=V3
C    V3M=VNORM
C    v3m = v3/(1+psi)
         AKP=DXP/V3M
         DADY=B+2*Z*Y3
C    DL=PI*Q3/(2.*SO*DADY)
C    COMPUTATION OF WAVE CELERITY OF THE REACH
         CEL=(1+2./3.*PRA)*V3
C    COMPUTATION OF PARAMETER AK,AKP,THETA, AND TETAM
         AK =DX / CEL
         R=(B+Z*YMID)*YMID/(B+2.*YMID*Z1)
         THETAN=Q3*(1-(4./9.)*FSQ*PRA*PRA)
         THETAD=SO*(B+2.*Z*Y3)*(1+2./3.*PRA)*V3*DX
C    COMPUTATION OF DISPERSION COEFFICIENT AND WEIGHTING FACTOR FOR SOLUTE
         DL=PI*THETAN/(2.*SO*DADY)
C    DL=PI*Q3/(2.*SO*DADY)
         TETAM=0.5-DL/(V3M*DXP)
C    WRITING  THE  VALUES  OF  OUTFLOW,  VELOCITY,  DISPERSION  COEFFICIENT
C    AND THE WEIGHTING COEFFICIENT
         WRITE (8,*) QCOM(J),V3M,DL,TETAM
C    GM = (QCOM(J)-AI(J))*THETAN/(THETAD*Q3)
```

```
       GM =0.
       THETA=0.5-(THETAN/THETAD)*(0.5+0.125*GM+(1./16.)*GM*GM+(5./128.)*
    1      GM**3+(7./256)*GM**4)
       YCOM(J)=YMID+(QCOM(J)-QMID)/((B+2.*Z*YMID)*(1.+ 2./3.*PRA)*VM)


C  COMPUTATION OF STAGE AT THE INLET OF THE REACH
       IF (DX1 .EQ. DX) THEN
       Y1(J)=2.*YMID-YCOM(J)
       ENDIF
       IF (M .LE. 1) GOTO 9


C  COMPUTATION OF NON-DIMENSIONALISED WATER SURFACE SLOPE AT  THE INLET OF
C  THE REACH

       VELUP=AI(J)/((B+Z*Y1(J))*Y1(J)
       PRA=(B*(B+2.0*Z*Y1(J))+2.0*Z1*Z*Y1(J)*Y1(J))/((B+2.*Z*Y1(J))*
    1      (B+2.0*Z1*Y1(J)))
       CELUP=(1+2./3.*PRA)*VELUP
       DYDXUP(J) = -(AI(J)-AI(J-1))/(SO*DT*B*CELUP**2)
C  CONVERTING AK INTO HOURS
       IF(DX1 .EQ. DX)AK1=AK/3600.0
C  WRITING INFLOW OF THE LAST REACH AND THE CORRESPONDING AK AND
C  THETA.
       IF(DX1 .EQ. DX) WRITE(4,*) J, AI(J),AK1,THETA
       DYDX(J)=(YCOM(J)-Y1(J))/DX
       DYDX1(J)=DYDX(J)/SO
       WRITE(1,*)DYDX(J),DYDX1(J)
       IF (J .LT. N) GOTO 5
C  WRITING INFLOW AND CORRESPONDING NON-DIMENSIONALISED WATER SURFACE
C  SLOPE OF THE St.VENANT'S SOLUTION AND PRESENT SOLUTION
       IF (DX1 .eq. DX) WRITE(1,222) (J,AIN1(J), DYDXUP(J), DYDX(J), DYDX1(J)      1 J=2,N)
222    FORMAT (5X, I3,F8.0,2X,F10.6,5X,2F10.6)


C  OUTFLOW AND STAGE FROM THE SUB-REACH BECOMES INFLOW TO THE
C  NEXT SUB-REACH
       DO 28 I=1,N
       Y1(I)=YCOM(I)
       CI(I)=CCOM(I)
  28   AI(I)=QCOM(I)


C  CHECKING FOR THE COMPLETION OF THE ROUTING FOR THE LAST SUB-
C  REACH
  26   IF(DX1.LT.TTL) GOTO 7
C  WRITING THE INFLOW, AND OBSERVED AND COMPUTED OUTFLOW AND
C  STAGE
       WRITE (3,*)'NO. INFLOW     OUTFLOW   OBS   YCOM'
       WRITE (3,101)((J-1), AIN1(J), QCOM(J), QOBS(J), YCOM(J), J=1,N)
101    FORMAT (1X,1X,I4,1X,4F12.5)
C  WRITING THE COMPUTED OUTFLOW, INPUT CONCENTRATION, COMPUTED
C  OUTPUT CONCENTRATION, AND OBSERVED CONCENTRATION AT OUTPUT SECTION

       WRITE (3,111)((J-1),QCOM(J), CINT(J), CCOM(J), COBS(J), J=1,N)
111    FORMAT(1X,1X,I4,1X,4F12.5)
C  ENDIF
C  COMPUTATION OF SUM OF INFLOW, OBSERVED OUTFLOW, COMPUTED
C  OUTFLOW, INPUT, OUTPUT AND OBSERVED CONCENTRATIONS, AND Nash
C  - Sutcliffe criterion and error in volume of flow. The mass conservation computation for solute under
C  unsteady flow condition is not included
```

231

```fortran
      sumai=0.0
      SUMQC=0.0
      SUMQO=0.0
      sumCI=0.0
      SUMCC=0.0
      SUMCO=0.0
      DO 22 J=1,N
      SUMAI=SUMAI+AIN1(J)
      SUMQC=SUMQC+QCOM(J)
      SUMQO=SUMQO+QOBS(J)
      SUMCI=SUMCI+CINT(J)
      SUMCC=SUMCC+CCOM(J)
22    SUMCO=SUMCO+COBS(J)
      AVECI=SUMCI/NP
      AVECC=SUMCC/NP
      AVECO=SUMCO/NP
      AVEAI=SUMAI/N
      AVEQC=SUMQC/N
      AVEQO=SUMQO/N
      TOTVAR=0.0
      RESVAR=0.0
      TTCVAR=0.0
      RSCVAR=0.0
      DO 32 J=1,N
          TTCVAR=TTCVAR+(COBS(J)-AVECO)*(COBS(J)-AVECO)
          RSCVAR=RSCVAR+(COBS(J)-CCOM(J))*(COBS(J)-CCOM(J))
          TOTVAR=TOTVAR+(QOBS(J)-AVEQO)*(QOBS(J)-AVEQO)
32    RESVAR=RESVAR+(QOBS(J)-QCOM(J))*(QOBS(J)-QCOM(J))
      VRCEXP=(TTCVAR-RSCVAR)/TTCVAR*100.0
      CEVOL=(SUMCC-SUMCI)/SUMCI*100
      VAREXP=(TOTVAR-RESVAR)/TOTVAR*100.0
      EVOL=(SUMQC-SUMAI)/SUMAI*100
      WRITE (3,102)SUMAI,SUMQC,SUMQO
102   FORMAT(15X,'SUMAI=',F10.2,4X,'SUMQC=',F10.2,3X,'SUMQO=',F10.2)
      WRITE (3,104)VAREXP,EVOL
104   FORMAT(15X,'VAREXP=',F9.3,5X,'EVOL=',F9.2,2X,'%ERR=',F10.5)
C     Nash-Sutcliffe criterion and error in mass given below is applicable for dispersion under  steady flow only.
C     For dispersion under unsteady flow compute inflow and out flow mass separately.
C
      WRITE (3,77)SUMCI,SUMCC,SUMCO
77    FORMAT(15X,'SUMCI=',F10.3,4X,'SUMCC=',F10.3,3X,'SUMCO=',F10.3)
      WRITE (3,78)VRCEXP,CEVOL
78    FORMAT(15X,'VRCEXP=',F9.3,5X,'EVOL=',F9.2,2X,'%ERR=',F10.5)
      Y1(1)=Y1(2)
c     DO 106 I=1,N
c         QCOM(I)=0.0
c         YCOM(I)=0.0
c 106   AI(I)=AIN1(I)
      CLOSE(1)
      CLOSE(2)
      CLOSE(3)
      CLOSE(4)
      CLOSE(7)
      CLOSE(8)
      STOP
      END
```

232